

CO₂ Adsorption Enhancement via Modification of Porous Materials
by

Abedeh Gholidoust Saraidashti

A thesis submitted in partial fulfillment of the requirements for the degree of

Doctor of Philosophy

in

Environmental Engineering

Department of Civil and Environmental Engineering

University of Alberta

© Abedeh Gholidoust Saraidashti, 2017

ABSTRACT

CO₂ separation from flue gas streams is an essential issue as it is the main anthropogenic greenhouse gas contributing to global warming. Commercially used methods for CO₂ capture includes absorption in liquid amine solutions which has its own drawbacks such as pipeline corrosion, oxidative degradation of amines, foaming in the gas-liquid interface, high energy requirement for regeneration, and high maintenance costs. To overcome these problems, adsorption onto solid adsorbents is proposed as an alternative. Although microporous activated carbons and zeolites (e.g. 5A, 13X and Faujasite) have been previously utilized in CO₂ capture, their relatively low adsorption capacity as well as sensitivity to humidity can limit their usage. One of the remedies to enhance adsorption capacity of solid adsorbent is anchoring amine via amine impregnation. Additionally, new classes of porous materials called Metal Organic Frameworks (MOFs) with exceptional capture performance hold promise in this regard.

In the course of the current research, firstly activated carbons were synthesized from oil sands coke which is abundantly available in Alberta. Then the synthesized microporous activated carbons were impregnated with amines and the performance of amine impregnated activated carbons for CO₂ adsorption was investigated to find suitable conditions for amine impregnation and CO₂ adsorption. The application of MOF materials for CO₂ capture was also studied and a new method was proposed to overcome problems associated with low MOF capture capacity at atmospheric pressure and temperature. Finally, a MOF-based microwave sensor was used to monitor the adsorption progress based on the change in dielectric properties of MOF materials.

The first part of this study investigated the effect of different activation agents such as KOH and MgO on porosity and capture capacity of activated carbons prepared from oil sands coke. Research findings suggested that KOH activation results in a narrow pore size distribution

in micropore range, while adding MgO template provides mesoporous activated carbons with almost twice CO₂ adsorption capacity.

Further investigations were completed to study the effect of amine impregnation on CO₂ capture enhancement of activated carbons prepared from oil sands coke. The impact of different parameters such as impregnation ratio, amine type, humidity and adsorption temperature was evaluated. The results showed that secondary amine (Diethanolamine) provided more active sites with affinity for CO₂ compared to tertiary (methyl diethanolamine) and bulky amines (tetra ethylene pentamine). There is an optimum value in amine loading which results in maximum adsorption capacity, while exceeding this point causes a decrease in adsorption capacity possibly due to the blockage of accessible volume of pores. The optimum adsorption temperature for our research was discovered to be at 50 °C. Also, the adsorption capacity of tertiary amine (MDEA in our work) was found to be improved by almost 1.6 times in the presence of 20% water vapor in feed stream compared to dry condition.

In the next step, a novel MOF material combined with carbon nanotube (CNT) membrane was introduced. This study focuses on: 1) synthesis of MOF (MOF-74) and MOF-CNT using solvothermal method, 2) enhancement of MOF-CNT interfacial interaction by plasma treatment, 3) testing the MOF and MOF-CNT for carbon dioxide adsorption. The generation of new functional groups on the surface of CNT through plasma treatment provided favorable chemical affinity and stability to bridge MOF crystals and produce near-defect free MOF-membranes. Additionally, single-component CO₂ adsorption isotherms showed a large increase in CO₂ uptake (maximum of 10.70 mmol CO₂/g) for MOF-CNT-BP samples compared to the parent Mg-MOF-74 (maximum of 3.13 mmol CO₂/g).

Additionally, a new MOF material (MOF-199) was integrated with a microwave resonator sensor and its performance for CO₂ monitoring was compared to a commercial zeolite 13X. During the adsorption, the dielectric properties of MOF changed which could be detected by a change in resonant frequency. Despite the lower adsorption capacity of MOF-199 for low CO₂ concentrations (<45 %), it showed higher sensitivity than zeolite 13X, which can be related to the initial dielectric properties of the virgin adsorbent. The ability of the sensor to monitor low concentrations of CO₂ amplifies its potential in applications where information is required on the adsorbent replacement time.

PREFACE

The research completed in this dissertation was planned, designed, conducted, analyzed, and compiled by myself, and was fully reviewed and supervised by Dr. Zaher Hashisho in the Department of Civil and Environmental Engineering at the University of Alberta. The journal articles written from the present work are listed below, and the individual contributions of all the members from the Air Quality Characterization Lab in the Department of Civil and Environmental Engineering, and Department of Electrical Engineering at the University of Alberta and collaborators from Deakin University are indicated.

Chapter 3:

A version of this chapter has been published as: Gholidoust, A.; Atkinson, J.D.; Hashisho, Z.

Towards CO₂ adsorption enhancement via amine impregnated activated carbon, *Energy & Fuels*, Jan. 2017, 31 (2), pp 1756–1763.

- Dr. John Atkinson contributed to manuscript edits.

Chapter 4:

This chapter will be submitted for publication as a journal paper.

- Dr. Masoud Jahandar assisted in obtaining some of the adsorption isotherms.

Chapter 5:

This chapter will be submitted for publication as a journal paper.

- Mr. Andrea Merenda and Ms. Nouran Ashraf Elbadawi helped me in conducting XPS and SEM characterization analyses.
- Dr. Ludovic Dumeé, and Dr. Lingxue Kong contributed to manuscript edits.

Chapter 6:

This chapter was submitted for publication in *Sensors and Actuators B: Chemical*.

- Dr. Mohammad Zarifi from Electrical Department at the University of Alberta conducted CO₂ monitoring measurements with sensor as well as data analyses. He also contributed to manuscript drafting and edits.
- Mr. Pooya Shariaty, and Mohammad Abdolrazzaghi partly involved in CO₂ monitoring experiments as well as manuscript edits.
- Dr. Mojgan Daneshmand from Electrical Department at the University of Alberta contributed to manuscript edits.

I dedicate this dissertation to my beloved family.

A special gratitude to my loving parents, Azar and Shaban, who have always been a source of inspiration, encouragement and stamina to undertake my higher studies and to face eventualities of life with zeal, enthusiasm and fear of God

This dissertation is also dedicated to my dear husband, Saeid, for his patience, understanding, support, and encouragement.

Last but not least, I dedicate this dissertation to all amazing women around the world who go beyond the traditional norms and battle with the dark days.

ACKNOWLEDGEMENTS

First and foremost, I would like to express my deepest appreciation to my supervisor, Dr. Zaher Hashisho, for his continuous guidance, generous support, and invaluable comments and great understandings during my PhD studies. This work could not be accomplished without his experience, knowledge, and passion.

I would like to acknowledge financial support from Carbon Management Canada (CMC), SCENEREI Seed funding, the Natural Sciences and Engineering Research Council (NSERC) of Canada, as well as the infrastructure and instruments grants from Canada Foundation for Innovation, Alberta Advanced Education and Technology, National Institute for Nanotechnology (NINT), Alfred Deakin University, and Commonwealth Scientific and Industrial Research Organization (CSIRO) located in Waurin Ponds campus in Australia,

I am grateful to my funders, including but not limited to, Air & Waste Management Association (Air Quality Study and Research Scholarship), UK Energy Research Community (Research Excellence Award to attend the Summer School at Warwick University), Education Abroad Program (Education Abroad Individual Award), Canadian Prairies and Northern Section of the Air & Waste Management Association (Graduate Student Travel Award), the Carbon Management Canada (Student Travel Award), Faculty of Graduate Studies and Research at the University of Alberta (Travel Award), the Graduate Students Association at the University of Alberta (Graduate Student Travel Award).

I also acknowledge my defense committee members, Prof. Rajender Gupta, Dr. Yang Liu, Dr. Japan Trivedi, and Dr. Yaman Boluk, for their contributions to this work.

I highly appreciate the contribution of my co-authors: Dr. Zaher Hashisho, Dr. John Atkinson, Dr. Ludovic Dumeénil, Dr. Lingxue Kong, Dr. Mojgan Daneshmand, Dr. Mohammad Zarifi, Pooya Shariaty, Saeid Niknaddaf, and Mohammad Abdolrazzaghi.

I would also like to express my gratitude to the postdoctoral fellows of our research group: Dr. Heng Chen, Dr. John Atkinson, and Dr. Mohammad Zarifi for their support, comments, recommendations, and availability.

Thank you to a number of technicians in the Department of Civil and Environmental Engineering for their support and availability: Chen Liang, Elena Dlusskaya, Yupeng (David) Zhao, Jela Burkus, Maria Demeter, and Nancy Zhang from NINT department.

I am very thankful to my friends and colleagues in Air Quality Characterization Lab: Saeid Niknaddaf, Pooya Shariaty, Masoud Jahandar, Samineh Kamravaei, Mohammadreza Fayaz, and Monisha Alam, and my research peers from Institute of Frontier Material Characterization Lab: Andrea Merenda, Nouran Ashraf El-badawi, and James Wainaina Maina.

TABLE OF CONTENTS

CHAPTER 1. INTRODUCTION AND RESEARCH OBJECTIVES	1
1.1. Background and Motivation	1
1.1.1. Climate change and CO ₂ emission	1
1.1.1. CO ₂ capture via adsorption	2
1.1.2. Real-time monitoring of CO ₂ concentration using microwave resonator sensor	3
1.2. Objectives	4
1.3. Significance of the Research	5
1.4. Thesis Organization	6
1.5. References	6
CHAPTER 2. LITERATURE REVIEW	13
2.1. CO ₂ Capture Methods	13
2.1.1. Pre-combustion Capture	14
2.1.2. Oxy-fuel Combustion	14
2.1.3. Post-combustion Capture	15
2.2. Adsorption Materials	18
2.2.1. Activated Carbon	20
2.2.2. Amine Impregnated Activated Carbons	24
2.2.3. MOFs	27

2.3.	Microwave Sensing	38
2.3.1.	Introduction	38
2.3.2.	Microwave sensing application	39
2.3.3.	Material-assisted sensors	40
2.4.	References	42
CHAPTER 3. ENHANCING CO ₂ ADSORPTION VIA AMINE IMPREGNATED ACTIVATED CARBON FROM OIL SANDS COKE		64
3.1.	Introduction	64
3.2.	Experimental Section	67
3.2.1.	Activated Carbon Preparation	67
3.2.2.	Amine Impregnation	68
3.2.3.	Materials Characterization	69
3.2.4.	CO ₂ adsorption experiment	70
3.3.	Results	72
3.3.1.	Raw and activated delayed coke	72
3.3.2.	Impregnated activated carbon materials	75
3.3.3.	CO ₂ adsorption performance	78
3.3.4.	Effect of humidity on adsorption capacity of tertiary amine	83
3.3.5.	Effect of adsorption temperature	85
3.4.	Conclusion	88

3.5.	References	89
CHAPTER 4. SYNTHESIS OF MESOPOROUS CARBONS FOR CO ₂		
ADSORPTION FROM OIL SANDS COKE USING KOH ACTIVATION WITH A MgO		
TEMPLATE	98	
4.1.	Introduction	98
4.2.	Materials and Methods	100
4.2.1.	Chemicals	100
4.2.2.	Activated Carbon Preparation	100
4.3.	Characterization Methods	102
4.3.1.	Nitrogen adsorption measurement	102
4.3.2.	Bulk and surface elemental analysis	102
4.3.3.	CO ₂ adsorption measurement	103
4.3.4.	FTIR Spectroscopy	103
4.4.	Results and Discussion	104
4.4.1.	BET surface area and pore size distribution	104
4.4.2.	Elemental analysis	106
4.4.3.	CO ₂ adsorption performance	108
4.5.	Conclusion	113
4.6.	References	114

CHAPTER 5. PLASMA ENHANCED SEEDED GROWTH OF METAL ORGANIC
 FRAMEWORKS ACROSS CARBON NANOTUBE FABRICS AND THEIR POTENTIAL
 FOR CO₂ CAPTURE 121

5.1.	Introduction	121
5.2.	Materials and methods.....	125
5.2.1.	Chemicals and reactants	125
5.2.2.	CNTs growth and preparation	125
5.2.3.	CNT-BP fabrication	125
5.2.4.	CNT-BP surface functionalization by plasma treatment.....	126
5.2.5.	MOF crystals seeding and growth across the BPs	126
5.2.6.	Characterization tests	128
5.3.	Results and Discussions.....	129
5.3.1.	Carbon nanotube surface conditioning and assessment	129
5.3.2.	MOF-CNT-BP composite properties	137
5.3.3.	CO ₂ volumetric adsorption results	145
5.4.	Conclusions	152
5.5.	References	153

CHAPTER 6. SENSITIVITY ENHANCEMENT IN PLANAR MICROWAVE
 ACTIVE-RESONATOR USING METAL ORGANIC FRAMEWORK FOR CO₂ SENSING 163

6.1.	Introduction	163
------	--------------------	-----

6.2.	Materials and methods.....	167
6.2.1.	Chemicals and reactants.....	167
6.2.2.	MOF crystals seeding and growth.....	167
6.2.3.	X-Ray Diffraction (XRD) analysis	168
6.2.4.	X-ray photoelectron spectroscopy (XPS).....	168
6.2.5.	Scanning Electron Microscopy	169
6.3.	Experimental set-up.....	169
6.3.1.	Gas adsorption-VNA set-up.....	169
6.3.2.	CO ₂ volumetric adsorption.....	170
6.4.	Results	170
6.4.1.	Characterization Test Results.....	170
6.4.2.	Microwave Results.....	172
6.4.3.	Volumetric Adsorption Results.....	176
6.5.	Conclusions	178
6.6.	References	179
CHAPTER 7. CONCLUSIONS AND RECOMMENDATIONS		189
7.1.	Conclusions	189
7.2.	Recommendations	191
BIBLIOGRAPHY.....		192
APPENDIX A: SUPPLEMENTARY DATA FOR CHAPTER 3		236

APPENDIX B: SUPPLEMENTARY DATA FOR CHAPTER 5.....	240
---	-----

LIST OF TABLES

Table 2-1. Physical properties of conventional amines (National Center for Biotechnology Information (a, b, c, d), 2017).....	25
Table 2-2. Low pressure CO ₂ adsorption capacities for MOFs	36
Table 3-1. Physical and chemical properties of raw and activated delayed coke	73
Table 3-2. Physical, chemical and adsorption properties of raw and impregnated samples	76
Table 4-1. Surface characteristics of raw and activated delayed cokes, microwave heated in N ₂ gas stream.....	104
Table 4-2. Bulk composition of raw and activated delayed cokes, microwave heated in N ₂ gas stream	107
Table 4-3. Surface composition of raw and activated delayed coke, microwave heated in N ₂ gas stream	108
Table 5-1. Atomic concentration of elements in CNT-BP samples before and after treatment with O ₂ /Ar.....	130
Table 5-2. Atomic concentration of elements in CNT-BP samples before and after treatment with NH ₃	131
Table 5-3. Contact angle results for the plasma treated CNT-BPs	136
Table 5-4. Summary of the properties of the MOF-CNT-BP membrane composites	145
Table A1. The atomic percentage of different N1S components determined from relative area of corresponding XPS spectra	237
Table B1. Curve fitting results of XPS C1s spectra for O ₂ /Ar plasma treatment	241
Table B2. Curve fitting results of XPS C1s spectra for NH ₃ plasma treatment.....	241
Table B3. Raman feature of CNT-BP before and after plasma treatment with O ₂ /Ar and NH ₃	242

LIST OF FIGURES

Figure 2-1. CO ₂ capture from power generation plant (Olajire, 2010).....	14
Figure 2-2. Process flow diagram for amine-based CO ₂ capture (CSIRO, 2008).....	16
Figure 2-3 Solid adsorbents for CO ₂ capture.....	19
Figure 2-4. The concept of surface modification to increase compatibility with MOF (Hermes et al., 2005).....	28
Figure 3-1. Schematic diagram of CO ₂ adsorption set-up.....	72
Figure 3-2. Pore size distribution of as prepared and impregnated activated carbon.....	78
Figure 3-3. Adsorption capacity of (a) AC-DEA, (b) AC-MDEA and (c) AC-TEPA at different loadings. Adsorption completed at 66.6% CO ₂ in N ₂ , 50 °C temperature, and atmospheric pressure. Error bars indicate standard deviation of the mean of two sets of data.....	81
Figure 3-4. Working adsorption capacity of AC-DEA, with 1.15 mmol N/g AC loading for 66% CO ₂ in N ₂ over 15 cycles of adsorption and regeneration. Adsorption completed at 66.6% CO ₂ in N ₂ , 50 °C, and atmospheric pressure regeneration completed at 110 °C in 100 mL/min of N ₂ (99.999%. Error bars indicate standard deviation of the mean of two sets of data).....	83
Figure 3-5. Effect of moisture on CO ₂ adsorption capacity of MDEA-impregnated activated carbon. Adsorption completed at 20% CO ₂ in N ₂ , 50 °C temperature, and atmospheric pressure. Error bars indicate standard deviation of the mean of two sets of data.....	85
Figure 3-6. Adsorption capacity of (a) AC-DEA, and (b) AC-MDEA samples at different temperatures, 20% CO ₂ in N ₂ , and atmospheric pressure. Error bars indicate standard deviation of the mean of two sets of data.....	87
Figure 4-1. Pore size distribution of activated delayed cokes (KC: KOH/coke, MC: MgO/coke).....	106

Figure 4-2. Effect of activation agent ratio on the adsorption capacity of microwave activated carbon, 66.6% CO ₂ in N ₂ , T _{adsorption} =50°C, Error bars indicate standard deviation of the mean of two sets of data.....	109
Figure 4-3. Effect of activation purge gas and humidity on the adsorption behavior of activated carbons (KC=0.86, MC=2), microwave (MW) heating, CO ₂ flow rate= 200 ml/min, T _{adsorption} =50°C. Error bars indicate standard deviation of the mean of two sets of data.....	111
Figure 4-4. FTIR spectra of microwave activated carbons in N ₂ and CO ₂ gas stream	112
Figure 5-1 Preparation of MOF-CNT-BP sample.....	127
Figure 5-2. Impact of plasma treatment on surface affinity towards MOF crystals, (a) virgin CNT-BP, (b) single side plasma treated CNT-BP with NH ₃ for 3min and (c) single side plasma treated CNT-BP with O ₂ /Ar for 3min.....	139
Figure 5-3. Impact of plasma duration on surface affinity towards MOF crystals, (a) 3min, (b) 5min and (c) 7min, double side treated with O ₂ /Ar, crystallization time = 20h.....	140
Figure 5-4. Impact of side treatment on surface affinity towards MOF crystals, (a) side 1 of double side treated sample, (b) side 2 of double side treated sample and (c) single side treated sample, treated with NH ₃ , treatment duration=5min, crystallization time=15h	141
Figure 5-5. Effect of crystallization time on MOF growth, (a) 15h crystallization, (b) 20h crystallization, single side treated with O ₂ /Ar, treatment duration of 3 min	142
Figure 5-6. CO ₂ volumetric adsorption of virgin CNT-BP and Mg-MOF-74-CNT-BPs at 25°C, Impact of (a) plasma gas, (b) plasma treatment duration for samples treated with O ₂ /Ar, (c) plasma duration for samples treated with NH ₃ , (d) plasma treatment side effect, and (e) crystallization duration.....	148
Figure 5-7. Pore size distribution of virgin CNT-BP, Mg-MOF-74 and MOF-CNT-BP	149

Figure 6-1. Schematic diagram of gas adsorption set-up.....	170
Figure 6-2. Characterization results: (a) XRD spectra, (b) High resolution XPS spectra, and (c) SEM images of synthesized MOF-199 samples	172
Figure 6-3. (a) experimental setup with the microwave active resonator sensor, (b) resonant profile (S21) of the sensor without any material (blank), with MOF and Zeolite while being purged with He at a rate of 200 SCCM at room temperature.	173
Figure 6-4. (a) Resonant frequency-shift during the adsorption time for different CO ₂ concentration on MOF-199-M2, (b) resonant frequency shift versus different Concentration of CO ₂ in dry He, the error bar is standard deviation of 5 independent experiments per each concentration.....	174
Figure 6-5. Time variant resonant frequency shift of the sensor for different CO ₂ concentrations on zeolite 13X, (b) reliability experiment of resonant frequency versus CO ₂ , the error bar is standard deviation of 5 independent experiments per each concentration	175
Figure 6-6. Comparison between the measured resonant frequency-shift of the sensor, for different adsorbents at different concentrations of CO ₂ in dry He, the error bar is standard deviation of 5 independent experiments per each concentration.	176
Figure 6-7. CO ₂ volumetric adsorption of MOF-199 and Zeolite 13X samples, T=20°C.....	178
Figure A1. De-convoluted N1s spectra of (a) raw and (b) activated coke.....	237
Figure A2. N1s spectra of raw and activated coke, and (a) AC-DEA samples, (b) AC-MDEA samples, and (c) AC-TEPA samples.....	239
Figure B1. Carbon 1s electron spectra for (a) double side plasma treated CNT-BP with O ₂ /Ar for 7min, and (b) double side plasma treated CNT-BP with NH ₃ for 7 min	242

Figure B2. Raman spectrum of virgin CNT-BP, and single side plasma treated CNT-BP with O ₂ /Ar and NH ₃ for 3 min	243
Figure B3. SEM images of (a) virgin and (b) single side plasma treated CNT-BP with O ₂ /Ar for 15min	244
Figure B4. Gravimetric analysis of the Mg-MOF-74 decomposition for Mg-MOF-74 and MOF-CNT-BP (single side treated CNT-BP with O ₂ /Ar for 3 min, 20 h crystallization)	244

LIST OF ACRONYMS

AC	Activated Carbon
BET	Brunauer-Emmett-Teller
BP	Bucky paper
BTC	1, 2, 3-benzenetricarboxylate
CNT	Carbon nanotube
DAC	Data acquisition and control system
DEA	Diethanolamine
DMF	N,N-dimethylformamide
DFT	Density functional theory model
FTIR	Fourier Transform Infrared
GC-TCD	Gas chromatography-Thermal conductivity detector
GHG	Greenhouse gas
IPCC	Intergovernmental panel on climate change
MEA	Monoethanolamine
MDEA	Methyl-diethanolamine
MOFs	Metal Organic Frameworks
MW	Microwave irradiation
<i>P</i>	Pressure (kPa)
<i>q</i>	The adsorbed amount (mmol/g)
RH	Relative humidity
SEM	Scanning Electron Microscopy
<i>T</i>	Temperature (K)

t	Time in (s)
TEPA	Tetra-ethylene pentamine
TF	Tube Furnace
TGA	Thermal Gravimetric Analysis
TGA/DSC	Thermal Gravimetric Analyzer/ Differential Scanning Calorimetry
XRD	X-ray Diffraction

CHAPTER 1. INTRODUCTION AND RESEARCH OBJECTIVES

1.1. Background and Motivation

1.1.1. Climate change and CO₂ emission

Fossil fuel combustion for energy production is responsible for about 40% of global carbon dioxide (CO₂) emissions (Zhang et al., 2010). This is the leading contributor to global warming and associated climate change (Zhang et al., 2010). Flue gas released from fossil fuel combustion contains 10-12% CO₂ and is a concern to a number of industries (energy generation, space industry, military establishments, natural gas processing, etc.) (Littel et al., 1992, Koh et al., 1999, Veawab et al., 1999, Huang et al., 2002, Chang et al., 2003).

A promising method to reduce CO₂ emissions is CO₂ capture and sequestration (Xu et al., 2002). A number of technologies have been investigated for capturing CO₂ from flue gases, including cryogenic processes (Zanganeh et al., 2009), membrane separation, absorption, and adsorption (Zhang et al., 2010, Garcia et al., 2011, Ko et al., 2011, Khalil et al., 2012, Supasinee Pipatsantipong, 2012). Absorption with amines is the most established technique for controlling industrial CO₂ emissions (Supasinee Pipatsantipong, 2012). This technique, however, suffers from corrosion of pipes and surrounding equipment, and low aqueous phase amine concentrations (Franchi et al., 2005). To mitigate these deficiencies, liquid amines can be added to the surface of solid supports (Caballero et al., 1993, Leal et al., 1995, Satyapal et al., 2001, Birbara et al., 2002, Huang et al., 2002, Xu et al., 2002, Contarini et al., 2003, Nalette et al., 2004). These materials modify the fundamental CO₂ control mechanism by incorporating amines that are typically used for absorption into adsorbents, benefiting from the high CO₂ capacity of amines but limiting the disadvantages associated with liquid absorbents.

1.1.1. CO₂ capture via adsorption

Solid sorbents can be categorized as molecular sieves or zeolites, activated carbons (Saha and Deng, 2010), calcium oxides (Lee et al., 2008), hydrotalcites (Hutson et al., 2004), metal organic frameworks (MOF) (Walton et al., 2007) and amino-polymers (Li et al., 2008, Yang et al., 2010).

Activated carbon is widely used for adsorption applications. It is resistant to acidic and basic conditions, can have tailored physical and chemical properties, can be regenerable, is thermally stable, and is inexpensive (Bullin and Polasek, 1990, Aksoylu et al., 2001, Xiong et al., 2003, Gray et al., 2004, Gomes et al., 2008). Activated carbon is typically prepared from coals or lingo-cellulosic materials (Hasib-ur-Rahman et al., 2010) via carbonization and physical or chemical activation. Petroleum coke has also been used as an activated carbon precursor (Chang et al., 2000, Kawano et al., 2008), but few studies have used oil sands coke.

Activated carbon's surface chemistry impacts its adsorption properties (Ugarte and Swider-Lyons, 2005, Gauden and Wisniewski, 2007). The surface of activated carbon can be modified (Lee et al., 2013) by oxidation, heat treatment, and/or chemical treatment with acids, bases, or metals (Sun et al., 2007, Lee et al., 2013). To the best of our knowledge, however, systematic studies investigating carbon surface modifications using microwave heating and chemical treatments to directly improve CO₂ capture have not been reported.

MOFs are crystalline, porous materials that possess high surface area (up to 5000 m²/g) and void volume (55-90%) (D'Alessandro et al., 2010) with chemical functionalities that can be tailored by modifying the metal group or organic linker. Although MOFs have high capacity for acidic gases such as CO₂ at pressures > 50 bar, their performance at lower pressures is not

favorable (Liang et al., 2009). One promising method to boost their functionality at low pressures is to modify their structure by embedding these materials on a polymeric support.

1.1.2. Real-time monitoring of CO₂ concentration using microwave resonator sensor

As stated in section 1.1.1, adsorption is a promising method to capture and remove CO₂ from air. In order to make it more economical and environment friendly, the adsorbent will be regenerated after cycles of adsorption. Thus the recovery of adsorbent is a substantially important attribute of the process, where it will provide information about when to replace the adsorbent and manage the process economically. Detecting the concentration of target gas after adsorption in the off-gas stream can provide this information, which is viable through using highly sensitive gas sensors. Hence, it is of great interest to develop gas sensors to detect and monitor CO₂ levels in gas streams. Developing highly sensitive, selective, stable, and cost effective CO₂ sensors at room temperature is a challenge (Kreno et al., 2012). CO₂ sensors functioning at room temperature are highly applicable for indoor and outdoor air quality control, and air quality monitoring in mines (Stegmeier et al., 2009). A wide range of techniques for the measurement of gas concentration have been developed which work based on various operating principles, such as optical, resistive, or capacitive sensing. Despite their vast applications, optical sensors have some disadvantages for CO₂ sensing as they are bulky and expensive with high chances of interference from CO, since CO has similar absorption in the same IR range (Lübbbers and Opitz, 1975, Leiner 1991). On the other hand, resistive sensors which operate based on the change of the electronic resistance of a sensitive layer (mostly semiconducting metal oxide) upon interaction with a target gas (Wagner et al., 2013), suffer from electrical noise (Lübbbers and Opitz, 1975, Leiner, 1991, Wagner et al., 2013). Amongst all, capacitive sensors coupled with selective adsorbent materials such as zeolite or MOF count as a good candidate for CO₂ sensing

application (Wark et al., 2003, Wagner et al., 2013). In this work, microwave resonator sensor coupled with MOF material was used to monitor the concentration changes of CO₂ at room temperature via detecting changes in the permittivity of MOF.

1.2.Objectives

Significant researches have been dedicated to increase the CO₂ capture capacity. Traditional approaches such as aqueous ammonia-based absorption, or liquid amine absorption have a number of shortcomings prompting new approaches for alternative technologies for CO₂ separation from flue gas.

The overall objective of this work is to develop solid adsorbent materials which mitigate the problems associated with traditional methods (i.e. liquid amine absorption) and can provide high capacity for CO₂ at atmospheric pressure and lower temperatures comparing to other adsorbents such as zeolites (with adsorption temperatures >75°C) (Chatti et al., 2009). The specific objectives of research done are presented as follows:

1. To transform an underutilized waste material (oil sands coke) into an activated carbon that has high capacity for CO₂ adsorption. For this purpose, oil sands coke was activated using different activation agents and the adsorption capacity of synthesized samples was measured.
2. To enhance the adsorption capacity of activated carbon (derived from oil sands coke) using alkali amines. To this end, the effect of the following parameters on the CO₂ adsorption capacity of the amine-impregnated samples is investigated:
 - Activated carbon support pore size distribution
 - Amine loading (impregnation temperature and concentration)
 - CO₂ adsorption temperature

- Humidity
3. To develop a synthesis method for metal organic frameworks (MOFs) by incorporating the MOF crystals on the surface of carbon nanotube (CNT) membrane using plasma technology and to investigate their CO₂ adsorption capacities, whereby the impact of several parameters were investigated:
 - Plasma treatment time
 - Plasma side treatment
 - Plasma gas
 - MOF crystallization time
 4. To explore the potential for using MOF in sensor applications. Microwave resonator sensor coupled with MOF was used for this purpose. The performance of MOF-199 as CO₂ adsorbent was compared to zeolite 13x. Microwave resonator sensor monitors the variation in dielectric properties of the adsorbents.

1.3. Significance of the Research

Using delayed coke from oil sands as a precursor for activated carbon can transform a petroleum waste material into an effective CO₂ adsorbent and lower the GHG footprint of the oil sands. Modifying this prepared activated carbon with amines is expected to improve CO₂ uptake capacity further, potentially creating an industrially-viable adsorbent for CO₂ capture. On the other hand, structure modification of MOFs provides an opportunity to enhance their storage capacity at lower pressures. Since MOFs have diverse properties, the findings of this research can be used in several applications such as CO₂ capture and monitoring. The outcome of this investigation can be used in designing an effective gas detection system for monitoring traces of CO₂ in gas streams.

1.4. Thesis Organization

This thesis is written in an article-integrated format as specified by The Faculty of Graduate Study and Research (FGSR) at the University of Alberta. CHAPTER 1 provides a brief background and motivation of the work. Pertinent literature about carbon dioxide capture technologies is reviewed and explained in chapter CHAPTER 2. The literature review presents general information about CO₂ capture technologies such as amine-based absorption, membrane separation and adsorption materials such as activated carbons, MOFs, and zeolites.

Chapter 3 of this thesis describes the synthesis, characterization, and capture capacity measurement of activated carbons from oil sands coke, as well as amine-impregnated activated carbons. Chapter 4 investigated the CO₂ capture capacities of mesoporous activated carbons. In chapter 5, the synthesis of MOFs and MOF-CNTs, and their CO₂ adsorption behavior were experimentally studied at room temperature and pressure. Chapter 6 discusses a new potential of MOF materials for CO₂ sensing using microwave resonator sensor. Chapter 7 presents the general conclusions from this study based on the experimental results, and the carried out analyses. Major findings are summarized, followed by recommendations for future work.

1.5. References

- Aksoylu, A. E., Madalena M., Freitas A., Pereira M. F. R., and Figueiredo J. L. (2001). The effects of different activated carbon supports and support modifications on the properties of Pt/AC catalysts. *Carbon* **39**(2): 175-185.
- Birbara, P. J., Filburn T. P., Michels H. and Nalette T. A. (2002). Sorbent system and method for absorbing carbon dioxide from the atmosphere of a closed habitable environment. *U. S. Patent. US6364938 B1*

- Bullin J. A. and Polasek J. C. (1990). The use of MDEA and mixtures of amines for bulk CO₂ removal. *Sixty-Ninth GPA Annual Convention*, Lakewood, Colorado
- Caballero, A., Dexpert H., Didillon B., LePeltier F., Clause O., and Lynch J. (1993). In situ x-ray absorption spectroscopic study of a highly dispersed platinum-tin/alumina catalyst. *The Journal of Physical Chemistry* **97**(43): 11283-11285.
- Chang, A. C. C., Chuang S. S. C., Gray M., and Soong Y. (2003). In-Situ Infrared Study of CO₂ Adsorption on SBA-15 Grafted with Y-(Aminopropyl)triethoxysilane. *Energy & Fuels* **17**(2): 468-473.
- Chang, C.F., Chang C.Y., and Tsai W.T. (2000). Effects of Burn-off and Activation Temperature on Preparation of Activated Carbon from Corn Cob Agrowaste by CO₂ and Steam. *Journal of Colloid and Interface Science* **232**(1): 45-49.
- Chatti, R., Bansiwala A. K., Thote J. A., Kumar V., Jadhav P., Lokhande S. K., Biniwale R. B., Labhsetwar N. K., and Rayalu S. S. (2009). Amine loaded zeolites for carbon dioxide capture: Amine loading and adsorption studies. *Microporous and Mesoporous Materials* **121**(1-3): 84-89.
- Contarini, S., Barbini M., Del Piero G., Gambarotta E., Mazzamurro G., Riocci M., Zappelli P., Gale J., and Kaya Y. (2003). Solid Sorbents for the Reversible Capture of Carbon Dioxide. *Greenhouse Gas Control Technologies - 6th International Conference*. Oxford, Pergamon: 169-174.
- D'Alessandro, D. M., Smit B., and Long J. R. (2010). Carbon Dioxide Capture: Prospects for New Materials. *Angewandte Chemie International Edition* **49**(35): 6058-6082.

- Franchi, R. S., Harlick P. J. E., and Sayari A. (2005). Applications of Pore-Expanded Mesoporous Silica. 2. Development of a High-Capacity, Water-Tolerant Adsorbent for CO₂. *Industrial & Engineering Chemistry Research* **44**(21): 8007-8013.
- Garcia, S., Gil M. V., Martin C. F., Pis J. J., Rubiera F., and Pevida C. (2011). Breakthrough adsorption study of a commercial activated carbon for pre-combustion CO₂ capture. *Chemical Engineering Journal* **171**(2): 549-556.
- Gauden, P. A. and Wisniewski M. (2007). CO₂ sorption on substituted carbon materials: Computational chemistry studies. *Applied Surface Science* **253**(13): 5726-5731.
- Gomes, H. T., Machado B. F., Ribeiro A., Moreira I., Rosario M. R., Silva A.M.T., Figueiredo J. L., and Faria J. L. (2008). Catalytic properties of carbon materials for wet oxidation of aniline. *Journal of Hazardous Materials* **159**(2-3): 420-426.
- Gray, M. L., Soong Y., Champagne K. J., Baltrus J., Stevens Jr R. W., Toochinda P., and Chuang S. S. C. (2004). CO₂ capture by amine-enriched fly ash carbon sorbents. *Separation and Purification Technology* **35**(1): 31-36.
- Hasib-ur-Rahman, M., Sijaj M., and Larachi F. (2010). Ionic liquids for CO₂ capture: Development and progress. *Chemical Engineering and Processing: Process Intensification* **49**(4): 313-322.
- Huang, H. Y., Yang R. T., Chinn D. , and Munson C. L. (2002). Amine-Grafted MCM-48 and Silica Xerogel as Superior Sorbents for Acidic Gas Removal from Natural Gas. *Industrial & Engineering Chemistry Research* **42**(12): 2427-2433.
- Hutson, N. D., Speakman S. A., and Payzant E. A. (2004). Structural Effects on the High Temperature Adsorption of CO₂ on a Synthetic Hydrotalcite. *Chemistry of Materials* **16**(21): 4135-4143.

- Kawano, T., Kubota M., Onyango M. S., Watanabe F., and Matsuda H. (2008). Preparation of activated carbon from petroleum coke by KOH chemical activation for adsorption heat pump. *Applied Thermal Engineering* **28**(8–9): 865-871.
- Khalil, S. H., Aroua M. K., and Daud W. M. A. W. (2012). Study on the improvement of the capacity of amine-impregnated commercial activated carbon beds for CO₂ adsorbing. *Chemical Engineering Journal* **183**(0): 15-20.
- Ko, Y. G., Shin S. S. , and Choi U. S. (2011). Primary, secondary, and tertiary amines for CO₂ capture: Designing for mesoporous CO₂ adsorbents. *Journal of Colloid and Interface Science* **361**(2): 594-602.
- Koh, C. A., Montanari T., Nooney R. I., Tahir S. F. , and Westacott R. E. (1999). Experimental and Computer Simulation Studies of the Removal of Carbon Dioxide from Mixtures with Methane Using AlPO₄-5 and MCM-41. *Langmuir* **15**(18): 6043-6049.
- Kreno, L. E., Leong K., Farha O. K., Allendorf M., Van Duyne R. P., and Hupp J. T. (2012). Metal–Organic Framework Materials as Chemical Sensors. *Chemical Reviews* **112**(2): 1105-1125.
- Leal, O., Bolivar C., Ovalles C. S., Garcia J. J., and Espidel Y. (1995). Reversible adsorption of carbon dioxide on amine surface-bonded silica gel. *Inorganica Chimica Acta* **240**(1-2): 183-189.
- Lee, C. S., Ong Y. L., Aroua M. K., and Daud W. M. A. W. (2013). Impregnation of palm shell-based activated carbon with sterically hindered amines for CO₂ adsorption. *Chemical Engineering Journal* **219**(0): 558-564.

- Lee, S. C., Chae H. J., Lee S. J., Choi B. Y., Yi C. K., Lee J. B., Ryu C. K., and Kim J. C. (2008). Development of Regenerable MgO-Based Sorbent Promoted with K_2CO_3 for CO_2 Capture at Low Temperatures. *Environmental Science & Technology* **42**(8): 2736-2741.
- Leiner, M. J. P. (1991). Luminescence chemical sensors for biomedical applications: scope and limitations. *Analytica Chimica Acta* **255**(2): 209-222.
- Li, P., Ge B., Zhang S., Chen S., Zhang Q., and Zhao Y. (2008). CO_2 Capture by Polyethylenimine-Modified Fibrous Adsorbent. *Langmuir* **24**(13): 6567-6574.
- Liang, Z., Marshall M., and Chaffee A. L. (2009). CO_2 Adsorption-Based Separation by Metal Organic Framework (Cu-BTC) versus Zeolite (13X). *Energy & Fuels* **23**(5): 2785-2789.
- Littel, R. J., Versteeg G. F., and Van Swaaij W. P. M. (1992). Kinetics of CO_2 with primary and secondary amines in aqueous solutions II. Influence of temperature on zwitterion formation and deprotonation rates. *Chemical Engineering Science* **47**(8): 2037-2045.
- Lübbbers, D. W. and Opitz N. (1975). The pCO_2 -/ pO_2 -optode: a new probe for measurement of pCO_2 or pO_2 in fluids and gases (authors transl). *Zeitschrift für Naturforschung. Section C: Biosciences* **30**(4): 532-533.
- Nalette, T. A., Papale W., and Filburn T. P. (2004). Carbon dioxide scrubber for fuel and gas emissions. U. S. Patent. **6755892**.
- Saha, D. and Deng S. (2010). Adsorption equilibrium and kinetics of CO_2 , CH_4 , N_2O , and NH_3 on ordered mesoporous carbon. *Journal of Colloid and Interface Science* **345**(2): 402-409.
- Satyapal, S., Filburn T., Trela J., and Strange J. (2001). Performance and Properties of a Solid Amine Sorbent for Carbon Dioxide Removal in Space Life Support Applications. *Energy & Fuels* **15**(2): 250-255.

- Stegmeier, S., Fleischer M., Tawil A., Hauptmann P., Egly K., and Rose K. (2009). Mechanism of the interaction of CO₂ and humidity with primary amino group systems for room temperature CO₂ sensors. *Procedia Chemistry* **1**(1): 236-239.
- Sun, Y., Wang Y., Zhang Y., Zhou Y., and Zhou L. (2007). CO₂ sorption in activated carbon in the presence of water. *Chemical Physics Letters* **437**(1-3): 14-16.
- Supasinee Pipatsantipong, P. R., Santi Kulprathipanja (2012). Towards CO₂ adsorption enhancement via polyethyleneimine impregnation. *International Journal of Chemical and Biological Engineering* **6**: 291-295.
- Ugarte, N.P. and Swider-Lyons K. E. (2005). Low-Platinum tin-oxide electrocatalysts for PEM fuel cell cathodes. *Proton Conducting Membrane Fuel Cells III*. M. Murthy and T. F. Fuller: 67-73.
- Veawab, A., Tontiwachwuthikul P. , and Chakma A. (1999). Corrosion Behavior of Carbon Steel in the CO₂ Absorption Process Using Aqueous Amine Solutions. *Industrial & Engineering Chemistry Research* **38**(10): 3917-3924.
- Wagner, T., Haffer S., Weinberger C., Klaus D., and Tiemann M. (2013). Mesoporous materials as gas sensors. *Chemical Society Reviews* **42**(9): 4036-4053.
- Walton, K. S., Millward A. R., Dubbeldam D., Frost H., Low J. J., Yaghi O. M., and Snurr R. Q. (2007). Understanding Inflections and Steps in Carbon Dioxide Adsorption Isotherms in Metal-Organic Frameworks. *Journal of the American Chemical Society* **130**(2): 406-407.
- Wark, M., Rohlfing Y., Altindag Y., and Wellmann H. (2003). Optical gas sensing by semiconductor nanoparticles or organic dye molecules hosted in the pores of mesoporous siliceous MCM-41. *Physical Chemistry Chemical Physics* **5**(23): 5188-5194.

- Xiong, R., Ida J. , and Lin Y. S. (2003). Kinetics of carbon dioxide sorption on potassium-doped lithium zirconate. *Chemical Engineering Science* **58**(19): 4377-4385.
- Xu, X., Song C., Andresen J. M., Miller B. G., and Scaroni A. W. (2002). Novel Polyethylenimine-Modified Mesoporous Molecular Sieve of MCM-41 Type as High-Capacity Adsorbent for CO₂ Capture. *Energy & Fuels* **16**(6): 1463-1469.
- Yang, Y., Li H., Chen S., Zhao Y., and Li Q. (2010). Preparation and Characterization of a Solid Amine Adsorbent for Capturing CO₂ by Grafting Allylamine onto PAN Fiber. *Langmuir* **26**(17): 13897-13902.
- Zanganeh, K. E., Shafeen A., and Salvador C. (2009). CO₂ Capture and Development of an Advanced Pilot-Scale Cryogenic Separation and Compression Unit. *Energy Procedia* **1**(1): 247-252.
- Zhang, Z., Xu M., Wang H., and Li Z. (2010). Enhancement of CO₂ adsorption on high surface area activated carbon modified by N₂, H₂ and ammonia. *Chemical Engineering Journal* **160**(2): 571-577.

CHAPTER 2. LITERATURE REVIEW

2.1. CO₂ Capture Methods

Since the industrial revolution, the amount of carbon dioxide emission has risen by more than a third from 280 parts per million (ppm) by volume to 368 ppm in 2000, and 388 ppm in 2010 (Rackley, 2010). Based on Intergovernmental Panel on Climate Change (IPCC) (IPCC, 2001), the rise in carbon dioxide emission may result in an increase in CO₂ level in the atmosphere up to 570 ppm in 2100 causing an approximate raise of 1.9°C in the mean global temperature.

Several approaches have been investigated to reduce the total carbon dioxide emission into the atmosphere including reduction of carbon intensity by using alternative to fossil fuels such as hydrogen and renewable energies, reduction in energy intensity by the efficient use of energy, and carbon capture and sequestration from point source emissions such as power plants (Yang et al., 2008).

A promising method to reduce CO₂ emissions is CO₂ capture and sequestration (Xu et al., 2002) as other alternatives to fossil fuels such as hydrogen, biomass, and solar energy are still under development and are not commercially viable. The main approaches to reduce the carbon dioxide emission from power generation plants can be categorized as: 1) pre-combustion capture through de-carbonation of the fuel prior to combustion, 2) oxy-fuel combustion by changing the combustion process to produce carbon dioxide as a pure combustion product and 3) post-combustion capture which is based on carbon dioxide separation from combustion product (Rackley, 2010). Figure 2-1 illustrates these approaches.

2.1.1. Pre-combustion Capture

In pre-combustion capture, the fuel (coal or biomass) is de-carbonized by gasification, in which it reacts with oxygen or air to produce carbon monoxide and hydrogen. Comparing to post-combustion capture, carbon dioxide concentration and partial pressure would be higher which simplifies the carbon dioxide capture process, and is counted as an advantage of this method compared to post-combustion capture. On the other hand, the generating facility increases the total capital costs (Olajire, 2010).

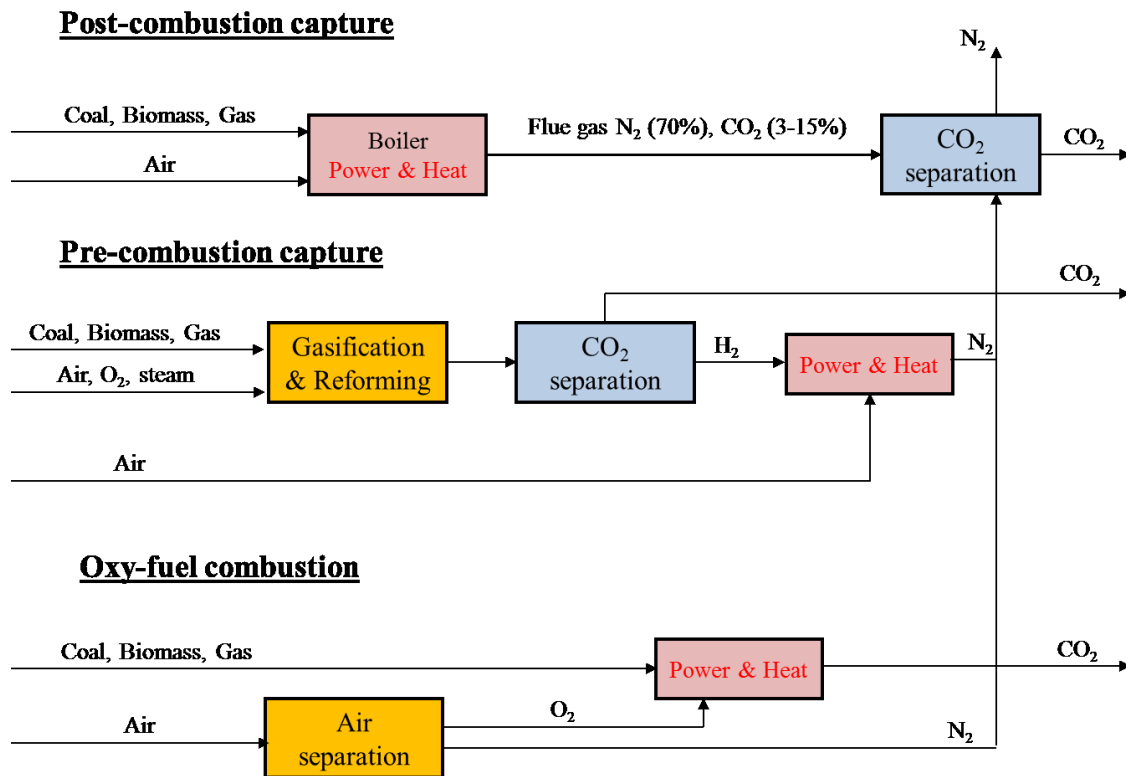


Figure 2-1. CO_2 capture from power generation plant (Olajire, 2010)

2.1.2. Oxy-fuel Combustion

In Oxy-fuel technique, the flue gas combustion occurs in oxygen rather than air, increasing carbon dioxide concentration in the product compared to post-combustion method. The carbon dioxide concentration reaches to almost 80% (Figueroa et al., 2008) which facilitates

its separation and purification techniques, but the need for large quantities of oxygen and air separation section raise the capital cost and energy consumption.

2.1.3. Post-combustion Capture

The last technique is post-combustion capture in which carbon dioxide is removed from the flue gas before emission to the atmosphere. Low partial pressure of carbon dioxide in the flue gas (Olajire, 2010) and relatively high temperature of the flue gas depending on the type of fuel (e.g., 120 and 180°C for black and brown coal, respectively (CSIRO, 2008)) make carbon dioxide separation more challenging. Although low concentration carbon dioxide in the flue gas highlights the need for strong chemical sorbents, post-combustion capture is still a promising technique due to its adaption to existing units (Figuerola et al., 2008).

A number of technologies have been applied for post combustion capture of CO₂ from flue gases, including cryogenic processes (Zanganeh et al., 2009), membrane separation, absorption, and adsorption (Zhang et al., 2010, Garcia et al., 2011, Ko et al., 2011, Khalil et al., 2012, Pipatsantipong et al., 2012). The following paragraphs mainly discuss post-combustion capture technologies from fossil fuel power plants which can be categorized as conventional technologies such as amine-based absorption, membrane separation and new emerging technologies such as adsorption using porous materials like activated carbon and metal organic frameworks.

2.1.3.1. Amine-based Absorption

Absorption is the most established technique for controlling industrial CO₂ emissions (Pipatsantipong et al., 2012) and involves an exothermic reaction of a sorbent (typically amine or carbonate solution) with carbon dioxide in the gas stream (Rackley, 2010) and occurs at large scale amine absorbers (scrubbers). There are three types of amines used in this process including primary, secondary and tertiary amines. Primary amines have higher reaction rate with carbon

dioxide while secondary amines and tertiary amines require lower regeneration energy due to weak interaction with carbon dioxide (Figuerola et al., 2008). Amine-based carbon dioxide separation from flue gas is illustrated in Figure 2-2. The scrubber contains 25-30% aqueous amine (normally monoethanolamine, MEA) solution at high pressure (60-70 atm) and the flue gas enters to packed absorber column at atmospheric pressure and temperature around 50°C (Freguia and Rochelle, 2003). The amine reaction with carbon dioxide results in the formation of carbamate species. After carbon dioxide separation, water washed flue gas is released from the top of the absorber whereas the rich solvent (contains high amount of carbon dioxide) passes through a stripper working at high temperature (100-140°C) (D'Alessandro and McDonald, 2010) and pressure (1-10 bar) (CSIRO, 2008) to release carbon dioxide in high purity (over 99%) which may be compressed for further applications such as long-term storage for deep geological formation like saline aquifers or depleted oil/gas fields (D'Alessandro and McDonald, 2010).

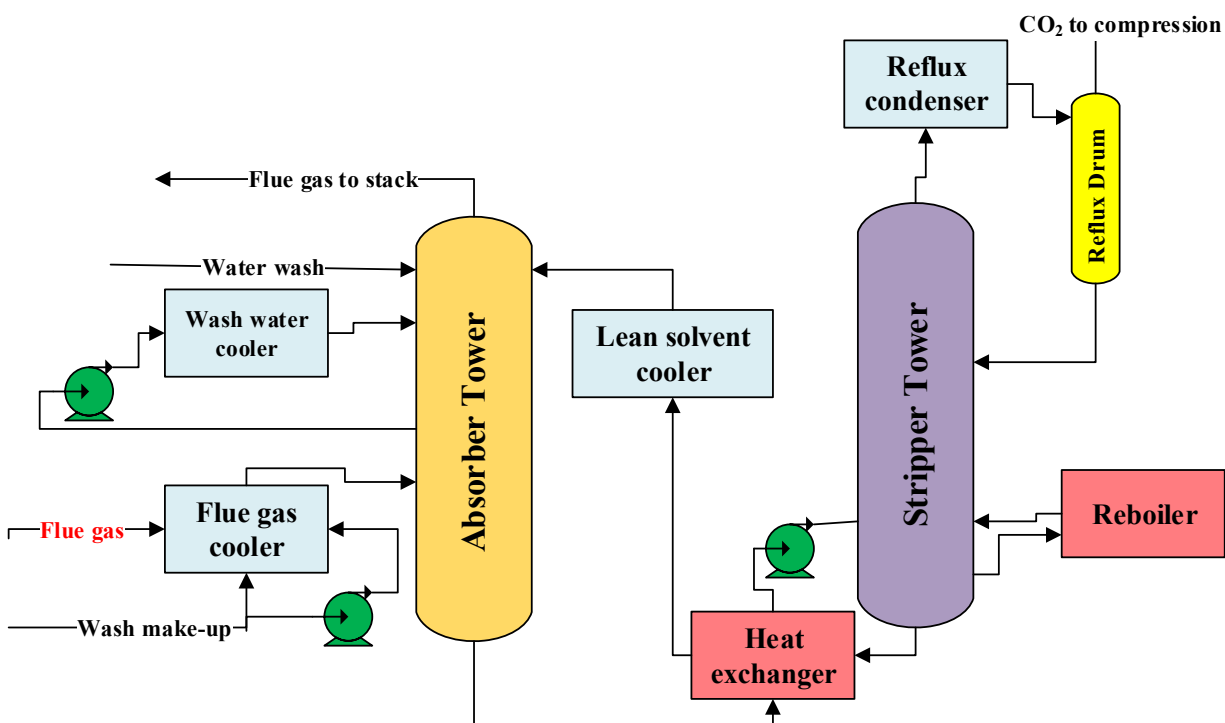


Figure 2-2. Process flow diagram for amine-based CO₂ capture (CSIRO, 2008)

This technique, however, suffers from degradation of amines in the presence of oxygen, SO₂, NO₂ and HCl which requires additional solvent recovery and waste disposal (Rackley, 2010), corrosion of pipes and surrounding equipment, low aqueous phase amine concentrations (Franchi et al., 2005), and high energy consumption causing electricity costs to increase by 35 – 85% (R. Veneman et al., 2013).

2.1.3.2. Membrane Separation

Membrane technology for gas separation has been widely applied in many industrial separation processes. Membranes separate components of a mixture based on different driving forces such as pressure difference, concentration difference and electrical potential difference between the feed and the permeate phases (Matsuura, 2009). Different separation mechanisms have been investigated so far including: 1) solution/diffusion, 2) adsorption/diffusion, and 3) molecular sieve and ionic transport (Olajire, 2010). When flue gas passes through the membrane, CO₂ separation occurs based on one of the followings: partial pressure difference of CO₂ between feed and permeate, or a reversible chemical reaction with porous inorganic materials such as zeolites, ceramic and metal organic frameworks (Shackley and Gough, 2006). In conventional dense membranes, solubility difference of gas molecules into membrane material serves as a driving force for separation. However, it (i.e. solubility difference) creates a trade-off between selectivity (separation quality) and permeability (energy consumption); selectivity requires thicker membrane, whereas the permeation resistance would increase with membrane thickness (Lu, 2012). While pure polymer membrane strategy presents limitations related to permeability-selectivity trade-off behavior (Robeson, 1991, Robeson, 2008, Lin et al., 2016), a new class of membranes or inorganic membranes (such as metal organic frameworks) offer significant separation, stability and selectivity.

2.1.3.3. *Adsorption via solid sorbents*

Adsorption of CO₂ requires relatively low energy consumption, is cost-effective, and can operate over a wide range of temperatures and pressures (Xu et al., 2005). Adsorbents can be regenerated, allowing for their reuse in cyclic adsorption/desorption systems. Ideally, a regenerated adsorbent will have the same capacity, selectivity, and adsorption kinetics as the initial material (Plaza et al., 2009). Based on the adsorbent-adsorbate interaction, the adsorption can be categorized in two groups: chemical adsorption (chemisorption) and physisorption. In chemisorption, the adsorbate and adsorbent are united by covalent bonds. Surface functional groups on the adsorbent may encourage chemisorption by providing sites for bond formation (Mattson et al., 1969, De Jonge et al., 1996). In physical adsorption, or physisorption, the adsorbate and adsorbent are linked by weaker van der Waals' interactions. Hence, the heat of adsorption associated with chemisorption is higher than for physisorption. Irreversible adsorption is associated with chemisorption or strong physisorption because the interactions are stronger and more difficult to reverse (Mattson et al., 1969).

2.2. **Adsorption Materials**

As discussed in section 2.1.3.1. and 2.1.3.2. , recent carbon capture technologies have some drawbacks that impede them to meet the requirements set by U.S. Department of Energy's National Energy Technology Laboratory (DOE/NETL) which aims to reach 90% CO₂ capture at less than 35% increase in the cost of electricity (COE) (Fout and Jones, 2009). Hence, alternative approaches are required that offer higher CO₂ capture efficiency at low operational cost. Solid adsorbents provide variety of adsorption processes including pressure, vacuum or temperature swing adsorption cycles, while circumventing major problem associated with absorption with liquid amines that is corrosion. Solid adsorbents also provide the possibility to take advantage of multiple regeneration options including isothermal regeneration under vacuum, and regeneration

by a desorbent which can reduce energy consumption (Pirngruber et al., 2009). Many solid adsorbent materials have been proposed for adsorption processes such as activated carbon, zeolites and metal organic frameworks (MOFs) which based on their working temperature can be categorized to low, medium and high temperature adsorbents as illustrated in Figure 2-3.

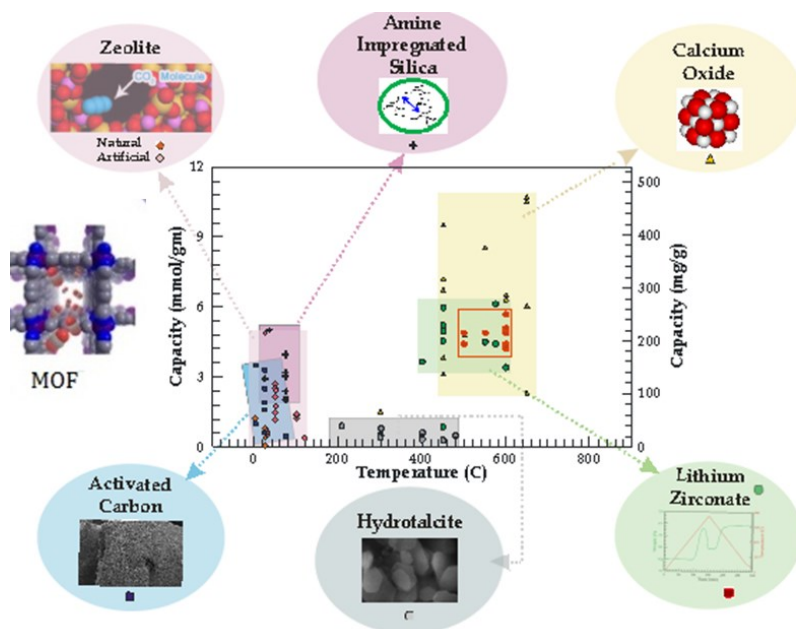


Figure 2-3 Solid adsorbents for CO₂ capture

In order to compete with conventional technologies for CO₂ capture from flue gas, these materials need to fulfill the following requirements: 1) high adsorption capacity (at least 2-4 mmol CO₂/g) at low pressure (Ho et al., 2008) to reduce the amount of adsorbent, 2) high selectivity for CO₂: which is defined as the ratio of CO₂ capture capacity to other bulk gas components (mainly N₂ and O₂), and determines the purity of CO₂ captured to meet the purity requirement and separation process costs (Pirngruber et al., 2009), 3) fast adsorption/desorption kinetic to allow high gas velocity in fixed bed adsorption column and short adsorption/desorption cycle time, 4) moderate heat of adsorption to speed up the regeneration process, 5) high water stability, since flue gases inherently contain water (5-7% by volume) (Keskin et al., 2010 ,

Granite and Pennline, 2002), 6) high mechanical stability to preserve the microstructure of adsorbent under severe operational conditions such as high temperature or flue gas flow rate, and finally 7) low operating costs including separation, adsorbent regeneration, and cost of raw adsorbent. According to a sensitivity analysis performed by Tarka et al. (2006), the baseline cost for an economic sorbent should be \$10/kg of sorbent. The main adsorption mechanisms using solid adsorbents are: 1) kinetic effect where the components in gas mixture have different diffusion rates, 2) molecular sieve effect where the separation is based on difference in size/shape of certain components, and 3) thermodynamic effect which is based on adsorbate-adsorbent interaction (Li et al., 2009).

2.2.1. Activated Carbon

To mitigate the deficiencies associated with conventional liquid amine absorption method, research is underway to develop porous supports impregnated with liquid amines that can be used for CO₂ control. These materials modify the fundamental CO₂ control mechanism, benefiting from the high CO₂ capacity of amines but limiting the negatives associated with liquid absorbents. One of the most commonly investigated porous supports is activated carbon that can be obtained from variety of carbon- containing materials such as sugar cane, sunflower seeds (Liou, 2010), industrial by-products (e.g. petroleum coke pitch (Small et al., 2012)), and biomass materials such as wood sawdust (Foo and Hameed, 2012) and coconut shell (Hu and Srinivasan, 2001), which makes activated carbon a favorable adsorbent in terms of low cost raw material. Oil sands coke can be used as a precursor for activated carbon due to its low cost and high carbon content (Chen and Hashisho, 2012). Moreover, activated carbon has a wide range of surface characteristics such as pore size distribution, pore structure, and active surface area due to the variety of its raw material (Choi et al., 2009). The activated carbon production process

from its raw materials includes carbonization and activation as described in the following section.

2.2.1.1. Carbonization

Carbonization is a crucial step because at this stage, the micropore structure starts to form. During carbonization, the precursor is heated (between 500-1200°C) in an inert atmosphere to isolate char (Davini, 2002) that has poor surface properties (Bandosz, 2006). The char has only incipient porous structure which is not accessible and needs to be upgraded or activated. Non-carbon elements such as H₂O, and H₂ are released during this step, increasing the relative carbon content of the isolated char (Choi et al., 2009).

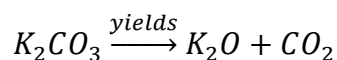
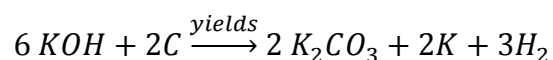
2.2.1.2. Activation

Thermal activation partially oxidizes the char with steam, carbon dioxide or air, during which carbon atoms react with gas, resulting in some mass removal. Activation adds pores to the char, increasing the surface area and pore volume of the carbonaceous material (Davini, 2002). The pore sizes can be classified into three major groups that correspond to micropores (less than 2 nm), mesopores (between 2 and 50 nm), and macropores (larger than 50 nm).

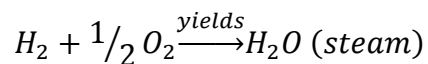
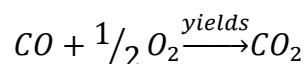
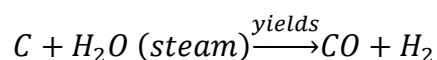
2.2.1.3. Physical and Chemical Activation

Physical activation of oil sands coke has been investigated using steam and/or CO₂ for partial gasification of chars at high temperatures (800 – 1000°C) (Di-Panfilo and Egiebor, 1996, Shawwa et al., 2001, Bandosz, 2006, Marsh and Rodriguez-Reinoso, 2006, Stavropoulos and Zabaniotou, 2009, Small et al., 2012). This process takes 1 – 6 h of heating and results in activated carbon with low surface area and pore volume (319 m²/g and 0.244 cm³/g) (Di-Panfilo and Egiebor, 1996) and low methylene blue adsorption capacity (100.5 mg/g) (Shawwa et al., 2001). Chemical activation requires less activation time to produce high surface area (1100 – 1200 m²/g) material (Bandosz, 2006, Marsh and Rodriguez-Reinoso, 2006). In this process, chemicals such as KOH, H₃PO₄ or ZnCl₂ open the micropores, leading to a well-developed

carbon structure (Ahmadpour and Do, 1996). For example, during activation with KOH, KOH reacts with the carbon skeleton, producing solid and gaseous products. At the same time carbon burn-off occurs resulting in porosity development. Experimental evidence shows that hydrogen and metallic potassium are formed during the reaction, as well as CO and CO₂ (which come from the carbon skeleton) and potassium oxide (Bandosz, 2006):



The following reactions are assumed to occur during physical activation (Bandosz, 2006):



Generally, chemical activation is performed at lower temperatures than physical activation (Ahmadpour and Do, 1996, Macia-Agullo et al., 2004).

2.2.1.4. Microwave activation

Recently, microwave activation has drawn attention due to its high energy efficiency, high heating rates, volumetric heating from inside to outside, and selective heating (Chen and Hashisho, 2012). The mechanism of microwave heating is based on the absorption of microwaves by a dielectric material, whereby the electromagnetic energy is converted into thermal energy or heat. Dielectric materials contain polar molecules. These molecules generally have a random orientation. In a microwave field, the polarity alternates very rapidly, changing the rotation of molecules which leads to friction with the surrounding medium, and heat is

generated. The ability of a material to convert absorbed energy into heat is characterized by its “dielectric loss factor” (Cherbański and Molga, 2009). Microwave heating is effective for materials with a high dielectric loss factor and permittivity, including carbonaceous materials (Chung, 2001). Chen et al. (Chen and Hashisho, 2012) applied microwave heating with steam for activating oil sands coke, finding that the method removes sulfur from and introduces oxygen to the surface and bulk of the cokes while increasing specific surface area and pore volume.

2.2.1.5. Effect of temperature on CO₂ adsorption of activated carbon

At room temperature (25°C) and atmospheric pressure, activated carbon (AC) adsorbs 110 mg CO₂ / g AC (Kamarudin and Mat, 2009). Because adsorption is exothermic, capacity decreases with increasing temperature (Pipatsantipong et al., 2012). Many industrial separations require high temperatures (up to 400°C) – it is not practical to install large scale heat exchangers in most processes – so it is beneficial to prepare CO₂ adsorbents with high capacity and selectivity at high temperatures.

2.2.1.6. Effect of pressure on CO₂ adsorption of activated carbon

Typically, CO₂ adsorption capacity on microporous ACs is lower than on mesoporous zeolites or molecular sieves at low pressures (< 1.7 bar) and ambient temperature (Chue et al., 1995). However, for a Pressure Swing Adsorption (PSA) process, at higher pressures, activated carbons surpass zeolites in terms of CO₂ uptake due to micropore filling (Siriwardane et al., 2001). This may be attributed to higher carbon surface areas compared to zeolites (897 vs. 506 m²/g for AC and zeolite 13X, respectively). Although, zeolites have higher CO₂ capacity per unit of specific surface area, and their surface affinity for CO₂ may be superior to carbon, because of the shape of equilibrium isotherm for AC, it can perform better than zeolite 13X at elevated pressures (Kumar, 1989, Siriwardane et al., 2001).

2.2.2. Amine Impregnated Activated Carbons

Preparation of activated carbon with basic surface properties can improve adsorption of acid gas (Lee et al., 2013, Sun et al., 2007). To make carbon basic, acidic oxygen functional groups can be removed with heat treatment ($> 700^{\circ}\text{C}$) in an inert atmosphere, or by adding basic surface groups, including amines (Menendez et al., 1996). Addition of functional groups can be achieved by impregnation or high temperature chemical treatments (Plaza et al., 2007, Pevida et al., 2008).

Ammonia treatment of carbon between 400 and 900°C will replace oxygen groups with amines (Krishnankutty and Vannice, 1995). This method is simple, low cost, and has the ability to load large amounts of amine (by increasing their basicity from 0 to 8.6 wt% on activated carbon) (Mahurin et al., 2011), but is not a sustainable method due to safety concerns, corrosiveness, and difficulties transporting and storing NH_3 (Davies, 2006). Wet impregnation is an alternative technique where the carbon is immersed in a solution containing the desired additives. The solution diffuses into carbon's pores based on a concentration gradient driving force and then the solvent is removed by evaporation or filtration (Morbidelli et al., 2001, Xu et al., 2002). Both impregnation techniques can alter the physical properties of the adsorbent by blocking narrow pores due to pore filling with the impregnant (Lee et al., 2013, Wei et al., 2010, Xu et al., 2002, Maroto-Valer et al., 2005, Jadhav et al., 2007, Khalil et al., 2012).

2.2.2.1. Amine selection

Alkanoamines have hydroxyl groups in their structure, decreasing their vapor pressure and reducing product losses during regeneration (Tontiwachwuthikul et al., 2011). Hydroxyl groups also increase the amine's solubility in aqueous solutions while the amino group provides the required alkalinity to adsorb CO_2 (Tontiwachwuthikul et al., 2011). Alkanoamines can be categorized into three groups (Wong and Bioletti, 2002):

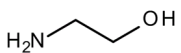
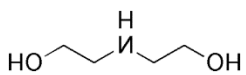
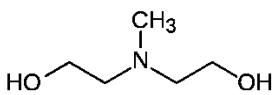
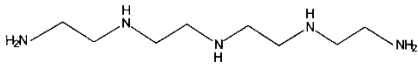
Primary amines (e.g., monoethanol amine (MEA), diglycolamine (DGA))

Secondary amines (e.g., diethanolamine (DEA), di-isopropylamine (DIPA))

Tertiary amines (e.g., triethanolamine (TEA), methyl-diethanolamine (MDEA))

Traditionally, MEA is used for CO₂ absorption because it has the lowest molecular weight and the highest theoretical CO₂ absorption capacity (0.4 kg of CO₂ per kg of sorbent (Rivera-Tinoco and Bouallou, 2010)). This theoretical capacity, however, has not been achieved in practice due to corrosion problem (Veawab et al., 2008). DEA is also commonly used because it has a lower vapor pressure than MEA and is less susceptible to volatilization (Kamarudin and Mat, 2009). Also, the chemistry of DEA-CO₂ benefits from moisture, which is found in most CO₂-containing mixtures (Franchi et al., 2005). Secondary amines also have lower heat of reaction with CO₂ than primary amines (360 cal/g vs. 455 cal/g), resulting in lower regeneration temperatures (Wong and Bioletti, 2002). Tertiary amines benefit from an even lower heat requirement (320 Cal/g for MDEA vs 455 Cal/g for MEA) for CO₂ liberation from spent solvents. Tertiary amines also have lower tendency for degradation products than primary and secondary amines, lower corrosion rates, and an easier regeneration process; however, because they react with CO₂ slowly, they require more liquid circulation to remove CO₂ (Wong and Bioletti, 2002). A list of common amines used for amine impregnation method is listed in Table 2-1.

Table 2-1 Physical properties of conventional amines (National Center for Biotechnology Information (a, b, c, d), 2017)

Amine name	Formula	Structure	Molecular weight (g/mol)	Density (g/cc)	Boiling point (°C)
MEA	C ₂ H ₇ NO		61.08	1.01	171
DEA	C ₄ H ₁₁ NO ₂		105.14	1.09	280
MDEA	C ₅ H ₁₃ NO ₂		119.16	1.08	247
TEPA*	C ₈ H ₂₃ N ₅		189.3	0.99	190-240

*Tetra ethylene pentamine

2.2.2.2. Amine interaction with CO₂

Activated carbon functionalized with amines can chemically or physically adsorb CO₂. Alkanoamines remove CO₂ via exothermic reactions between CO₂ and the impregnated amine group (Wong and Bioletti, 2002). The interaction of CO₂ with amines has been explained by several mechanisms (Lee et al., 2013, Satyapal et al., 2001, Zelenak et al., 2008). Primary and secondary amines directly react with CO₂ to produce carbamate through the formation of zwitterions. In the first step, the ion pair of the amine attacks the carbon atom from CO₂ to form a zwitterion. Then, carbamate is formed via de-protonation of the zwitterion by a free base provided by the amine molecule, H₂O, or OH (Sartori and Savage, 1983). Tertiary amines react with CO₂ differently. Instead of a direct reaction with CO₂, they catalyze the formation of bicarbonate. This mechanism, which involves base-catalyzed hydration of CO₂, was first reported by Donaldson (Donaldson and Nguyen, 1980).

2.2.3. MOFs

MOFs are crystalline materials with structures based on coordination bonds formed between metal cations as nodes (e.g. Al^{3+} , Cr^{3+} , Mg^{2+} , Cu^{2+} , or Zn^{2+}) and electron donors as linking groups, such as amines or carboxylates. The rigid pore structure of MOFs results from the self-assembly of these components, typically in solution, which do not collapse upon solvent removal or when “guest” molecules occupy the pores. The topology of MOFs depends on the metal ion coordination and the geometry of the organic linker groups, called secondary building units (SBUs), which control the network symmetry (Tranchemontagne et al., 2009). MOFs are applied in adsorption applications because they have high surface area (up to $5000 \text{ cm}^2/\text{g}$), and can have tailored pore size distributions, allowing for increased adsorption capacity and improved adsorption kinetics. Other beneficial properties of MOFs include charge transfer capabilities (ligand to metal or metal to ligand), high thermal stability, and electronic properties (Eddaoudi et al., 2001).

2.2.3.1. MOF Synthesis

Typical MOF synthesis follows the solvothermal method of heating a mixture of a metal salt and an organic acid in a solvent for 12 – 48 h. This method yields high purity, and structured crystals, although it requires long reaction times (Mueller et al., 2006). It was found that for some protocols, heat can be replaced by other stimulus such as ultrasound (Suslick et al., 1986), and microwave (Klinowski et al., 2011). Methods other than solvothermal include mechanochemical (Pichon et al., 2006) which is solvent free and room temperature catalysis (Díaz-García et al., 2014). The MOF synthesis methods developed so far produce MOFs in powder forms which makes them difficult to function in gas separation applications. The agglomeration of MOF crystals in the solution makes it difficult to direct the growth into a certain position, termed as “growing to position”. Recently, efforts made to overcome this

obstacle by growth of MOFs on a surface in-situ or by seeding-secondary growth approach through blending already synthesized MOF crystals with other materials, mostly polymers (Jahan et al., 2010). In these methods, MOF crystal nucleation is less likely to occur on top of the already formed crystals, hence “piling up” of the crystals is avoided.

2.2.3.2. *In-situ and seeding-secondary growth of MOF membranes*

In this method, MOF crystals grow on a surface which is modified or processed to make it compatible with MOF growth. The surface modification is usually made by introducing active (functional) groups which can react with metal ions or organic groups on MOF surface, as illustrated in Figure 2-4. Then the template is immersed in the MOF mother solution for in-situ growth of MOF, which allows the MOF layer to grow on the template by solvothermal method directly. In seeded growth, the template is usually coated by a seeded layer of MOF of interest, then placed into the mother solution for secondary solvothermal treatment (Li et al., 2015).

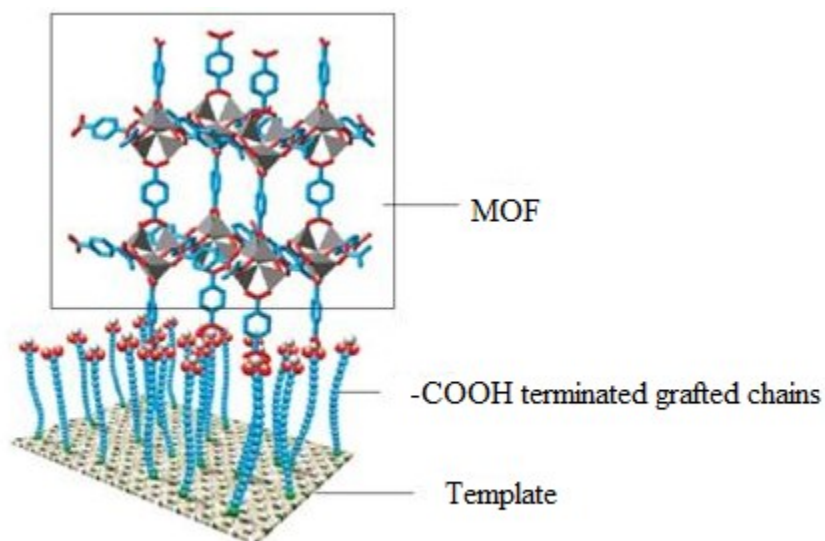


Figure 2-4. The concept of surface modification to increase compatibility with MOF

(Hermes et al., 2005)

Different types of materials have been studied for supporting MOF crystals, including poly (acrylonitrile) (PAN) (Centrone et al., 2010), polypropylene fiber mats (Zhao et al., 2014), or carbon based materials such as carbon nanotubes (CNTs) and graphite (Petit and Bandoz, 2011). Amongst all, CNTs are of exceptional research interest for their mechanical strength, potential in adsorption and catalysis, and tunable chemistry (Bradshaw et al., 2012). Preparing a defect-free MOF-membrane faces challenges such as poor membrane-MOF bonding, poor membrane stability and macroscopic crack formation during activation. Also, achieving good dispersion of the CNTs in a polymer is known to be difficult because of the limitations due to their hydrophobic and inert nature. The dispersion in polar solvents, for instance, is a strong requirement for the synthesis procedure of some composite materials such as specific drug delivery agents (Bianco et al., 2005), as well as for the incorporation in mixed matrix membrane (MMM) (Khan et al., 2012). For this purpose, different routes have been explored and reviewed to modify the surface of CNTs.

2.2.3.3. Membrane surface modification methods

Typical surface modification methods include reactions in solution for chemical functionalization, exposition to radiative sources such as x-ray, gamma ray or ultra violet - ozone, and plasma treatments (Datsyuk et al., 2008, Jiang et al., 2009, Ma et al., 2010). Another possible reason to chemically functionalize the surface of CNTs is to introduce some specific chemical groups which will act as a grafting agent in a further reaction, aiming at incorporating other functionalities. However the surface functionalization is still not fully understood in terms of surface chemistry and control of the introduction of the functionalities, while the loss in crystallinity and damage on the sidewalls which can generate amorphous carbon have been reported as an important drawback which must be limited. Solution reactions are by far the most volume to surface efficient functionalization routes and typically lead to fast kinetics. Generally,

an efficient technique requires the use of a strong oxidizing agent in order to graft hydrophilic oxygenated functionalities, typically alcohols or carboxylic acids, mostly at the tips or on defect sites which are expected to be the most reactive spots on the structure (Lin et al., 2003).

The surface functionalization reaction usually requires particularly harsh chemicals, such as HNO_3 , $\text{HNO}_3/\text{H}_2\text{SO}_4$, H_2O_2 , KMnO_4 , which are not environmental friendly (Shieh et al., 2007, Smith et al., 2009). Moreover, due to the harsh conditions related to the use of chemicals such as H_2SO_4 or HNO_3 , most oxidation reaction result in some undesirable damage introduced on the sidewalls and on the tips of CNT (Wiltshire et al., 2004, Datsyuk et al., 2008). As a consequence, these issues limit their application to a relatively narrow range of surface modifications (Karousis et al., 2010).

On the other hand the high penetrability of irradiative chemical pathways by x-ray or gamma ray irradiation may be performed in gaseous phases and are not limited to the surface of the material (Wang et al., 2009, Yang et al., 2009, Dumée et al., 2014). However these techniques are limited to reagents which can be brought physically in contact with the sites to be grafted (Dumée et al., 2014). UV-ozone and surface plasma treatments on the other hand offer highly versatile routes to the surface modification of graphene materials (Lin et al., 2010, Wang et al., 2013).

2.2.3.3.1 *Plasma treatment*

While acid treatments and x-ray or gamma ray irradiation present some obstacles in terms of controlling the reaction conditions when harsh chemicals are applied and introduction of undesirable structural damage, plasma treatment offers the possibility to chemically modify a polymeric surface by introducing new functional groups with a clean, fast and possibly safe process (Barton et al., 1999, Barton et al., 2000). Plasma consists of a mixture of excited

species such as radicals, electrons, ions and UV light. The application of an intense source of energy to an atom results in the breaking up of its outer shell, generating negatively charged electrons and positively charged ions and radicals. While energy is provided by a high frequency generator, an electron from the feed gas is shot out from the outer shell. The negatively charged components consequently move towards the anode, meeting and colliding with other molecules thus generating more radicals and positive ions which are accelerated towards the cathode. Ionized molecules are not the only responsible species for the plasma functionalization, in fact during the process IR/UV radiations are created even though they have less significance compared to the impact of radicals and ions (Rauscher et al., 2010).

Having to deal with different charged species, and tuning the plasma parameters in order to fully understand the effects, make it challenging to obtain the most suitable conditions. Several studies have been carried out to demonstrate how nitrogen or oxygenated functionalities can be introduced via plasma treatment by making use of a wide range of feed gas, commonly oxygen or ammonia (Felten et al., 2013, McEvoy et al., 2013, Singh et al., 2013). As previously mentioned, one of the most aimed functionalization of CNTs consists of grafting oxygenated groups such as alcohols or carboxylic ones, not only to improve the wettability and, as a consequence, the stability in polar solvents, but also as a first step to introduce further molecules which can find $-OH$ and $-COOH$ as their most suitable reaction partners.

In order to achieve the targeted functionalization, a wide range of feed gases has been explored and investigated. Zhao et al. (2012) reviewed the application of an Ar or Ar/O₂ mixture as the feed gas in order to introduce some oxygenated functionalities on the surface of CNT forests. They reported that the CNT surface may reach a saturation level in terms of the amount of O₂ that can be introduced. Chen et al. (2009) also confirmed this phenomenon must be taken

into account. Consequently, the authors made the assumption that the CNT surface can reach a specific level of saturation due to the oxidation level and the molecular steric hindrance.

Interestingly, Zhao and his coworkers (Zhao et al., 2012) found out that an Ar/O₂ mixture is more efficient in introducing the targeted functionalities than an O₂ one. The possible explanation is related to the role of Ar which may be able to enhance the quantity of active oxygen present in the plasma environment. Nonetheless, oxygen or an oxygen and argon mixture are not the only feed gases which have been investigated for the purpose. Hussain et al. (2012) observed that water can possibly introduce some oxygenated groups even though high pressure may be a drawback since a layer of water can be formed on the surface, preventing the action of ions and radicals to be efficient.

However, it is complex to assess which plasma feed gas is the most suitable for a specific purpose since many parameters are involved varying from the gas partial pressure to the treatment time, plasma power and plasma work pressure.

Furthermore, the reactivity of the free radicals generated across the surface of the graphene materials has not been studied to date. The assessment of the reactivity of these groups is primordial to expand manufacturing routes and to ultimately prove the advantages of the plasma technique compared to a classic acid treatment.

2.2.3.4. CO₂ Separation using MOFs

Porous materials are used for separating mixtures of gases or liquids in applications including O₂ and N₂ separations from air, removal of volatile organic compounds, and CO₂ capture. For CO₂ capture in particular, adsorbents should be chemically stable, low-cost, easy to prepare, and regenerable. Thermodynamic effects (adsorbate-adsorbate and/or adsorbate-adsorbent interactions) and kinetic effects (differences in diffusion rates of different components in a gas mixture) impact adsorption processes (D'Alessandro et al., 2010). Since MOFs provide

high specific surface area and tailorable pore structures, they provide advantages over many other porous materials used in separation applications, possibly negating their relatively high costs and warranting additional investigations.

2.2.3.5. *MOFs with high selectivity for CO₂ adsorption*

MOF properties can be tuned by selecting appropriate metal ions and organic linkers, enabling them to be tailored for specific adsorption applications. MOFs have 3D structures and most have high surface areas (up to 5,000 m²/g) (D'Alessandro et al., 2010), comparable or even higher than activated carbon and zeolites. Yaghi et al. (Millward and Yaghi, 2005) completed the first systematic study linking CO₂ capacity and MOF surface area, showing that high surface area MOF-177 has high CO₂ capacity at high pressures (60.0 wt% at 35 bar). The same group identified the impact of metal ions on CO₂ adsorption by varying the properties of MOF-74. Breakthrough experiments showed that Mg-MOF-74 captures 96% more CO₂ than Zn-MOF-74 because of different metal ion-CO₂ interactions. The presence of open metal sites in MOF structure provides a mechanism for the separation of (quadru) polar/non polar gas pairs such as CO₂/CH₄. It was reported that selective adsorption of CO₂ is due to the coordination of CO₂ to the metal ion in an end-on fashion, i.e., O=C=O...Cu²⁺ (D'Alessandro et al., 2010). Accordingly, MOF-199 (called also HKUST-1, or Cu₃(BTC)₂) which consists of paddlewheel Cu₂(COO⁻) units connected through btc₃-ligands offers this feature. During the synthesis of MOF-199, solvent molecules bound on the axial sites of each Cu²⁺ metal center which will be removed in vacuum at elevated temperatures, creating open binding sites for guest molecules. In fact, these sites act as charge-dense point charges, which selectively separate component of gas mixtures based on their polarity, dipole or quadrupole moment (Sumida et al., 2012). Also the metal type plays a significant role for tuning and optimizing the adsorptive properties of the isostructural frameworks. Dietzel et al. (2009) examined the influence of metal center on the

capacity and selectivity of $[M_2(\text{dobdc})(\text{H}_2\text{O})]$ towards CO_2 and reported the highest adsorption capacity for $[\text{Mg}_2(\text{dobdc})]$ which is more than double of any other metal ions in the framework (e.g. $M = \text{Mg}, \text{Mn}, \text{Fe}, \text{Co}, \text{Ni}, \text{Zn}$). Similarly, different organic linkers can be applied to change the porosity and structure of MOFs. Furukawa et al. (2010) modified the structure of MOF-177 by using an expanded organic linker, obtaining MOF-200 with 35, 19, and 63% higher surface area, porosity, and CO_2 capacity at 25°C and 50 bar, respectively.

Since CO_2 capture from flue gases is most practical at ambient pressure, increasing low pressure CO_2 capacity of MOFs should be investigated. Currently, the best reported MOF for ambient pressure CO_2 adsorption is Mg-MOF-74 (Britt et al., 2009), which has available Mg^{2+} sites that allow for a CO_2 capacity of 35.2 wt% at 298 K and 1 bar. The open metal sites are essential for achieving high capacities. Since actual flue gas streams contain only 10-12 wt% CO_2 , selectivity for CO_2 and against other gases (e.g., N_2 , O_2 and H_2O) is essential (Simmons et al., 2011).

2.2.3.6. *The binding nature of CO_2 in MOFs*

Past research identifies unsaturated metal centers (UMCs) as CO_2 binding sites on Mg-MOF-74 and MOF-199 because of enhanced electrostatic interaction with CO_2 molecules (Wu et al., 2010). CO_2 molecules bind to Mg^{2+} sites in Mg-MOF-74. For MOF-199, CO_2 molecules bind to Cu^{2+} sites at low CO_2 concentration, while pore filling in small cage windows is the adsorption mechanism at high CO_2 concentrations. (Wu et al., 2010). Most often, accessible small cages and channels in the MOF structure interact with CO_2 molecules via van der Waals' interactions (Wu et al., 2010). Cho et al. (2012), measured the heat of CO_2 adsorption on Co-MOF-74 and reported a sharp decrease with increasing CO_2 loading. This behavior indicates that for low CO_2 concentrations, CO_2 preferentially binds to energetic adsorption sites (open metal sites), while for high CO_2 loadings, these sites are saturated and adsorption proceeds by small

cage window filling (Vaidhyanathan et al., 2009, Bao et al., 2011, Cho et al., 2012). A large number of MOFs has been investigated experimentally for CO₂ adsorption and other gas separations, as summarized in Table 2-2. The results are collected at ambient temperature, with pressure ranging from low pressure (<1.2 bar) to atmospheric pressure. Low temperature and pressure adsorption is mainly controlled by chemical feature of surface, whereas high pressure adsorption isotherms are mostly influenced by the surface area of MOFs. The focus of this work will be on CO₂ adsorption at ambient temperature and pressure, which most resembled to post combustion CO₂ capture application (at ~ 1 bar).

Table 2-2. Low pressure CO₂ adsorption capacities for MOFs

Material	Common name	BET surface area (m ² /g)	Uptake Temp (°C)	Pressure (bar)	Adsorption Capacity (wt %)	Reference
Zn/DOBDC*		816	23	1	5.8	(Caskey et al., 2008)
Mg/DOBDC		1,495	23	1	23.6	(Caskey et al., 2008)
Ni ₂ (dobdc)*	Ni-MOF-74, CPO-27-Ni	936	25	1	23.9	(Yazaydın et al., 2009)
Ni ₂ (dobdc)	Ni-MOF-74, CPO-27-Ni	1,070	23	1	22.6	(Caskey et al., 2008)
Zn ₂ (dobdc)	Zn-MOF-74, CPO-27-Zn		23	1	19.8	(Yazaydın et al., 2009)
Co ₂ (dobdc)	Co-MOF-74, CPO-27-Co	957	25	1	24.9	(Yazaydın et al., 2009)
Zn ₄ O (BDC-NH ₂) ₃	IRMOF-3	2,160	25	1.1	5.1	(Millward and Yaghi, 2005)
Mg(tcpbda)*			25	1	6.5	(Bao et al., 2011)

$\text{Cu}_3(\text{BTC})_2^*$	HKUST-1	934	22	1	12.5	(Xie et al., 2012)
$\text{Zn}_4\text{O}(\text{BDC})_3$	MOF-5, IRMOF-1	2,304	23	1	8.5	(Zhao et al., 2009)
$\text{Zn}(\text{IDC})^*$	IMOF-3	802	25	1	8.6	(Debatin et al., 2010)
$\text{Cr}_3\text{O}(\text{H}_2\text{O})_2\text{F}(\text{BDC})_3$	MIL-101(Cr)	2,674	46	1	4.2	(Chowdhury et al., 2009)
$\text{Cu}_2(\text{bptc})(\text{H}_2\text{O})_2(\text{DMF})_3^*$	MOF-505	1,547	25	1.1	12.6	(Millward and Yaghi, 2005)
$\text{Al}(\text{OH})(\text{bpydc})$	MOF-253	2,160	25	1	6.2	(Bloch et al., 2010)
$\text{Ni}_2(\text{pbmp})^*$	Ni-STA-12		31	1	9.9	(Miller et al., 2008)
$\text{Zn}_4\text{O}(\text{BDC}-\text{C}_2\text{H}_4)_3$	IRMOF-6	2,516	25	1.2	4.6	(Millward and Yaghi, 2005)
$\text{In}(\text{OH})(\text{BDC})$	MIL-53(Al), USO-1-Al	1,300	25	1	10.6	(Arstad et al., 2008)
$\text{Ni}_2(\text{BDC})_2(\text{DABCO})^*$	USO-2-Ni	1,925	25	1	10	(Arstad et al., 2008)
$\text{Cu}_3(\text{BPT})_2$	UMCM-150		25	1	10.2	(Yazaydin et al., 2009)

*BDC: benzenedicarboxylate, BPT: Biphenyl-3,4',5-tricarboxylate, DOBDC: 2,5-dihydroxyterephthalate, tcbpda: N,N,N',N'-tetrakis(4-carboxyphenyl)biphenyl-4,4'-diamine, BTC: 1,3,5-benzenetricarboxylic, IDC: imidazole-4,5-dicarboxylate, DMF: N,N-dimethyl formamide, bpydc: 2,2'-bipyridine-5,5'-dicarboxylic, pbmp: N,N'-piperazinebismethylenephosphonate, DABCO: 1,4-diazabicyclo[2.2.2]octane

2.3. Microwave Sensing

2.3.1. Introduction

Low cost and highly selective sensors with the capability to sense trace amounts of gases have become indispensable for environmental monitoring in gas phase (e.g. carbon level emission, volatile organic compound emission, indoor air quality), and biomedical and industrial applications (Nayak et al., 2015). One of the significant application of such sensitive sensors can be in CO₂ level detection in atmosphere.

On the other hand, as stated earlier, adsorption of CO₂ onto a solid adsorbent is one of the promising methods to efficiently reduce CO₂ emissions. In order to make it more economical and sustainable, the adsorbent needs to be regenerated after each adsorption cycle. Hence, the adsorbent recovery becomes important where it needs information about when to replace the adsorbent and manage the process economically. CO₂ sensors can provide such information by monitoring changes of carbon dioxide concentration in the gas stream. The most common approaches in CO₂ sensor technology is based on infrared (IR) spectroscopy and gas chromatography. Unfortunately these devices are bulky and have expensive readout circuitry with high chances of interference from CO, as CO has similar absorption in the same IR range (Lübbers and Opitz, 1975, Leiner, 1991). Other major CO₂ sensors work based on chemical reaction between the CO₂ gas and the sampling module of the sensor such as polymer membrane or porous adsorbents (Wang et al., 2014). The main function in these sensors is recognition of the CO₂ molecule and transduction of this recognition into a readable signal. This signal can be a change in parameters such as pH, resistance, conductivity, or capacitance of the system. Among them, capacitive sensors show great potential for CO₂ monitoring. They monitor the change in the permittivity of a material as a function of the concentration of the target gas (Wark et al.,

2003, Wagner et al., 2013). Microwave sensors work based on the interaction between electromagnetic waves and testing materials. The incident waves may be affected by the test object via attenuation, reflection or change in its velocity. The variation in transmitted and reflected microwave powers is specific for each material (Zarifi et al., 2015). In this concept, microwave resonator sensors draw more attention due to their low-cost, robust, non-destructive, sensitive, and long life-time features (Ebrahimi et al., 2014, Korostynska et al., 2014, Afshar et al., 2015, Ateeq et al., 2016, Wang et al., 2016, Zarifi et al., 2016).

The microwave sensor is capable of monitoring changes in the dielectric properties of its vicinity through measuring variation of resonant frequency (f_r), at which the maximum power transmission occurs. Dielectric properties of material includes dielectric constant (ϵ'), and loss factor (ϵ'') (Zarifi et al., 2015). Dielectric constant is a measure of substance's ability to be polarized by an electromagnetic field, and loss factor is the material's ability in converting the absorbed energy into heat (Cherbański et al., 2011).

2.3.2. Microwave sensing application

Microwave sensors have been utilized in environmental applications in different media, e.g., solid, liquid and gas. Cheng (2014) used an integrated microwave resonator sensor to monitor the temperature in harsh environment (above 1000 °C). The temperature was monitored by measuring the changes in resonant frequency of microwave resonator, which in fact depends on the substrate (alumina) permittivity. Liancheng and his coworkers (Liangcheng et al., 2013) using microwave sensor determined the moisture content in bio-filter media, e.g., wood chips and composts. The impedance of the bio-filter media was directly measured using an impedance analyzer and interpreted as a predictor of moisture content. Microwave sensors have also been used to detect water pollution in underground pipelines using the difference between dielectric

properties of fresh and contaminated water (Abdelgwad, 2014). McGrath et al. (2006) developed a microwave carbon nanotube resonator sensor which was capable of monitoring traces of ammonia. Upon exposure to the gas, the shift in resonance frequency indicates the presence of gas, which achieved a sensitivity of 4000 Hz/ppm for ammonia. Sohrabi et al. (2014) proposed a new method to detect concentrations of volatile organic compounds such as ethanol and acetone by using a deposited swelling polymer (polydimethylsiloxane; PDMS) film on top of a micro-strip ring resonator. In their work, changes in the PDMS thickness and permittivity were detected by a shift in the resonance frequency of the resonator.

2.3.3. Material-assisted sensors

Recently, various sensitive materials (e.g. amino groups, modified silicates, and metal-oxide semiconductors (MOS)) have been investigated for the use in mass sensitive and capacitive CO₂ sensors which work based on sensing of changes in material properties due to chemical interaction between target gas and material. However, they come with disadvantages such as long response time, the poor reversibility and sensitivity, and high temperature requirement (200-400 °C) (Stegmeier et al., 2009, Yamagiwa et al., 2014). In a new approach, MOFs have been investigated for sensor applications due to their tunable nanoporosity and high surface area. The connection of metal ions with organic linkers in the framework creates a regulated nanospace, where guest molecules can be incorporated into it through molecular sieving effect, π - π interaction, hydrogen bonding and electrostatic interaction (Yamagiwa et al., 2014). The combination of MOFs with a transducer (e.g., cantilever, quartz-crystal microbalance (QCM)) has been reported as sensing materials with high detection sensitivities (Goeders et al., 2008, Ameloot et al., 2009). However, due to the difficulty of loading MOF crystals onto the tiny region of such tools (Xu et al., 2014), new approaches such as MOF coating and seeding growth

on the sensor surface have been developed (Ameloot et al., 2009). In a research by Ameloot et al. (2009), MOF-199 was coated on pure copper electrodes through electrochemical formation, and integrated with QCM. The as-synthesized MOF-based microsystem was used as a humidity sensor working based on the changes in vibration frequency of a piezoelectrically driven quartz crystal upon water vapor adsorption. The well-known MOF-199 structure was chosen because of highly stable bimetallic tetracarboxylate arrangement as well as its good water sorption capacity (25-30 wt %) (Ameloot et al., 2009). Zhuang et al. (2013) developed a new method for practical gas sensors on textiles by ink-jet printing of MOF-199. The printed patterns of MOF-199 have the unique properties of fast colour change upon exposure to different gases, as it was shown to change colour from turquoise to dark blue, yellow, and brown after exposure to NH_3 , HCl , and H_2S vapour respectively (Zhuang et al., 2013). In addition to aforementioned unique properties of MOF-199 for sensor application, in MOF-199 (or $\text{Cu}_3(\text{BTC})_2$), the Cu^{2+} ions are accessible coordination sites with high potential for binding to other molecules, whereas in many MOF structures (e.g., MOF-5), the coordination sites of the metal ions are blocked by the ligands (Biemmi et al., 2007). Also MOF-199 offers a rapid interaction of multivalent metals with quadrupolar CO_2 molecule (Gutiérrez-Sevillano et al., 2013).

It should be noted that, in spite of remarkable properties of MOFs, their application for sensing function is still in its infancy. Hitherto, we do not have any MOF-based gas sensors acceptable for the sensor market. New approaches to MOF film deposition and sensor fabrication are required to improve the reproducibility and make them suitable for long-term applications. In this work we integrated MOF-199 (as highly applied in sensor applications) with a new designed microwave resonator sensor to evaluate its function for CO_2 detection and monitoring.

2.4. References

- Abdelgwad A. H. , Said T. M. , Gody A. M. (2014). Microwave Detection of Water Pollution in Underground Pipelines. *International Journal of Wireless and Microwave Technologies* **4**(3): 1-15.
- Afshar, S., Salimi E., Braasch K., Butler M., Thomson D., and Bridges G. (2015). Multi-frequency DEP cytometer employing a microwave interferometer for the dielectric analysis of micro-particles. *2015 IEEE MTT-S International Microwave Symposium*.
- Ahmadpour, A. and Do D. D. (1996). The preparation of active carbons from coal by chemical and physical activation. *Carbon* **34**(4): 471-479.
- Ameloot, R., Stappers L., Fransaer J., Alaerts L., Sels B. F., and De Vos D. E. (2009). Patterned Growth of Metal-Organic Framework Coatings by Electrochemical Synthesis. *Chemistry of Materials* **21**(13): 2580-2582.
- Arstad, B., Fjellvag H., Kongshaug K. O., Swang O., and Blom R. (2008). Amine functionalised metal organic frameworks (MOFs) as adsorbents for carbon dioxide. *Adsorption* **14**(6): 755-762.
- Ateeq, M., Shaw A., Garrett R., and Dickson P. (2016). Feasibility study on using microwave sensing technique to analyse silver-based products. *Journal of Electromagnetic Waves and Applications*: 1-17.
- Bandosz, T. J. (2006). Activated carbon surfaces in environmental remediation, *Oxford,UK*.

- Bao, Z., Yu L., Ren Q., Lu X., and Deng S. (2011). Adsorption of CO₂ and CH₄ on a magnesium-based metal organic framework. *Journal of Colloid and Interface Science* **353**(2): 549-556.
- Barton, D., Bradley J. W., Gibson K. J., Steele D. A., and Short R. D. (2000). An In Situ Comparison between VUV Photon and Ion Energy Fluxes to Polymer Surfaces Immersed in an RF Plasma. *The Journal of Physical Chemistry B* **104**(30): 7150-7153.
- Barton, D., Bradley J. W., Steele D. A., and Short R. D. (1999). Investigating Radio Frequency Plasmas Used for the Modification of Polymer Surfaces. *The Journal of Physical Chemistry B* **103**(21): 4423-4430.
- Bianco, A., Kostarelos K., and Prato M. (2005). Applications of carbon nanotubes in drug delivery. *Current opinion in chemical biology* **9**(6): 674-679.
- Biemmi, E., Scherb C., and Bein T. (2007). Oriented Growth of the Metal Organic Framework Cu₃(BTC)₂(H₂O)₃·xH₂O Tunable with Functionalized Self-Assembled Monolayers. *Journal of the American Chemical Society* **129**(26): 8054-8055.
- Bloch, E. D., Britt D., Lee C., Doonan C. J., Uribe-Romo F. J., Furukawa H., Long J. R., and Yaghi O. M. (2010). Metal Insertion in a Microporous Metal–Organic Framework Lined with 2,2'-Bipyridine. *Journal of the American Chemical Society* **132**(41): 14382-14384.
- Bradshaw, D., Garai A., and Huo J. (2012). Metal-organic framework growth at functional interfaces: thin films and composites for diverse applications. *Chemical Society Reviews* **41**(6): 2344-2381.

- Britt, D., Furukawa H., Wang B., Glover T. G., and Yaghi O. M. (2009). Highly efficient separation of carbon dioxide by a metal-organic framework replete with open metal sites. *Proceedings of the National Academy of Sciences* **106**(49): 20637-20640.
- Caskey, S. R., Wong-Foy A. G., and Matzger A. J. (2008). Dramatic Tuning of Carbon Dioxide Uptake via Metal Substitution in a Coordination Polymer with Cylindrical Pores. *Journal of the American Chemical Society* **130**(33): 10870-10871.
- Centrone, A., Yang Y., Speakman S., Bromberg L., Rutledge G. C., and Hatton T. A. (2010). Growth of Metal–Organic Frameworks on Polymer Surfaces. *Journal of the American Chemical Society* **132**(44): 15687-15691.
- Chen, C., Liang B., Ogino A., Wang X., and Nagatsu M. (2009). Oxygen functionalization of multiwall carbon nanotubes by microwave-excited surface-wave plasma treatment. *The Journal of Physical Chemistry C* **113**(18): 7659-7665.
- Chen, H. and Hashisho Z. (2012). Effects of microwave activation conditions on the properties of activated oil sands coke. *Fuel Processing Technology* **102**(0): 102-109.
- Cheng, H. (2014). Integrated microwave resonator/antenna structures for sensor and filter applications, *Thesis for Doctor of Philosophy*, University of Central Florida.
- Cherbański, R. and Molga, E. (2009). Intensification of desorption processes by use of microwaves-An overview of possible applications and industrial perspectives. *Chemical Engineering and Processing: Process Intensification*, **48**: 48-58.

- Cherbański, R., Komorowska-Durka M., Stefanidis G. D., and Stankiewicz A. I. (2011). Microwave Swing Regeneration vs Temperature Swing Regeneration, Comparison of Desorption Kinetics. *Industrial & Engineering Chemistry Research* **50**(14): 8632-8644.
- Cho, H.Y., Yang D.A., Kim J., Jeong S.Y., and Ahn W.S. (2012). CO₂ adsorption and catalytic application of Co-MOF-74 synthesized by microwave heating. *Catalysis Today* **185**(1): 35-40.
- Choi, S., Drese J. H., and Jones C. W. (2009). Adsorbent Materials for Carbon Dioxide Capture from Large Anthropogenic Point Sources. *ChemSusChem* **2**(9): 796-854.
- Chowdhury, P., Bikkina C., and Gumma S. (2009). Gas Adsorption Properties of the Chromium-Based Metal Organic Framework MIL-101. *The Journal of Physical Chemistry C* **113**(16): 6616-6621.
- Chue, K. T., Kim J. N., Yoo , Cho S. H. , and Yang R. T. (1995). Comparison of Activated Carbon and Zeolite 13X for CO₂ Recovery from Flue Gas by Pressure Swing Adsorption. *Industrial & Engineering Chemistry Research* **34**(2): 591-598.
- Chung, D. D. L. (2001). Electromagnetic interference shielding effectiveness of carbon materials. *Carbon* **39**(2): 279-285.
- CSIRO (2008). Post-Combustion Capture (PCC). *COAL21 Post Combustion CO₂ Capture Meeting*, Canberra
- D'Alessandro, D. M., and T. McDonald (2010). Toward carbon dioxide capture using nanoporous materials. *Pure and Applied Chemistry*. **83**: 57.
- D'Alessandro, D. M., Smit B., and Long J. R. (2010). Carbon Dioxide Capture: Prospects for New Materials. *Angewandte Chemie International Edition* **49**(35): 6058-6082.

- Datsyuk, V., Kalyva M., Papagelis K., Parthenios J., Tasis D., Siokou A., Kallitsis I., and Galiotis C. (2008). Chemical oxidation of multiwalled carbon nanotubes. *Carbon* **46**(6): 833-840.
- Davies, M. (2006). Corrosion: Environments and Industries *ASM Handbook*_ASM International. **13C**: 727 - 735.
- Davini, P. (2002). Flue gas treatment by activated carbon obtained from oil-fired fly ash. *Carbon* **40**(11): 1973-1979.
- De Jonge, R. J., Breure A. M., and Van Andel J. G. (1996). Reversibility of adsorption of aromatic compounds onto powdered activated carbon (PAC). *Water Research* **30**(4): 883-892.
- Debatin, F., Thomas A., Kelling A., Hedin N., Bacsik Z., Senkovska I., Kaskel S., Junginger M., Müller H., Schilde U., Jäger C., Friedrich A., and Holdt H. J. (2010). In Situ Synthesis of an Imidazolate-4-amide-5-imidate Ligand and Formation of a Microporous Zinc–Organic Framework with H₂-and CO₂-Storage Ability. *Angewandte Chemie International Edition* **49**(7): 1258-1262.
- Díaz-García, M., Mayoral Á., Díaz I., and Sánchez-Sánchez M. (2014). Nanoscaled M-MOF-74 Materials Prepared at Room Temperature. *Crystal Growth & Design* **14**(5): 2479-2487.
- Dietzel, P. D. C., Besikiotis V., and Blom R. (2009). Application of metal-organic frameworks with coordinatively unsaturated metal sites in storage and separation of methane and carbon dioxide. *Journal of Materials Chemistry* **19**(39): 7362-7370.

- Di-Panfilo, R. and Egiebor N. O. (1996). Activated carbon production from synthetic crude coke. *Fuel Processing Technology* **46**(3): 157-169.
- Donaldson, T. L. and Nguyen Y. N. (1980). Carbon Dioxide Reaction Kinetics and Transport in Aqueous Amine Membranes. *Industrial & Engineering Chemistry Fundamentals* **19**(3): 260-266.
- Dumée, L. F., Feng C., He L., Allieux F.M., Yi Z., Gao W., Banos C., Davies J. B. and Kong L. (2014). Tuning the grade of graphene: Gamma ray irradiation of free-standing graphene oxide films in gaseous phase. *Applied Surface Science* **322**(0): 126-135.
- Ebrahimi, A., Withayachumnankul W., Al-Sarawi S. F. and Abbott D. (2014). Metamaterial-Inspired Rotation Sensor With Wide Dynamic Range. *IEEE Sensors Journal* **14**(8): 2609-2614.
- Eddaoudi, M., Moler D. B., Li H., Chen B., Reineke T. M., O'Keeffe M., and Yaghi O. M. (2001). Modular Chemistry: Secondary Building Units as a Basis for the Design of Highly Porous and Robust Metal–Organic Carboxylate Frameworks. *Accounts of Chemical Research* **34**(4): 319-330.
- Felten, A., Eckmann A., Pireaux J. J., Krupke R. and Casiraghi C. (2013). Controlled modification of mono- and bilayer graphene in O₂, H₂ and CF₄ plasmas. *Nanotechnology* **24**(35): 355705.
- Figuerola, J. D., Fout T., Plasynski S., McIlvried H., and Srivastava R. D. (2008). Advances in CO₂ capture technology—The U.S. Department of Energy's Carbon Sequestration Program. *International Journal of Greenhouse Gas Control* **2**(1): 9-20.

- Foo, K. Y. and Hameed B. H. (2012). Mesoporous activated carbon from wood sawdust by K_2CO_3 activation using microwave heating. *Bioresource technology* **111**: 425-432.
- Franchi, R. S., Harlick P. J. E., and Sayari A. (2005). Applications of Pore-Expanded Mesoporous Silica. 2. Development of a High-Capacity, Water-Tolerant Adsorbent for CO_2 . *Industrial & Engineering Chemistry Research* **44**(21): 8007-8013.
- Freguia, S. and Rochelle G. T. (2003). Modeling of CO_2 capture by aqueous monoethanolamine. *AIChE Journal* **49**(7): 1676-1686.
- Furukawa, H., Ko N., Go Y. B., Aratani N., Choi S. B., Choi E., Yazaydin Ö., Snurr R. Q., O’Keeffe M., Kim J., and Yaghi O. M. (2010). Ultrahigh Porosity in Metal-Organic Frameworks. *Science* **329**(5990): 424-428.
- Garcia, S., Gil M. V., Martin C. F., Pis J. J., Rubiera F., and Pevida C. (2011). Breakthrough adsorption study of a commercial activated carbon for pre-combustion CO_2 capture. *Chemical Engineering Journal* **171**(2): 549-556.
- Goeders, K. M., Colton J. S., and Bottomley L. A. (2008). Microcantilevers: Sensing Chemical Interactions via Mechanical Motion. *Chemical Reviews* **108**(2): 522-542.
- Granite, E. J. and Pennline H. W. (2002). Photochemical Removal of Mercury from Flue Gas. *Industrial & Engineering Chemistry Research* **41**(22): 5470-5476.
- Gutiérrez-Sevillano, J. J., Vicent-Luna J. M., Dubbeldam D., and Calero S. (2013). Molecular Mechanisms for Adsorption in Cu-BTC Metal Organic Framework. *The Journal of Physical Chemistry C* **117**(21): 11357-11366.

- Hermes, S., Schröder F., Chelmowski R., Wöll C., and Fischer R. A. (2005). Selective Nucleation and Growth of Metal–Organic Open Framework Thin Films on Patterned COOH/CF₃-Terminated Self-Assembled Monolayers on Au(111). *Journal of the American Chemical Society* **127**(40): 13744-13745.
- Ho, M. T., Allinson G. W., and Wiley D. E. (2008). Reducing the Cost of CO₂ Capture from Flue Gases Using Pressure Swing Adsorption. *Industrial & Engineering Chemistry Research* **47**(14): 4883-4890.
- Hu, Z. and Srinivasan M. P. (2001). Mesoporous high-surface-area activated carbon. *Microporous and Mesoporous Materials* **43**(3): 267-275.
- Hussain, S., Amade R., Jover E., and Bertran E. (2012). Functionalization of carbon nanotubes by water plasma. *Nanotechnology* **23**(38): 385604.
- IPCC (2001). *Climate Change 2001: Impacts, Adaptation and Vulnerability*.
- Jadhav, P. D., Chatti R. V., Biniwale R. B., Labhsetwar N. K., Devotta S., and Rayalu S. S. (2007). Monoethanol Amine Modified Zeolite 13X for CO₂ Adsorption at Different Temperatures. *Energy & Fuels* **21**(6): 3555-3559.
- Jahan, M., Bao Q., Yang J.X., and Loh K. P. (2010). Structure-Directing Role of Graphene in the Synthesis of Metal–Organic Framework Nanowire. *Journal of the American Chemical Society* **132**(41): 14487-14495.
- Jiang, X., Gu J., Bai X., Lin L., and Zhang Y. (2009). The influence of acid treatment on multi-walled carbon nanotubes. *Pigment & Resin Technology* **38**(3): 165-173.
- Kamarudin, K. S. N. and Mat H. (2009). Synthesis and modification of micro and mesoporous materials as CO₂ adsorbents, *Thesis for Master of Science, University of Technology of Malaysia*.

- Karousis, N., Tagmatarchis N., and Tasis D. (2010). Current progress on the chemical modification of carbon nanotubes. *Chemical Reviews* **110**(9): 5366-5397.
- Keskin, S., Van Heest T. M., and Sholl D. S. (2010). Can Metal–Organic Framework Materials Play a Useful Role in Large-Scale Carbon Dioxide Separations? *ChemSusChem* **3**(8): 879-891.
- Khalil, S. H., Aroua M. K., and Daud W. M. A. W. (2012). Study on the improvement of the capacity of amine-impregnated commercial activated carbon beds for CO₂ adsorbing. *Chemical Engineering Journal* **183**(0): 15-20.
- Khan, M., Filiz V., Bengtson G., Shishatskiy S., Rahman M., and Abetz V. (2012). Functionalized carbon nanotubes mixed matrix membranes of polymers of intrinsic microporosity for gas separation. *Nanoscale Research Letters* **7**(1): 1-12.
- Klinowski, J., Almeida Paz F. A., Silva P., and Rocha J. (2011). Microwave-Assisted Synthesis of Metal-Organic Frameworks. *Dalton Transactions* **40**(2): 321-330.
- Ko, Y. G., Shin S. S. , and Choi U. S. (2011). Primary, secondary, and tertiary amines for CO₂ capture: Designing for mesoporous CO₂ adsorbents. *Journal of Colloid and Interface Science* **361**(2): 594-602.
- Korostynska, O., Mason A., and Al-Shamma'a A. (2014). Microwave sensors for the non-invasive monitoring of industrial and medical applications. *Sensor Review* **34**(2): 182-191.
- Krishnankutty, N. and Vannice M. A. (1995). Effect of Pretreatment on Surface Area, Porosity, and Adsorption Properties of a Carbon Black. *Chemistry of Materials* **7**(4): 754-763.

- Kumar, R. (1989). Adsorption column blowdown: adiabatic equilibrium model for bulk binary gas mixtures. *Industrial & Engineering Chemistry Research* **28**(11): 1677-1683.
- Lee, C. S., Ong Y. L., Aroua M. K., and Daud W. M. A. W. (2013) Impregnation of palm shell-based activated carbon with sterically hindered amines for CO₂ adsorption. *Chemical Engineering Journal* **219**(0): 558-564.
- Leiner, M. J. P. (1991). Luminescence chemical sensors for biomedical applications: scope and limitations. *Analytica Chimica Acta* **255**(2): 209-222.
- Li, J.R., Kuppler R. J., and Zhou H.C. (2009). Selective gas adsorption and separation in metal-organic frameworks. *Chemical Society Reviews* **38**(5): 1477-1504.
- Li, W., Zhang Y., Li Q., and Zhang G. (2015). Metal-organic framework composite membranes: Synthesis and separation applications. *Chemical Engineering Science* **135**: 232-257.
- Liangcheng, Y., Xinlei W., Ted L. F., Richard S. G., and Yuanhui Z. (2013). Impedance-Based Moisture Sensor Design and Test for Gas-Phase Biofilter Applications. *American Society of Agricultural and Biological Engineers* **56**(4). 1613-1621.
- Lin, R., Ge L., Diao H., Rudolph V., and Zhu Z. (2016). Propylene/propane selective mixed matrix membranes with grape-branched MOF/CNT filler. *Journal of Materials Chemistry A* **4**(16): 6084-6090.
- Lin, T., Bajpai V., Ji T., and Dai L. (2003). Chemistry of carbon nanotubes. *Australian journal of chemistry* **56**(7): 635-651.
- Lin, Y.C., Lin C.Y., and Chiu P.W. (2010). Controllable graphene N-doping with ammonia plasma. *Applied Physics Letters* **96**(13): 133110.

- Liou, T.H. (2010). Development of mesoporous structure and high adsorption capacity of biomass-based activated carbon by phosphoric acid and zinc chloride activation. *Chemical Engineering Journal* **158**(2): 129-142.
- Lu, H. (2012). Interfacial Synthesis of Metal-organic Frameworks. *Thesis for Master of Science, McMaster University*.
- Lübbers, D. W. and Opitz N. (1975). The pCO₂-/pO₂-optode: a new probe for measurement of pCO₂ or pO₂ in fluids and gases (authors transl). *Zeitschrift für Naturforschung. Section C: Biosciences* **30**(4): 532-533.
- Ma, P.C., Siddiqui N. A., Marom G., and Kim J.K. (2010). Dispersion and functionalization of carbon nanotubes for polymer-based nanocomposites: A review. *Composites Part A: Applied Science and Manufacturing* **41**(10): 1345-1367.
- Macia-Agullo, J. A., Moore B. C., Cazorla-Amoros D., and Linares-Solano A. (2004). Activation of coal tar pitch carbon fibres: Physical activation vs. chemical activation. *Carbon* **42**(7): 1367-1370.
- Mahurin, S. M., Lee J. S., Wang X., and Dai S. (2011). Ammonia-activated mesoporous carbon membranes for gas separations. *Journal of Membrane Science* **368**(1-2): 41-47.
- Maroto-Valer, M. M., Tang Z., and Zhang Y. (2005). CO₂ capture by activated and impregnated anthracites. *Fuel Processing Technology* **86**(14-15): 1487-1502.
- Marsh, H. and Rodriguez-Reinoso F. (2006). *Activated Carbon*, Elsevier Ltd: Oxford: 243-365.

- Matsuura, T. (2009). Membrane Separation Technologies. *Wastewater Recycling, Reuse, and Reclamation*. S. Vigneswaran, EOLSS Publications. **I**: 98-135.
- Mattson, J. A., Mark H. B., Malbin M. D., Weber W. J. and Crittenden J. C. (1969). Surface chemistry of active carbon: Specific adsorption of phenols. *Journal of Colloid and Interface Science* **31**(1): 116-130.
- McEvoy, N., Nolan H., Ashok Kumar N., Hallam T., and Duesberg G. S. (2013). Functionalisation of graphene surfaces with downstream plasma treatments. *Carbon* **54**: 283-290.
- McGrath, M. P. and Pham A. (2006). Carbon Nanotube Based Microwave Resonator Gas Sensors. *International Journal of High Speed Electronics and Systems* **16**(04): 913-935.
- Menendez, J. A., Phillips J., Xia B., and Radovic L. R. (1996). On the Modification and Characterization of Chemical Surface Properties of Activated Carbon: In the Search of Carbons with Stable Basic Properties. *Langmuir* **12**(18): 4404-4410.
- Miller, S. R., Pearce G. M., Wright P. A., Bonino F., Chavan S., Bordiga S., Margiolaki I., Guillou N., Férey G., Bourrelly S., and Llewellyn P. L. (2008). Structural Transformations and Adsorption of Fuel-Related Gases of a Structurally Responsive Nickel Phosphonate Metal–Organic Framework, Ni-STA-12. *Journal of the American Chemical Society* **130**(47): 15967-15981.
- Millward, A. R. and Yaghi O. M. (2005). Metal-Organic Frameworks with Exceptionally High Capacity for Storage of Carbon Dioxide at Room Temperature. *Journal of the American Chemical Society* **127**(51): 17998-17999.

- Morbidelli M., Gavriilidis A., and Varma A. (2001). *Catalyst design*, Cambridge University Press, UK: 149-150.
- Mueller, U., Schubert M., Teich F., Puetter H., Schierle-Arndt K., and Pastre J. (2006). Metal-organic frameworks-prospective industrial applications. *Journal of Materials Chemistry* **16**(7): 626-636.
- National Center for Biotechnology Information. PubChem Compound Database (2017); (a) CID=74819, <https://pubchem.ncbi.nlm.nih.gov/compound/74819>; (b) CID=8113, <https://pubchem.ncbi.nlm.nih.gov/compound/8113>; (c) CID=7767, <https://pubchem.ncbi.nlm.nih.gov/compound/7767>; (d) CID=8197, <https://pubchem.ncbi.nlm.nih.gov/compound/8197>
- Nayak, A. K., Ghosh R., Santra S., Guha P. K., and Pradhan D. (2015). Hierarchical nanostructured WO₃-SnO₂ for selective sensing of volatile organic compounds. *Nanoscale* **7**(29): 12460-12473.
- Olajire, A. A. (2010). CO₂ capture and separation technologies for end-of-pipe applications – A review. *Energy* **35**(6): 2610-2628.
- Petit, C. and Bandosz T. J. (2011). Synthesis, Characterization, and Ammonia Adsorption Properties of Mesoporous Metal–Organic Framework (MIL(Fe))–Graphite Oxide Composites: Exploring the Limits of Materials Fabrication. *Advanced Functional Materials* **21**(11): 2108-2117.
- Pevida, C., Plaza M. G., Arias B., Feroso J., Rubiera F., and Pis J. J. (2008). Surface modification of activated carbons for CO₂ capture. *Applied Surface Science* **254**(22): 7165-7172.

- Pichon, A., Lazuen-Garay A., and James S. L. (2006). Solvent-free synthesis of a microporous metal-organic framework. *CrystEngComm* **8**(3): 211-214.
- Pipatsantipong, S., Rangsunvigit P., and Kulprathipanja S. (2012). Towards CO₂ adsorption enhancement via polyethyleneimine impregnation. *International Journal of Chemical and Biological Engineering* **6**: 291-295.
- Pirngruber, G. D., Cassiano-Gaspar S., Louret S., Chaumonnot A., and Delfort B. (2009). Amines immobilized on a solid support for postcombustion CO₂ capture: A preliminary analysis of the performance in a VSA or TSA process based on the adsorption isotherms and kinetic data. *Energy Procedia* **1**(1): 1335-1342.
- Plaza, M. G., Pevida C., Arenillas A., Rubiera F., and Pis J. J. (2007). CO₂ capture by adsorption with nitrogen enriched carbons. *Fuel* **86**(14): 2204-2212.
- Plaza, M. G., Pevida C., Arias B., Feroso J., Rubiera F., and Pis J. J. (2009). A comparison of two methods for producing CO₂ capture adsorbents. *Energy Procedia* **1**(1): 1107-1113.
- R. Veneman, Kamphuis H., and Brilman D. W. F. (2013). Post combustion CO₂ capture using supported amine sorbents: A process integration study. *Energy Procedia*: 1-9.
- Rackley, S. A. (2010). *Carbon Capture and Storage*, Butterworth-Heinemann/Elsevier.
- Rauscher, H., Perucca M., and Buyle G. (2010). Plasma Technology for Hyperfunctional Surfaces: Food, Biomedical and Textile Applications, *Wiley*.
- Rivera-Tinoco, R. and Bouallou C. (2010). Comparison of absorption rates and absorption capacity of ammonia solvents with MEA and MDEA aqueous blends for CO₂ capture. *Journal of Cleaner Production* **18**(9): 875-880.

- Robeson, L. M. (1991). Correlation of separation factor versus permeability for polymeric membranes. *Journal of Membrane Science* **62**(2): 165-185.
- Robeson, L. M. (2008). The upper bound revisited. *Journal of Membrane Science* **320**(1–2): 390-400.
- Wong S. and Bioletti R. (2002). Carbon Dioxide Separation Technologies. Edmonton, Alberta, *Alberta Research Council Inc (ARC)*
- Sartori, G. and Savage D. W. (1983). Sterically hindered amines for carbon dioxide removal from gases. *Industrial & Engineering Chemistry Fundamentals* **22**(2): 239-249.
- Satyapal, S., Filburn T., Trela J. and Strange J. (2001). Performance and Properties of a Solid Amine Sorbent for Carbon Dioxide Removal in Space Life Support Applications. *Energy & Fuels* **15**(2): 250-255.
- Shackley, S. and Gough C. (2006). Carbon Capture and Its Storage: An Integrated Assessment, *Ashgate*.
- Shawwa, A. R., Smith D. W., and Segó D. C. (2001). Color and chlorinated organics removal from pulp mills wastewater using activated petroleum coke. *Water Research* **35**(3): 745-749.
- Shieh, Y.-T., Liu G.-L., Wu H.-H., and Lee C.-C. (2007). Effects of polarity and pH on the solubility of acid-treated carbon nanotubes in different media. *Carbon* **45**(9): 1880-1890.
- Simmons, J. M., Wu H., Zhou W., and Yildirim T. (2011). Carbon capture in metal-organic frameworks-a comparative study. *Energy & Environmental Science* **4**(6): 2177-2185.

- Singh, G., Botcha V. D., Narayanam P. K., Sutar D. S., Talwar S. S., Srinivasa R. S., and Major S. S. (2013). Effect of ammonia plasma treatment on graphene oxide LB monolayers. *AIP Conference Proceedings* **1512**(1): 702-703.
- Siriwardane, R. V., Shen M.S., Fisher E. P., and Poston J. A. (2001). Adsorption of CO₂ on Molecular Sieves and Activated Carbon. *Energy & Fuels* **15**(2): 279-284.
- Small, C., Ulrich A. C., and Hashisho Z. (2012). Adsorption of Acid Extractable Oil Sands Tailings Organics onto Raw and Activated Oil Sands Coke. *Journal of Environmental Engineering* **138**(8): 833-840.
- Small, C. C., Hashisho Z., and Ulrich A. C. (2012). Preparation and characterization of activated carbon from oil sands coke. *Fuel* **92**(1): 69-76.
- Smith, B., Wepasnick K., Schrote K. E., Cho H. H., Ball W. P., and Fairbrother D. H. (2009). Influence of surface oxides on the colloidal stability of multi-walled carbon nanotubes: A structure– property relationship. *Langmuir* **25**(17): 9767-9776.
- Sohrabi, A., Shaibani P. M., Zarifi M. H., Daneshmand M., and Thundat T. (2014). A novel technique for rapid vapor detection using swelling polymer covered microstrip ring resonator. *2014 IEEE MTT-S International Microwave Symposium (IMS2014)*.
- Stavropoulos, G. G. and Zabaniotou A. A. (2009). Minimizing activated carbons production cost. *Fuel Processing Technology* **90**(7–8): 952-957.
- Stegmeier, S., Fleischer M., Tawil A., Hauptmann P., Egly K., and Rose K. (2009). Mechanism of the interaction of CO₂ and humidity with primary amino group systems for room temperature CO₂ sensors. *Procedia Chemistry* **1**(1): 236-239.

- Sumida, K., Rogow D. L., Mason J. A., McDonald T. M., Bloch E. D., Herm Z. R., Bae T. H., and Long J. R. (2012). Carbon Dioxide Capture in Metal–Organic Frameworks. *Chemical Reviews* **112**(2): 724-781.
- Sun, Y., Wang Y., Zhang Y., Zhou Y., and Zhou L. (2007). CO₂ sorption in activated carbon in the presence of water. *Chemical Physics Letters* **437**(1-3): 14-16.
- Suslick, K. S., Hammerton D. A., and Cline R. E. (1986). Sonochemical hot spot. *Journal of the American Chemical Society* **108**(18): 5641-5642.
- Tarka, T. J., Ciferno J. P., McMahan L. G. , and Fauth D. (2006). CO₂ Capture Systems Using Amine Enhanced Solid Sorbents. *5th Annual Conference on Carbon Capture & Sequestration, Alexandria, VA, USA.*
- Fout T., J. T. M. and Jones A. P. (2009). DOE/NETL’s Carbon Capture R&D Program for Existing Coal-Fired Power Plants. Energy, National Energy Technology Laboratory
- Tontiwachwuthikul, P., Wee A. G. H., Idem R., Maneeintr K. , Fan G.J. , Amornvadee V., Amr H., Aroonwilas A. , Chakma A. (2011). Method of capturing carbon dioxide from gas streams. *US Patent, US 7910078 B2*
- Tranchemontagne, D. J., Mendoza-Cortes J. L., O’Keeffe M., and Yaghi O. M. (2009). Secondary building units, nets and bonding in the chemistry of metal-organic frameworks. *Chemical Society Reviews* **38**(5): 1257-1283.
- Vaidhyanathan, R., Iremonger S. S., Dawson K. W. , and Shimizu G. K. H. (2009). An amine-functionalized metal organic framework for preferential CO₂ adsorption at low pressures. *Chemical Communications* (35): 5230-5232.

- Veawab, A., Aroonwilas A., Chakma A., and Tontiwachwuthikul P. (2008). Solvent Formulation for CO₂ Separation from Flue Gas Streams, Faculty of Engineering, University of Regina.
- Wagner, T., Haffer S., Weinberger C., Klaus D., and Tiemann M. (2013). Mesoporous materials as gas sensors. *Chemical Society Reviews* **42**(9): 4036-4053.
- Wang, B., Long J., and Teo K. (2016). Multi-Channel Capacitive Sensor Arrays. *Sensors* **16**(2): 150.
- Wang, P., Liu Z. G., Chen X., Meng F. L., Liu J. H., and Huang X. J. (2013). UV irradiation synthesis of an Au-graphene nanocomposite with enhanced electrochemical sensing properties. *Journal of Materials Chemistry A* **1**(32): 9189-9195.
- Wang, X., Li X., Zhang L., Yoon Y., Weber P. K., Wang H., Guo J., and Dai H. (2009). N-doping of graphene through electrothermal reactions with ammonia. *Science* **324**(5928): 768-771.
- Wang, Y., Chyu M. K., and Wang Q. M. (2014). Passive wireless surface acoustic wave CO₂ sensor with carbon nanotube nanocomposite as an interface layer. *Sensors and Actuators A: Physical* **220**: 34-44.
- Wark, M., Rohlfig Y., Altindag Y., and Wellmann H. (2003). Optical gas sensing by semiconductor nanoparticles or organic dye molecules hosted in the pores of mesoporous siliceous MCM-41. *Physical Chemistry Chemical Physics* **5**(23): 5188-5194.

- Wei, J., Liao L., Xiao Y., Zhang P., and Shi Y. (2010) Capture of carbon dioxide by amine-impregnated as-synthesized MCM-41. *Journal of Environmental Sciences* **22**(10): 1558-1563.
- Wiltshire, J., Khlobystov A., Li L., Lyapin S., Briggs G., and Nicholas R. (2004). Comparative studies on acid and thermal based selective purification of HiPCO produced single-walled carbon nanotubes. *Chemical Physics Letters* **386**(4): 239-243.
- Wu, H., Simmons J. M., Liu Y., Brown C. M., Wang X. S., Ma S., Peterson V. K., Southon P. D., Kepert C. J., Zhou H. C., Yildirim T., and Zhou. W. (2010). Metal–Organic Frameworks with Exceptionally High Methane Uptake: Where and How is Methane Stored? *Chemistry – A European Journal* **16**(17): 5205-5214.
- Wu, H., Simmons J. M., Srinivas G., Zhou W., and Yildirim T. (2010). Adsorption Sites and Binding Nature of CO₂ in Prototypical Metal-Organic Frameworks: A Combined Neutron Diffraction and First-Principles Study. *The Journal of Physical Chemistry Letters* **1**(13): 1946-1951.
- Xie, J., Yan N., Qu Z., and Yang S. (2012). Synthesis, characterization and experimental investigation of Cu-BTC as CO₂ adsorbent from flue gas. *Journal of Environmental Sciences* **24**(4): 640-644.
- Xu, P., Li X., Yu H., and Xu T. (2014). Advanced Nanoporous Materials for Micro-Gravimetric Sensing to Trace-Level Bio/Chemical Molecules. *Sensors* **14**(10): 19023.

- Xu, X., Song C., Andresen J. M., Miller B. G., and Scaroni A. W. (2002). Novel Polyethylenimine-Modified Mesoporous Molecular Sieve of MCM-41 Type as High-Capacity Adsorbent for CO₂ Capture. *Energy & Fuels* **16**(6): 1463-1469.
- Xu, X., Song C., Miller B. G., and Scaroni A. W. (2005). Adsorption separation of carbon dioxide from flue gas of natural gas-fired boiler by a novel nanoporous Molecular basket adsorbent. *Fuel Processing Technology* **86**(14-15): 1457-1472.
- Yamagiwa, H., Sato S., Fukawa T., Ikehara T., Maeda R., Mihara T., and Kimura M. (2014). Detection of Volatile Organic Compounds by Weight-Detectable Sensors coated with Metal-Organic Frameworks. *Scientific Reports* **4**: 6247.
- Yang, D., Velamakanni A., Bozoklu G., Park S., Stoller M., Piner R. D., Stankovich S., Jung I., Field D. A., Ventrice C. A., and Ruoff R. S. (2009). Chemical analysis of graphene oxide films after heat and chemical treatments by X-ray photoelectron and Micro-Raman spectroscopy. *Carbon* **47**(1): 145-152.
- Yang, H., Xu Z., Fan M., Gupta R., Slimane R. B., Bland A. E., and Wright I. (2008). Progress in carbon dioxide separation and capture: A review. *Journal of Environmental Sciences* **20**(1): 14-27.
- Yazaydin, A. Ö., Snurr R. Q., Park T. H., Koh K., Liu J., LeVan M. D., Benin A. I., Jakubczak P., Lanuza M., Galloway D. B., Low J. J., and Willis R. R. (2009). Screening of Metal–Organic Frameworks for Carbon Dioxide Capture from Flue Gas Using a Combined Experimental and Modeling Approach. *Journal of the American Chemical Society* **131**(51): 18198-18199.

- Zanganeh, K. E., Shafeen A., and Salvador C. (2009). CO₂ Capture and Development of an Advanced Pilot-Scale Cryogenic Separation and Compression Unit. *Energy Procedia* **1**(1): 247-252.
- Zarifi, M. H., Fayaz M., Goldthorp J., Abdolrazzaghi M., Hashisho Z., and Daneshmand M. (2015). Microbead-assisted high resolution microwave planar ring resonator for organic-vapor sensing. *Applied Physics Letters* **106**(6): 062903.
- Zarifi, M. H., Rahimi M., Daneshmand M., and Thundat T. (2016). Microwave ring resonator-based non-contact interface sensor for oil sands applications. *Sensors and Actuators B: Chemical* **224**: 632-639.
- Zelenak, V., Halamova D., Gaberova L., Bloch E., and Llewellyn P. (2008). Amine-modified SBA-12 mesoporous silica for carbon dioxide capture: Effect of amine basicity on sorption properties. *Microporous and Mesoporous Materials* **116**(1-3): 358-364.
- Zhang, Z., Xu M., Wang H., and Li Z. (2010). Enhancement of CO₂ adsorption on high surface area activated carbon modified by N₂, H₂ and ammonia. *Chemical Engineering Journal* **160**(2): 571-577.
- Zhao, B., Zhang L., Wang X., and Yang J. (2012). Surface functionalization of vertically-aligned carbon nanotube forests by radio-frequency Ar/O₂ plasma. *Carbon* **50**(8): 2710-2716.
- Zhao, J., Losego M. D., Lemaire P. C., Williams P. S., Gong B., Atanasov S. E., Blevins T. M., Oldham C. J., Walls H. J., Shepherd S. D., Browe M. A., Peterson G. W., and Parsons G. N. (2014). Highly Adsorptive, MOF-Functionalized Nonwoven

Fiber Mats for Hazardous Gas Capture Enabled by Atomic Layer Deposition.

Advanced Materials Interfaces **1**(4): 1400040-n/a

Zhao, Z., Li Z., and Lin Y. S. (2009). Adsorption and Diffusion of Carbon Dioxide on Metal–Organic Framework (MOF-5). *Industrial & Engineering Chemistry Research* **48**(22): 10015-10020.

Zhuang, J. L., Ar D., Yu X. J., Liu J. X. and Terfort A. (2013). Patterned Deposition of Metal-Organic Frameworks onto Plastic, Paper, and Textile Substrates by Inkjet Printing of a Precursor Solution. *Advanced Materials* **25**(33): 4631-4635.

CHAPTER 3. ENHANCING CO₂ ADSORPTION VIA AMINE IMPREGNATED ACTIVATED CARBON FROM OIL SANDS COKE

3.1. Introduction

Large-scale CO₂ control is essential to minimize global impacts associated with climate change (Chang et al., 2003, Zhang et al., 2010). The concentration of CO₂ in different gas streams varies from about 13% in coal-fired power plant flue gas to about 60% in hot stove gas in steel welding process (Xiaochun Xu and Bruce G. Miller, 2003). CO₂ capture and sequestration is a potential approach to reduce CO₂ emissions (Xu et al., 2002). Cryogenic processes, membrane separation, chemical absorption, and adsorption have been investigated in the literature for CO₂ capture. In particular, chemical absorption with amines (wet scrubbing) is currently being implemented on industrial scale for CO₂ capture (Zhang et al., 2010, Ko et al., 2011, Khalil et al., 2012, Pipatsantipong et al., 2012). While effective at capturing CO₂, wet scrubbing is energy intensive (R. Veneman et al., 2013), and suffers from corrosion, solvent leakage, and limited amine availability in the aqueous phase due to poor solubility (Franchi et al., 2005). To remedy these problems, liquid amines are added to solid supports (Xu et al., 2002). These materials modify the fundamental CO₂ control mechanism by incorporating amines that are typically used for absorption into adsorbents, benefiting from the high CO₂ capacity of amines but limiting the challenges associated with liquid absorbents.

Solid sorbents use physisorption or chemisorption to capture CO₂ (Ko et al., 2011). Tested sorbents for CO₂ capture include zeolites (Chatti et al., 2009), activated carbons (Saha and Deng, 2010), calcium oxides (Lee et al., 2008), hydrotalcites (Hutson et al., 2004), metal

organic frameworks (Walton et al., 2007), amino-polymers (Yang et al., 2010), and organic-inorganic hybrids (Alauzun et al., 2005). Zeolites, activated carbons, and organic-inorganic hybrids operate at room temperature, while the others require temperatures $> 100^{\circ}\text{C}$ (Choi et al., 2009, Ko et al., 2011). Although Zeolite 13X outperforms other adsorbents at atmospheric pressure and dry conditions, it requires stringent moisture control and high temperature regeneration ($300 - 400^{\circ}\text{C}$) (Franchi et al., 2005).

Activated carbon (AC) is a widely used adsorbent because it is inexpensive, is physically stable in acidic and/or basic solutions, has modifiable pore structure and surface chemistry, and can, often, be regenerated at low cost (Gray et al., 2004). AC precursors can be any organic material such as coal, wood, and fruit/nut shells (Hu and Srinivasan, 2001, Kang et al., 2011, Foo and Hameed, 2012, Zhang et al., 2012). Oil sands coke in the Athabasca basin, produced as a by-product of bitumen upgrading, is readily available at low cost and has high carbon content (approximately 80 – 85% by weight) (Small et al., 2012), making it a suitable precursor for AC production.

Upgrading oil sands bitumen requires a complex thermal treatment and produces coke as a byproduct (Fedorak and Coy, 2006). Current estimates indicate a total of 1 billion m^3 of coke production over the lifetime of oil sands operations in Alberta. Most of the coke is currently stockpiled on-site, and only small quantities are consumed as fuel for steam and electricity generation (Furimsky, 1998). However, the use of coke as a fuel cannot keep up with the rate of coke production. In addition, coke combustion produces CO_2 , promoting the stigma associated with the CO_2 -intensive oil sands operations. Hence, there is a need for better management and use for stockpiled coke. Transforming this waste into AC provides a solution to both waste management and CO_2 capture needs.

Additionally, the high nitrogen content (1.6 wt%) of this material compared to other AC precursors (Plaza et al., 2007, Dong-II Jang and Park, 2011), makes the produced AC basic and preferred for acid gas adsorption. This is due to the incorporation of pyridine-like nitrogen functionalities in the carbon structure during high temperature activation (up to 950 °C) (Bandosz, 2006, Sullivan et al., 2012, Zhang et al., 2012). Also according to previous investigation (Chen and Hashisho, 2012), delayed coke could yield AC with higher surface area than fluid coke (1063 vs. 658 m²/g), hence delayed coke was used as precursor in this study.

Modification of a carbon's surface chemistry, including oxidation, amination, sulfonation, bromination, and metal impregnation, impacts its adsorption properties (Ugarte and Swider-Lyons, 2005, Lee et al., 2013). For acid gas adsorption, including CO₂, increasing the basicity of the adsorbent through amination is expected to increase its capacity for the contaminant (Lee et al., 2013).

Impregnation with low molecular weight amines, including diethanolamine (DEA), methyl-diethanolamine (MDEA), and tetra-ethylene pentamine (TEPA), can accomplish this goal (Heydari-Gorji et al., 2011). The choice of the impregnant depends on process and material parameters including amine size and molecular weight, adsorbate dimensions and potential for steric hindrances, adsorbent pore size distribution, and regeneration conditions (Rivera-Tinoco and Bouallou, 2010, Tontiwachwuthikul et al., 2011).

Traditionally, monoethanolamine (MEA) is used for CO₂ absorption because it has the lowest molecular weight and the highest theoretical CO₂ absorption capacity (9.09 mmol CO₂/g of absorbent (Rivera-Tinoco and Bouallou, 2010)). This theoretical capacity, however, has not been achieved in practice due to corrosion of scrubber vessels and ductwork in amine plants caused by amine degradation (Veawab et al., 1999) Different types of amine modified adsorbents

have been studied. Yue et al. (2006) used SBA-15 and modified it with TEPA. The highest adsorption capacity achieved was 3.43 mmol CO₂/g adsorbent at 50 wt% and 100°C. DEA is also commonly used because it has a lower vapor pressure than MEA and is less susceptible to volatilization (Kamarudin and Mat, 2009). TEPA, on the other hand, is a weaker base than DEA, and its weakened N-H bond allows for regeneration under less intense conditions (e.g., lower temperatures, lower pressures) (Bonenfant et al., 2003).

In this work, a unique AC was prepared from waste oil sands coke and was then modified with different amines (DEA, MDEA, and TEPA). The aim of this work was to evaluate the modified oil sands AC for CO₂ adsorption as, to the best of our knowledge, systematic studies investigating CO₂ capture using AC prepared from this unique waste precursor have not been reported. Also, the impact of preparation and processing parameters, including amine loading, adsorption temperature, and humidity, on the CO₂ capture capacity of the amine-impregnated samples were studied.

3.2. Experimental Section

3.2.1. Activated Carbon Preparation

Delayed oil sands coke, a by-product of bitumen thermal cracking, was provided by Suncor Energy. KOH (ACS grade, Fisher scientific) was used as activation agent. Diethanolamine, methyl-diethanolamine and tetra ethylenepentamine (reagent grade, Sigma Aldrich) were used for impregnation.

Delayed coke was ground, sieved (180-212 µm), and dried overnight at 110 °C (Chen and Hashisho, 2012). KOH (dissolved in H₂O) was used as activation agent and was mixed with an equal mass of dry coke. The mixture was heated at 110°C until all water evaporated. 25 – 30 g of the dried powder was added to a crucible covered with glass wool, and placed in a quartz

reactor (inner diameter = 2.6 cm, height = 20 cm) purged with 500 ml/min of humidified N₂. Dry nitrogen passed through an impinger containing water before purging the activation reactor. The sample was heated for 20 min in a 2.45 GHz multimode microwave applicator (Kenmore, 721.80602) with 800 W nominal power output. After activation, the product was washed with water and 1 M hydrochloric acid to remove KOH, and then was dried overnight at 110°C before use.

3.2.2. Amine Impregnation

DEA, MDEA, and TEPA were added to the activated carbon prepared from delayed coke. Different amounts of each amine were dissolved in 20 ml of water (based on activated carbon pore volume and amine loading) and added to a beaker containing 5 g of activated carbon. The theoretical amount of amine loading on the support is defined by equation 1 (Choi et al., 2009, Lee et al., 2013):

$$\text{Maximum Percentage of amine impregnated on a support} = \text{Pore volume of support} \times \text{Density of amine} \times 100 \quad (\text{eq. 1})$$

The slurry was stirred in a rotary evaporator (Brinkman-RE120) for 2 h at 40°C before separation by vacuum filtration. Prepared materials were dried at 110°C before use and stored in a desiccator afterwards.

Amine loading was quantified with acid titration (Cummings et al., 1990). Each amine solution was titrated with hydrochloric acid (1 M) before and after impregnation. Free amine concentration was determined based on the volume of consumed acid [45], and difference in basicity of amine solution before and after measurements was attributed to uptake by the activated carbon.

3.2.3. Materials Characterization

3.2.3.1. Iodine number

The iodine number of prepared activated carbon was determined following American Society for Testing and Materials method D4607 (ASTM, 2006) and interpreted as the amount of iodine adsorbed (in mg iodine / g adsorbent) at a residual iodine concentration of 0.018 N.

3.2.3.2. Nitrogen adsorption

Nitrogen adsorption isotherms were obtained at 77 K using a surface area analyzer (Quantachrome Instruments, Autosorb-1MP). Prior to the measurement, samples were degassed at 120°C (atmospheric pressure) for 5 h. Specific surface area and micropore volume were determined from the N₂ adsorption isotherm using the Brunauer-Emmett-Teller (BET) equation and the V-t method, respectively. The pore size distribution was determined using density functional theory (DFT) for slit-shaped pores (Bandosz, 2006, Dunne and Manos, 2010), and total pore volume was recorded at $p/p_0 = 0.95$ (Zhang et al., 2010). The average pore diameter (D_p) was calculated as $D_p = 4 V_p/S_{BET}$, assuming cylindrical shape pores, where V_p and S_{BET} are the pore volume and BET surface area of the material.

3.2.3.3. Bulk and surface elemental composition

The bulk composition (carbon, hydrogen, nitrogen, sulfur, and oxygen) of prepared samples was characterized using a CHNS elemental analyzer (Vario MICRO). Oxygen in the sample is determined by mass difference ($100\% - C \text{ wt}\% - H \text{ wt}\% - N \text{ wt}\% - S \text{ wt}\%$), assuming that ash content is negligible (Thompson, 2008). The method detection limits are: carbon, 0.25%, nitrogen 0.25%, hydrogen 0.25%, oxygen 0.25% and sulfur 0.27%.

The surface composition of prepared samples was characterized using X-Ray Photoelectron Spectroscopy (XPS, Kratos AXIS 165) with Mono Al K α radiation at 210 W and 14 kV, under ultrahigh vacuum (10^{-9} Torr). Spectra were calibrated to a C1s peak location of

284.5 eV. The method detection limit is 0.1%. Casa XPS Software was used to process the XPS scans and the results were reported in terms of weight concentration (%wt.). The weight concentration of each element was calculated based on its atomic percentage multiplied by its atomic mass, divided by the summation of weight concentration of other elements in the compound.

3.2.3.4. pH at point of zero charge

The pH value of the point of zero charge (pH_{PZC}) for delayed coke and activated delayed coke was measured with a pH meter (OAKTON pH700). 2 wt% carbon in deionized water was stirred for > 24 h. The pH measurements were conducted in duplicates and the average was reported as the pH_{PZC} for that material (Atkinson et al., 2013).

3.2.4. CO₂ adsorption experiment

The prepared sorbents were screened for CO₂ adsorption performance using a thermogravimetric analyzer (TGA/DSC 1, Mettler Toledo). 10 mg of sample was placed in an alumina crucible, heated at 10° C/min to 120°C in 100 mL/min N₂, and then held at this temperature for 30 min to remove water vapor. The temperature was then ramped down to the adsorption set-point at 10°C/min, and the sample was held at this temperature until a stable weight was reached, at which point the gas was switched to 200 mL/min of 99.99% CO₂ mixed with 100 mL/min of N₂ (66.6% CO₂ in N₂). Different adsorption temperatures (40, 50, 60 and 75°C) were tested based on previous studies (Pirngruber et al., 2009, Khalil et al., 2012) to achieve optimum temperature for CO₂ adsorption.

The adsorption capacity was determined in mmol of adsorbate (CO₂) / g of adsorbent. In order to evaluate the stability performance of impregnated samples, 15 adsorption-regeneration cycles were completed on the sample with the highest CO₂ adsorption capacity. Adsorption was

followed by regeneration in the TGA at 110 °C (heating rate of 10 °C/min) in 100 mL/min of N₂ (99.999%).

To study the adsorption behavior of impregnated samples at CO₂ levels closer to those in the flue gas, adsorption tests were also completed at a lower concentration of CO₂ (20% CO₂ in N₂) obtained using a flow of 50 mL/min of 99.99% CO₂ and 200 mL/min of N₂. In order to measure the effect of humidity on adsorption behavior of samples, breakthrough tests were completed. The adsorption setup consisted of an adsorption tube, a power application module, and a data acquisition and control system (DAC) (Figure 3-1). Further information about the adsorption setup is available elsewhere (Lashaki et al., 2012). 2 g of as-prepared or amine-impregnated activated carbon was added to a stainless steel tube (inner diameter = 0.88 cm, length = 10.16 cm), with glass wool at the top and bottom. The adsorption feed gas (20% CO₂ in dry N₂) was humidified (to 0 – 40% RH as discussed in section 3.3.4.) by water injection using a syringe pump and introduced into the adsorption tube at 0.25 SLPM. Effluent CO₂ was analyzed every 20 seconds for 10 min using Gas Chromatography-Thermal Conductivity Detection (GC-TCD). Adsorption experiments were completed at 50°C, measured with a 0.5 mm outer diameter thermocouple in the center of the adsorbent bed and the adsorption tube was wrapped with a heating tape to maintain the adsorption temperature. A DAC system that included a LabVIEW program (National Instruments) and a proportional-integral-derivative algorithm controlled power application to the heating tape to maintain the tube at 50 °C during adsorption.

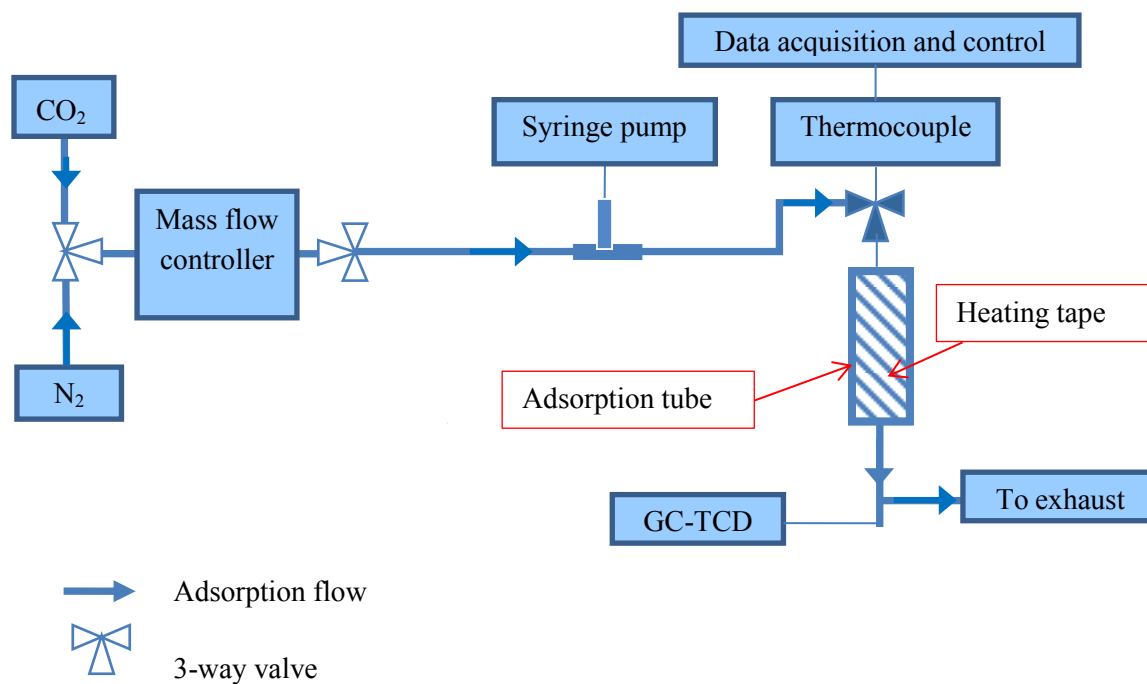


Figure 3-1. Schematic diagram of CO₂ adsorption set-up

3.3. Results

3.3.1. Raw and activated delayed coke

Physical, chemical, and N₂ adsorption properties of the raw delayed coke and the activated delayed coke are described in Table 3-1. Activation vastly increases the pore volume and specific surface area of the product, making it a potentially effective adsorbent for gas-phase applications. This is consistent with the literature for microwave activation of raw delayed coke (Chen and Hashisho, 2012). Comparing to commercial activated carbons with a range of surface area (846-1943 m²/g) (Houshmand et al., 2012, Siriwardane et al., 2001, Sun et al., 2007, Pevida et al., 2008) our prepared AC possess reasonable surface area ($S_{\text{BET}} = 1068 \text{ m}^2/\text{g}$) for this application.

During activation, volatile components are released from the precursor, generating a small degree of porosity inside the carbon structure. KOH reactivity within the high carbon-content structure removes reactive carbon sites during activation, generating micropores that vastly increase the surface area and pore volume of the product (Marsh and Rodriguez-Reinoso, 2006, Chen and Hashisho, 2012) (Table 3-1). Carbon burn-off yields CO and CO₂ and is governed by diffusion control, burning the carbon only on the surface of particles and not in the bulk (Bandosz, 2006). Accordingly, upon activation the carbon content on the surface decreased from 87 to 84.4%.

The nearly 50x higher iodine number for the activated material compared to the raw coke also suggests strong adsorption performance in applications that require large micropores / small mesopores.

Table 3-1. Physical and chemical properties of raw and activated delayed coke

		Raw delayed oil sands coke	Activated carbon
Bulk composition, CHNS analysis (%wt.)	N	1.4	1.6
	C	82.3	87.4
	H	3.7	1.0
	S	6.8	1.4
	O	5.8	8.6
Surface composition, XPS (%wt.)	N	0.9	1.4
	C	87.0	84.4
	K	0.0	1.7
	O	6.5	10.9

	S	4.0	0.8
	Si	1.6	0.8

Relative surface nitrogen content of the AC (Table 3-1-XPS results) increased from 0.9 to 1.4 wt% following activation and is quite high compared to many commercially available carbonaceous adsorbents (typically from 0.05 to 0.22 N%) (Xu et al., 2008, Liou, 2010). This increase is primarily attributed to the removal of acidic carbon/oxygen functionalities with the high temperature treatment, increasing the relative nitrogen content and basicity of the sample (Zhang et al., 2010). Nitrogen addition through high temperature reactions between the carrier gas and the carbon structure may also occur but is expected to be minor (Bandosz, 2006). This trend is confirmed by pH_{PZC} results for delayed coke and AC. Activation increased the pH_{PZC} from 7.1 to 9.6, indicating that basic functional groups are present. To confirm the presence of pyridine and pyrrolic functional groups upon activation, the XPS spectra with corresponding nitrogen peak models for delayed coke as well as AC is presented in Figure A1. Peaks at 398.2 and 399.5 eV correspond to pyridine-like and pyrrole-like nitrogen, respectively. Graphitic nitrogen is present at 401.1 eV, and the high energy peak at 402.6 eV is attributed to oxidized nitrogen (Liu et al., 2015). Percentages of pyridinic, pyrrolic, graphitic, and oxidized nitrogen are summarized in X-ray Photo electron Spectroscopy Measurement (Appendix A)

In a XPS spectrum, peak intensities of different elements correspond to their atomic percentage present in a sample. The atomic percentage of each element then can be easily converted to weight percentage by multiplying by its molecular weight.

From Table A1, the total percentage of pyridinic and pyrrolic nitrogen increases by 17% after activation, which is consistent with pH_{PZC} results that show a more basic material.

A comparison to other carbons in the literature indicates that this as-prepared AC compares chemically to carbons that have been tailored to have basic properties by high temperature ammonia treatment (Zhang et al., 2010). Removing the need for this post-preparation modification step provides a significant advantage for activated carbons prepared from delayed coke. Also the relative carbon content in the bulk increased from 82.3 to 87.4% after activation, due to the loss of other elements such as sulfur. This is consistent with previous research (Lee and Choi, 2000) indicating sulfur loss when the activation of petroleum coke resulted in high surface area activated carbon. However, there was an increase in oxygen content from 5.7 to 8.6% upon activation possibly due to incomplete acid wash after activation, as traces of K was observed in XPS analysis after activation.

3.3.2. Impregnated activated carbon materials

Table 3-2 describes the physical, chemical, and adsorption properties of the activated carbon samples impregnated with varying amounts of DEA, MDEA, and TEPA. Acid titration measurements showed that amine loading for AC-DEA samples ranged from 0.22 to 1.78 mmol N/g AC, while it ranged from 0.15 to 2.25 mmol N/g AC for AC-MDEA samples, and from 0.52 to 2.85 mmol N/g AC for AC-TEPA samples (Table 3-2). Results from CHNS and XPS analyses support increased nitrogen content following impregnation with amines (Table 3-2). In general, these results show higher nitrogen content on the surface of the impregnated materials compared to the bulk, which might be attributed to diffusion limitations, especially for large amines.

Table 3-2. Physical, chemical and adsorption properties of raw and impregnated samples

Sample	Amine loading (mmol N/g AC)	Iodine Number (mg/g)	BET surface area (m ² /g)	Pore volume (cc/g)	Micropore volume (cc/g)	Average pore diameter (Å)	N% surface	N% bulk
Raw delayed coke	–	22	2.70	0.00	0.00	-	0.90	1.40
Activated carbon (AC)	–	1068	889.01	0.29	0.20	5.73	1.40	1.60
AC-DEA	0.22	847	251.03	0.17	0.10	13.20	2.74	1.64
AC-DEA	0.52	581	118.10	0.08	0.04	16.87	2.88	2.15
AC-DEA	0.62	479	93.95	0.07	0.03	16.81	3.37	2.44
AC-DEA	1.15	339	82.10	0.06	0.04	15.43	3.51	2.60
AC-DEA	1.78	254	56.75	0.05	0.03	14.13	3.25	2.52
AC-MDEA	0.49	631	273.00	0.16	0.14	15.75	2.22	1.08
AC-MDEA	0.56	529	250.40	0.15	0.12	15.43	3.27	1.85
AC-MDEA	2.14	343	168.30	0.10	0.07	15.04	2.59	2.58
AC-MDEA	2.25	301	134.40	0.08	0.06	14.74	2.47	2.72
AC-TEPA	0.52	501	102.00	0.04	0.02	21.53	4.85	3.11
AC-TEPA	0.89	103	25.20	0.01	0.00	23.32	7.66	4.07
AC-TEPA	1.03	291	71.00	0.02	0.00	23.60	5.15	3.18
AC-TEPA	1.77	262	63.06	0.02	0.00	23.71	5.86	3.40
AC-TEPA	2.85	86	17.60	0.03	0.00	29.54	9.99	4.46

For each type of amine, decreasing iodine numbers with increasing nitrogen loading was observed, which supports partial pore filling associated with nitrogen impregnation (Chang et al., 2003). This result is consistent with the decrease in BET surface area and total pore volume (Khalil et al., 2012). Figure 3-2 presents pore size distribution of as prepared and impregnated activated carbon samples. Activated carbon is mostly (~69%) microporous while impregnation with amine results in lower microporosity. Samples impregnated with DEA (AC-DEA) have larger decreases in pore volume and surface area than samples impregnated with MDEA (AC-MDEA). For example, samples with about 0.5 mmol N/g AC, BET surface area is 53% lower for AC-DEA compared to AC-MDEA. This may be because DEA (molecule diameter=3.75 Å) more readily fills the carbon's micropores compared to the bulkier MDEA (molecule diameter= 8.81 Å) (Yin et al., 2008). Therefore, despite having similar loadings, AC-MDEA (0.56 mmol N/g AC) has 300% higher micropore volume than AC-DEA (0.52 mmol N/g AC) (Figure 3-2) and is consistent with its average pore diameter (15.43 Å) which is less than the value for AC-DEA (16.87 Å). On the other hand, for the same range of amine loading, samples impregnated with TEPA (AC-TEPA) (molecule diameter=19.36 Å) have the lowest surface area. This might be due to steric hindrance effect of five amine molecules in TEPA structure and is consistent with average pore diameter results presented in

Table 3-2 3-2. Loss of capacity via pore blockage must be balanced with adsorption improvements associated with the added chemical functionalities, as will be discussed in the CO₂ adsorption results (Section 3.3.3.).

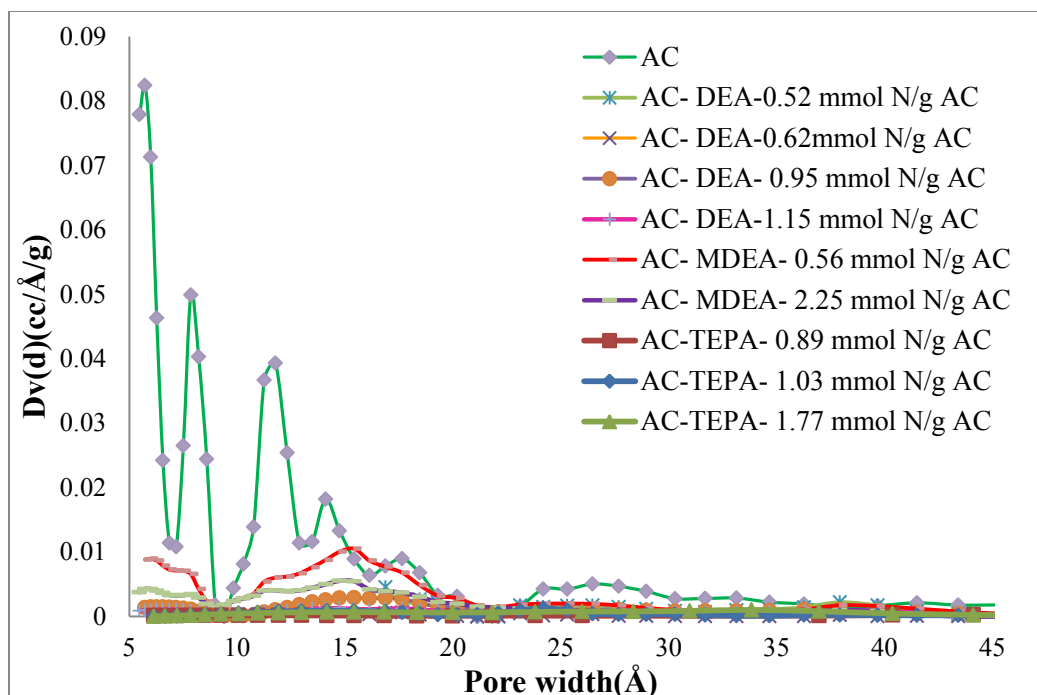
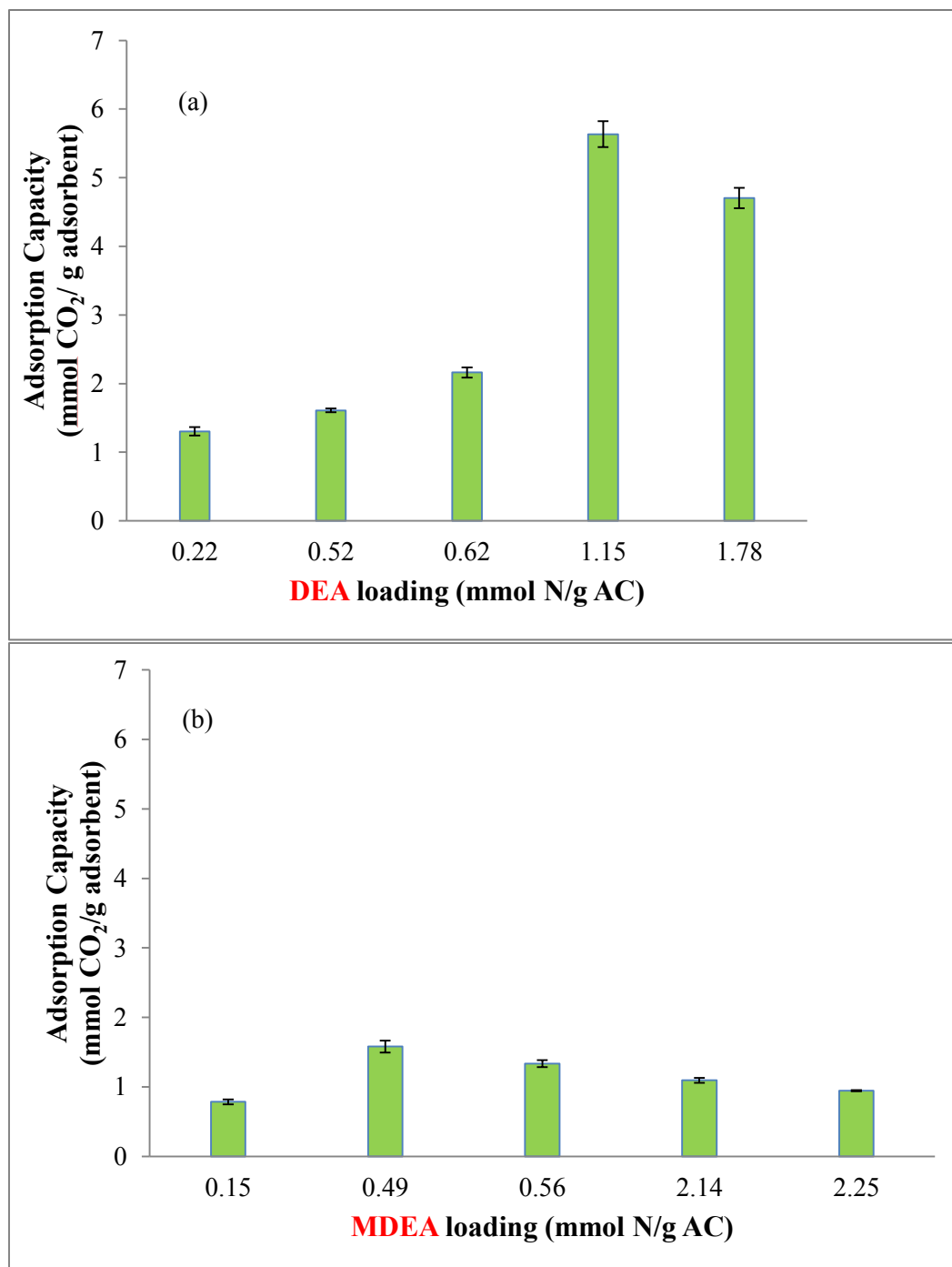


Figure 3-2. Pore size distribution of as prepared and impregnated activated carbon

3.3.3. CO₂ adsorption performance

The impact of amine loading on CO₂ adsorption capacity was examined using screening tests in a TGA. These tests were conducted at a CO₂ concentration that exceeds typical coal-fired power plants levels (Xiaochun Xu and Bruce G. Miller, 2003) to measure the maximum adsorption capacity of prepared materials. The CO₂ adsorption capacity for all three sets of impregnated samples increased with amine loading then decreased, indicating that there is an optimum preparation condition. For AC-DEA, the maximum CO₂ adsorption capacity is 5.63 mmol CO₂/g adsorbent, nearly 75% higher than the 3.3 mmol/g capacity of zeolite 13X (Bao et al., 2011) and almost 5 times higher than commercial AC impregnated with MEA (Khalil et al., 2012) at the same condition, which occurs for a DEA loading of 1.15 mmol N/g AC. Beyond this point, it is hypothesized that additional amine added to the carbon blocks the internal pore structure, preventing the CO₂ from accessing the amine that is added to the bulk of the structure

(Khalil et al., 2012). The unavailability of amine sites for CO₂ adsorption could be attributed to agglomeration of amine, which causes diffusion limitations for CO₂ to access the amine molecules (Srikanth and Chuang, 2012). Although the maximum amine loading can be achieved by filling almost all available pore volume of porous support with liquid amine (as discussed in section 3.3.2.), the adsorption rate will decrease as diffusion through amine-filled pores would be significantly slower than through the empty pores (Fryxell and Cao, 2012).



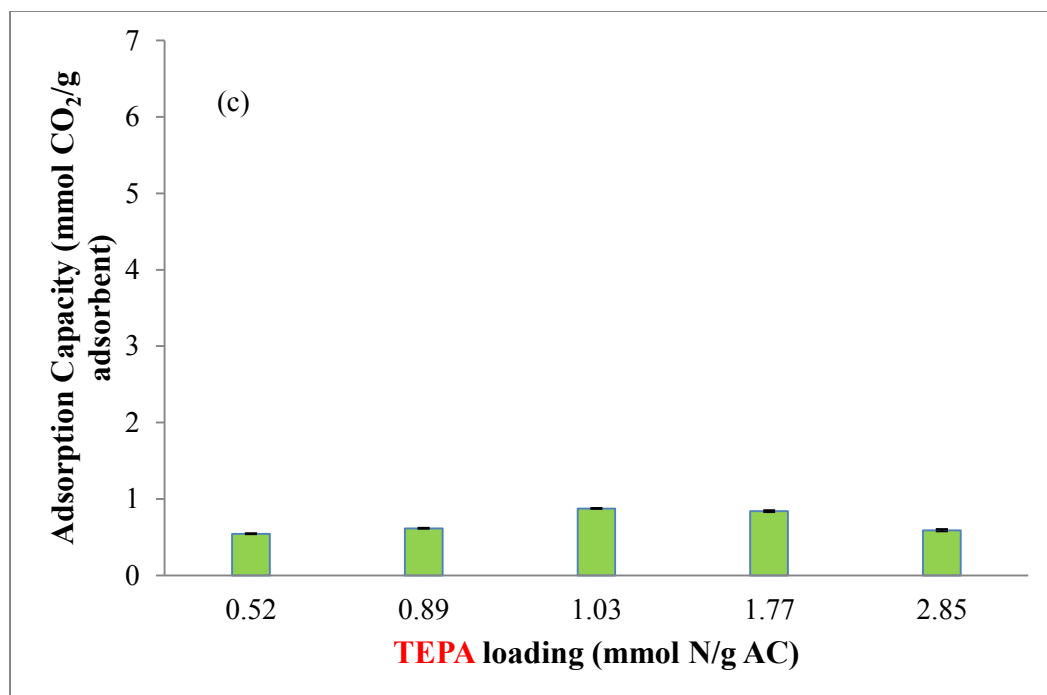


Figure 3-3. Adsorption capacity of (a) AC-DEA, (b) AC-MDEA and (c) AC-TEPA at different loadings. Adsorption completed at 66.6% CO₂ in N₂, 50 °C temperature, and atmospheric pressure. Error bars indicate standard deviation of the mean of two sets of data

In case of AC-MDEA (tertiary amine), the maximum CO₂ adsorption is 1.58 mmol CO₂/g adsorbent which occurs at amine loading equal to 0.49 mmol N/g AC. This amount is about one third of the maximum adsorption capacity of samples impregnated with DEA (secondary amine). The results here show that activated carbon impregnated with secondary amine is more prone to react with CO₂ than with tertiary amine. This is in good agreement with previous reports suggesting that amine reactivity follows the order of primary > secondary > tertiary (Xu et al., 2002, Ko et al., 2011, Lee et al., 2013). This trend can be attributed to the nature of reaction between CO₂ and amine sites. Primary and secondary amines react directly with CO₂ and produce ammonium carbamate through the formation of zwitterions (Zelenak et al., 2008, Ko et al., 2011). The amine's lone electron pair first attacks the carbon atom in CO₂

(forming a zwitterion), and then a second amine deprotonates the zwitterion to produce ammonium carbamate (Ko et al., 2011). Hence, the adsorption performance of carbons modified with primary or secondary amines depends on the amine's ability to split or bind to the proton (Zelenak et al., 2008). Tertiary amines like MDEA follow a different mechanism in which CO₂ binds to the amine in the presence of H₂O. The mechanism involves base-catalyzed hydration of CO₂ to form bicarbonate (Donaldson and Nguyen, 1980, Ko et al., 2011). It is hypothesized that the adsorption capacity of AC-MDEA samples would increase if moisture were added to the gas stream. However, moisture has negligible effect on the adsorption capacity of DEA loaded supports such as zeolite 13X and MCM-41 (Franchi et al., 2005).

Adsorption capacity of AC-TEPA sample, which is a sterically hindered amine composed of several primary and secondary carbons, is up to 84 and 45% lower than AC-DEA and AC-MDEA, respectively (Figure 3-3). This is consistent with the literature, which describes steric hindrances causing amine isolation and preventing CO₂ adsorption (Ko et al., 2011).

The stability of AC-DEA sample with the highest CO₂ adsorption capacity was studied through multi cycles with, each adsorption and subsequent thermal regeneration was considered as a cycle. As illustrated in Figure 3-4, the adsorption capacity of sample AC-DEA, with 1.15 mmol N/g AC loading for the feed gas containing 66% CO₂ in N₂ after 15 cycles was found to be sufficiently close (within 14%) to the original one, following impregnation. The adsorption capacity in the first cycle was 5.63 mmol CO₂/g adsorbent, and the capacity dropped only 14% (to 4.81 mmol CO₂/g adsorbent) after 15 adsorption/ regeneration cycles. It is notable that other comparable studies (Mulgundmath and Tezel, 2010, Khalil et al., 2012) have shown 50 to 85% reduction in CO₂ capture performance after one adsorption/regeneration cycle.

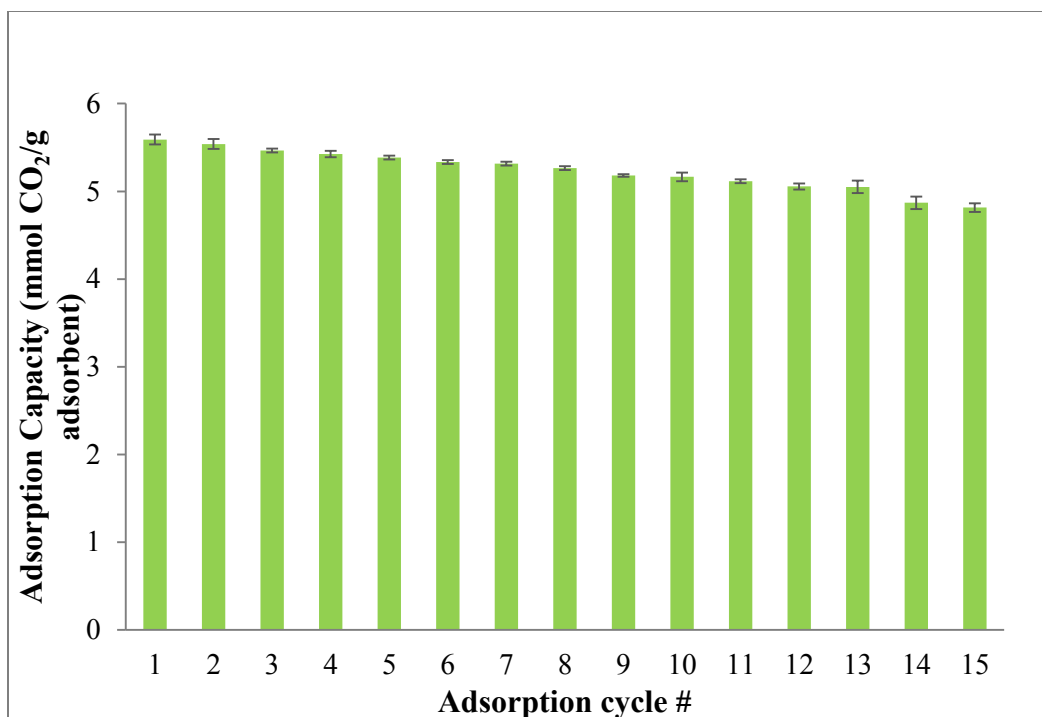


Figure 3-4. Working adsorption capacity of AC-DEA, with 1.15 mmol N/g AC loading for 66% CO₂ in N₂ over 15 cycles of adsorption and regeneration. Adsorption completed at 66.6% CO₂ in N₂, 50 °C, and atmospheric pressure regeneration completed at 110 °C in 100 mL/min of N₂ (99.999%. Error bars indicate standard deviation of the mean of two sets of data)

3.3.4. Effect of humidity on adsorption capacity of tertiary amine

As discussed in the previous section, the mechanism of reaction between tertiary amine (MDEA in our study) and CO₂ will accelerate in the presence of water. Therefore, the effect of water vapor on CO₂ adsorption was studied, using breakthrough tests. The tests were completed in a stainless steel tube under dry and humid conditions for AC-MDEA samples.

Figure 3-5 shows the effect of RH on CO₂ adsorption capacity of AC-MDEA. Adsorption capacity reached a maximum with increasing RH to 20%, and then decreased. This behavior can be explained based on the relative amount of water vapor to CO₂ in the feed stream. When the water vapor content of the feed stream is less than CO₂ content, CO₂ adsorption capacity will

increase with increases in water vapor concentration; however after it reaches the saturation point, the CO₂ capture capacity decreases due to competition between H₂O and CO₂ on active sites. The increase in CO₂ adsorption capacity by raising the water vapor content up to 20% can be attributed to catalytic effect of H₂O on the reaction between CO₂ and amine groups (Donaldson and Nguyen, 1980). Moreover, moisture stabilizes carbonate-like species by hydrogen bonding with adsorbed H₂O, increasing the performance of the adsorbent (Donaldson and Nguyen, 1980). Although adsorption capacity of AC-MDEA samples increased up to 200% in the presence of 20% RH, their performance is 2.5 times lower than AC-DEA.

Xu et al. (Xu et al., 2005) also reported that when water vapor concentration in the feed stream is less than that of CO₂, CO₂ adsorption capacity increases rapidly with increasing water vapor content, but when the water vapor concentration becomes higher than CO₂ concentration, CO₂ adsorption is inhibited in the presence of excess water.

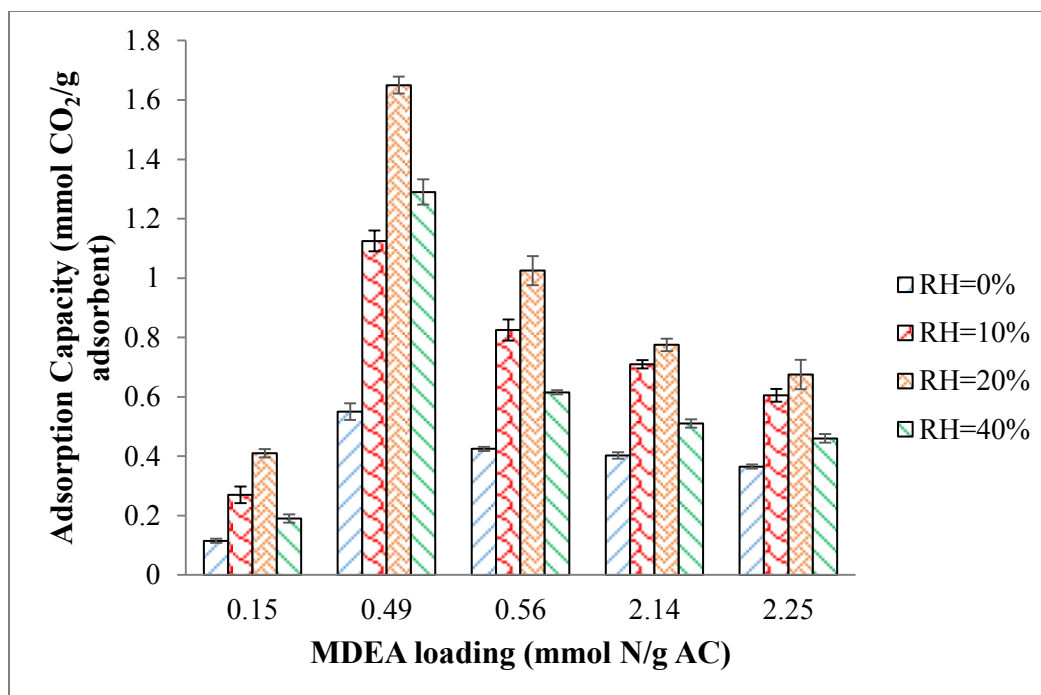
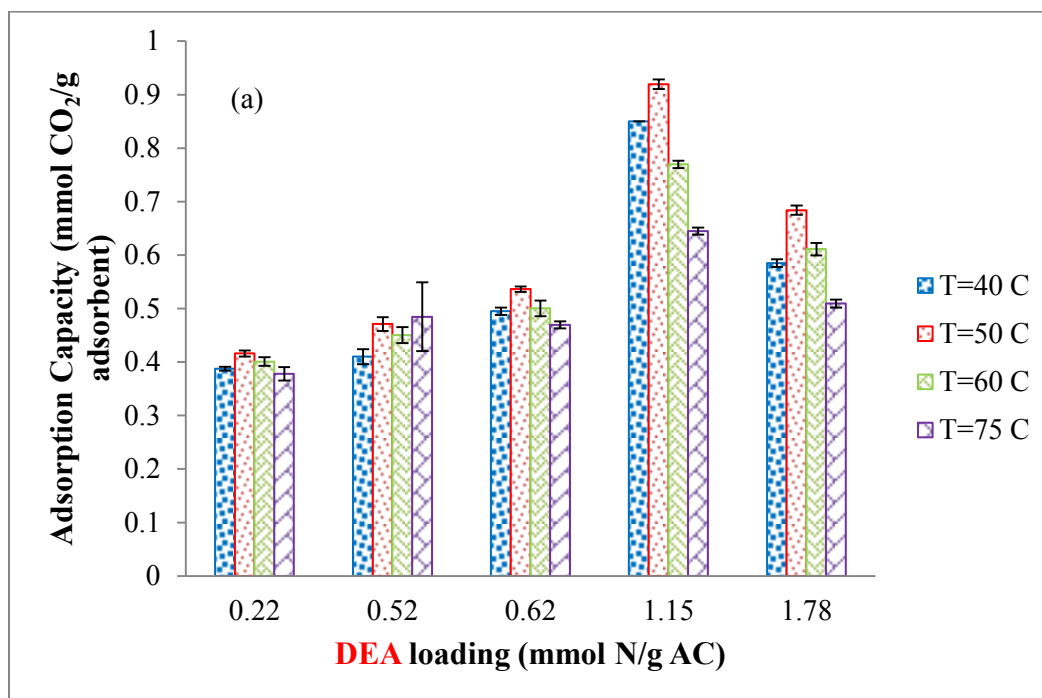


Figure 3-5. Effect of moisture on CO₂ adsorption capacity of MDEA-impregnated activated carbon. Adsorption completed at 20% CO₂ in N₂, 50 °C temperature, and atmospheric pressure. Error bars indicate standard deviation of the mean of two sets of data

3.3.5. Effect of adsorption temperature

CO₂ adsorption capacity of amine-impregnated samples was quantified at 40, 50, 60, and 75 °C at 20% CO₂ concentration in N₂ using a stainless steel tube (Figure 3-6). For all three amines, the CO₂ adsorption capacity increased from 40 to 50 °C, but decreased with further temperature increases. Improvements at low temperatures are attributed to increased CO₂ diffusion to reactive amine sites, and decreased performance at higher temperatures is believed to be associated with the exothermic chemisorption process (Lee et al., 2011). In other words, there is an optimum temperature (50 °C in this case) that balances diffusion limitations with reaction/thermodynamic limitations (Pipatsantipong et al., 2012). Lee et al. showed similar

trends in CO₂ capacity with changing temperature, identifying an optimum adsorption temperature of 45 °C (Lee et al., 2011).



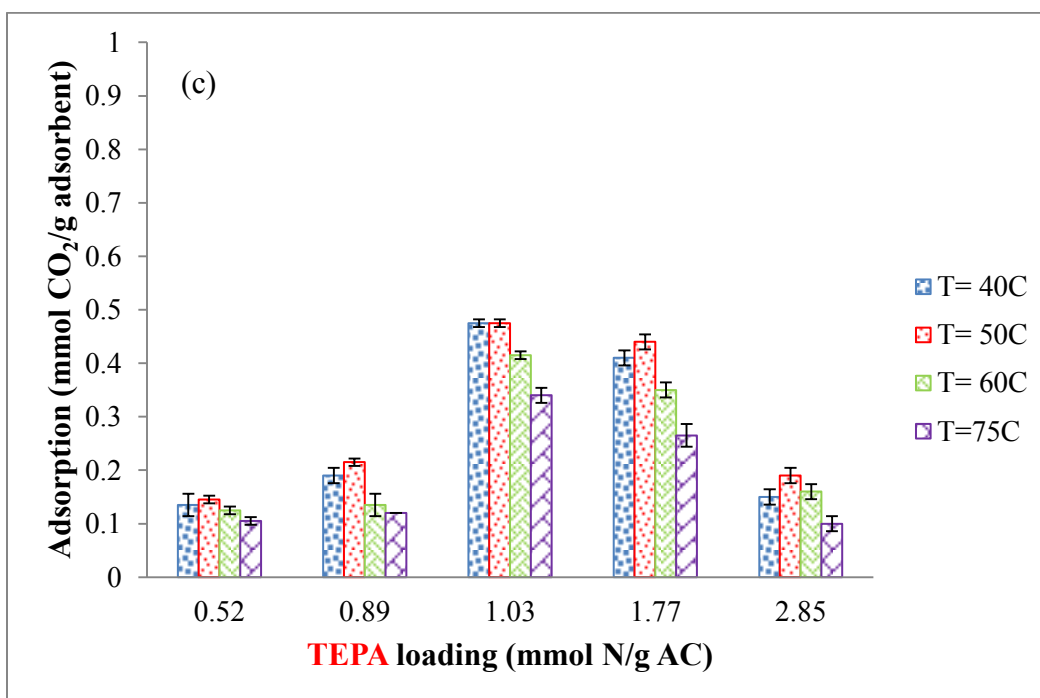
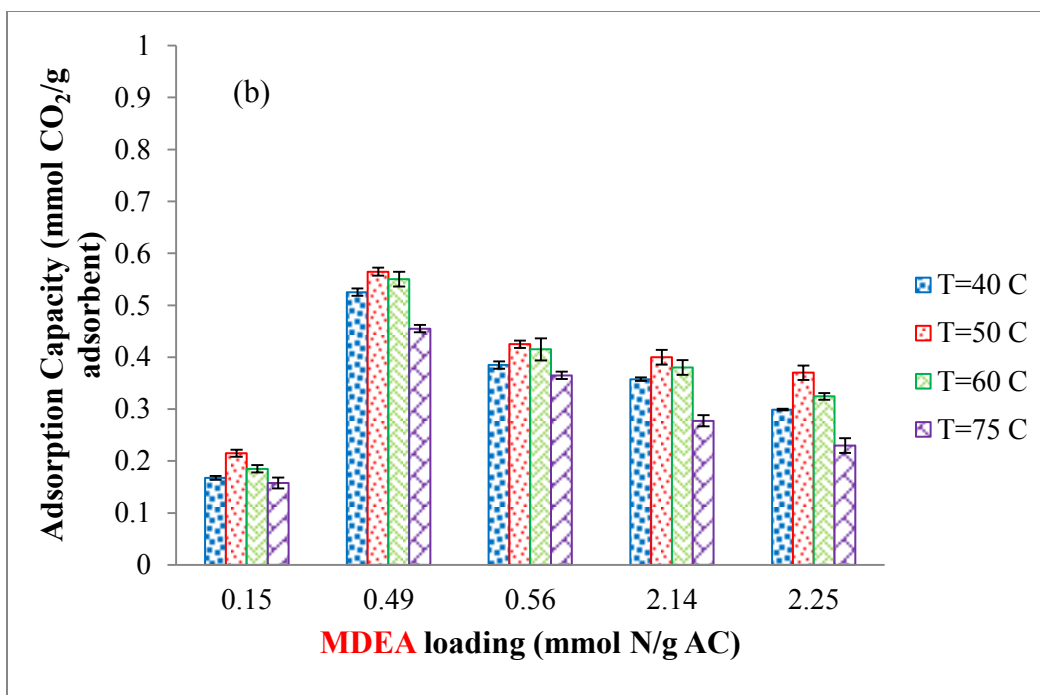


Figure 3-6. Adsorption capacity of (a) AC-DEA, and (b) AC-MDEA samples at different temperatures, 20% CO₂ in N₂, and atmospheric pressure. Error bars indicate standard deviation of the mean of two sets of data

Note that adsorption capacity of amine-impregnated samples at room temperature was lower than the as-prepared activated carbon which is 1.34 mmol CO₂/g adsorbent. According to Plaza et al. (Plaza et al., 2007), activated carbon has higher adsorption capacity than amine-impregnated activated carbon at room temperature due to a higher contribution of physisorption, which is limited in the case of the modified sorbents due to pores blockage by amines. Maroto-Valer et al. (Maroto-Valer et al., 2005) theorized that only pores < 1 nm are responsible for CO₂ uptake by physisorption. Since the amine coating blocks these narrow pores, amine impregnation is not the best approach for increasing the adsorption of CO₂ at room temperature. It should be highlighted that other species in flue gas can be physically adsorbed into activated carbon, lowering its separation factor. To reach a higher separation factor, chemical adsorption is adopted to selectively separate target gas from flue gas (Xu et al., 2002). Hence, there should be a balance between physisorption and chemisorption contribution (Plaza et al., 2007).

3.4. Conclusion

Oil sands coke was activated using microwave heating then impregnated with amines (DEA, MDEA, or TEPA). Evaluation of bulk and surface composition of the amine impregnated activated carbon indicated that most of the amine is deposited on the surface, which makes it more accessible for CO₂ molecules. The amine impregnated activated carbons were tested for CO₂ adsorption. In general, the surface area of the impregnated activated carbon decreased with increasing amine loading and the size of amine molecule.

Comparing the adsorption performance of three amine types showed that secondary amine had the highest adsorption capacity followed by tertiary and bulky amines. AC-DEA samples had a maximum CO₂ adsorption capacity of 5.63 mmol CO₂/ g adsorbent for a DEA loading of 1.15mmol N/g AC. Further increase in amine loading resulted in a decrease in

adsorption capacity possibly due to the blockage of accessible volume of pores. Our best sample (with 5.63 mmol CO₂/ g adsorbent capacity) experienced only 14% decrease in adsorption capacity after 15 cycles of adsorption- desorption, which makes this sample viable for multi-cycle use. The experimental results also confirmed the enhancement of capture capacity of AC-MDEA samples in the presence of 20% RH. The effect of temperature on adsorption capacity of amine modified samples was also investigated. For all three sets of amine impregnated samples, increasing temperature from 50 to 75 °C lead to a decrease in CO₂ adsorption capacity. These results are encouraging because they show that oil sands coke can be readily transformed to a high surface area and selective adsorbent for CO₂ which not only decreases the stockpile of a waste byproduct but also reduces the net greenhouse gases contribution of the oil sands operations. Our results demonstrated effectiveness of synthesized adsorbent for CO₂ capture. Further studies will investigate adsorbent performance under more representative flue gas conditions.

3.5. References

- Alauzun, J., Mehdi A., Reya C. and Corriu R. J. P. (2005). CO₂ as a Supramolecular Assembly Agent: A Route for Lamellar Materials with a High Content of Amine Groups. *Journal of the American Chemical Society* **127**(32): 11204-11205.
- ASTM (2006). Standard Test Method for Determination of Iodine Number of Activated Carbon D4607, American Society for Testing and Materials.
- Atkinson, J. D., Zhang Z., Yan Z., and Rood M. J. (2013). Evolution and impact of acidic oxygen functional groups on activated carbon fiber cloth during NO oxidation. *Carbon* **54**: 444-453.

- Bandosz, T. J. (2006). *Activated Carbon Surfaces in Environmental Remediation*, Elsevier Science.
- Bao, Z., Yu L., Ren Q., Lu X., and Deng S. (2011). Adsorption of CO₂ and CH₄ on a magnesium-based metal organic framework. *Journal of Colloid and Interface Science* **353**(2): 549-556.
- Bonenfant, D., Mimeault M., and Hausler R. (2003). Determination of the Structural Features of Distinct Amines Important for the Absorption of CO₂ and Regeneration in Aqueous Solution. *Industrial & Engineering Chemistry Research* **42**(14): 3179-3184.
- Chang, A. C. C., Chuang S. S. C., Gray M., and Soong Y. (2003). In-Situ Infrared Study of CO₂ Adsorption on SBA-15 Grafted with Y-(Aminopropyl)triethoxysilane. *Energy & Fuels* **17**(2): 468-473.
- Chatti, R., Bansawal A. K., Thote J. A., Kumar V., Jadhav P., Lokhande S. K., Biniwale R. B., Labhsetwar N. K., and Rayalu S. S. (2009). Amine loaded zeolites for carbon dioxide capture: Amine loading and adsorption studies. *Microporous and Mesoporous Materials* **121**(1-3): 84-89.
- Chen, H. and Hashisho Z. (2012). Effects of microwave activation conditions on the properties of activated oil sands coke. *Fuel Processing Technology* **102**(0): 102-109.
- Choi, S., Drese J. H., and Jones C. W. (2009). Adsorbent Materials for Carbon Dioxide Capture from Large Anthropogenic Point Sources. *ChemSusChem* **2**(9): 796-854.
- Cummings A. L., Veatch F. C., Keller A. E., Mecum S. M. and Kammiller R. M. (1990). An analytical method for determining bound and free alkanolamines in heat stable salt contaminated solutions. *AICHE 1990 Summer national meeting symposium gas processing*, Ponca City, OK.

- Donaldson, T. L. and Nguyen Y. N. (1980). Carbon Dioxide Reaction Kinetics and Transport in Aqueous Amine Membranes. *Industrial & Engineering Chemistry Fundamentals* **19**(3): 260-266.
- Dong-Il Jang and Park S. J. (2011). Influence of Amine Grafting on Carbon Dioxide Adsorption Behaviors of Activated Carbons. *Bulletin of the Korean Chemical Society* **32**(9): 3377-3381.
- Dunne, L. J. and Manos G. (2010). Adsorption and Phase Behaviour in Nanochannels and Nanotubes. New York.
- Fedorak, P. M. and Coy D. L. (2006). Oil sands cokes affect microbial activities. *Fuel* **85**(12-13): 1642-1651.
- Foo, K. Y. and Hameed B. H. (2012). Mesoporous activated carbon from wood sawdust by K_2CO_3 activation using microwave heating. *Bioresource Technology* **111**(0): 425-432.
- Franchi, R. S., Harlick P. J. E., and Sayari A. (2005). Applications of Pore-Expanded Mesoporous Silica. 2. Development of a High-Capacity, Water-Tolerant Adsorbent for CO_2 . *Industrial & Engineering Chemistry Research* **44**(21): 8007-8013.
- Fryxell, G. E. and Cao G. (2012). Environmental Applications of Nanomaterials: Synthesis, Sorbents and Sensors. *World Scientific*
- Furimsky, E. (1998). Gasification of oil sand coke: Review. *Fuel Processing Technology* **56**(3): 263-290.
- Gray, M. L., Soong Y., Champagne K. J., Baltrus J., Stevens R. W., Toochinda P., and Chuang S. S. C. (2004). CO_2 capture by amine-enriched fly ash carbon sorbents. *Separation and Purification Technology* **35**(1): 31-36.

- Heydari-Gorji, A., Belmabkhout Y., and Sayari A. (2011). Polyethylenimine-Impregnated Mesoporous Silica: Effect of Amine Loading and Surface Alkyl Chains on CO₂ Adsorption. *Langmuir* **27**(20): 12411-12416.
- Houshmand, A., Daud W., Lee M.G., and Shafeeyan M. (2012) Carbon Dioxide Capture with Amine-Grafted Activated Carbon. *Water, Air, & Soil Pollution* **223**(2): 827-835.
- Hu, Z. and Srinivasan M. P. (2001). Mesoporous high-surface-area activated carbon. *Microporous and Mesoporous Materials* **43**(3): 267-275.
- Hutson, N. D., Speakman S. A., and Payzant E. A. (2004). Structural Effects on the High Temperature Adsorption of CO₂ on a Synthetic Hydrotalcite. *Chemistry of Materials* **16**(21): 4135-4143.
- Kamarudin, K. S. N. and Mat H. (2009). Synthesis and modification of micro and mesoporous materials as CO₂ adsorbents. *Thesis for Master of Science, University of Technology of Malaysia*.
- Kang, S., Jian-chun J., and Dan-dan C. (2011). Preparation of activated carbon with highly developed mesoporous structure from *Camellia oleifera* shell through water vapor gasification and phosphoric acid modification. *Biomass and Bioenergy* **35**(8): 3643-3647.
- Khalil, S. H., Aroua M. K., and Daud W. M. A. W. (2012). Study on the improvement of the capacity of amine-impregnated commercial activated carbon beds for CO₂ adsorbing. *Chemical Engineering Journal* **183**(0): 15-20.
- Ko, Y. G., Shin S. S., and Choi U. S. (2011). Primary, secondary, and tertiary amines for CO₂ capture: Designing for mesoporous CO₂ adsorbents. *Journal of Colloid and Interface Science* **361**(2): 594-602.

- Lashaki, M. J., Fayaz M., Wang H., Hashisho Z., Philips J. H., Anderson J. E., and Nichols M. (2012). Effect of Adsorption and Regeneration Temperature on Irreversible Adsorption of Organic Vapors on Beaded Activated Carbon. *Environmental Science & Technology* **46**(7): 4083-4090.
- Lee, C. S., Ong Y. L., Aroua M. K., and Daud W. M. A. W. (2013). Impregnation of palm shell-based activated carbon with sterically hindered amines for CO₂ adsorption. *Chemical Engineering Journal* **219**(0): 558-564.
- Lee, D., Jin Y., Jung N., Lee J., Lee J., Jeong Y. S., and Jeon S. (2011). Gravimetric Analysis of the Adsorption and Desorption of CO₂ on Amine-Functionalized Mesoporous Silica Mounted on a Microcantilever Array. *Environmental Science & Technology* **45**(13): 5704-5709.
- Lee, S. C., Chae H. J., Lee S. J., Choi B. Y., Yi C. K., Lee J. B., Ryu C. K., and Kim J. C. (2008). Development of Regenerable MgO-Based Sorbent Promoted with K₂CO₃ for CO₂ Capture at Low Temperatures. *Environmental Science & Technology* **42**(8): 2736-2741.
- Lee, S. H. and Choi C. S. (2000). Chemical activation of high sulfur petroleum cokes by alkali metal compounds. *Fuel Processing Technology* **64**(1-3): 141-153.
- Liou, T. H. (2010). Development of mesoporous structure and high adsorption capacity of biomass-based activated carbon by phosphoric acid and zinc chloride activation. *Chemical Engineering Journal* **158**(2): 129-142.
- Liu, Y., Chen T., Lu T., Sun Z., Chua D. H. C., and Pan L. (2015). Nitrogen-doped porous carbon spheres for highly efficient capacitive deionization. *Electrochimica Acta* **158**: 403-409.

- Maroto-Valer, M. M., Tang Z., and Zhang Y. (2005). CO₂ capture by activated and impregnated anthracites. *Fuel Processing Technology* **86**(14-15): 1487-1502.
- Marsh H. and Rodriguez-Reinoso F. (2006). Activated carbon. Oxford, Elsevier, Ltd.
- Mulgundmath, V. and Tezel F. H. (2010). Optimisation of carbon dioxide recovery from flue gas in a TPSA system. *Adsorption* **16**(6): 587-598.
- Pevida, C., Plaza M. G., Arias B., Feroso J., Rubiera F., and Pis J. J. (2008). Surface modification of activated carbons for CO₂ capture. *Applied Surface Science* **254**(22): 7165-7172.
- Pipatsantipong, S., Rangsunvigit P., and Kulprathipanja S. (2012). Towards CO₂ adsorption enhancement via polyethyleneimine impregnation. *International Journal of Chemical and Biological Engineering* **6**: 291-295.
- Pirngruber, G. D., Cassiano-Gaspar S., Louret S., Chaumonnot A., and Delfort B. (2009). Amines immobilized on a solid support for postcombustion CO₂ capture: A preliminary analysis of the performance in a VSA or TSA process based on the adsorption isotherms and kinetic data. *Energy Procedia* **1**(1): 1335-1342.
- Plaza, M. G., Pevida C., Arenillas A., Rubiera F., and Pis J. J. (2007). CO₂ capture by adsorption with nitrogen enriched carbons. *Fuel* **86**(14): 2204-2212.
- R. Veneman, Kamphuis H., and Brilman D. W. F. (2013). Post combustion CO₂ capture using supported amine sorbents: A process integration study. *Energy Procedia*: 1-9.
- Rivera-Tinoco, R. and Bouallou C. (2010). Comparison of absorption rates and absorption capacity of ammonia solvents with MEA and MDEA aqueous blends for CO₂ capture. *Journal of Cleaner Production* **18**(9): 875-880.

- Saha, D. and Deng S. (2010). Adsorption equilibrium and kinetics of CO₂, CH₄, N₂O, and NH₃ on ordered mesoporous carbon. *Journal of Colloid and Interface Science* **345**(2): 402-409.
- Siriwardane, R. V., Shen M. S., Fisher E. P., and Poston J. A. (2001). Adsorption of CO₂ on Molecular Sieves and Activated Carbon. *Energy & Fuels* **15**(2): 279-284.
- Small, C., Ulrich A., and Hashisho Z. (2012). Adsorption of Acid Extractable Oil Sands Tailings Organics onto Raw and Activated Oil Sands Coke. *Journal of Environmental Engineering* **138**(8): 833-840.
- Srikanth, C. S. and Chuang S. S. C. (2012). Spectroscopic Investigation into Oxidative Degradation of Silica-Supported Amine Sorbents for CO₂ Capture. *ChemSusChem* **5**(8): 1435-1442.
- Sullivan, P., Moate J., Stone B., Atkinson J. D., Hashisho Z., and Rood M. J. (2012). Physical and chemical properties of PAN-derived electrospun activated carbon nanofibers and their potential for use as an adsorbent for toxic industrial chemicals. *Adsorption* **18**(3): 265-274.
- Sun, Y., Wang Y., Zhang Y., Zhou Y., and Zhou L. (2007). CO₂ sorption in activated carbon in the presence of water. *Chemical Physics Letters* **437**(1-3): 14-16.
- Thompson, M. (2008). CHNS Elemental Analyzers. *The Royal Society of Chemistry* **29**.
- Tontiwachwuthikul, P., Wee A. G. H., Idem R., Maneeintr K. , Fan G.J. , Amornvadee V., Amr H., Aroonwilas A. , Chakma A. (2011). Method of capturing carbon dioxide from gas streams. *US Patent, US 7910078 B2*

- Ugarte, N.P. and Swider-Lyons K. E. (2005). Low-Platinum tin-oxide electrocatalysts for PEM fuel cell cathodes. *Proton Conducting Membrane Fuel Cells III*. M. Murthy and T. F. Fuller: 67-73.
- Veawab, A., Tontiwachwuthikul P., and Chakma A. (1999). Corrosion Behavior of Carbon Steel in the CO₂ Absorption Process Using Aqueous Amine Solutions. *Industrial & Engineering Chemistry Research* **38**(10): 3917-3924.
- Walton, K. S., Millward A. R., Dubbeldam D., Frost H., Low J. J., Yaghi O. M., and Snurr R. Q. (2007). Understanding Inflections and Steps in Carbon Dioxide Adsorption Isotherms in Metal-Organic Frameworks. *Journal of the American Chemical Society* **130**(2): 406-407.
- Xu, D. P., Yoon S. H., Mochida I., Qiao W. M., Wang Y. G., and Ling L. C. (2008). Synthesis of mesoporous carbon and its adsorption property to biomolecules. *Microporous and Mesoporous Materials* **115**(3): 461-468.
- Xu, X., Song C., Andresen J. M., Miller B. G., and Scaroni A. W. (2002). Novel Polyethylenimine-Modified Mesoporous Molecular Sieve of MCM-41 Type as High-Capacity Adsorbent for CO₂ Capture. *Energy & Fuels* **16**(6): 1463-1469.
- Xu, X., Song C., Miller B. G., and Scaroni A. W. (2005). Influence of Moisture on CO₂ Separation from Gas Mixture by a Nanoporous Adsorbent Based on Polyethylenimine-Modified Molecular Sieve MCM-41. *Industrial & Engineering Chemistry Research* **44**(21): 8113-8119.
- Xu, X., Song C., Wincek R., Andresen J. M., Scaroni A. W., Miller B. G. (2003). Separation of CO₂ from Power Plant Flue Gas Using a Novel CO₂ “Molecular Basket” Adsorbent *Fuel Chemistry Division Preprints* **48**(1): 162.

- Yang, Y., Li H., Chen S., Zhao Y., and Li Q. (2010). Preparation and Characterization of a Solid Amine Adsorbent for Capturing CO₂ by Grafting Allylamine onto PAN Fiber. *Langmuir* **26**(17): 13897-13902.
- Yin, C. Y., Aroua M. K., and Daud W. M. A. W. (2008). Polyethyleneimine impregnation on activated carbon: Effects of impregnation amount and molecular number on textural characteristics and metal adsorption capacities. *Materials Chemistry and Physics* **112**(2): 417-422.
- Yue, M. B., Chun Y., Cao Y., Dong X., and Zhu J. H. (2006). CO₂ Capture by As-Prepared SBA-15 with an Occluded Organic Template. *Advanced Functional Materials* **16**(13): 1717-1722.
- Zelenak, V., Halamova D., Gaberova L., Bloch E., and Llewellyn P. (2008). Amine-modified SBA-12 mesoporous silica for carbon dioxide capture: Effect of amine basicity on sorption properties. *Microporous and Mesoporous Materials* **116**(1-3): 358-364.
- Zhang, Z., Wang K., Atkinson J. D., Yan X., Li X., Rood M. J., and Yan Z. (2012). Sustainable and hierarchical porous Enteromorpha prolifera based carbon for CO₂ capture. *Journal of Hazardous Materials* **229–230**: 183-191.
- Zhang, Z., Xu M., Wang H., and Li Z. (2010). Enhancement of CO₂ adsorption on high surface area activated carbon modified by N₂, H₂ and ammonia. *Chemical Engineering Journal* **160**(2): 571-577.

CHAPTER 4. SYNTHESIS OF MESOPOROUS CARBONS FOR CO₂ ADSORPTION FROM OIL SANDS COKE USING KOH ACTIVATION WITH A MgO TEMPLATE

4.1. Introduction

Activated carbon is widely used for gas adsorption due to its low cost, the variety of its pore structures and surface chemistry, and efficient regeneration (Bullin and Polasek, 1990, Aksoylu et al., 2001, Xiong et al., 2003, Gray et al., 2004, Gomes et al., 2008). In general applications of activated carbon, microporous structure plays an important role, but recently, mesoporous activated carbon has drawn increasing attention because it possesses a high pore volume and a wide range of pore size which increases the accessibility of pores for target adsorbate (Durá et al., 2016).

The pore structure of carbons is mainly dependent on the carbon precursor and the activation/preparation methods. Therefore, significant efforts have been devoted to modifying the existing methods and finding suitable precursors to obtain activated carbon with higher specific surface area or larger mesopore volume (Yang and Qiu, 2010). One of the methods to produce mesoporous carbon is adding a template into the carbon precursor in the preparation step. In hard template techniques, the pores of inorganic template matrix are filled with carbon precursors to make a composite which is subsequently carbonized followed by acid treatment to wash out the inorganic template (Xia et al., 2010). A number of hard templates such as zeolite (Xia et al., 2011), silicate (Yoon et al., 2011) and colloidal particles (Woo et al., 2009) have been used which result in microporous, mesoporous and macroporous carbons, respectively. Soft templates such as calcium carbonate (Xu et al., 2010) and magnesium oxide (MgO) (Morishita et al., 2010) have also been used for this purpose.

Previous studies showed that microwave activation is a fast and effective way to promote the surface area and total pore volume of activated carbon (Chen and Hashisho, 2012, Gholidoust et al., 2017). Foo (Foo and Hameed, 2012) and Li (Li et al., 2016) have also reported that microwave heating is more effective than chemical treatment to optimize the pore structure of activated carbon. In fact, changes to the pore characteristics of carbon during activation depends on carbon burn-off which in turn depends on the activation temperature and time. Different agents have been used for this purpose including air, oxygen, carbon dioxide and steam. Air and oxygen have a fast and exothermic reaction with carbon, while steam and carbon dioxide react under endothermic condition which makes the carbon burn-off more controllable compared to the other two aforementioned agents. Therefore, steam and carbon dioxide are preferred for activation (Bandosz, 2006).

In general, activated carbon can be prepared from different precursors such as coals, petroleum coke, and lignocellulosic materials (Hasib-ur-Rahman et al. 2010, Kawano et al., 2008) through a variety of physical or chemical activation processes. Although petroleum coke has been commonly used as precursor for preparing activated carbon (Chang et al., 2000, Lee and Choi, 2000), a few studies investigated activation of oil sands coke. In Alberta, Canada, oil sands coke, a by-product of bitumen upgrading, can be a suitable precursor for activated carbon as it has high carbon content (approximately 80-85% by weight) and is widely available at low cost (Small et al., 2012). Current estimates indicate a total of 1 billion m³ of coke production over the entire lifetime of oil sands operations in Alberta (Furimsky, 1998). Most of the produced coke is stockpiled on-site (Furimsky, 1998) and only small quantities is burnt to generate steam and electricity (Allen, 2008). However, coke combustion produces CO₂, emphasizing the need for sustainable management and use of stockpiled coke. Transforming this

by-product into activated carbon can help in managing coke stockpile and reduces CO₂ emissions.

The aim of this work is to prepare mesoporous oil sands activated carbon and evaluate its performance for CO₂ adsorption. Oil sands coke was utilized as a precursor for mesoporous activated carbon and was activated using MgO template in a one-step microwave heating coupled with KOH. MgO was selected as a template because it can be easily dissolved in dilute acidic solutions. Specific surface area and pore size distribution were measured to investigate the effect of activation agent on the structure of activated oil sands coke. Performance of activated oil sands coke was then investigated for CO₂ adsorption. To the best of our knowledge, systematic studies investigating CO₂ capture using activated carbon prepared from this unique waste precursor have not been reported.

4.2. Materials and Methods

4.2.1. Chemicals

Delayed oil sands coke was provided by Suncor Energy. Potassium hydroxide (KOH, Fisher, ACS grade) and Magnesium oxide (MgO, Fisher, ACS grade) were used as the activation agents.

4.2.2. Activated Carbon Preparation

Prior to activation, delayed coke was ground, sieved into selected sizes (180-212 μm), then dried overnight in a laboratory oven at 110 °C. Two activation methods were used in this research: (a) preparation using a single activation agent, and (b) preparation using two activation agents.

Preparation using a single activation agent: In this method, KOH was dissolved in de-ionized water and mixed with delayed coke at 1:1 ratio. The prepared mixture was then dried in the oven at 110 °C until it reached a stable weight. A 25-30 g sample of the dried mixture was loaded onto a crucible and covered with quartz wools to prevent heat loss. The crucible was then placed inside a quartz reactor (diameter 2.6cm, height 20cm) purged with a flow of 500 ml/min of humidified N₂. Dry nitrogen passed through an impinger containing water before purging the activation reactor. The sample was heated for 20 min in a 2.45 GHz customized kitchen microwave (Kenmore, 721.80602) with 800W nominal power output. The power output of the microwave oven was controlled by varying the duty cycle of the magnetron. After the activation, the resulting mixture was washed with de-ionized water and diluted hydrochloric acid to remove the impurities until neutralization and then dried overnight in the oven at 110 °C. The temperature of the reactants in the crucible was measured using a high temperature thermocouple (OMEGA-KMQXL) right after the completion of microwave-assisted activation process.

Preparation using two activation agents: In this method, dried delayed coke was first mixed with MgO (with mesh sizes between 104 µm-74 µm) and KOH and then pulverized at different mass ratios (the total mass of mixture was fixed at 27g). The mixture was then placed in a crucible inside a quartz reactor and heated using a microwave oven (the same one as described above) for 30 min in a 600 ml/min of humidified nitrogen purge flow. In order to study the effect of heating method, the samples were also activated by conventional heating using tube furnace (Linberg Blue M, HTF55342C) and dry/humidified purge gases (N₂ and CO₂). The sample temperature was first raised from room temperature to 150 °C, held at this temperature for 1h to remove any moisture, and then ramped up to 900 °C at 10 °C/min. The sample was then held at this temperature for 1h. After heating, the resultant mixture was washed with de-ionized water

and 2 M H₂SO₄ to remove the residual ions until it reached neutral pH, then the mixture was dried at 100 °C for 24 h. Samples prepared in this method are named based on KOH/coke ratio (KC) and MgO/coke ratio (MC).

4.3. Characterization Methods

4.3.1. Nitrogen adsorption measurement

Nitrogen adsorption isotherms were measured using a surface area analyzer (Quantachrome Instruments, Autosorb-1MP) at 77 K. Prior to the measurement, the samples were outgassed at 150 °C under vacuum for 5 h. The specific surface area was determined from N₂ adsorption isotherm by the standard Brunauer-Emmett-Teller (BET) method using nitrogen in the relative pressure range of 0.05-0.99. Micropore volume was evaluated using the V-t model. The pore size distribution was determined using the density functional theory (DFT) for slit pores (Bandosz, 2006, Dunne and Manos, 2010). The total pore volume was based on the conversion of the adsorption amount at $p/p_0 = 0.95$ to a volume of liquid N₂ (Zhang et al., 2010).

4.3.2. Bulk and surface elemental analysis

The bulk composition (carbon, hydrogen, nitrogen, sulfur, and oxygen) of prepared samples was characterized using a CHNS elemental analyzer (Vario MICRO). Oxygen in the sample is determined by mass difference ($100\% - \text{C wt}\% - \text{H wt}\% - \text{N wt}\% - \text{S wt}\%$), assuming that ash content is negligible (Thompson, 2008).

The surface composition of the prepared activated carbon was determined using X-ray photoelectron spectroscopy (XPS). The analysis was conducted using Kratos AXIS 165 instrument with Mono Al K α radiation at 210 W and 14 kV under ultrahigh vacuum (10^{-9} Torr). All the spectra were calibrated to C1s peak at 284.5 eV.

4.3.3. CO₂ adsorption measurement

The adsorption performance of the sorbents was analyzed using a thermo-gravimetric analyzer (TGA/ DSC 1, Mettler Toledo). The adsorption performance of selected samples were screened at 40, 50, 60 and 75°C based on previous studies (Pirngruber et al., 2009, Khalil et al., 2012) (results not included) and the optimum CO₂ adsorption temperature was obtained at 50 °C. Typically, about 10 mg of sample was placed in a small alumina crucible, heated to 120 °C in 100 ml/min N₂ and held at this temperature for 30 minutes to remove water vapor. The temperature was then ramped down at 10 °C/min to the adsorption set-point (50 °C), and the sample was held at this temperature until a stable weight was reached, at which point the gas was switched to 200 mL/min of 99.99% CO₂ mixed with 100 mL/min of N₂ (66.6% CO₂ in N₂). The amount of adsorbed CO₂ was determined by sample weight change before and after the adsorption. The adsorption capacity was determined in mmol of adsorbate (CO₂) / g of adsorbent.

4.3.4. FTIR Spectroscopy

FTIR spectra were recorded between 4000 and 500 cm⁻¹ using a Thermo Nicolet 8700 spectrometer for samples activated in N₂ and CO₂ atmosphere to evaluate the surface functional groups. The analysis discs were prepared by first mixing 1 mg of dried sample with 500 mg of KBr (Merck, spectroscopy grade) in an agate mortar and then pressing the resulting mixture at 10 tonnes cm⁻² for 15 min under vacuum.

4.4. Results and Discussion

4.4.1. BET surface area and pore size distribution

The BET surface area and pore size distribution of microwave activated carbons have been determined to evaluate the effect of different activation agents. Surface characteristics of microwave activated carbons are summarized in Table 4-1.

Table 4-1. Surface characteristics of raw and activated delayed cokes, microwave heated in N₂ gas stream

Sample	BET surface area (m ² /g)	Total pore volume (cc/g)	Micropore volume (cc/g)
Delayed oil sands coke	2.7	0.004	0.00
AC-KC ¹ =1	816	0.23	0.17
AC-KC=0.43, MC=0.5	81.1	0.07	0.01
AC-KC=1.5, MC=4	385.1	0.41	0.03
AC-KC=1, MC=2	210.4	0.19	0.08
AC-KC=0.86, MC=2	274.8	0.24	0.01
AC-KC=0.66, MC=1.33	115.9	0.09	0.003

¹ AC: Activated Carbon, KC: KOH/coke, MC: MgO/coke

BET surface area for sample activated with 1:1 KOH to coke (KC=1) has the highest value, indicating the effectiveness of KOH as an activation agent in microwave activation method (Chen and Hashisho, 2012, Gholidoust et al., 2017). This sample has a microporous structure as can be seen from the pore size distribution in Figure 4-1. It is postulated that the pores in the delayed coke are interconnected due to the release of volatile components from its

uniform structure during the coking process. Hence, KOH can spread inside the interconnected pores and make a well-developed micropore structure (Jack et al., 1979, Dabrowski et al., 2005, Marsh and Rodriguez-Reinoso, 2006, Chen and Hashisho, 2012). Using MgO causes a significant change in the delayed coke porous structure (Table 4-1). In fact, MgO is the main reason for pore widening of the delayed coke, as increasing MC ratio from 0.5 to 4 resulted in almost 60% increase in total pore volume when comparing samples with KC=0.43, MC=0.5, and KC=1.5, MC=4, respectively. Although the KC ratio is different in these two samples, it does not conflict with the pore widening effect of MgO. In fact, increasing the KC ratio from 0.43 to 1.5 caused a decrease in pore volume, as it was observed in samples with the same MC ratios, but different KC ratios (i.e. KC=1, MC=2, and KC=0.86, MC=2). At a constant MC ratio, increasing KC ratio from 0.86 to 1 resulted in a 20% decrease in total pore volume (from 0.24 to 0.19cc/g).

Adding MgO to coke also causes a decrease in micropore volume. For instance, the micropore volume was 0.17 cc/g for KOH only activation (KC=1) but it decreased to 0.08 cc/g for combined KOH and MgO activation (KC=1 and MC=2). Although, the presence of KOH in the mixture results in the formation of micropores, decreasing KOH/coke ratio causes deformation of micropores and formation of mesopores (He et al., 2012).

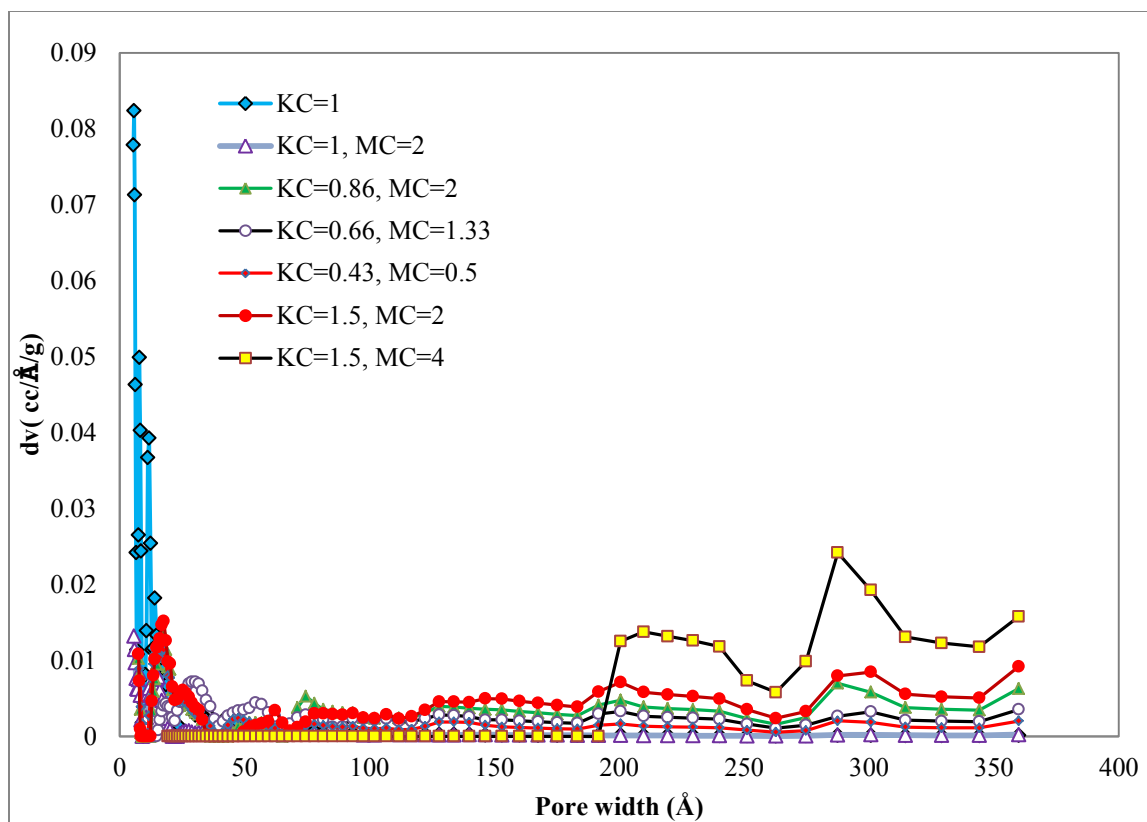


Figure 4-1. Pore size distribution of activated delayed cokes (KC: KOH/coke, MC: MgO/coke)

4.4.2. Elemental analysis

Table 4-2 lists the bulk composition of delayed coke before and after activation based on proportional weight change of five elements (C, H, N, S and O). Sulfur content of delayed coke has drastically (about 80%) decreased after activation with KOH while carbon and oxygen content has increased. The loss of sulfur content during activation is consistent with results from previous studies (Lee and Choi, 2000, Chen and Hashisho, 2012). For the samples activated with combined MgO and KOH, the carbon content is reversely proportional to KC ratios. The results confirm the effective removal of impurities and improving the carbon proportion during the activation. Comparing the samples activated with KOH only, and combined KOH and MgO, one can conclude an order of magnitude increase in oxygen content in the latter. In fact, K-containing compounds can easily be removed by washing with distilled water, whereas MgO used in this

experiment can readily react with water during the water-washing process and form brucite ($\text{Mg}(\text{OH})_2$) which is the main reason of high oxygen content in samples activated using MgO template. Accordingly, the trend in oxygen content is consistent with the MC ratio. Moreover, hydrogen content has generally decreased upon activation. During activation, KOH reacts with the carbon skeleton, producing solid and gaseous products such as hydrogen, CO and CO_2 (which come from the carbon skeleton) and potassium oxide (Bandosz, 2006).

Table 4-2. Bulk composition (%wt.) of raw and activated delayed cokes, microwave heated in N_2 gas stream

Sample	N%	C%	H%	S%	O%
Delayed oil sands coke	1.6± 0.1	82.3± 0.0	3.7± 0.1	6.8± 0.1	5.7± 3.0
AC- KC=1	1.4± 0.1	87.4± 0.2	1.2± 0.1	1.4± 0.0	8.6± 3.5
AC- KC=1, MC=2	0.4 ± 0.0	23.1± 0.0	0.7± 0.0	0.6± 0.0	75.2± 0.0
AC- KC=0.86, MC=2	0.3± 0.1	22.2± 9.0	2.2± 0.1	0.8± 0.0	74.4± 9.3
AC- KC=0.66, MC=1.33	0.4± 0.1	33.5± 11.9	1.6± 0.3	0.9± 0.1	63.6± 11.8
AC- KC=0.43, MC=0.5	0.9 ± 0.0	63.9± 5.1	0.8± 0.0	1.6± 0.0	32.7± 5.1
AC- KC=1.5, MC=4	0.1± 0.0	12.3± 2.9	2.5± 0.1	0.9± 0.0	84.1± 2.8

Surface composition of raw and activated delayed coke is summarized in Table 4-3. Similar to bulk composition, surface oxygen content of delayed coke shows up to 7 times increase upon activation with MgO and KOH, while there is up to 100% decrease in surface sulfur content. In general, the trend in Mg and K content is consistent with MC and KC ratios, respectively.

It is also worthy to compare the sulfur content of bulk and surface of activated carbon from Table 4-2 and Table 4-3. The sulfur content on the surface of activated carbon is 57% lower than its value in the bulk, indicating that activation can effectively remove sulfur from the surface. Introducing MgO in the activation step provides activated carbons with lower carbon content and almost no sulfur on the surface.

Table 4-3. Surface composition (%wt.) of raw and activated delayed coke, microwave heated in N₂ gas stream

Sample	N%	C%	Mg%	K%	S%	O%
Delayed oil sands coke	1.4	87	0	0	4.0	6.5
AC- KC=1	0.9	84.4	0	1.7	0.8	10.9
AC- KC=1, MC=2	1.1	14.8	24.8	1.3	0.6	57.4
AC- KC=0.86, MC=2	0.5	11.1	30.5	0.8	3.2	53.9
AC- KC=0.66, MC=1.33	0.7	24.7	31.2	0.6	0.4	42.4
AC- KC=0.43, MC=0.5	1.4	23.6	23.3	0.6	3.0	48.1
AC- KC=1.5, MC=4	0.5	12.8	31.3	2.4	0.0	53.0

4.4.3. CO₂ adsorption performance

CO₂ adsorption tests were completed in 66.6 % CO₂ in N₂ at 50 °C and atmospheric pressure using a TGA. Adsorption capacity of activated carbons is presented in Figure 4-2. The highest adsorption capacity (3.17 mmol CO₂/g adsorbent) was observed for the sample with KC ratio of 1 and MC ratio of 2. Comparing samples with the same MC ratio (MC=2), decreasing KC ratio from 1 to 0.86 results in a decrease in adsorption capacity from 3.17 to 3.01 (Figure 4-2). The presence of KOH as an activation agent is necessary for the formation of micropores

and has an optimum ratio to coke of 1:1 to achieve a high surface area activated carbon (Chen and Hashisho, 2012), Lower ratios of KOH is not efficient enough to diffuse to the inside of the delayed coke particles and forming interconnected pores.

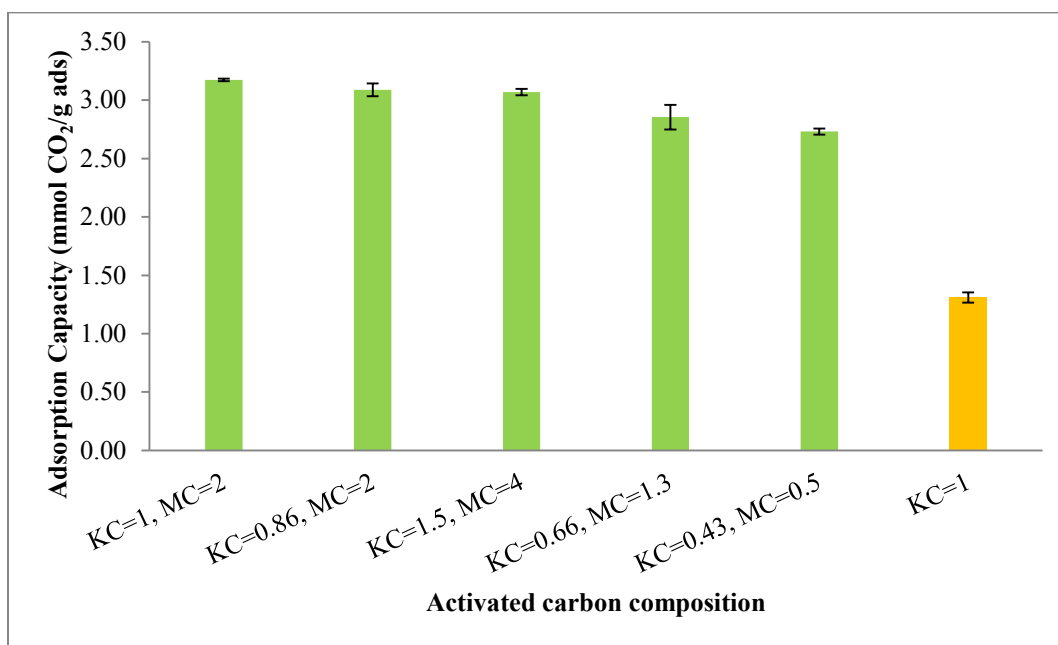


Figure 4-2. Effect of activation agent ratio on the adsorption capacity of microwave activated carbon, 66.6% CO₂ in N₂, T_{adsorption}=50°C, Error bars indicate standard deviation of the mean of two sets of data

Comparing the adsorption capacity of samples activated with KOH, and combined KOH and MgO, the former showed lower adsorption capacity (1.31 mmol CO₂/g ads), indicating that MgO template enhances the CO₂ capture by providing wider pore size distribution. The increase in adsorption capacity can be attributed to the higher entropy of adsorption associated with large degree of freedom of CO₂ molecules adsorbed on the surface of mesoporous activated carbon. These CO₂ molecules have higher mobility and less restriction than the ones adsorbed on the

surface of microporous activated carbon (Durá et al., 2016). However, based on our research findings there should be a balance between mesopore and micropore volume. Increasing the ratio of MgO/coke at a fixed amount of KOH in 27g of coke-MgO-KOH mixture, causes pore collapse due to the over-activation related to higher KOH/coke ratio in the mixture (He et al., 2012). Therefore, at a particular MgO/coke ratio, all the mesopores will collapse and the structure of the activated carbon will be mainly macroporous which is not favorable for the adsorption of relatively small molecules like CO₂ (with kinetic diameter of 3.9 Å (Siriwardane et al., 2001)). This suggests that MgO/Coke ratio has an optimum ratio which turned out to be 2 in our experimental work.

Figure 4-3 shows the effect of activation purge gas and humidity on the adsorption capacity of activated carbon (KC=0.86, MC=2) prepared under different activation conditions. Samples prepared under humid condition (either in N₂ or CO₂) show higher adsorption capacity than samples prepared under dry atmosphere. Steam is a common activation agent and physical activation could occur if the activation atmosphere is rich in water vapor. The impregnation of the coke with KOH created additional pores in the coke which facilitated the access of water molecules to the carbon skeleton for additional activation. In addition, potassium acts as a catalyst which increases the rate of the reaction between the water molecules and the carbon atoms (Jankowska et al., 1991, Patrick, 1995, Wu et al., 2005). As a result, the use of humidified nitrogen resulted in higher surface area and consequently higher CO₂ adsorption than dry nitrogen.

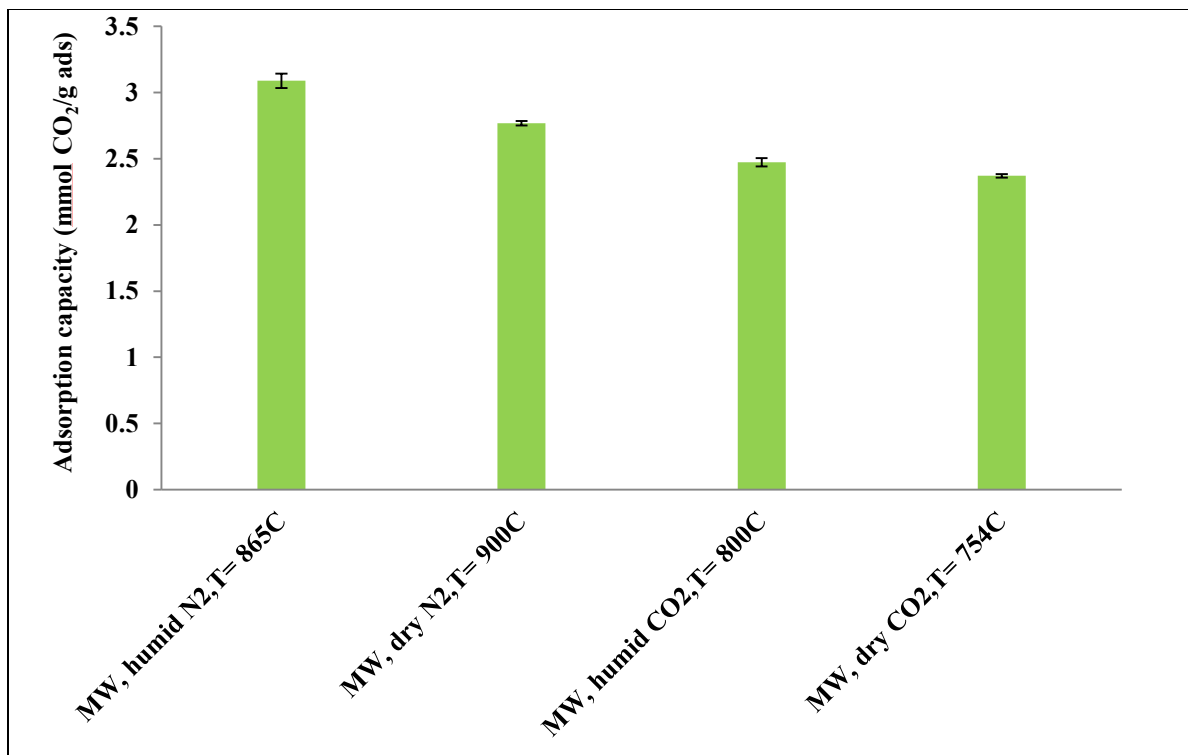


Figure 4-3. Effect of activation purge gas and humidity on the adsorption behavior of activated carbons (KC=0.86, MC=2), microwave (MW) heating, CO₂ flow rate= 200 ml/min, T_{adsorption} =50°C. Error bars indicate standard deviation of the mean of two sets of data

The adsorption results show that samples activated in N₂ atmosphere have almost 25% higher CO₂ uptake capacity compared to those activated in CO₂. Activation with N₂ shows significant formation of nitrile (C≡N) at temperatures around 850 °C which increases the basicity of activated carbon (Rathore et al., 2010). The high temperature activation with N₂ results in an increase in quaternary nitrogen, where N atoms are incorporated into the graphitic layer in substitution of C atoms and increases the polarity and basicity of carbon surface (Bandosz, 2006). Microwave heating of delayed coke in nitrogen atmosphere raises its temperature so fast and uniformly which results in decomposition of surface acidic (e.g. carboxylic and lactone) groups and removal in the form of CO or CO₂. In addition, it is possible some N from N₂

atmosphere react with carbon surface forming some nitrogen complex. Consequently, the relative basic content will be increased (Zhang et al., 2010), hence increases the affinity of activated carbon to acidic CO₂.

FTIR analysis (Figure 4-4) of carbon samples activated in N₂ and CO₂ atmosphere was carried out for ascertaining various functional groups.

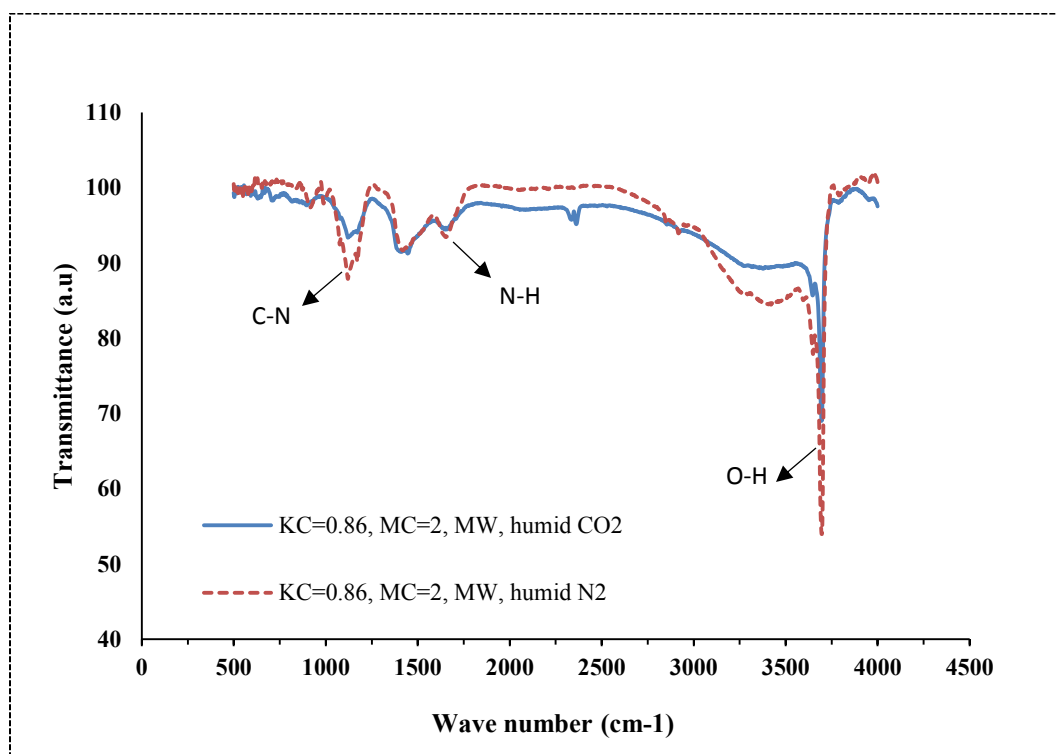


Figure 4-4. FTIR spectra of microwave activated carbons in N₂ and CO₂ gas stream

The peaks observed at $\sim 1118 \text{ cm}^{-1}$ and $\sim 1666 \text{ cm}^{-1}$ (Figure 4-4) correspond to C-N and N-H stretching of amide (Coates, 2006). These two bands are more pronounced for the sample activated in nitrogen gas stream, indicating more basic surface. These N-containing groups possess an isolated electron in their nitrogen atom; hence, the activated carbon surface becomes alkaline and shows strong affinity to acidic species such as CO₂ (Rathore et al., 2010).

Additionally, a major presence of O-H band was detected at $\sim 3690 \text{ cm}^{-1}$ (Figure 4-4) which was assigned to OH stretching vibration (Ahmad et al., 2013). There is a noticeable reduction in the spectrum of the O-H band (lower intensity) in carbon activated in CO_2 atmosphere. Ahmad et al. (Ahmad et al., 2013), also reported significant reduction of surface O-H groups at high carbonization temperatures ($>500 \text{ }^\circ\text{C}$) using CO_2 as activation agent, which is followed by the formation of aromatic groups. This well-organized activated carbon with dense aromatic groups has fewer reactive sites (Ahmad et al., 2013). It is also postulated that during activation at elevated temperatures ($>700 \text{ }^\circ\text{C}$), CO_2 can affect the surface functional groups of coke and increase the acidic groups which is not favorable for adsorption of acidic gases such as CO_2 (Bandosz, 2006).

In Figure 4-4, of the washed samples with distilled water and sulfuric acid, no IR absorption bands for the Mg compounds (IR bands of 1470, and 1540 cm^{-1}) including $\text{MgCO}_3/\text{H}_2\text{O}$, $\text{MgCO}_3/2\text{H}_2\text{O}$, MgCO_3 , $\text{Mg}_2\text{CO}_3(\text{OH})_2/3\text{H}_2\text{O}$ and Mg were found. Therefore, we expect that MgO has only served as a template though MgO can react with water to form $\text{Mg}(\text{OH})_2$ (IR absorption bands of 800, 850, and 880 cm^{-1}) in the presence of H_2O in the water-washing step (Li et al., (2014)).

4.5. Conclusion

Activated carbon was prepared from delayed coke by microwave-assisted heating using KOH coupled with the MgO template. Evaluation of bulk and surface composition of activated carbon samples indicated that samples activated with combined KOH and MgO have one order of magnitude higher oxygen content comparing to those activated with KOH only. Also, the general trend in Mg and K content is consistent with MC and KC ratios, respectively. Comparing the pore volume of activated carbons showed that KOH is necessary for micropore formation,

but there is an optimum ratio for KOH to coke which in this research was 1:1, and further increase of KOH results in pore collapse. It was found that pore volume of activated carbons directly increases with the portion of MgO template in the carbon, which indicates the essential role of MgO template in pore widening and formation of mesopores. This effect was validated through comparing samples activated with KOH only, and combined KOH and MgO. Activated carbons were tested for CO₂ adsorption at 50°C using a TGA. The highest adsorption capacity of 3.17 mmol CO₂/g AC was obtained for sample with KC=1, and MC=2 which was attributed to the wider pore size distribution and higher entropy of adsorption for CO₂ molecules. Comparing the adsorption performance of samples activated under CO₂ and N₂ stream, showed that CO₂ was not as efficient as N₂, and yielded activated carbons with almost 25% lower CO₂ adsorption capacity, which was due to a decrease in the amount of surface basic groups (which are reactive sites for adsorption of acidic gases such as CO₂), as confirmed by FTIR analyses. The results clearly indicated that microwave-assisted KOH activation coupled with the MgO template is an effective approach to the preparation of high capacity CO₂ adsorbents from oil sands coke and better management of this by-product.

4.6. References

- Ahmad, F., Daud W. M. A. W., Ahmad M. A., Radzi R., and Azmi A. A. (2013). The effects of CO₂ activation, on porosity and surface functional groups of cocoa (*Theobroma cacao*) – Shell based activated carbon. *Journal of Environmental Chemical Engineering* **1**(3): 378-388.
- Aksoylu, A. E., Madalena M., Freitas A., Pereira M. F. R., and Figueiredo J. L. (2001). The effects of different activated carbon supports and support modifications on the properties of Pt/AC catalysts. *Carbon* **39**(2): 175-185.

- Allen, E. W. (2008). Process water treatment in Canada's oil sands industry: I. Target pollutants and treatment objectives. *Journal of Environmental Engineering and Science* **7**(2): 123-138.
- Bandosz, T. J. (2006). *Activated Carbon Surfaces in Environmental Remediation*, Elsevier Science.
- Bullin J. A. and Polasek J. C. (1990). The use of MDEA and mixtures of amines for bulk CO₂ removal, *Sixty-Ninth GPA Annual Convention*, Lakewood, Colorado
- Chang, C. F., Chang C. Y., and Tsai W. T. (2000). Effects of Burn-off and Activation Temperature on Preparation of Activated Carbon from Corn Cob Agrowaste by CO₂ and Steam. *Journal of Colloid and Interface Science* **232**(1): 45-49.
- Chen, H. and Hashisho Z. (2012). Effects of microwave activation conditions on the properties of activated oil sands coke. *Fuel Processing Technology* **102**(0): 102-109.
- Chen, H. and Hashisho Z. (2012). Fast preparation of activated carbon from oil sands coke using microwave-assisted activation. *Fuel* **95**: 178-182.
- Coates, J. (2006). Interpretation of Infrared Spectra, A Practical Approach. Encyclopedia of Analytical Chemistry, John Wiley & Sons, Ltd.
- Dabrowski, A., Podkoscielny P., Hubicki Z., and Barczak M. (2005). Adsorption of phenolic compounds by activated carbon: a critical review. *Chemosphere* **58**(8): 1049-1070.
- Dunne, L. J. and Manos G. (2010). Adsorption and Phase Behaviour in Nanochannels and Nanotubes. New York.

- Durá, G., Budarin V. L., Castro-Osma J. A., Shuttleworth P. S., Quek S. C. Z., Clark J. H., and North M. (2016). Importance of Micropore–Mesopore Interfaces in Carbon Dioxide Capture by Carbon-Based Materials. *Angewandte Chemie International Edition* **55**(32): 9173-9177.
- Foo, K. Y. and Hameed B. H. (2012). Mesoporous activated carbon from wood sawdust by K_2CO_3 activation using microwave heating. *Bioresource technology* **111**: 425-432.
- Furimsky, E. (1998). Gasification of oil sand coke: Review. *Fuel Processing Technology* **56**(3): 263-290.
- Gholidoust, A., Atkinson J. D., and Hashisho Z. (2017). Enhancing CO_2 Adsorption via Amine-Impregnated Activated Carbon from Oil Sands Coke. *Energy & Fuels* **31**(2): 1756-1763.
- Gomes, H. T., Machado B. F., Ribeiro A., Moreira I., Rosario M. R., Silva A. N. M. T., Figueiredo J. L., and Faria J. L. (2008). Catalytic properties of carbon materials for wet oxidation of aniline. *Journal of Hazardous Materials* **159**(2-3): 420-426.
- Gray, M. L., Soong Y., Champagne K. J., Baltrus J., Stevens R. W., Toochinda P., and Chuang S. S. C. (2004). CO_2 capture by amine-enriched fly ash carbon sorbents. *Separation and Purification Technology* **35**(1): 31-36.
- Hasib-ur-Rahman, M., Sijaj M., and Larachi F. (2010). Ionic liquids for CO_2 capture: Development and progress. *Chemical Engineering and Processing: Process Intensification* **49**(4): 313-322.

- He, X., Li R., Qiu J., Xie K., Ling P., Yu M., Zhang X., and Zheng M. (2012). Synthesis of mesoporous carbons for supercapacitors from coal tar pitch by coupling microwave-assisted KOH activation with a MgO template. *Carbon* **50**(13): 4911-4921.
- Jack, T. R., Sullivan E. A., and Zajic J. E. (1979). Comparison of the structure and composition of cokes from the thermal cracking of Athabasca Oil Sands bitumen. *Fuel* **58**(8): 585-588.
- Jankowska, H., Świątkowski A., and Choma J. (1991). Active carbon, E. Horwood.
- Kawano, T., Kubota M., Onyango M. S., Watanabe F., and Matsuda H. (2008). Preparation of activated carbon from petroleum coke by KOH chemical activation for adsorption heat pump. *Applied Thermal Engineering* **28**(8-9): 865-871.
- Khalil, S. H., Aroua M. K., and Daud W. M. A. W. (2012). Study on the improvement of the capacity of amine-impregnated commercial activated carbon beds for CO₂ adsorbing. *Chemical Engineering Journal* **183**(0): 15-20.
- Lee, S. H. and Choi C. S. (2000). Chemical activation of high sulfur petroleum cokes by alkali metal compounds. *Fuel Processing Technology* **64**(1-3): 141-153.
- Li, L., Tang L., Liang X., Liu Z., and Yang Y. (2016). Adsorption Performance of Acetone on Activated Carbon Modified by Microwave Heating and Alkali Treatment. *Journal of Chemical Engineering of Japan* **49**(11): 958-966.
- Li, S., Wang Z.J., Chang T-T (2014) Temperature Oscillation Modulated Self-Assembly of Periodic Concentric Layered Magnesium Carbonate Microparticles. *PLoS ONE* **9**(2): e88648.

- Marsh, H. and Rodriguez-Reinoso F. (2006). Activated carbon. Oxford, Elsevier, Ltd.
- Morishita, T., Tsumura T., Toyoda M., Przepiorski J., Morawski A. W., Konno H., and Inagaki M. (2010). A review of the control of pore structure in MgO-templated nanoporous carbons. *Carbon* **48**(10): 2690-2707.
- Patrick, J. W. (1995). Porosity in Carbons: Characterization and Applications, Wiley.
- Pirngruber, G. D., Cassiano-Gaspar S., Louret S., Chaumonnot A., and Delfort B. (2009). Amines immobilized on a solid support for postcombustion CO₂ capture: A preliminary analysis of the performance in a VSA or TSA process based on the adsorption isotherms and kinetic data. *Energy Procedia* **1**(1): 1335-1342.
- Rathore, R. S., Srivastava D. K., Agarwal A. K., and Verma N. (2010). Development of surface functionalized activated carbon fiber for control of NO and particulate matter. *Journal of Hazardous Materials* **173**(1): 211-222.
- Siriwardane, R. V., Shen M. S., Fisher E. P., and Poston J. A. (2001). Adsorption of CO₂ on Molecular Sieves and Activated Carbon. *Energy & Fuels* **15**(2): 279-284.
- Small, C., Ulrich A., and Hashisho Z. (2012). Adsorption of Acid Extractable Oil Sands Tailings Organics onto Raw and Activated Oil Sands Coke. *Journal of Environmental Engineering* **138**(8): 833-840.
- Thompson, M. (2008). CHNS Elemental Analyzers. *The Royal Society of Chemistry* **29**.
- Woo, S.W., Dokko K., Nakano H., and Kanamura K. (2009). Incorporation of polyaniline into macropores of three-dimensionally ordered macroporous carbon electrode for electrochemical capacitors. *Journal of Power Sources* **190**(2): 596-600.

- Wu, M., Zha Q., Qiu J., Han X., Guo Y., Li Z., Yuan A., and Sun X. (2005). Preparation of porous carbons from petroleum coke by different activation methods. *Fuel* **84**(14–15): 1992-1997.
- Xia, Y., Mokaya R., Grant D. M., and Walker G. S. (2011). A simplified synthesis of N-doped zeolite-templated carbons, the control of the level of zeolite-like ordering and its effect on hydrogen storage properties. *Carbon* **49**(3): 844-853.
- Xia, Y., Yang Z., and Mokaya R. (2010). Templated nanoscale porous carbons. *Nanoscale* **2**(5): 639-659.
- Xiong, R., Ida J., and Lin Y. S. (2003). Kinetics of carbon dioxide sorption on potassium-doped lithium zirconate. *Chemical Engineering Science* **58**(19): 4377-4385.
- Xu, B., Peng L., Wang G., Cao G., and Wu F. (2010). Easy synthesis of mesoporous carbon using nano-CaCO₃ as template. *Carbon* **48**(8): 2377-2380.
- Yang, J. and Qiu K. (2010). Preparation of activated carbons from walnut shells via vacuum chemical activation and their application for methylene blue removal. *Chemical Engineering Journal* **165**(1): 209-217.
- Yoon, S., Oh S. M., Lee C. W., and Ryu J. H. (2011). Pore structure tuning of mesoporous carbon prepared by direct templating method for application to high rate supercapacitor electrodes. *Journal of Electroanalytical Chemistry* **650**(2): 187-195.
- Zhang, Z., Xu M., Wang H., and Li Z. (2010). Enhancement of CO₂ adsorption on high surface area activated carbon modified by N₂, H₂ and ammonia. *Chemical Engineering Journal* **160**(2): 571-577.

CHAPTER 5. PLASMA ENHANCED SEEDED GROWTH OF METAL ORGANIC FRAMEWORKS ACROSS CARBON NANOTUBE FABRICS AND THEIR POTENTIAL FOR CO₂ CAPTURE

5.1. Introduction

Adsorption onto solid sorbents hold promise for carbon dioxide (CO₂) capture due to their high efficiency, low energy requirements, and often ease of regeneration (Rao and Rubin, 2002). However, most of the currently used adsorbents such as molecular sieves or zeolites, activated carbons (Saha and Deng, 2010), silica gel (Zhang et al., 1998), and hydrotalcites (Hutson et al., 2004) have relatively low adsorption capacities (0.3- 4.4 mmol CO₂/g) for CO₂ at atmospheric pressure and require high operating pressures and temperature (Rao and Rubin, 2002). Therefore, alternative adsorbents, performing at low temperature and pressure needs to be considered.

Metal organic frameworks (MOF) (Walton et al., 2007) have recently drawn great attention mainly because they have high surface area and tailorable pore structure, and are suitable for the capture, release, permeation, storage, or sensing (Kumar et al., 2015) of gas molecules. The presence of open metal sites across MOF crystals enables for selective adsorption of target gases such as CO₂ (Bao et al., 2011), and offers very specific functionalities and properties relevant to carbon capture. MOF-74 series were shown to offer strong adsorption sites for CO₂ (Caskey et al., 2008, Dietzel et al., 2009, Bae et al., 2012) with the adsorption capacity of 26 and 30 wt% for Ni-MOF-74 and Mg-MOF-74 at 423K, respectively. The Mg-MOF has a higher heat of adsorption compared to MOFs of other metal ions and take up more CO₂ molecules per unit cell than its analogues (Dietzel et al., 2009). Caskey et al. also attributed this behavior to the smaller molecular size of Mg that increases the ionic character of Mg-O bond between unsaturated Mg²⁺ ions and oxygen atoms in CO₂ molecule (Caskey et al., 2008).

Micron-sized MOF crystals formed from traditional solvothermal MOF synthesis reaction are not necessarily best fitted for separation/adsorption applications due to difficulty to control their growth into shapes other than their particulate form (Lu, 2012). The development of MOF thin film materials where MOF crystals are intimately interconnected to form defect-free membranes has therefore been extensively investigated (Zacher et al., 2009, Carne et al., 2011). One of the promising methods is to embed MOF crystals across a polymer membrane to form mixed matrix membranes (MMM). MOF-based MMMs currently outperform pure MOF from economic point of view, since only a small amount of MOF is required to cover the support and no expensive support is necessarily needed for MOF-based MMM (Adatoz et al., 2015). A variety of polymer materials such as electrospun fiber mats including poly(acrylonitrile) (PAN) (Centrone et al., 2010), polypropylene fiber mats (Zhao et al., 2014) have been applied for supporting MOF crystals. MOF-crystals on polymer fiber matrices have been integrated through different methods including encapsulation in electrospun fibers (Ostermann et al., 2011) or immobilization on fiber through solvothermal synthesis (Küsgens et al., 2009), but unfortunately these methods resulted in small MOF loading fraction and poor MOF crystal quality (Zhao et al., 2014). Also an important challenge that needs to be addressed is interface compatibility between the MOF and the polymer (Basu et al., 2011), which results in physical agglomeration of MOFs upon manufacturing. Therefore, new strategies to develop continuous MOF membranes supported onto nano-porous materials have been investigated. Additionally, the lack of chemical diversity of these materials has opened the route to the design of more chemically versatile platforms.

Carbon nanotubes (CNTs) recently attracted great attention as growth platform materials for their high chemical stability, tuneable chemistry, and excellent mechanical strength (Majumder et al., 2005, Li et al., 2014). A hybrid MIL-101/MWCNT has been fabricated by Anbia *et al.*,

(Anbia and Hoseini, 2012) where the crystal structure and morphology was identical to that of virgin MIL-101 but CO₂ adsorption capacity was increased from 0.84 to 1.35mmol/g at 298K and 10 bar. Yang *et al.* (Yang et al., 2010), reported an improvement in H₂ storage by incorporating MOF-5 into Pt-loaded multi-walled carbon nanotubes (MWCNTs), at both 77K and 298K, and over a wide range of pressure. Dumée *et al.* fabricated ZIF-18 on CNT bucky paper support via secondary growth method. The mixed gas permeation performance of synthesized hybrid metal organic framework membranes towards CO₂, and N₂ revealed high selectivity of N₂ over CO₂ (Selectivity = 33) (Dumee et al.). Lin *et al.* (Lin et al., 2015) by in situ growth of NH₂-MIL-101(Al) on the external surface of CNTs, introduced amino groups and active sites for selective separation of CO₂ from CH₄ (Selectivity = 25.4). The developed CNT-MOF composites can also be promising for application in adsorption such as CO₂ capture. The major limitation with the incorporation of CNTs across any composite material relates to the control of the interface between the different phases which may lead to poor heterogeneous nucleation sites for MOFs to grow on the surface of bare substrate (Yoo et al., 2009, Bux et al., 2011, Liu et al., 2011). Specifically, when considering the growth of nanostructures from the surface of CNTs, the surface active sites should be optimized to ensure appropriate surface coverage density. Different methods, including chemical reaction in solution, exposure to radiative sources such as x-ray, gamma ray or ultra violet-ozone and plasma have been developed to introduce functional groups on the surface of CNT (Datsyuk et al., 2008, Jiang et al., 2009, Ma et al., 2010). Exposure to strong acids, such as nitric acid (HNO₃) and sulfuric acid (H₂SO₄) (Taborski et al., 1995, Hamon et al., 1999), ozone oxidation (Hou et al., 2008, Vandsburger et al., 2009) and plasma oxidation have been investigated as routes to anchor oxygenated groups such as hydroxyl or carboxylic groups across the surface on CNTs. Although

chemical treatments are by far the most effective route, wet-oxidation was shown to lead to loss in crystallinity and damage of the CNT walls (Wang et al., 2009). Plasma gas treatments, on the other hand, are versatile routes to generate specific functional group densities and do not affect the bulk properties of materials (Wang et al., 2009). The plasma treatment process has been well studied since the 1960's (Morita et al., 1990) and has quickly evolved into a valuable technique to engineer the surface properties of CNTs via appropriate plasma parameters such as type of gas, treatment time and input power (Chevallier et al., 2001). Several research studies on plasma treatment of CNTs revealed the enhanced chemical performance and interfacial adhesion by embedding oxygen-containing functional groups on the surface of CNT (Chen et al., 2009, Chen et al., 2010, Ham et al., 2014).

The purpose of this study is to investigate the synthesis of a new class of porous materials working at low pressure and possessing high adsorption capacity for CO₂ gas. The seeding and growth of a thin, active, and selective layer of Mg-MOF-74 across the surface of plasma functionalized CNT- Bucky paper (CNT-BP), a new class of randomly oriented carbon nanotube fabrics, was studied through a broad range of plasma conditions. The changes of the atomic contents and structure properties of CNT-BPs as a function of plasma gas and treatment time were analyzed using X-ray photoelectron spectroscopy (XPS) and Raman spectroscopy. Contact angle analysis was performed to measure the impact of plasma treatment on surface wettability of CNT-BPs. Morphological characteristic of CNT-BPs and its interface with MOF was observed by Scanning Electron Microscopy (SEM). The CO₂ capture capacity of MOF-CNT-BP samples was investigated by volumetric analysis at 25 °C and 1 atm.

5.2. Materials and methods

5.2.1. Chemicals and reactants

All chemicals in this study including 2,5 dihydroxyterephthalic acid (98%), N,N, dimethylformamide (99.8% anhydrous), Ethanol (90% anhydrous), and Isopropanol (99.5%) were purchased from Sigma Aldrich except for Magnesium nitrate hexahydrate (98%) which was acquired from Fisher Scientific.

5.2.2. CNTs growth and preparation

The growth of the multiwall CNTs was performed by Chemical Vapor Deposition (CVD) as detailed elsewhere (Huynh and Hawkins, 2010). Fe_2O_3 as the catalyst was deposited on silicon wafers (100 mm dia., N/phosphorous (1-0-0) type, 1-10 Ω/cm (SQI Inc.)) by thermal evaporation by a resistively-heated alumina-lined tungsten boat. Prior to the test, the CVD reactor was evacuated and flushed with a flow of helium (Air Liquide, 99.999%) then the temperature was ramped to the set-point. Acetone-free acetylene supply (Air Liquide, 99.9999%) was switched into the reactor with the helium flow when required.

5.2.3. CNT-BP fabrication

CNTs formed as forests on silicon wafers were scrapped from their supports and suspended in isopropanol. The suspensions were then bath-sonicated for 5min at 240 W (using UNISONIC FXP10M) and up to 5 times at an initial temperature of -17 °C (Dumée et al., 2013). The temperature of the system was maintained below 5 °C during sonication by adding ice cubes into the sonication bath reservoir. BPs were then formed by vacuum filtrating the CNTs suspension onto a poly (ether sulfone) membrane (0.2 mm pore size – Millipore) until completely dried. The BPs could then be peeled off to form self-supporting substrates as previously reported (Dumée et al., 2013).

5.2.4. CNT-BP surface functionalization by plasma treatment

Plasma treatments were performed on a 13.56 MHz high frequency plasma system (Diener PICO PC (SN 80001)). Plasma parameters such as the chamber pressure (0.2 mbar) and power (80 W) were fixed, while a time-based dose matrix was performed in order to induce a range of seeding moieties densities across the surface of the CNTs. The plasma method was conducted in either O₂/Ar or NH₃ gas glows. The plasma exposure duration was varied between 3, 5 and 7 min and both the temperature of the sample stage and chamber were recorded. CNT-BPs were fixed on the curved glass plate with double-sided tape and placed inside the chamber.

5.2.5. MOF crystals seeding and growth across the BPs

In a typical preparation of Mg-MOF-74, 2,5-Dihydroxyterephthalic acid (0.333 g) and magnesium nitrate hexahydrate (1.425 g) were dissolved in 150 mL of a solvent mixture of dimethyl formamide, ethanol and de-ionized (DI) water (15:1:1) and placed in a 400 mL sealed Schott bottle. The solution was then sonicated for 30 min to get a homogeneous solution. In order to make sure that both sides of the membranes were exposed to the solution, the BP samples were placed vertically within a hollow Teflon (PTFE polymer with melting point 320 °C) holder placed inside a Teflon-lined autoclave. The solution was then heated at 125 °C in an oven (HERAEUS, UT6120) for 20 h to achieve full crystal growth. After growth, the mother liquor was decanted using cellulose acetate filter papers (Whatman, grade 5) under vacuum filtration. The yellow crystalline product was washed 3 times with methanol (10 mL), then immersed in 10 mL fresh methanol and decanted. The purification steps were repeated with fresh methanol 3 times over 4 days to exchange the DMF guest. CNT-BPs were separated from the solution and oven dried at 80 °C for 5 h. The solution was then vacuum-dried at 250 °C for 5 h to remove remaining methanol traces. For simplicity, the samples are named based on their

preparation methods from now on. For example, MCN3, 2s-Cr15 represents MOF-CNT-BP sample which has been treated with ammonia (N) for the duration of 3 min and 1 side, while crystallization (Cr) took 15 h. Similarly, MCO7, 2s-Cr20 refers to MOF-CNT-BP treated with 30% oxygen (O) in argon for the duration of 7 min and 2 sides, while crystallization (Cr) took 20 h. Figure 5-1 illustrates the schematic of MOF-CNT-BP preparation, step by step.

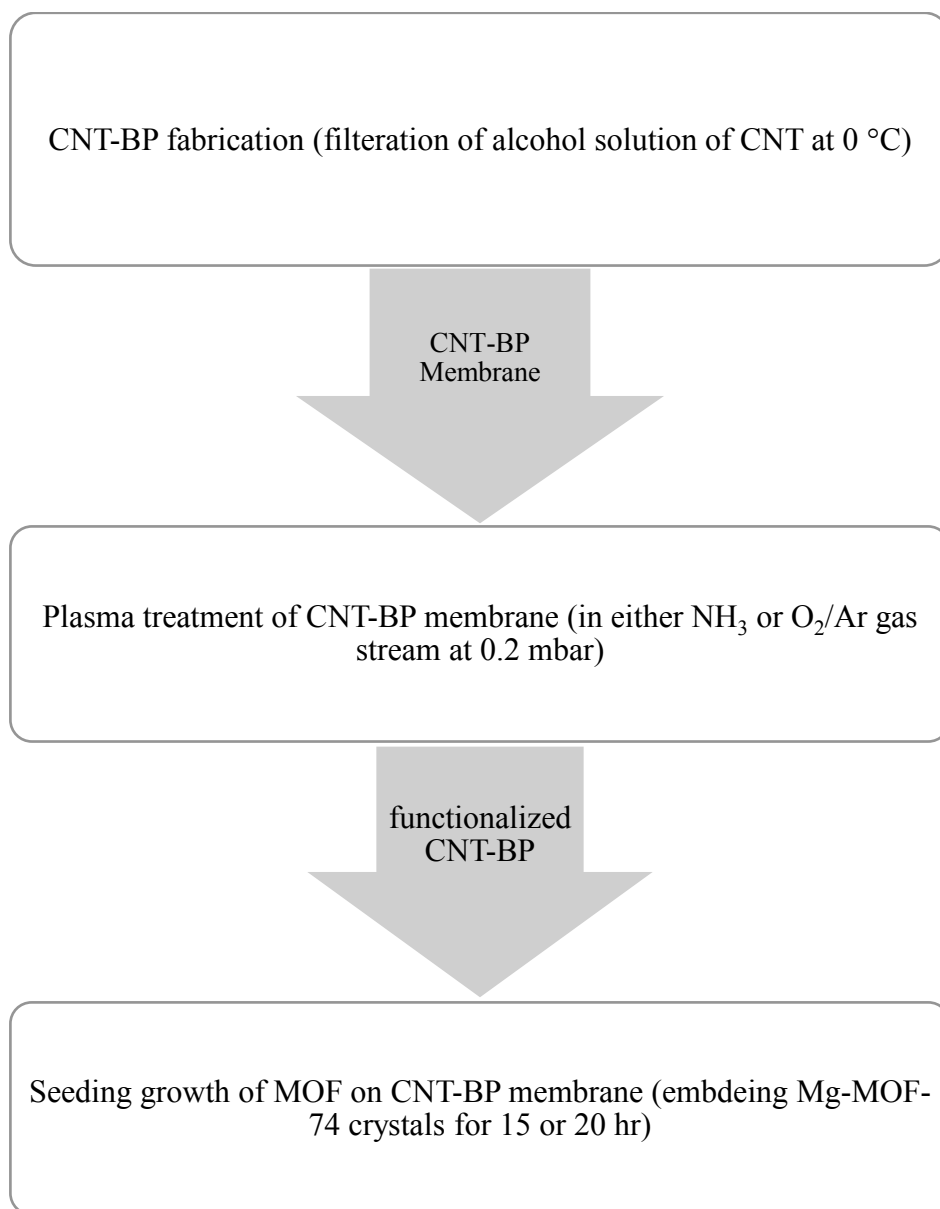


Figure 5-2 Preparation of MOF-CNT-BP sample

5.2.6. Characterization tests

X-ray photoemission spectroscopy (XPS) spectra were acquired at a pass energy of 160 eV with a 1 eV/step and a pressure in the analysis chamber of 5×10^{-9} torr with an AXIS Nova (Kratos Analytical Ltd., UK). The samples were irradiated with Al $K\alpha$ radiation ($h\nu = 1486.6$ eV) from a mono-chromated source operating at 150 W. Analysis was performed on a plasma treated CNT-BPs prior to MOF crystals coverage.

Raman spectra of CNT-BPs were obtained using Raman microscope (Renishaw, InVia Basis). Argon ion laser with the excitation wavelength of 514 nm and maximum output power of 50 mW was used as light source. A Leica N PLAN confocal microscope with a resolution up to $2\mu\text{m}$ was coupled to the Raman spectrometer. All measurements were collected at 50x magnification with a 10 s exposure time and 10 accumulations. The samples were scanned in the range of 500 to 3500 cm^{-1} with 2 cm^{-1} spectral resolution.

Static or dynamic contact angles across the membranes were measured using a camera (KSV Instruments, CAM 101). At least 50 pictures were acquired after 2 s of drop impact. The solution used was DI- water.

Scanning Electron Micrographs (SEMs) were acquired on a Supra 55VP FEG-SEM at an accelerating voltage of 3 keV and a working distance of 5 mm. The samples were mounted on aluminum stubs with carbon tape and coated with a 6 nm thick layer of Au prior to analysis to minimize charging and prevent beam damage across the crystals.

Thermogravimetric analysis tests (TGA) were conducted on the MOF-CNT-BP samples on a Thermogravimetric Analyzer (TA instruments, TA Q50). Tests were carried out under N_2 stream at a heating rate of $10\text{ }^\circ\text{C}/\text{min}$ for a temperature profile from $25\text{ }^\circ\text{C}$ to $500\text{ }^\circ\text{C}$.

Nitrogen adsorption isotherms were obtained using a sorption analyzer (Quantachrome Instruments, Autosorb-iQ2) at relative pressure range from 10^{-6} to 0.99 at 77K. Prior to the measurement, samples were degassed at 120 °C (atmospheric pressure) for 5h. Specific surface area was determined from the N₂ adsorption isotherms using the Brunauer-Emmett-Teller (BET) at relative pressure ranges from 0.01 to 0.07 and total pore volume was determined at $p/p_0 = 0.95$. Pore size distributions (PSD) were also obtained from nitrogen adsorption isotherm using Horváth-Kawazoe (HK) method which was developed for graphitic slit pores in microporous carbons and is suitable for PSD determination in MOFs (Bae et al., 2009).

CO₂ volumetric adsorption measurements were conducted on Autosorb-iQ2 (Quantachrome Instruments) at 25 °C. The samples were out-gassed prior to the measurement at 250 °C under vacuum for 10h.

5.3. Results and Discussions

5.3.1. Carbon nanotube surface conditioning and assessment

The functionalization of CNTs to introduce oxygen rich groups, such as alcohols or carboxylic species, are extremely valuable routes not only to improve the wettability of the graphitic structures but also as a first step as anchoring points towards specific grafting. Different plasma parameters, such as the choice of feed gas (Chen et al., 2010, Zhao et al., 2012), and plasma treatment time were used to determine specific levels of functionalization (Chen et al., 2009). In this work, specific plasma treatments were used to enhance the surface chemistry of CNTs prior to the growth of MOF. Virgin and plasma treated CNT-BPs with O₂/Ar or NH₃ have been analyzed with XPS in order to investigate the functional groups attached to the surface of CNT-BP.

Table 5-1 and

Table 5-2 present the atomic concentrations of samples treated with O₂/Ar and NH₃, respectively. From Table 5-1, the amount of oxygen atomic concentration of virgin CNT-BP has increased from 3.3 to 13.9, 15.0 and 15.2% after plasma treatment with O₂/Ar for 3, 5 and 7min, respectively. Plasma treatment with O₂/Ar led to a large increase in surface oxygen and nitrogen concentration, while the carbon concentration decreased. As for the O₂/Ar plasma, the attack of the O^{*} radicals from the feed gas, most likely led to the formation of active sites and then of C-O bonds on the surface of the bucky papers. Due to the stabilization by hydrogen atom transfer from the neighbors (carbon nanotube edges passivated with hydrogen) (Buonocore et al., 2008), C-OH bonds are formed, while C=O bonds are the consequence of an intramolecular reorganization of C-C bonds. Conversely, the carboxylic groups stem from the attack of O^{*} radicals on the previously generated C=O bonds (Chen et al., 2009).

Table 5-1. Atomic concentration of elements in CNT-BP samples before and after treatment with O₂/Ar

Sample	C (%)	N (%)	O (%)
Virgin CNT-BP	96.1	0.7	3.2
Treated CNT-BP, O ₂ /Ar, 3min	85.2	0.9	13.9
Treated CNT-BP, O ₂ /Ar, 5min	84.1	0.9	15.0
Treated CNT-BP, O ₂ /Ar, 7min	83.8	1.0	15.2

Table 5-2. Atomic concentration of elements in CNT-BP samples before and after treatment with NH_3

Sample	C (%)	N (%)	O (%)
Virgin CNT-BP	96.1	0.7	3.2
Treated CNT-BP, NH_3 , 3min	90.1	1.9	8.0
Treated CNT-BP, NH_3 , 5min	89.5	2.1	8.4
Treated CNT-BP, NH_3 , 7min	88.2	2.7	9.1

When increasing plasma treatment time from 3 to 5min, the surface oxygen concentration increased by 7.8%, while extending plasma treatment from 5min to 7min resulted in a small increase (1.4%) in the surface oxygen concentration. This phenomenon can be attributed to the surface saturation of oxygenated groups at long time plasma treatment (Zhao et al., 2012). In the case of plasma treatment with NH_3 (

Table 5-2), the oxygen atomic concentration increased with plasma treatment duration as it was 8.0, 8.4 and 9.1% for 3, 5 and 7min treatment, respectively. Compared to O_2/Ar plasma treatment, NH_3 plasma introduced lower amount of oxygen on the surface whereas its surface nitrogen concentration was almost two folds higher.

Figure B1a presents high resolution C1s spectra of plasma treated CNT-BP with O_2/Ar for 7min on both sides after de-convolution based on their binding energies as described in Table

B1. The carbon 1s spectrum was fitted with five Gaussian peaks components that represent (1) sp^2 -hybridized graphite-like carbon atoms (C=C at 284.1 ± 0.2 eV), (2) SP^3 hybridized carbon atoms (C-C at 285.1 ± 0.2 eV), (3) carbon bonded to one oxygen atom (C-O at 286.2 ± 0.2 eV such as alcohol and ether species) or (4) (C=O at 287.2 ± 0.2 eV such as ketone and aldehyde species) and (5) carbon bonded to two oxygen atoms, such as O-C=O at 288.9 ± 0.2 eV corresponding to carboxylic and ester functional groups. The C1s peak intensity varied depending on plasma gas and treatment time. The quantitative analysis presented in Table B1 indicates that plasma treatment resulted in reduction of the sp^2 C=C fraction, and increase in the C-O, C=O or O-C=O fractions. These trends, suggests that plasma treatments oxidized the C=C bonds to form new C-Ox groups. When oxygen plasma gas treatment is used, various oxidative reactions are believed to occur. Free radicals will form on the treated surface and can react with active species from oxygen plasma environment (Steen et al., 2001, Tang et al., 2007).

In both cases of O_2/Ar and NH_3 plasma treatment (Table B1, and Table B2) the C-O fraction first increases, and then decreases with increasing treatment time, whereas the C=O and O-C=O fraction increases. This is possibly due to the reaction mechanism of generation of C-O, and transformation to C=O and O-C=O bonds that was proposed by Chen *et al.* (Chen et al., 2009). It is postulated that C=C bonds are more susceptible to plasma attack due to the presence of active π bonds (Ago et al., 1999, Tang et al., 2007). In fact, the dissociated π bonds act as active sites on C=C which are prone for radical generation. Hence a decrease in C=C fraction, may result in C-O production and then C-OH bonds through stabilization by hydrogen atom transfer from neighboring chain. During plasma treatment, oxygen radicals will also be generated on the surface of CNT-BP, and can react with C-C bonds, forming C=O bonds. As for O-C=O, it is believed the plasma- generated radicals on C=O bind to active oxygen atoms and after

stabilization with H^+ transfer, will form carboxylic species ($HO-C=O$). For samples treated with O_2/Ar , when the plasma treatment time increases from 3 to 5min, the $C=C$ fraction decreases from 28.1 to 20.8% while $C=O$ fraction increases significantly from 12.9 to 29.4. When plasma treatment time extends to 7min, there is almost no change in $C=C$ fraction, while $C=O$ fraction drops from 29.4 to 24.4%, suggesting that there is a saturation state for the surface oxidation for which the CNT surface cannot accept any more oxygen species from plasma environment due to oxidation level. Hence, with increasing plasma treatment time from 5 to 7min, no further oxidation on $C=C$ bonds will occur and no more $C=O$ bond will form; whereas, $O-C=O$ fraction reaches a significant amount of 9.9%, which is possibly due to the reaction between radicals on $C=O$ and active oxygen atoms.

The NH_3 plasma treated samples exhibited a very different behaviour comparing to the O_2/Ar treatments. The $C1s$ peak (Figure B1b) is composed of three main peaks: peak (1) corresponding to $C-C$ and $C-H$ bond at 284.8eV, peak (2) belonging to $C-O$ or $C-N$ at 286.4eV, and peak (3) corresponding to $O=C-O$ bond at 288.8eV. In some cases, a new peak (4) also appear at a binding energy of 287.4 eV, which can be attributed to amide carbon atoms in $O=C-N$ group (Vesel and Mozetic, 2008). Also $C-N$ bond from amino group is expected to appear at (~285.8 eV), but is not shown due to the difficulty to distinguish between peaks (1) or (2). It is hard to determine the exact type of nitrogen functional group and differentiate it from oxygen functional groups, as there is a strong overlap of peaks for oxygen and nitrogen containing functionalities and they appear at similar binding energies (Vesel et al., 2008).

Comparing the XPS results from Table B2, it can be observed that with an increase in NH_3 plasma treatment time from 3 to 5mins, the fraction of peak (1) corresponding to $C-C$ decreases from 62.7 to 54.0%, while the fraction of peak (2) which can be attributed to either $C-$

O or C-N increases from 23.1 to 31.7%. Extending NH_3 treatment up to 7min, C-C bond (peak 1) fraction decreases to 33.8%, but fraction of peak (2) stays almost the same (30.8%) and a new bond at 287.2 eV evolves with 26% fraction that can be attributed to O=C-N as well as C=O species. A decrease of peak (1) can be due to replacement of hydrogen atoms from benzene ring with amino groups (C-NH₂) or even hydroxyl (-OH) groups (Vesel and Mozetic, 2008). On the other hand, the O-C=O fraction remains unchanged with increasing NH_3 plasma exposure time from 3 to 5mins, suggesting surface saturation at a very short exposure time in NH_3 comparing to O_2/Ar , due to differences in the probability of oxygen and nitrogen incorporation into the surface, as it was also reported elsewhere (Vesel et al., 2008). As it can be concluded from Table B2, samples treated with NH_3 have high intensity peak attributed to carboxylic groups while for samples treated with O_2/Ar , the intensity of this peak is small and only significant if they were exposed to plasma for long time (7min). Our measurements suggested that O_2/Ar plasma treatment preferentially forms hydroxyl and carbonyl groups on the surface, which is in a good accordance with research findings in the literature (Ago et al., 1999).

The incorporation of such functional groups induced changes to the lattice of the CNT walls. Raman analysis was therefore used to evaluate the crystallinity of the CNT materials, and assess potential disorder across the CNTs surface generated from the plasma treatment step (Sveningsson et al., 2001). Figure B2 presents the Raman spectra of CNT-BP before and after 3min of both 30% O_2/Ar and NH_3 plasma treatments. In case of virgin CNT-BP, the G peak at 1570.6 cm^{-1} , implies the presence of crystalline graphitic carbon in CNT-BP (Sveningsson et al., 2001) and is a result of in-plane vibrations of sp^2 bonded carbon atoms (Ferrari and Basko, 2013) whereas occurrence of the D peak at 1342.6 cm^{-1} is attributed to the defects in the curved graphitic sheet, sp^3 carbon (Sveningsson et al., 2001).

The ratio (R) of D/G intensity is a measure of the defects present on graphene structure. From Table B3, the R ratio is 0.51 for the virgin CNT-BP, and slightly increases to 0.60 and 0.69 for NH₃ and O₂/Ar treated CNT-BP, respectively which can be due to the enhancement of surface defects and embedment of oxygen atoms. Chen et al. (Chen et al., 2009) also reported an enhanced oxygen fraction on the surface of MWCNT upon plasma treatment with O₂/Ar mixture. The R ratio for CNT-BP treated with O₂/Ar is even more than that of CNT-BP treated with NH₃, which can be due to presence of more oxygenated groups on the surface as it was also confirmed by the XPS results.

Comparing to the virgin CNT-BP, a blue shift (increase in Raman frequency) of peak G takes place which can be due to the increased disorder and defects density in plasma treated CNT-BP (Yu et al., 2004). Slight increase of the D/G intensity ratio (R) and blue shift of peak G position in treated CNT-BP samples are indicative of surface structure change of CNT-BP and introduction of oxygen groups. Comparing the plasma conditions applied more oxygen functionalities have been embedded on the surface of CNT-BP with 30% O₂/Ar gas.

The wettability of the CNT-BP materials is largely a function of the amount of amorphous carbons present across the surface lattice, nature of the functional groups, and the roughness of the materials. Contact angle measurements are presented in Table 5-3 and show a decrease in contact angle after oxygen and ammonia plasma treatment, which correspond to a higher hydrophilicity of CNT-BP surface. For one-sided plasma treated samples, the shielded side showed that a water drop beaded up on the CNT-BP surface, whereas for the side facing the plasma, water wicks into the CNT-BP. The oxygen- plasma treated samples exhibit lower values of contact angle which can be attributed to a higher hydrophilic character. Even after a short exposure time (3min and one side), for both typed of gas used, the surface shows an enhanced

hydrophilicity by decrease in contact angle value from 123.52° to 34.3° and 39.6° for virgin CNT-BP, oxygen treated and NH₃ plasma treated CNT-BP samples, respectively. However, NH₃ plasma treatment seems to be less efficient in surface wettability. After 3min exposure on one side, oxygen-plasma treated CNT-BPs show contact angle value of 34.3°, while this value for NH₃-plasma treated CNT-BPs increases to 39.6°.

Table 5-3. Contact angle results for the plasma treated CNT-BPs

Sample	Contact angle with water (deg)	
	Side 1	Side 2
Virgin CNT-BP	123.52	122.98
MCO3,1s-Cr15	34.32	87.86
MCO3,2s-Cr15	25.46	–
MCO3,2s-Cr20	25.09	–
MCO5,2s-Cr20	20.60	31.23
MCO7,1s-Cr15	27.13	71.53
MCO7,2s-Cr20	24.28	–
MCN3,1s-Cr20	39.63	–
MCN3,2s-Cr15	40.10	–
MCN3,2s-Cr20	40.10	33.45
MCN5,1s-Cr15	39.06	–
MCN5,2s-Cr15	30.10	21.27
MCN7,1s-Cr20	38.52	–
MCN7,2s-Cr15	20.92	–

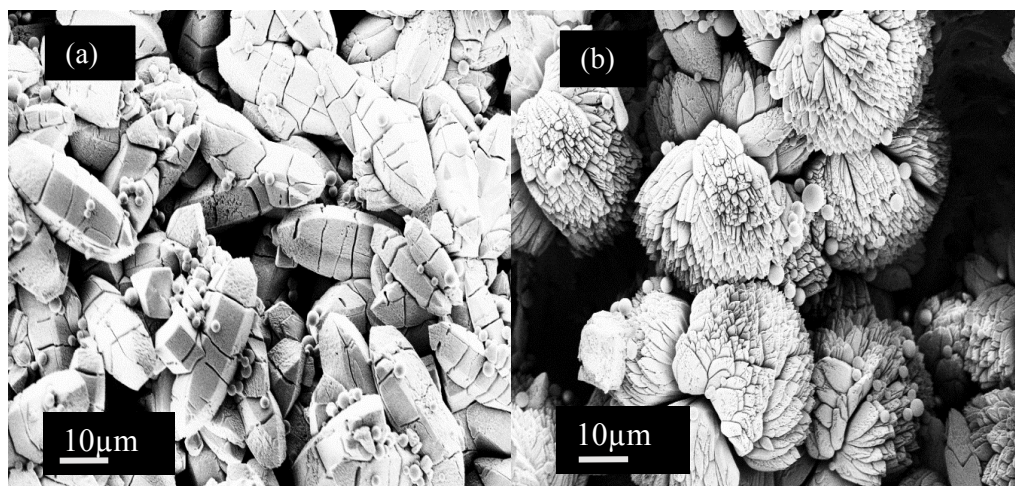
The difference becomes more obvious when samples get treated with plasma on both sides, as 3min oxygen- plasma treatment on both sides caused a decrease in the contact angle value to 25.4°, while for that of NH₃- plasma treated sample is about 40.1°. Junkar *et al.* (Junkar *et al.*, 2009), also studied nitrogen and oxygen plasma treatment on polyethylene terephthalate polymer and reported a lower surface wettability with nitrogen plasma treatment compared to oxygen treatment.

Interestingly, when CNT-BPs were treated with plasma on one side, depending on the exposure time, the other side facing impervious material (glass plate) showed a lower contact angle value comparing to the virgin CNT-BP. This might be due to the diffusion of plasma through the material which can affect surface chemistry of the non-treated side. It was previously reported (Chakraborty *et al.*, 2013) that at high residence time of plasma, depending on the average pore size of the fabrics, active chemical species might penetrate through the fabric layers and affect lower layers. The difference in contact angle values between sides of double sided plasma treated CNT-BPs can be attributed to this fact. From the contact angle results in Table 5-3, it can be concluded that extending plasma exposure time results in higher hydrophilicity.

5.3.2. MOF-CNT-BP composite properties

The morphology of the CNT-BP and MOF-CNT-BP materials was assessed by SEM in order to evaluate its interface with MOF and MOF seeding density. Figure B3 presents SEM of virgin CNT-BP and plasma treated CNT-BP with O₂/Ar for 15min. Comparing plasma treated and virgin CNT-BP illustrates that there is no mechanical damage on the sidewalls of the sample even after long (i.e. 15 min) plasma treatment. The effect of plasma treatment on surface

reactivity with MOF crystals is shown in Figure 5-3. Virgin BP shows almost no affinity towards MOF crystals as indicated by poor MOF coverage while the affinity of surface increases after plasma treatment with NH_3 and O_2/Ar . This enhancement is attributed to the CNT-BP surface characteristic change by plasma treatment which enhances the growth of MOF nano-crystals by creating a large number of potential nucleation sites. Also, comparing SEM images of samples treated with O_2/Ar and NH_3 indicates that the former provides more MOF coverage on CNT surface than the latter. This might be related to the formation of hydroxyl groups on the CNT surface upon plasma treatment. It has been proven that the interaction between acidic species with $-\text{OH}$ is energetically more favorable than that at carbon atoms attached to $-\text{OH}$ with $\text{C}=\text{O}$ bond (in the carboxylic group) (D'Souza and Kadish, 2014). Since plasma treated samples were immersed in the solution of an organic acid and organic solvent, so the presence of $-\text{OH}$ group is much more favorable than carboxylic groups.



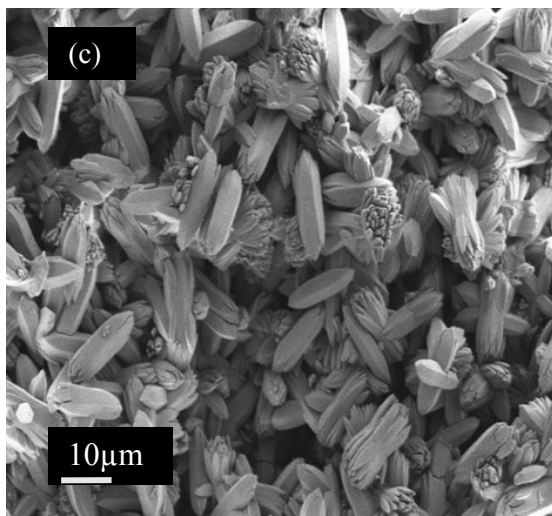


Figure 5-3. Impact of plasma treatment on surface affinity towards MOF crystals, (a) virgin CNT-BP, (b) single side plasma treated CNT-BP with NH_3 for 3min and (c) single side plasma treated CNT-BP with O_2/Ar for 3min

On the other hand, the formation of hydrogen bonds between the CNTs and solvent molecules, such as water or alcohols, will facilitate wettability and ameliorate the interactions between MOF solution and CNT, resulting in higher MOF crystals seeding densities and coverage across the CNT-BP surface (Gascon et al., 2008). The effect of plasma treatment duration is illustrated in Figure 5-4. From 3min to 5min treatment, the crystals accumulate on the stem and form a cluster. While prolonging the plasma duration to 7min results in a mixture of single and clustered crystals on the surface.

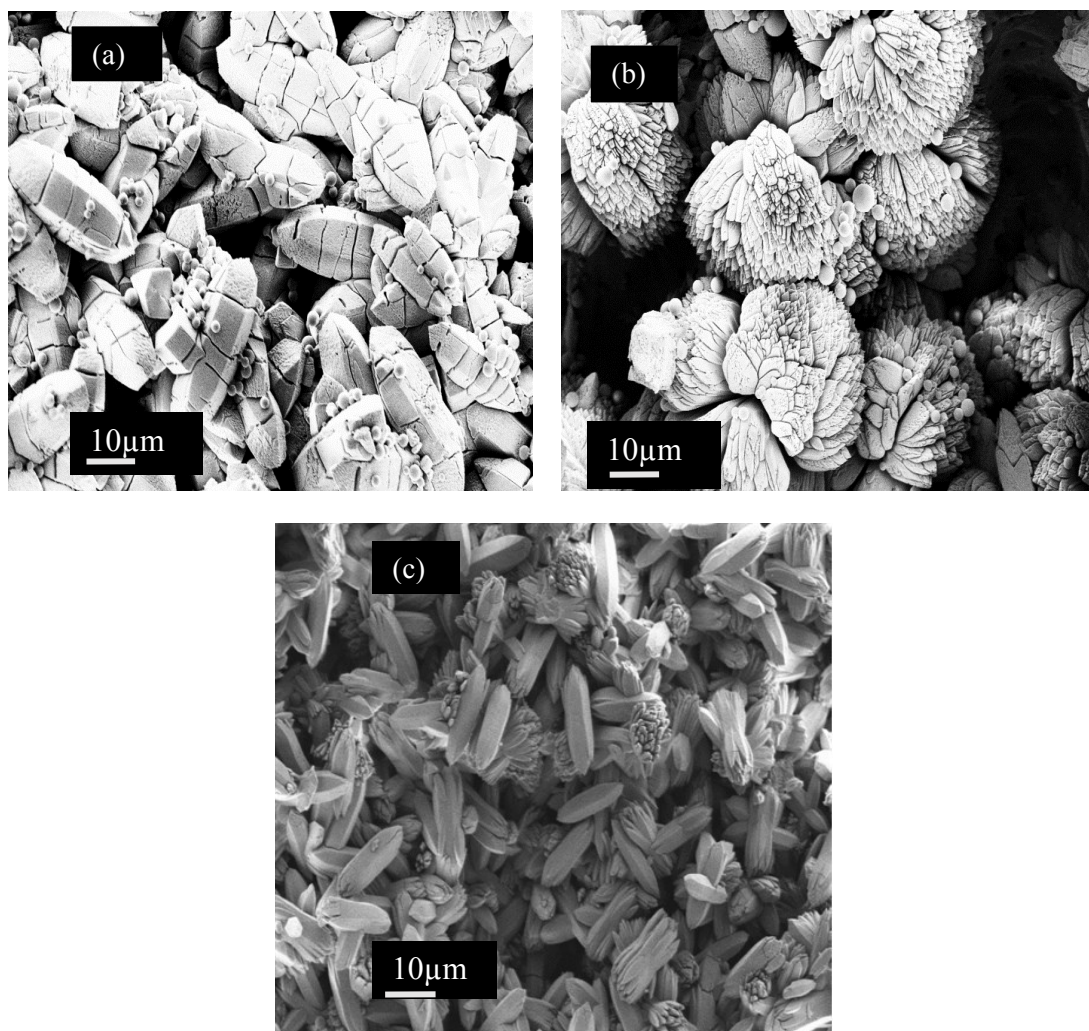


Figure 5-4. Impact of plasma duration on surface affinity towards MOF crystals, (a) 3min, (b) 5min and (c) 7min, double side treated with O_2/Ar , crystallization time = 20h

Figure 5-5 shows the impact of single or double sided plasma treatment on surface MOF coverage. The density of MOF crystals on each side of the double-side treated samples was found to be lower than that of the samples treated only on one side. This might be due to the competition between crystal seeds to sit on the active sites located on both sides of double-side treated CNT-BPs. As stated earlier, although both sides of CNT-BPs were treated under the same condition, due to the plasma diffusion, the wettability, hence density of active species on one of

the sides could be higher. Accordingly, the density of MOF crystals on one side of double-side treated CNT-BP was higher than the other one.

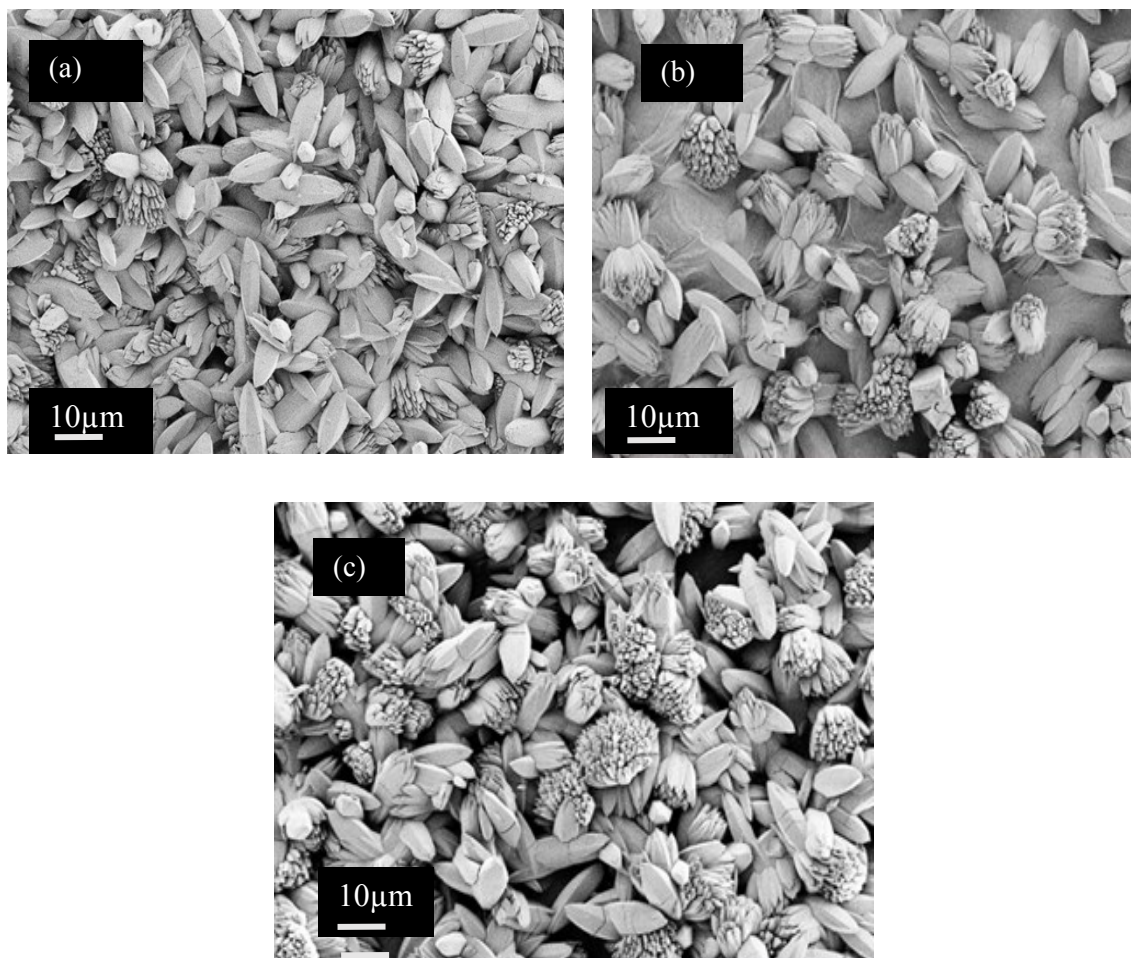


Figure 5-5. Impact of side treatment on surface affinity towards MOF crystals, (a) side 1 of double side treated sample, (b) side 2 of double side treated sample and (c) single side treated sample, treated with NH_3 , treatment duration=5min, crystallization time=15h

Figure 5-6 shows the impact of MOF crystallization time on the size of crystals. For crystallization time equal to 15 h (Figure 5-6a), the first micrometric-sized crystals of MOF were obtained, and therefore the crystallinity of the mixture increased. Employing longer crystallization time up to 20 h (Figure 5-6b), provided enough time for the crystals to grow and

fully develop, which shows the typical faceted morphology for this synthesis (Sanchez-Lainez et al., 2015). It can be concluded that longer crystallization time results in formation of larger crystals and yields clusters of crystals attached to each other from stem.

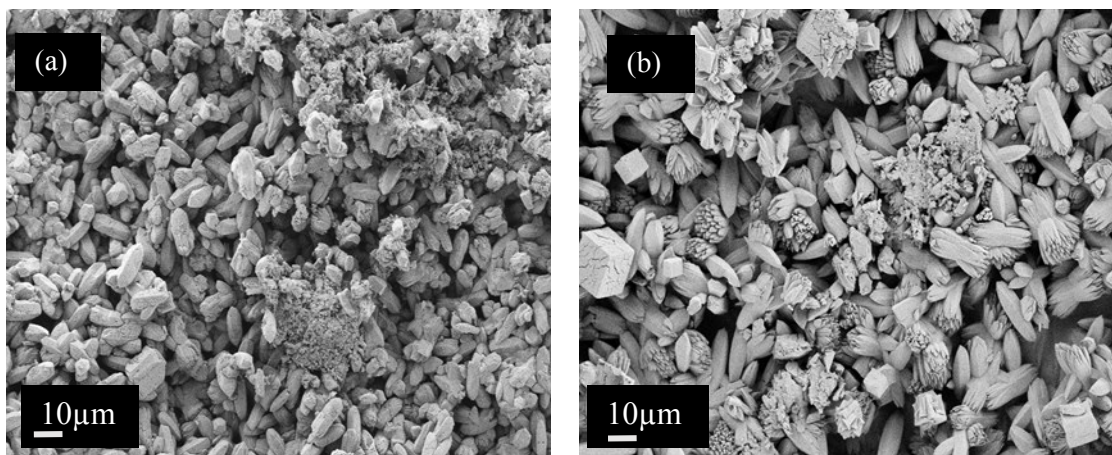


Figure 5-6. Effect of crystallization time on MOF growth, (a) 15h crystallization, (b) 20h crystallization, single side treated with O₂/Ar, treatment duration of 3 min

The thermal stability of the MOF-CNT-BP structures was also investigated by TGA analysis. Thermal properties of adsorbent materials are critical since in some separation processes (such as CO₂ separation from flue gas) the temperature may reach as high as 232 °C (Wong, 2009). The TG curves of MOF-CNT-BP and Mg-MOF-74 presented in Figure B4 show a clear reduction in weight as soon as samples are exposed to the dry nitrogen gas stream in the TGA furnace and is attributed to the removal of hydration water molecules from the crystal structure. After a first sharp decrease of ~7.8% in weight of MOF-CNT-BP up to 120 °C, which is corresponding to non-coordinated water removal, the rate of weight loss level off until it reach to 166 °C. The second weight loss, corresponding to 27.2%, was however related to the removal of metal-coordinated water and solvent molecules within the MOF structure (Bernini et al., 2015), and was continued until the decomposition of framework to magnesium oxide which commence at

above 400 °C (Dietzel et al., 2008). Comparing to Mg-MOF-74, the TG curve inclination of MOF-CNT-BP was sharper and exhibited a continuous decrease in weight up to 305 °C which may be attributed to further removal of solvent molecules, since MOF-CNT-BP samples were dried at low temperature (80 °C) to preserve the CNT properties, while the Mg-MOF-74 crystals were dried and activated at 250 °C. This trend can be clearly observed from DTG curve where MOF-CNT-BP showed a peak centered at 261 °C while Mg-MOF-74 reached a plateau from 166 to 305 °C, indicating that most of the solvent within the framework was already removed during the MOF activation process.

The third weight loss in the TG curve of MOF-CNT-BP, corresponding to 18.6% occurred above 400 °C which is related to the decomposition of the framework and yields magnesium oxide (Dietzel et al., 2008, Jiao et al., 2015). For all MOF-CNT-BP samples, the decomposition temperature is higher than that of Mg-MOF-74 (435 vs 430 °C) indicating a slight improvement in thermal stability of Mg-MOF-74 over CNT-BP compared to parent Mg-MOF-74. The whole decomposition process to render MgO from Mg-MOF-74 involves a weight loss of 53.6%, corresponding to complete removal of all water molecules within the framework which accompanies with collapse of the framework and is in good agreement with reported value (57%) by other researchers (Dietzel et al., 2008).

After total decomposition of framework to MgO at ~550 °C, the TG curve of Mg-MOF-74-CNT-BP, reach a plateau indicating stability of CNT-BP under nitrogen atmosphere. Similar studies showed almost intact structure of MWCNTs under anaerobic condition even up to 800 °C (Mahajan et al., 2013).

The specific surface area of adsorbents is critical to evaluate the activity and adsorption capacity of materials. Table 5-4 presents the BET surface area and pore volume of the MOF-CNT-BP samples. Compared to virgin CNT and Mg-MOF-74 with a specific surface area of 254.8 and 637.8 m²/g and an average pore volume of 0.7 and 0.4 cc/g, respectively, the surface area and pore volume for all MOF-CNT-BP samples decreased. The lower surface area of the MOF-CNT-BP samples in the present work can be attributed not only to the presence of Mg species in the CNT pores, but also to the different condition applied for synthesis, since MOF-CNT-BP samples dried at low temperature (80 °C). The outgassing temperature was determined based on the optimal temperature at which the non-coordinated water molecules remaining at the framework channels can be evacuated, without removing metal-coordinated water.

Table 5-4 shows when samples outgassed at 120 °C under nitrogen atmosphere, the nitrogen adsorption capacity and consequently the specific surface area is low, showing that the pores remain mostly blocked with guest molecules, probably DMF. DTG curve for MOF-CNT-BP sample in Figure B4 also shows a continual weight loss from 166 to 368 °C, which is even after removal of non-coordinated water molecules and can be attributed to the evacuation of framework from guest molecules. But when samples were outgassed at 250 °C, the nitrogen adsorption and surface area strongly increased. Bernini and coworkers (Bernini et al., 2015) studied the effect of outgas temperature on adsorption properties of Mg-MOF-74 and reported that at low outgas temperature (100 °C), most of MOF pores remain blocked due to the presence of solvent molecules.

Table 5-4. Summary of the properties of the MOF-CNT-BP membrane composites

Sample	MOF (%)	Pore Volume (cc/g)	BET Surface area (m ² /g), outgassed at 120°C	Decrease in surface area (%)	BET Surface area (m ² /g), outgassed at 250°C
Virgin CNT-BP	0	0.70	–		254.8
Mg-MOF-74	–	0.40	–		637.8
MCO3,1s-Cr15	55.8	0.16	27.2	89.3	78.2
MCO3,2s-Cr15	60.3	0.07	22.1	91.3	–
MCO3,2s-Cr20	70.9	0.19	61.7	76.0	–
MCO5,2s-Cr20	61.8	3.12	–	–	–
MCO7,1s-Cr15	74.2	0.35	77.2	69.7	201.7
MCO7,2s-Cr20	64.1	0.06	13.0	94.9	74.2
MCN3,1s-Cr20	64.9	0.11	22.4	91.2	–
MCN3,2s-Cr15	67.6	0.06	20.9	91.8	–
MCN3,2s-Cr20	56.3	0.14	49.7	80.5	287.3
MCN5,1s-Cr15	69.9	0.21	48.1	81.1	164.1
MCN5,2s-Cr15	56.7	0.44	80.7	68.3	–
MCN5,2s-Cr20	61.1	0.55	58.4	77.1	–
MCN7,1s-Cr20	63.9	0.09	47.9	81.2	–
MCN7,2s-Cr15	53.2	0.28	54.5	78.6	–

5.3.3. CO₂ volumetric adsorption results

Figure 5-7 presents the CO₂ volumetric adsorption of all MOF-CNT-BP samples. Figure 5-7a compares CO₂ adsorption of Mg-MOF-74 and MOF-CNT-BP at 25°C and 1 atm. Mg-MOF-

74 has a CO₂ adsorption capacity of only 3.1 mmol/g, while incorporated Mg-MOF-74 on a CNT-BP (treated with O₂/Ar, for 3min) has the highest CO₂ adsorption capacity of 10.7 mmol/g suggesting enhanced affinity towards CO₂ due to the presence of CNT-BPs.

The CNT-BP has an interpenetrating structure and hierarchical nanopores that improve the storage capability of the composite. In fact, MOF with a structure full of void spaces, is not beneficial for the retention of small molecules at ambient conditions owing to weak dispersive forces, whereas incorporating CNT-BP which is made of dense array of layers enhances the dispersive forces (Petit et al., 2010).

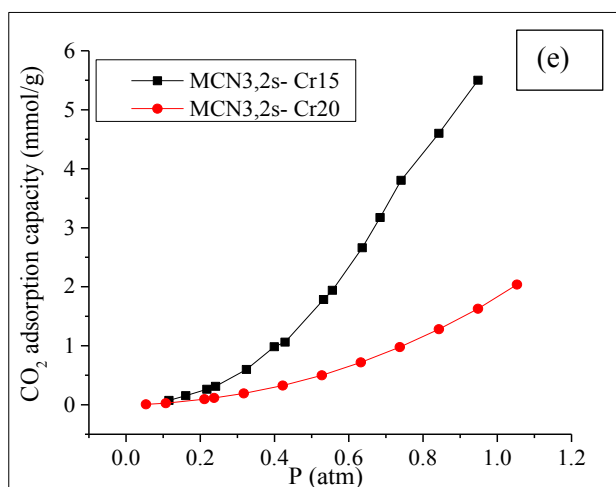
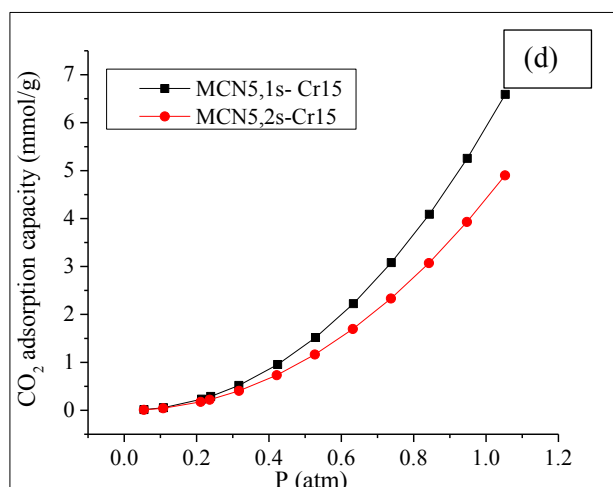
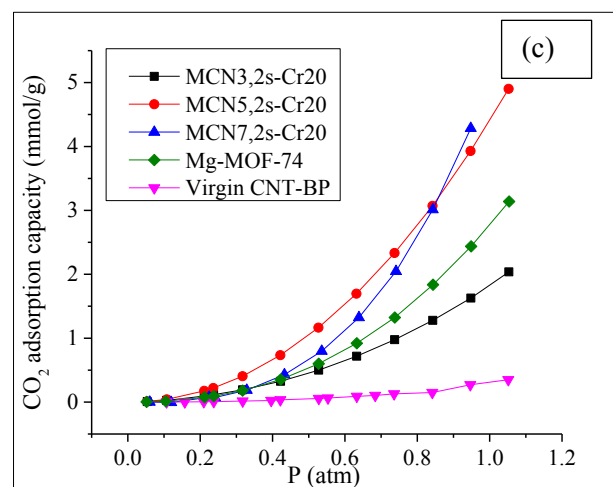
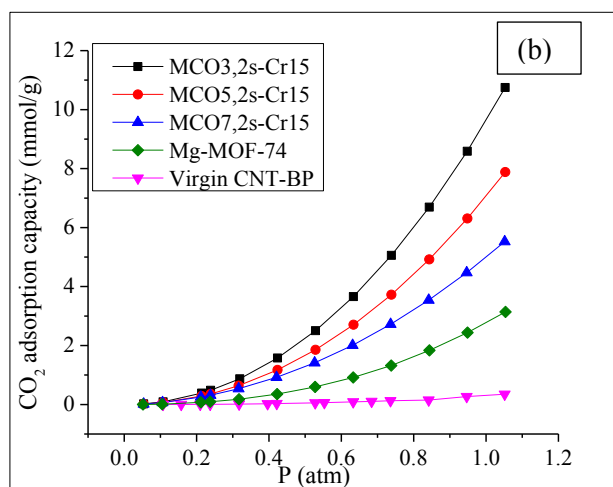
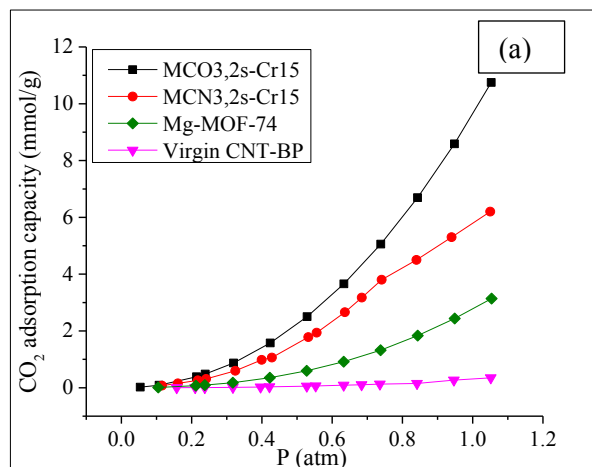


Figure 5-7. CO₂ volumetric adsorption of virgin CNT-BP and Mg-MOF-74-CNT-BPs at 25°C, Impact of (a) plasma gas, (b) plasma treatment duration for samples treated with O₂/Ar, (c) plasma duration for samples treated with NH₃, (d) plasma treatment side effect, and (e) crystallization duration

The pore size distribution (PSD) of MOF-CNT-BP samples is shown in Figure 5-8, representing the mesoporous structure of these materials, which further improves the storage capacity. The PSD data can be divided into two regimes with pore sizes of <20 Å (I) and 20-50 Å (II). These two classes reflect the role of incorporated CNT-BPs in pore structure change. As it can be seen from Figure 5-8, Mg-MOF-74 has microporous structure with pores distributed in the first range (<20 Å), while Virgin CNT-BP is mesoporous and its incorporation to MOF material resulted in a mesoporous composite of MOF-CNT-BP. The new porosity may be caused by new pores created at the interface between the MOF units and the CNT layers owing to the coordination of the oxygen groups of CNT-BP with the metallic centers of the MOF (Zu et al., 2014). The presence of new porosity enhances the dispersive forces which is the main attribute to the enhanced CO₂ adsorption (Petit et al., 2010).

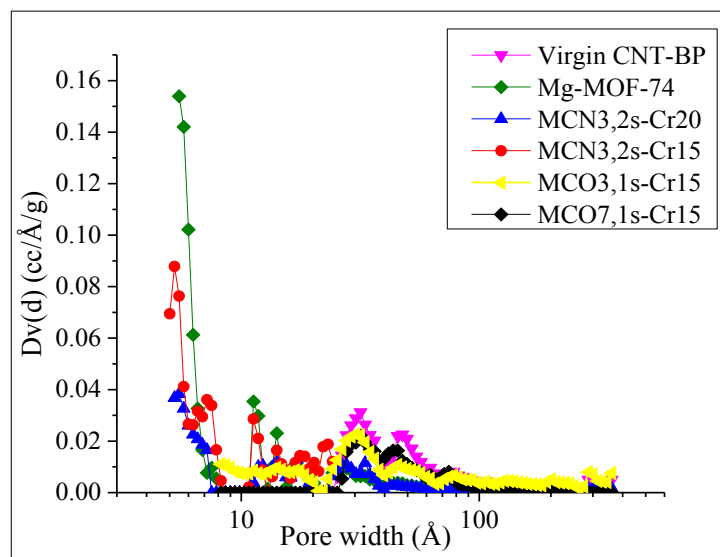


Figure 5-8. Pore size distribution of virgin CNT-BP, Mg-MOF-74 and MOF-CNT-BP

Also, SEM analysis of MOF-CNT-BPs confirms a highly interconnected network between MOF and CNT-BP with retained shape of MOF crystals suggesting good prior contact between MOF and CNT-BP which alleviates any drawback during MOF crystallization and growth such as agglomeration of crystals in the solution. Research studies on different MOF-carbon membranes revealed the fact that interfacial interaction between MOF and carbonaceous surface results in superior adsorption properties over parental MOF owing to the synergetic effect of the parent materials such as well- separation of the MOFs, and inhibition of distortion and bundling in CNT (Petit and Badosz, 2011).

CO₂ volumetric adsorption results can be categorized in four groups:

(a) The effect of plasma gas

Figure 5-7a compares the CO₂ uptake capacity of MOF-CNT-BP samples (MCO₃, 2s-Cr₁₅ and MCN₃, 2s-Cr₁₅) which has same preparation conditions but different plasma gas treatment,

i.e., O₂/Ar and NH₃, respectively. The results highlights that sample treated with O₂/Ar have higher affinity (10.7mmol/g) towards CO₂ than the one treated with NH₃ (6.2mmol/g). This behavior can be attributed to a better distribution of MOF crystals on CNT-BP's upon treatment with O₂/Ar than NH₃. Plasma treatment with O₂/Ar provides better wettability on the surface of CNT-BP as it introduces carbonyl and hydroxyl groups which enhances the interaction of CNT surface with water and polar solvents in the MOF solution and as a result, a better coverage of MOF on CNT surface would be provided, while NH₃ treatment functionalize surface with carboxylic groups as it was confirmed by XPS results. Raman spectroscopy results also confirmed the presence of oxygen functional group on the surface after plasma treatment with O₂/Ar.

(b) The effect of plasma treatment time

Figure 5-7b presents the adsorption capacity of samples treated with O₂/Ar at different exposure times of 3, 5 and 7min which are 10.7, 7.9 and 5.5mmol/g, respectively. This decreasing trend in adsorption capacity can be related to the amount of hydroxyl group on the surface. As also presented in Table B1, the C-O fraction first increases, and then decreases with increasing treatment time, whereas the C=O and O-C=O fraction increases. It is possibly due to the reaction mechanism of generation of C-O, and transformation to C=O and O-C=O bonds as proposed by Chen et al. (Chen et al., 2009). A combination of CO₂ adsorption capacities and contents of hydroxyl groups implied that CO₂ uptake capacities seemed to be correlated with the content of hydroxyl groups.

For samples treated with NH₃ plasma (Figure 5-7c), a sharp increase in CO₂ adsorption was observed as the plasma treatment time increased from 3 to 5min (2.0 to 4.9mmol/g) but as the treatment time increased to 7min, the adsorption capacity remained unchanged. This is likely

related to a saturation of surface dipoles stemming from the plasma treatment (Merenda, 2015). We can attribute the adsorption trend to the changes in surface functionalities as discussed earlier in section 5.3.1. From Table B2, the amount of surface hydroxyl group increased by about 37% when plasma exposure time changed from 3 to 5min, but it remained intact when prolonging the plasma treatment by 7min.

(c) The effect of plasma side treatment

The CO₂ adsorption capacities of samples treated with NH₃ plasma is shown in Figure 5-7d to investigate the effect of side treatment. Compared to MCN5, 1s-Cr15 which has been treated with NH₃ for 5min on one side, sample MCN5, 2s-Cr15 with similar plasma treatment but on both sides, shows 25% lower CO₂ uptake (4.90 vs. 6.59mmol/g). As it was earlier mentioned in SEM analysis, one side plasma treatment provides more active sites on CNT-BP surface compared to double side treatment. Hence the density of MOF crystals would be higher in the former case, and accordingly more CO₂ adsorption is expected.

(d) The effect of crystallization time

The effect of crystallization time on sample MCN3, 2s-Cr15 and MCN3, 2s-Cr20 is presented in Figure 5-7e. The CO₂ uptake of MCN3, 2s-Cr15 was greater by a factor of 1.9 than that of MCN3, 2s-Cr20. Based on SEM results, 15h crystallization yielded relatively smaller MOF crystals as they have limited time for growth compared to 20h crystallization. This might be attributed to a decrease of the channel length in each grain of the adsorbent (MOF), which results in high accessibility under the same condition, since diffusion is a limiting parameter in CO₂ access into the MOF crystal. In other words, the sorption ability of MOF-CNT-BP improved 1.9 times with a decrease in MOF crystal size. Our result is in good agreement with Kim group's

work (Kim et al., 2016), where they reported an enhanced CO₂ adsorption kinetics by reducing the amine-modified MOF crystal size.

5.4. Conclusions

The significant outcomes of this study are related to the impact of the plasma treatment on the CNT surface and its function towards gas adsorption. The Raman spectroscopy analysis demonstrated that plasma treatment on CNT was successful to functionalize the surface by inducing oxygenated groups on the surface which has been correlated more to the surface chemistry rather than mechanical change in carbon structure. The contact angle test confirmed that plasma treatment has drastically transformed hydrophobic surface to hydrophilic surface which by XPS analysis, determined to be due to the presence of hydroxyl groups more than carboxylic groups. It was observed that plasma treatment with 30% O₂ /Ar was more effective than treatment with NH₃ in terms of increasing the surface hydroxyl groups. The presence of a surface saturation mechanism was also confirmed, which is consistent with the literature. Given the plasma parameters applied, short plasma duration seems to be ample to introduce as much functionalities as allowed. Moreover SEM micrographs showed that plasma treatment was an effective method to anchor MOF crystals on the surface of CNT-BP. The study of crystallization time effect on capture capacity of prepared MOF-CNT-BP samples revealed that limiting the crystallization time results in smaller crystals which diminishes the diffusion resistance and enhances CO₂ access to MOF crystals. CO₂ adsorption was considerably higher on the hybrid MOF-CNT-BP compared to that of the parent materials (10.7 mmol/g for MOF-CNT-BP vs 3.1 and 0.35 mmol/g for Mg-MOF-74 and virgin CNT, respectively). A significant improvement in adsorption capacity of the MOF-CNT-BP samples was ascribed to the positive features deriving from compositing the parent materials. In this respect, growth of MOF on CNT-BP platforms

was found to benefit their formation and functionality through number of ways including increased dispersive forces, preventing agglomeration and enhanced MOF-CNT interfacial interaction following plasma treatment.

5.5. References

- Adatoz, E., Avci A. K., and Keskin S. (2015). Opportunities and challenges of MOF-based membranes in gas separations. *Separation and Purification Technology* **152**: 207-237.
- Ago, H., Kugler T., Cacialli F., Salaneck W. R., Shaffer M. S. P., Windle A. H., and Friend R. H. (1999). Work Functions and Surface Functional Groups of Multiwall Carbon Nanotubes. *The Journal of Physical Chemistry B* **103**(38): 8116-8121.
- Anbia, M. and Hoseini V. (2012). Development of MWCNT@MIL-101 hybrid composite with enhanced adsorption capacity for carbon dioxide. *Chemical Engineering Journal* **191**: 326-330.
- Bae, Y. S., Dubbeldam D., Nelson A., Walton K. S., Hupp J. T., and Snurr R. Q. (2009). Strategies for Characterization of Large-Pore Metal-Organic Frameworks by Combined Experimental and Computational Methods. *Chemistry of Materials* **21**(20): 4768-4777.
- Bae, Y. S., Lee C. Y., Kim K. C., Farha O. K., Nickias P., Hupp J. T., Nguyen S. T., and Snurr R. Q. (2012). High Propene/Propane Selectivity in Isostructural Metal–Organic Frameworks with High Densities of Open Metal Sites. *Angewandte Chemie International Edition* **51**(8): 1857-1860.
- Bao, Z., Yu L., Ren Q., Lu X., and Deng S. (2011). Adsorption of CO₂ and CH₄ on a magnesium-based metal organic framework. *Journal of Colloid and Interface Science* **353**(2): 549-556.

- Basu, S., Cano-Odena A., and Vankelecom I. F. J. (2011). MOF-containing mixed-matrix membranes for CO₂/CH₄ and CO₂/N₂ binary gas mixture separations. *Separation and Purification Technology* **81**(1): 31-40.
- Bernini, M. C., Garcia Blanco A. A., Villarroel-Rocha J., Fairen-Jimenez D., Sapag K., Ramirez-Pastor A. J., and Narda G. E. (2015). Tuning the target composition of amine-grafted CPO-27-Mg for capture of CO₂ under post-combustion and air filtering conditions: a combined experimental and computational study. *Dalton Transactions* **44**(43): 18970-18982.
- Buonocore, F., Trani F., Ninno D., Matteo A. D., Cantele G., and Iadonisi G. (2008). Ab initio calculations of electron affinity and ionization potential of carbon nanotubes. *Nanotechnology* **19**(2): 025711.
- Bux, H., Feldhoff A., Cravillon J., Wiebcke M., Li Y. S., and Caro J. (2011). Oriented Zeolitic Imidazolate Framework-8 Membrane with Sharp H₂/C₃H₈ Molecular Sieve Separation. *Chemistry of Materials* **23**(8): 2262-2269.
- Carne, A., Carbonell C., Imaz I., and MasPOCH D. (2011). Nanoscale metal-organic materials. *Chemical Society Reviews* **40**(1): 291-305.
- Caskey, S. R., Wong-Foy A. G., and Matzger A. J. (2008). Dramatic Tuning of Carbon Dioxide Uptake via Metal Substitution in a Coordination Polymer with Cylindrical Pores. *Journal of the American Chemical Society* **130**(33): 10870-10871.
- Centrone, A., Yang Y., Speakman S., Bromberg L., Rutledge G. C., and Hatton T. A. (2010). Growth of Metal–Organic Frameworks on Polymer Surfaces. *Journal of the American Chemical Society* **132**(44): 15687-15691.

- Chakraborty, T., Bucknum M. J., and Castro E. A. (2013). Computational and Experimental Chemistry: Developments and Applications, Apple Academic Press.
- Chen, C., Liang B., Ogino A., Wang X, and Nagatsu M. (2009). Oxygen Functionalization of Multiwall Carbon Nanotubes by Microwave-Excited Surface-Wave Plasma Treatment. *The Journal of Physical Chemistry C* **113**(18): 7659-7665.
- Chen, C., Ogino A., Wang X., and Nagatsu M. (2010). Plasma treatment of multiwall carbon nanotubes for dispersion improvement in water. *Applied Physics Letters* **96**(13): 131504.
- Chevallier, P., Castonguay M., Turgeon S., Dubrulle N., Mantovani D., McBreen P. H., Wittmann J. C., and Laroche G. (2001). Ammonia RF-Plasma on PTFE Surfaces: Chemical Characterization of the Species Created on the Surface by Vapor-Phase Chemical Derivatization. *The Journal of Physical Chemistry B* **105**(50): 12490-12497.
- D'Souza, F. and Kadish K. M. (2014). Handbook of Carbon Nano Materials: (In 2 Volumes)Volume 5: Graphene — Fundamental PropertiesVolume 6: Graphene — Energy and Sensor Applications.
- Datsyuk, V., Kalyva M., Papagelis K., Parthenios J., Tasis D., Siokou A., Kallitsis I., and Galiotis C. (2008). Chemical oxidation of multiwalled carbon nanotubes. *Carbon* **46**(6): 833-840.
- Dietzel, P. D. C., Besikiotis V., and Blom R. (2009). Application of metal-organic frameworks with coordinatively unsaturated metal sites in storage and separation of methane and carbon dioxide. *Journal of Materials Chemistry* **19**(39): 7362-7370.
- Dietzel, P. D. C., Blom R., and Fjellvåg H. (2008). Base-Induced Formation of Two Magnesium Metal-Organic Framework Compounds with a Bifunctional Tetratopic Ligand. *European Journal of Inorganic Chemistry* **2008**(23): 3624-3632.

- Dumée, L., He L., Hill M., Zhu B., Duke M., Schutz J., She F., Wang H., Gray S., Hodgson P., and Kong L. (2013) Seeded growth of ZIF-8 on the surface of carbon nanotubes towards self-supporting gas separation membranes. *Journal of Materials Chemistry A* **1**(32): 9208-9214.
- Dumée, L., Sears K., Schütz J., Finn N., Duke M., and Gray S. (2013). Influence of the Sonication Temperature on the Debundling Kinetics of Carbon Nanotubes in Propan-2-ol. *Nanomaterials* **3**(1): 70.
- Dumée, L. F., Sears K., Marmiroli B., Amenitsch H., Duan X., Lamb R., Buso D., Huynh C., Hawkins S., Kentish S., Duke M., Gray S., Innocenzi P., Hill A. J., and Falcaro P. (2013). A high volume and low damage route to hydroxyl functionalization of carbon nanotubes using hard X-ray lithography. *Carbon* **51**: 430-434.
- Ferrari, A. C. and Basko D. M. (2013). Raman spectroscopy as a versatile tool for studying the properties of graphene. *Nat Nano* **8**(4): 235-246.
- Gascon, J., Aguado S., and Kapteijn F. (2008). Manufacture of dense coatings of $\text{Cu}_3(\text{BTC})_2$ (HKUST-1) on α -alumina. *Microporous and Mesoporous Materials* **113**(1-3): 132-138.
- Ham, S. W., Hong H. P., Kim J. H., Min S. J., and Min N. K. (2014). Effect of Oxygen Plasma Treatment on Carbon Nanotube-Based Sensors. *Journal of Nanoscience and Nanotechnology* **14**(11): 8476-8481.
- Hamon, M. A., Chen J., Hu H., Chen Y., Itkis M. E., Rao A. M., Eklund P. C., and Haddon R. C. (1999). Dissolution of Single-Walled Carbon Nanotubes. *Advanced Materials* **11**(10): 834-840.
- Hou, Z., Cai B., Liu H., and Xu D. (2008). Ar, O₂, CHF₃, and SF₆ plasma treatments of screen-printed carbon nanotube films for electrode applications. *Carbon* **46**(3): 405-413.

- Hutson, N. D., Speakman S. A., and Payzant E. A. (2004). Structural Effects on the High Temperature Adsorption of CO₂ on a Synthetic Hydrotalcite. *Chemistry of Materials* **16**(21): 4135-4143.
- Huynh, C. P. and Hawkins S. C. (2010). Understanding the synthesis of directly spinnable carbon nanotube forests. *Carbon* **48**(4): 1105-1115.
- Jiang, X., Gu J., Bai X., Lin L., and Zhang Y. (2009). The influence of acid treatment on multi-walled carbon nanotubes. *Pigment & Resin Technology* **38**(3): 165-173.
- Jiao, Y., Morelock C. R., Burtch N. C., Mounfield W. P., Hungerford J. T., and Walton K. S. (2015). Tuning the Kinetic Water Stability and Adsorption Interactions of Mg-MOF-74 by Partial Substitution with Co or Ni. *Industrial & Engineering Chemistry Research* **54**(49): 12408-12414.
- Junkar, I., Vesel A., Cvelbar U., Mozetič M., and Strnad S. (2009). Influence of oxygen and nitrogen plasma treatment on polyethylene terephthalate (PET) polymers. *Vacuum* **84**(1): 83-85.
- Kim, Y. K., Hyun S. M., Lee J. H., Kim T. K., Moon D., and Moon H. R. (2016). Crystal-Size Effects on Carbon Dioxide Capture of a Covalently Alkylamine-Tethered Metal-Organic Framework Constructed by a One-Step Self-Assembly. *Scientific Reports* **6**: 19337.
- Kumar, P., Deep A., and Kim K. H. (2015). Metal organic frameworks for sensing applications. *TrAC Trends in Analytical Chemistry* **73**: 39-53.
- Küsgens, P., Siegle S., and Kaskel S. (2009). Crystal Growth of the Metal—Organic Framework Cu₃(BTC)₂ on the Surface of Pulp Fibers. *Advanced Engineering Materials* **11**(1-2): 93-95.

- Li, S., Liao G., Liu Z., Pan Y., Wu Q., Weng Y., Zhang X., Yang Z., and Tsui O. K. C. (2014). Enhanced water flux in vertically aligned carbon nanotube arrays and polyethersulfone composite membranes. *Journal of Materials Chemistry A* **2**(31): 12171-12176.
- Lin, R., Ge L., Liu S., Rudolph V., and Zhu Z. (2015). Mixed-Matrix Membranes with Metal–Organic Framework-Decorated CNT Fillers for Efficient CO₂ Separation. *ACS Applied Materials & Interfaces* **7**(27): 14750-14757.
- Liu, Y., Zeng G., Pan Y., and Lai Z. (2011). Synthesis of highly c-oriented ZIF-69 membranes by secondary growth and their gas permeation properties. *Journal of Membrane Science* **379**(1–2): 46-51.
- Lu, H. (2012). Interfacial Synthesis of Metal-organic Frameworks. *Thesis for Master of Science, McMaster University*.
- Ma, P.-C., Siddiqui N. A., Marom G., and Kim J.K. (2010). Dispersion and functionalization of carbon nanotubes for polymer-based nanocomposites: A review. *Composites Part A: Applied Science and Manufacturing* **41**(10): 1345-1367.
- Mahajan, A., Kingon A., Kukovecz Á., Konya Z., and Vilarinho P. M. (2013). Studies on the thermal decomposition of multiwall carbon nanotubes under different atmospheres. *Materials Letters* **90**: 165-168.
- Majumder, M., Chopra N., Andrews R., and Hinds B. J. (2005). Nanoscale hydrodynamics: Enhanced flow in carbon nanotubes. *Nature* **438**(7064): 44-44.
- Merenda, A. (2015). Development of gate keepers gas separation membranes by selective growth of metal organic frameworks on the tips of carbon nanotubes. *Thesis for Master of Science, Politecnico di Torino*

- Morita, S., Hattori S., D'Agostino R. (1990). Applications of Plasma Polymers - Plasma Deposition, Treatment, and Etching of Polymers. San Diego, Academic Press: 423-461.
- Ostermann, R., Cravillon J., Weidmann C., Wiebcke M., and Smarsly B. M. (2011). Metal-organic framework nanofibers viaelectrospinning. *Chemical Communications* **47**(1): 442-444.
- Petit, C. and Bandosz T. J. (2011). Synthesis, Characterization, and Ammonia Adsorption Properties of Mesoporous Metal–Organic Framework (MIL(Fe))–Graphite Oxide Composites: Exploring the Limits of Materials Fabrication. *Advanced Functional Materials* **21**(11): 2108-2117.
- Petit, C., Mendoza B., and Bandosz T. J. (2010). Hydrogen Sulfide Adsorption on MOFs and MOF/Graphite Oxide Composites. *Journal of chemical physics and physical chemistry* **11**(17): 3678-3684.
- Rao, A. B., and Rubin E.S. (2002). A Technical, Economic and Environmental Assessment of Amine-based CO₂ Capture Technology for Power Plant Greenhouse Gas Control, *Environmental Science & Technology*, **36** (20): 4467–4475.
- Saha, D. and Deng S. (2010). Adsorption equilibrium and kinetics of CO₂, CH₄, N₂O, and NH₃ on ordered mesoporous carbon. *Journal of Colloid and Interface Science* **345**(2): 402-409.
- Sanchez-Lainez, J., Zornoza B., Mayoral A., Berenguer-Murcia A., Cazorla-Amoros D., Tellez C., and Coronas J. (2015). Beyond the H₂/CO₂ upper bound: one-step crystallization and separation of nano-sized ZIF-11 by centrifugation and its application in mixed matrix membranes. *Journal of Materials Chemistry A* **3**(12): 6549-6556.

- Steen, M. L., Butoi C. I., and Fisher E. R. (2001). Identification of Gas-Phase Reactive Species and Chemical Mechanisms Occurring at Plasma–Polymer Surface Interfaces. *Langmuir* **17**(26): 8156-8166.
- Sveningsson, M., Morjan R. E., Nerushev O. A., Sato Y., Bäckström J., Campbell E. E. B., and Rohmund F. (2001). Raman spectroscopy and field-emission properties of CVD-grown carbon-nanotube films. *Applied Physics A* **73**(4): 409-418.
- Taborski, J., Wüstenhagen V., Väterlein P., and Umbach E. (1995). Precoverage-dependent molecular orientation of big organic adsorbates: NDCA on Ni(111) and O/Ni(111). *Chemical Physics Letters* **239**(4–6): 380-386.
- Tang, S., Lu N., Wang J. K., Ryu S. K., and Choi H. S. (2007). Novel Effects of Surface Modification on Activated Carbon Fibers Using a Low Pressure Plasma Treatment. *The Journal of Physical Chemistry C* **111**(4): 1820-1829.
- Vandsburger, L., Swanson E., Tavares J., Meunier J. L., and Coulombe S. (2009). Stabilized aqueous dispersion of multi-walled carbon nanotubes obtained by RF glow-discharge treatment. *Journal of Nanoparticle Research* **11**(7): 1817-1822.
- Vesel, A., Junkar I., Cvelbar U., Kovac J., and Mozetic M. (2008). Surface modification of polyester by oxygen- and nitrogen-plasma treatment. *Surface and Interface Analysis* **40**(11): 1444-1453.
- Vesel, A. and Mozetic M. (2008). Modification of PET surface by nitrogen plasma treatment. *Journal of Physics: Conference Series* **100**(1): 012027.
- Walton, K. S., Millward A. R., Dubbeldam D., Frost H., Low J. J., Yaghi O. M., and Snurr R. Q. (2007). Understanding Inflections and Steps in Carbon Dioxide Adsorption Isotherms in Metal-Organic Frameworks. *Journal of the American Chemical Society* **130**(2): 406-407.

- Wang, S. C., Chang K. S., and Yuan C. J. (2009). Enhancement of electrochemical properties of screen-printed carbon electrodes by oxygen plasma treatment. *Electrochimica Acta* **54**(21): 4937-4943.
- Wong, S. (2009). Module 2: CO₂ capture: Post combustion flue gas separation.
- Yang, S. J., Cho J. H., Nahm K. S., and Park C. R. (2010). Enhanced hydrogen storage capacity of Pt-loaded CNT@MOF-5 hybrid composites. *International Journal of Hydrogen Energy* **35**(23): 13062-13067.
- Yoo, Y., Lai Z., and Jeong H. K. (2009). Fabrication of MOF-5 membranes using microwave-induced rapid seeding and solvothermal secondary growth. *Microporous and Mesoporous Materials* **123**(1-3): 100-106.
- Yu, K., Zhu Z., Zhang Y., Li Q., Wang W., Luo L., Yu X., Ma H., Li Z., and Feng T. (2004). Change of surface morphology and field emission property of carbon nanotube films treated using a hydrogen plasma. *Applied Surface Science* **225**(1-4): 380-388.
- Zacher, D., Shekhah O., Woll C., and Fischer R. A. (2009). Thin films of metal-organic frameworks. *Chemical Society Reviews* **38**(5): 1418-1429.
- Zhang, Z., Guan J., and Ye Z. (1998). R and D Note: Separation of a Nitrogen-Carbon Dioxide Mixture by Rapid Pressure Swing Adsorption. *Adsorption* **4**(2): 173-177.
- Zhao, B., Zhang L., Wang X., and Yang J. (2012). Surface functionalization of vertically-aligned carbon nanotube forests by radio-frequency Ar/O₂ plasma. *Carbon* **50**(8): 2710-2716.
- Zhao, J., Losego M. D., Lemaire P. C., Williams P. S., Gong B., Atanasov S. E., Blevins T. M., Oldham C. J., Walls H. J., Shepherd S. D., Browe M. A., Peterson G. W., and Parsons G. N. (2014). Highly Adsorptive, MOF-Functionalized Nonwoven Fiber Mats for Hazardous

Gas Capture Enabled by Atomic Layer Deposition. *Advanced Materials Interfaces* **1**(4): n/a-n/a.

Zu, D. D., Lu L., Liu X. Q., Zhang D. Y., and Sun L. B. (2014). Improving Hydrothermal Stability and Catalytic Activity of Metal–Organic Frameworks by Graphite Oxide Incorporation. *The Journal of Physical Chemistry C* **118**(34): 19910-19917.

CHAPTER 6. SENSITIVITY ENHANCEMENT IN PLANAR MICROWAVE ACTIVE-RESONATOR USING METAL ORGANIC FRAMEWORK FOR CO₂ SENSING

6.1. Introduction

Carbon dioxide is the main greenhouse gas emitted from sources such as fossil fuel power plants. Several approaches have been investigated to reduce the release of anthropogenic CO₂ amongst which carbon capture and storage (CCS) has been widely used (Yang et al., 2008). Meanwhile the CCS methods are effective and promising at capturing carbon dioxide, monitoring CO₂ at gas stream is still an attractive topic for environmental safety applications. To this end, it is of a great interest to develop gas sensors to detect and monitor changes of carbon dioxide concentration in a gas stream.

CO₂ sensors compatible with room temperature are playing an important role in many applications such as process control in food industry, indoor and outdoor air quality control, and monitors for biotechnology, etc. (Sala et al., 2000, Thomas et al., 2004, Stegmeier et al., 2009, Chiang et al., 2013). Recently, the application of material-assisted sensors is gaining interest for gas sensing, mostly due to the fact that strong inclusion of an analyte (target gas) in the sensing material facilitates its detection at lower limits (Kumar et al., 2015), and works based on sensing of the change in material properties due to chemical interaction between target gas and sensing material. Specifically, there has been increasing research and development on CO₂ monitoring and sensing using this technique which can be classified into two categories: (i) development of sensing devices and (ii) exploration and fabrication of novel sensing materials.

Sensing devices work based on various operating principles, such as capacitive, resistive, or optical sensing. Optical sensing works based on the measurement of IR absorption in the

range of 4200-4400nm, they are contactless but bulky and have expensive readout circuitry with high chances of interference from CO, as CO has similar absorption in the same IR range (Lübbers and Opitz, 1975, Leiner, 1991). Resistive sensors which operate based on the change of the electronic resistance of a sensitive layer (mostly semiconducting metal oxide) upon interaction with a target gas (Wagner et al., 2013), have several inherent advantages including immunity to interference from other gases and compact size but are also prone to electrical noise and drift such as temperature and humidity variation (Lübbers and Opitz, 1975, Leiner, 1991, Wagner et al., 2013). Capacitive sensors monitor the change in the permittivity of a material as a function of the concentration of a target gas (Wark et al., 2003, Wagner et al., 2013).

With respect to capacitive sensors, several configurations based on the interaction between specific gas (such as CO₂) and a coating material on sensor have been developed that are able to work at low temperature with high stability, sensitivity, and selectivity towards target gas. A group of the sensing materials, which have the ability of CO₂ detection at low temperature, are noble metal oxides such as SnO₂ acting as an electrode sensor for CO₂. In this approach, carbonates of alkali metals serve as solid electrolytes with high sensitivity towards CO₂ concentration change (Dobrovolsky et al., 1995). In addition, layered reduced graphene oxide (RGO) sprayed onto inter-digital electrodes (IDEs) was employed for sensing mechanism investigation on exposure to CO₂ gas mixture (Zhou et al., 2014). Ioannis *et al.*, proposed a zeolite (faujasite)-Metglas composite material for CO₂ detection using the change in resonance frequency of Metglas magnetoelastic strip (made of metallic alloys or composites of rare elements) (Giannakopoulos et al., 2005).

Recently Metal Organic Frameworks (MOFs) adsorbents have been intensely studied for adsorptive separation of gases such as CO₂ due to the unique properties of the framework (e.g.,

ultrahigh porosity, and presence of active metal ions within the framework). Previous studies showed that MOF-based sensors can provide real-time information on the concentration of different components in the exhaust gas such as NO_x , benefiting the diesel engine management system to finely tune the active emission control. This will significantly increase the engine efficiency and provide information on the lifetime of filters (Wales et al., 2015). Another interesting approach could be integrating them with sensing devices for chemo-sensing as well as bio-sensing applications (McKinlay et al., 2010, Jung et al., 2011). The most common type of MOFs for such application is Cu-based MOFs. Zybalyo et al. (Zybalyo et al., 2010), using Cu-BTC MOF (MOF-199) on QCM gold electrode studied the mass uptake of pyridine via corresponding binding energy. Allendorf et al. integrated the same MOF with a piezoresistive microcantilever, which selectively senses water and can be also served as a CO_2 detector when it is completely dehydrated (Allendorf et al., 2008). MOF-199 was also used for the fabrication of a capacitance film sensor (Liu et al., 2011). MOF-199 coated on silver nanoparticles functioned as a CO_2 sensor device and resulted in a 14-fold enhancement of the CO_2 sensing signal through selective uptake of CO_2 in the MOF pores (Kreno et al., 2010). The aforementioned examples confirm the versatility of MOF to be effectively integrated with various detection systems to serve as gas sensor. However, research on the synthesis and application of MOFs for CO_2 detection is in its infancy and needs further investigation.

Microwave resonator devices have demonstrated excellent potential for sensing applications in different applications including moisture detection (Kot et al., 2015), permittivity characterization (Ebrahimi et al., 2014, Galindo-Romera et al., 2016), Volatile Organic Compound (VOC) detection (Korostynska et al., 2014, Morán-Lázaro et al., 2016) and have demonstrated attractive readout circuitry method leading to low-cost, robust, non-destructive,

sensitive, and long life-time devices (Ebrahimi et al., 2014, Korostynska et al., 2014, Afshar et al., 2015, Ateeq et al., 2016, Wang et al., 2016, Zarifi et al., 2016). These sensors are sensitive to dielectric property (permittivity and conductivity) variation of interface materials, which alter the electric field distribution around the sensor, and enable contactless sensing operation. In many reported microwave gas sensors, an interface material such as polymer (Chen et al., 2013, Sohrabi et al., 2014, Bhadra et al., 2015, Zarifi et al., 2015), nanotubes and nanoparticles (Cismaru et al., 2016, Morán-Lázaro et al., 2016, Zarifi et al., 2016), activated carbon beads (Zarifi et al., 2015) and zeolite materials (Anderson et al., 1997, Dietrich et al., 2014, Chen et al., 2015, Dietrich et al., 2015, Zarifi et al., 2017) are used to enhance the sensitivity and selectivity to a targeted gas or vapor, where any changes in the interface material, is correlated with a variation in a readout parameter and thus to the concentration of the gas under test. The dielectric property variation in the intermediate material can be reflected in different amplitude, frequency, and quality-factor of transmission/reflection-characteristics of the sensor device.

Recent studies on selective CO₂ detection still need further investigation, both in development of sensor devices and sensing materials. In this work, a high resolution microwave resonator sensor (Zarifi et al., 2015, Zarifi et al., 2015, Zarifi and Daneshmand, 2016) is utilized for monitoring CO₂ adsorption, in a mixture of He/CO₂, on three different adsorbent materials at room temperature (20 °C). MOF-199 was synthesized by two different solvothermal methods and its CO₂ uptake was compared to that of a benchmark zeolite 13X. These materials were placed in the most sensitive area of the sensor and the changes in their permittivity during adsorption were monitored via tracking the resonant frequency variation of the sensor device. This approach clearly demonstrates the effect of material selection on the sensitivity and illustrates the potential of the sensor device for real-time monitoring of the adsorbent materials' lifetime.

6.2. Materials and methods

6.2.1. Chemicals and reactants

All chemicals in this study including N, N, dimethylformamide (DMF) (99.8% anhydrous), Ethanol (90% anhydrous), copper nitrate tri-hydrate (99%), and dichloromethane (anhydrous, 99.8%) were purchased from Sigma Aldrich. Copper nitrate hemipenta-hydrate (ACS reagent, 98%) and trimesic acid (98%), were acquired from Arcos Organics. Zeolite samples (13X) used in this work was pellets (2.5–5 mm) purchased from Advanced Specialty Gas Equipment.

6.2.2. MOF crystals seeding and growth

MOFs were prepared following two different procedures as described below:

1. In a typical preparation of MOF-199 (Rowsell and Yaghi, 2006), Trimesic acid (5g) and copper nitrate hemipenta-hydrate (10g) were dissolved in 250 mL of a solvent mixture of dimethyl formamide, ethanol and de-ionized (DI) water (1:1:1) placed into a 400 mL sealed Schott bottle. The solution was then sonicated for 30 min to get a homogeneous solution. The mixture was placed inside a Teflon-lined autoclave and heated at 85 °C in oven (Lindberg/Blue- BF51732 series) for 20 h to achieve full crystal growth. After growth, the mother liquor was decanted using cellulose acetate filter papers (Whatman, grade 5) under vacuum filtration. The blue crystalline product was washed with DMF (10 mL), then exchanged with dichloromethane and decanted. The purification steps were repeated over 2 days to exchange the DMF guest molecules. The product was then dried under vacuum at 170 °C for 24 h to remove remaining ethanol traces. (The prepared sample is referred as MOF-199-M1 throughout the paper)

2. In the second method (Chowdhury et al., 2009), copper nitrate trihydrate (4.48g) and trimesic acid (1.96g) were dissolved in a 50 ml solution of ethanol and DI water (1:1), then placed into a 100 mL sealed Schott bottle. The solution was then sonicated for 30 min to get a homogeneous solution. The mixture was placed inside a Teflon-lined autoclave and heated at 140 °C in oven (Lindberg/Blue- BF51732 series) for 48 h. After growth, the mother liquor was decanted using cellulose acetate filter papers (Whatman, grade 5) under vacuum filtration and washed with DI water. The purification steps were repeated over 2 days to exchange the guest molecules. The product was then dried under vacuum at 85 °C overnight. (The prepared sample is referred as MOF-199-M2 throughout the paper)

6.2.3. X-Ray Diffraction (XRD) analysis

In order to confirm the structure of the prepared MOFs with the literature, XRD analysis was performed. Powder XRD measurements were conducted with a Rigaku Ultima IV unit equipped with a D/Tex detector and Fe filter. The results were obtained with Co-K wavelength with the average wavelength of 1.790260 Å (Cobalt tube 38 kV, 38 mA). Samples were run from 5 to 90° on a continuous scan using a top-pack mount at 2° 2-θ per minute with a step size of 0.02°. Patterns were characterized using JADE 9.1 with the 2011 ICDD database.

6.2.4. X-ray photoelectron spectroscopy (XPS)

The surface composition of MOFs was determined using XPS. The analysis was conducted using Kratos AXIS 165 instrument with Mono Al K α radiation at 210 W and 14 kV under ultrahigh vacuum (10⁻⁹Torr). All the spectra were calibrated to C1s peak at 284.5 eV.

6.2.5. Scanning Electron Microscopy

Scanning Electron Micrographs (SEMs) were acquired on a Zeiss Sigma (Gemie) FEG-SEM at an accelerating voltage of 10 keV and a working distance of 21 mm. The samples were mounted on aluminum stubs with carbon tape and coated with a 6 nm thick layer of Au prior to analysis to minimize charging and prevent beam damage across the crystals.

6.3. Experimental set-up

6.3.1. Gas adsorption-VNA set-up

The experimental set-up for gas adsorption is illustrated in Figure 6-1. The sample was located on the sensor panel covered by a Teflon container (0.88cm inner diameter, 0.5cm long) to avoid any effect from surrounding environment. The sample was exposed to the feed gas which consisted of a mixture of dry helium (He, 99.998% purity) and dry CO₂ (99.9% purity). To adjust the concentration of CO₂ in the gas stream and control the gas flow rate, two separate mass flow controllers (Alicat Scientific) were used. The adsorbent permittivity was monitored during the adsorption by the sensor (Zarifi et al., 2015, Zarifi et al., 2015, Zarifi et al., 2017) connected to a Vector Network Analyzer (VNA-PXI 1075).

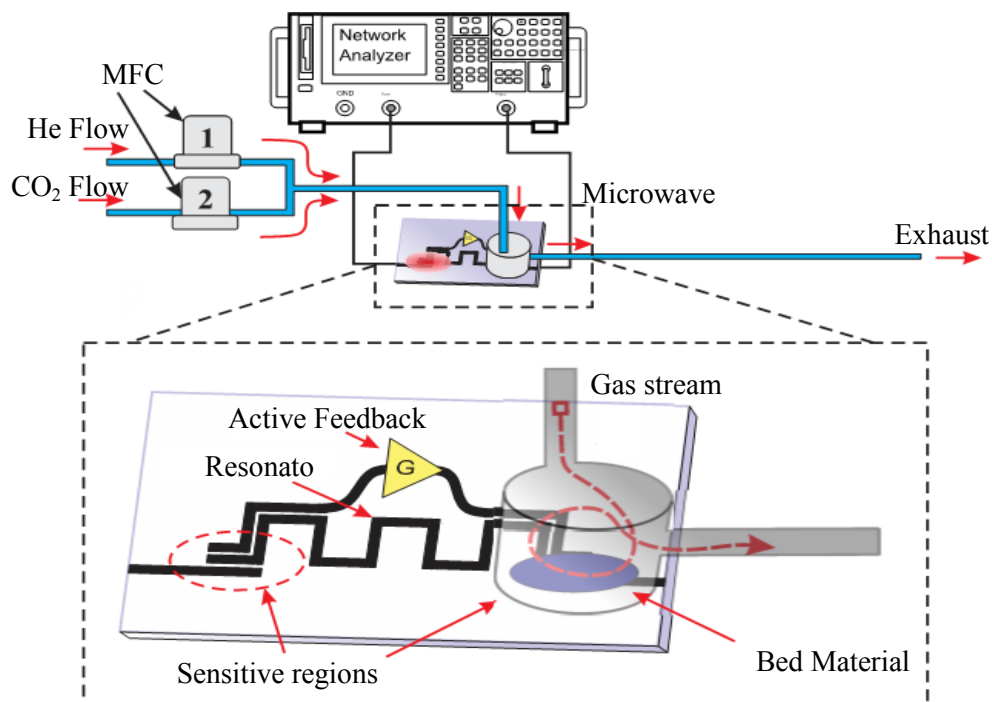


Figure 6-1. Schematic diagram of gas adsorption set-up

6.3.2. CO₂ volumetric adsorption

CO₂ volumetric adsorption measurements were conducted on a sorption analyser (Quantachrome model iQ2) at 298K. Prior to the measurements, the samples were outgassed at 110 °C under vacuum for 10 h. The adsorbed amount was determined from CO₂ adsorption isotherm by the Dubinin-Astakhov equation (Singh and Anil Kumar, 2016) in the pressure range from 0 to 1 atm.

6.4. Results

6.4.1. Characterization Test Results

Obtained XRD Patterns of MOF-199-M1 and MOF-199-M2 are presented in Figure 6-2a, showing the characteristic peaks associated with MOF-199 at 2θ : 9.51, 11.71 and 13.51, corresponding to (220), (222) and (400) diffraction peaks, respectively (Rowse and Yaghi, 2006, Casco et al., 2015). For MOF-199-M2, a small shift in peak positions to a lower angle was

observed. The peak shift might be due to a change in d-spacing of planes i.e., changing in lattice parameter. If the sample is strained the shifts will normally be greater at high angles than low angles, which seems to be the case in sample MOF-199-M2. These shifts reflect the change in interatomic distances in the material. The deviation in the peak position can be translated into macroscopic strain such as lattice vacancies (Epp, 2016), as it was also confirmed with XPS results.

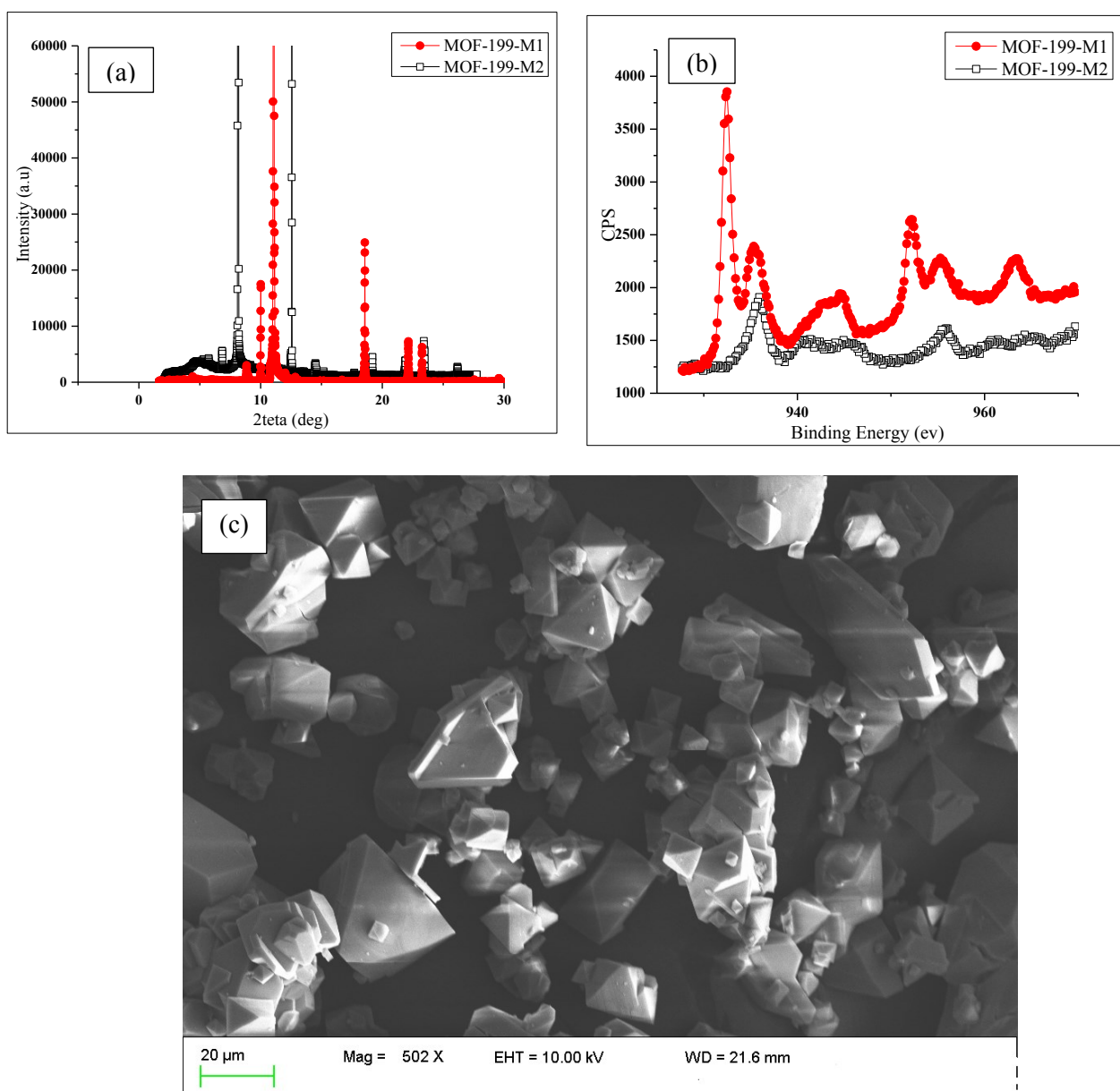


Figure 6-2. Characterization results: (a) XRD spectra, (b) High resolution XPS spectra, and (c) SEM images of synthesized MOF-199 samples

A typical XPS spectrum of Copper nanoparticle (as in MOF-199) was measured and the spectrum of Cu 2p_{3/2} is depicted in Figure 6-2b. The Cu²⁺ peaks appeared at 933, 935 and 942 eV, which attributed to CuO. The peak at lower binding energy (932.50 eV) is attributed to saturated metallic state of copper (Liu et al., 2004, Biesinger et al., 2010).

Comparing the XPS spectrum of as-prepared samples, one can conclude that sample MOF-199-M2 does not contain any saturated metal copper, i.e., Cu (0), and includes mostly of Cu (II). Figure 6-2b, presents a comparison of XPS peaks for MOF-199 prepared from different precursors. MOF-199-M1 shows much stronger peaks in intensity, which can be an indicative of solvent presence in the framework and can have a detrimental effect on gas adsorption capacity of sample.

Figure 6-2c presents SEM image of as prepared MOF-199 (the crystal structure of both types of MOF-199 is identical). The small octahedral crystals are typical MOF-199 crystals resulting from growth experiment, according to the literature (Liu et al., 2010).

6.4.2. Microwave Results

The setup for gas sensing experiments is presented in Figure 6-3a. Two DC signals were providing the bias voltage to the active circuitry of the sensor and microwave signals were fed through ports 1 and 2 to the resonator. Resonant profiles for device with no material (blank), with MOF-199-M1, 2 and Zeolite 13X were measured as the transmitted power to the reflected power ratio (S_{21}) and presented in Figure 6-3b. The resonant profiles were recorded while pure He was purging the adsorbents, and were used as the baseline for the further measurements. Zeolite 13X demonstrates two times larger shift on resonant frequency than MOF-199-M2

(Figure 6-3b), which confirms the higher dielectric constant of Zeolite 13X compared to MOF-199-M2 adsorbent (Usman et al., 2015). The environmental conditions such as temperature (20°C) and the relative humidity (14 %) were constant and monitored separately during the experiment. The sensor response for the adsorbents in presence of pure He was monitored for an hour prior to addition of CO₂ to the gas stream. The results confirmed a constant and invariant response for each adsorbent in the inert environment.

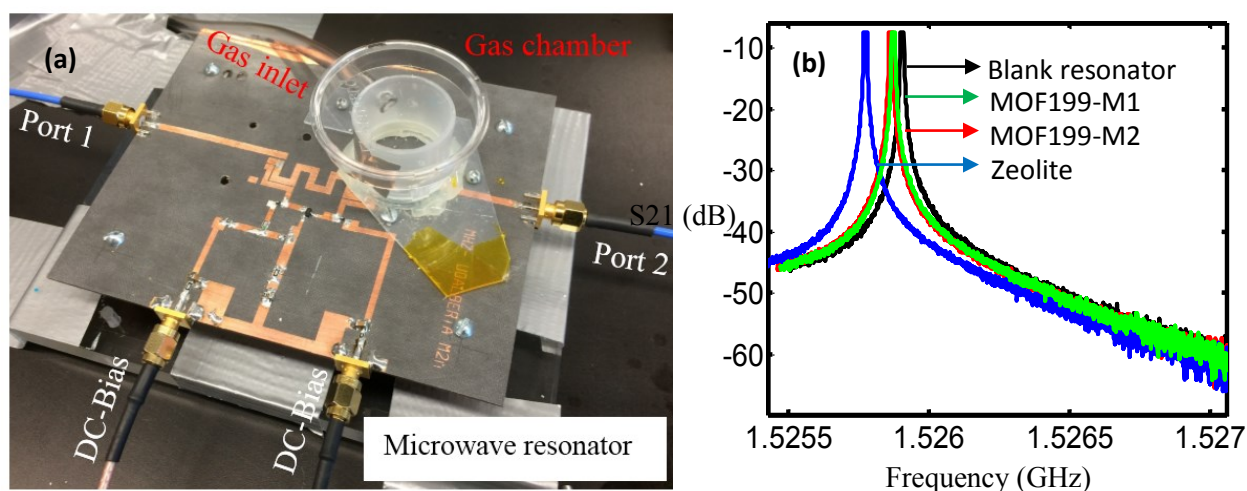


Figure 6-3. (a) experimental setup with the microwave active resonator sensor, (b) resonant profile (S21) of the sensor without any material (blank), with MOF and Zeolite while being purged with He at a rate of 200 SCCM at room temperature.

Different concentrations of CO₂-He mixture were passed over the adsorbents separately, while the adsorbent material was placed in the most sensitive region of the sensor. The material and sensor were in contact and the adsorbent was purged by He, at a constant rate of 200 SCCM.

During the adsorption process, CO₂ molecules occupy the adsorbent pores. Since the pore size of MOF-199 is within 1-6 nm range, the adsorbed molecules of CO₂ are present in more packed form than in the gas state, condense on the layer of previously adsorbed molecules, and form a liquid-like phase. Consequently the density of target gas is similar to that of liquid

adsorbate which results in a significant variation in effective permittivity and conductivity of the adsorbent.

Hence, adsorption of CO_2 on the MOF affects the effective permittivity of MOF. The permittivity variation in the MOF affects the electric field around the sensitive region of the sensor which is reflected in a change in the resonant profile of the sensor and can be related to the target gas concentration (Zarifi et al., 2015).

The resonant profile of the sensor is recorded using Labview-assisted VNA (NI-PXIe 1075) with sampling period of 10 sec. As shown in Figure 6-4a, the resonant frequency variation and its transient response demonstrate a strong dependence on CO_2 concentration in the stream. Figure 6-4b clearly presents the relation between the resonant frequency change and CO_2 concentration in the steady state condition.

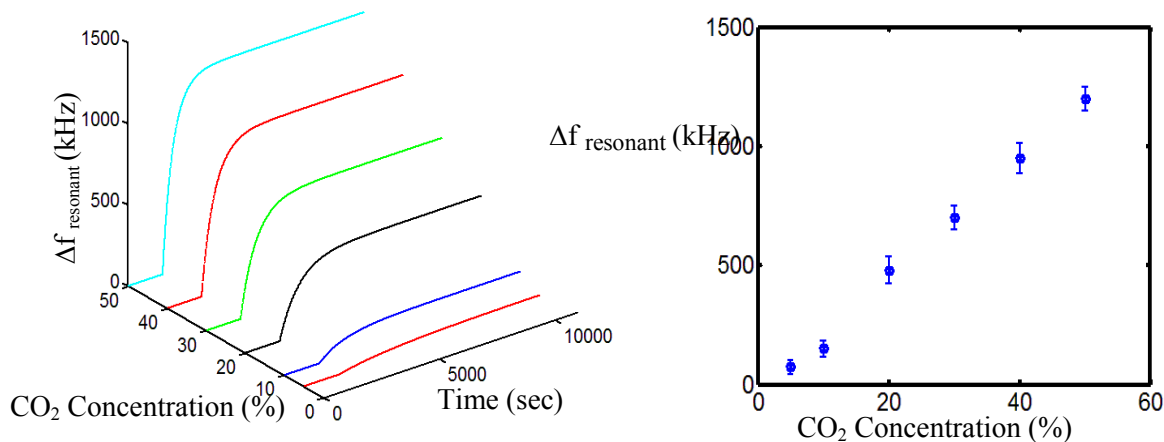


Figure 6-4. (a) Resonant frequency-shift during the adsorption time for different CO_2 concentration on MOF-199-M2, (b) resonant frequency shift versus different Concentration of CO_2 in dry He, the error bar is standard deviation of 5 independent experiments per each concentration.

The effect of bed material on the steady-state, resonant frequency variation for different CO₂ concentrations is studied by replacing the synthesized MOF material with Zeolite 13X as a standard commercially available adsorbent. The results of the resonant frequency-shift versus time for different CO₂ concentrations are presented in Figure 6-5.

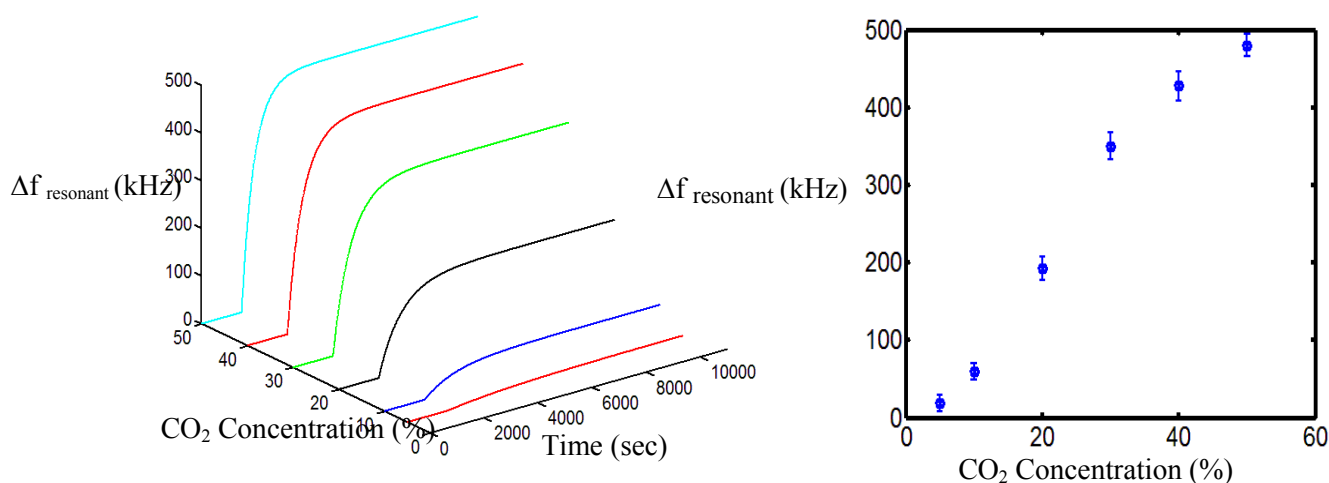


Figure 6-5. Time variant resonant frequency shift of the sensor for different CO₂ concentrations on zeolite 13X, (b) reliability experiment of resonant frequency versus CO₂, the error bar is standard deviation of 5 independent experiments per each concentration

The responses of the microwave resonator sensor (resonant frequency variation) are compared in Figure 6-6. Adsorption of a constant concentration of CO₂ on MOF-199-M2 demonstrates a large resonant frequency shift, representing a large variation in dielectric properties of the adsorbent material relative to its initial dielectric constant. Additionally, for higher CO₂ concentrations, MOF-199-M2 illustrates a linear response in comparison to the other adsorbents. Considering the effective permittivity change in the adsorbent and permittivity of condensed gas, the adsorption led to a significant variation on the effective permittivity and conductivity of the adsorbent (Zarifi et al., 2017). Variation of adsorbent capacity during

adsorption can be monitored by resonant frequency-shift in the sensor response, which is due to effective permittivity change in the bed [44].

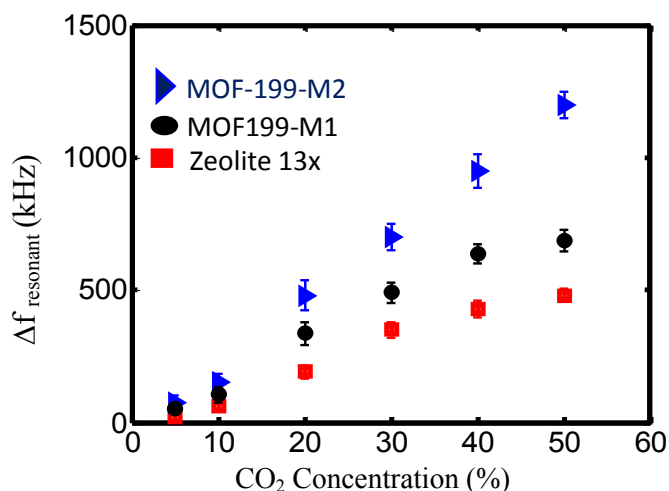


Figure 6-6. Comparison between the measured resonant frequency-shift of the sensor, for different adsorbents at different concentrations of CO₂ in dry He, the error bar is standard deviation of 5 independent experiments per each concentration.

6.4.3. Volumetric Adsorption Results

Volumetric adsorption profile of three different adsorbents was obtained and presented in Figure 6-7 for different CO₂ concentrations. The difference in CO₂ adsorption isotherm shapes is due to the different structural properties. In the case of MOF-199, increasing pressure (or CO₂ concentration) results in a linear increase in CO₂ sorption which is due to the specific interactions between CO₂ molecules and positive charges on the coordinatively unsaturated metal sites in the framework (Liang et al., 2009). It was suggested that CO₂ attaches to the Cu²⁺ through one of its oxygen atoms which induces multiple moments to the CO₂ molecule, causing effective interaction with open metal and overall binding enhancement (Wu et al., 2010). Hence presence of more Cu²⁺ in the framework increases the adsorption of CO₂, as shown by the XPS and volumetric adsorption results. After all unsaturated metal sites are occupied at higher CO₂

loading, the gas molecules will be adsorbed on the small cages (Wu et al., 2010) through strong quadrupole moments (Gutierrez-Sevillano et al., 2013).

On the other hand, in Zeolite 13X, the adsorption mechanism is mainly due to the slight acidity of CO₂ molecules which boost the interaction with basic inner micropore surface of zeolite with low Si/Al ratio (Aprea et al., 2010). Zeolite 13X consists of 12-ring window with dispersed Na⁺ ions. The adsorption principle between CO₂ molecule and Zeolite 13X involves two steps: CO₂ molecule will first contact with strong Na⁺ centers and quadrupole moments of CO₂ enhances this interaction causing the adsorbate molecule (CO₂) to be immobilized (J.A. Dunne, 1996). As presented in Figure 6-7, the first part of CO₂ adsorption on Zeolite 13X has a ramping curvature. When all Na⁺ centers are occupied, an induced weak electric field will be the dominant mechanism to affect adsorbate molecule; hence less CO₂ will be trapped, and the adsorption isotherm curvature will be changed (Deng et al., 2012).

Based on the volumetric adsorption results, MOF-199-M2 demonstrates higher adsorption capacity than MOF-199-M1 for all CO₂ concentrations. This behavior can be attributed to the presence of more unsaturated metal sites (Cu²⁺) in MOF-199-M2 as also was confirmed with XRD and XPS results. Previous studies identified unsaturated metal centers (UMCs) as CO₂ binding sites on MOF-199 because of enhanced electrostatic interaction with CO₂ molecules (Wu et al., 2010). CO₂ molecules bind to Cu²⁺ sites at low CO₂ concentration, while pore filling in small cage windows is the adsorption mechanism at high CO₂ concentrations (Wu et al., 2010). Higher adsorption capacity corresponds to more condensed gas in the adsorbent and larger variation in the effective permittivity of the adsorbent. Comparing these results to microwave sensor's response (Figure 6-6), demonstrates a conceptual agreement between the higher adsorption capacity and larger resonant frequency-shift for materials with

similar structure (like MOF-199-M1 and MOF-199-M2). Compared to synthesized MOF-199 materials, Zeolite 13X demonstrates higher adsorption capacity at lower CO₂ concentrations (<45 vol. %), but since Zeolite 13X has larger initial permittivity than the MOF-199 (Figure 6-3b). the microwave sensor shows less sensitivity to effective permittivity change in Zeolite 13X than the MOF-199. Additionally, the volumetric adsorption graphs demonstrate the potential application of microwave sensors at high CO₂ concentration (> 45 vol. %) using MOF-199-M2.

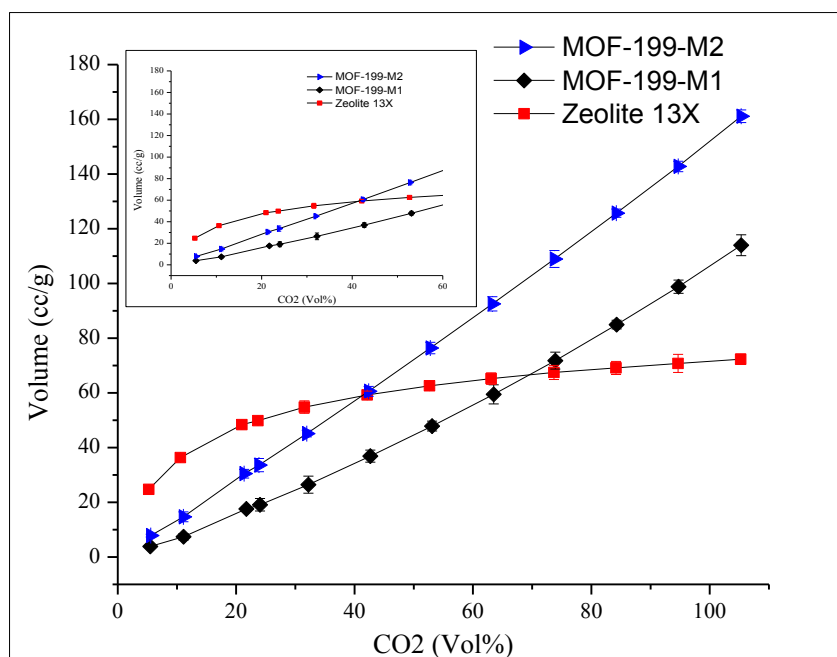


Figure 6-7. CO₂ volumetric adsorption of MOF-199 and Zeolite 13X samples, T=20°C

6.5. Conclusions

A high resolution active microwave resonator sensor was utilized to study real-time dielectric properties variation in zeolite-13X and MOF-199 bed exposed to different CO₂ concentrations in a dry inert gas stream. Despite the lower adsorption capacity of MOF-199 for

low CO₂ concentrations (<45 %), it has demonstrated higher sensitivity than zeolite-13X, which can be related to the initial dielectric properties of the fresh bed materials. In addition, the responses of the microwave sensor using two different synthesized MOF materials as adsorbents were compared, and MOF-199-M2 demonstrated higher sensitivity than MOF-199-M1 with respect to different CO₂ concentrations in the gas stream. XRD and XPS results revealed that structure difference of two types of MOF-199 was due to the presence of different amount of unsaturated Cu²⁺ ions. Adsorption of CO₂ on MOF-199-M2 demonstrated a larger resonant frequency variation compared to the other two adsorbents, which clearly demonstrates the potential of MOF-199-M2 as a sensitive material in microwave CO₂ sensor structures. The proposed structure is a low-cost, robust, small-size, real-time and planar sensor device, which is reinforced by adsorbent material. Further work will study the sensor performance in non-dry gas streams at different levels of humidity and its integration with different materials to improve the selectivity parameter of the sensor.

6.6. References

- Afshar, S., Salimi E., Braasch K., Butler M., Thomson D. and Bridges G. (2015). Multi-frequency DEP cytometer employing a microwave interferometer for the dielectric analysis of micro-particles. *2015 IEEE MTT-S International Microwave Symposium*.
- Allendorf, M. D., Houk R. J. T., Andruszkiewicz L., Talin A. A., Pikarsky J., Choudhury A., Gall K. A. and Hesketh P. J. (2008). Stress-Induced Chemical Detection Using Flexible Metal–Organic Frameworks. *Journal of the American Chemical Society* **130**(44): 14404-14405.

- Anderson, P. A., Armstrong A. R., Porch A., Edwards P. P. and Woodall L. J. (1997). Structure and Electronic Properties of Potassium-Loaded Zeolite L. *The Journal of Physical Chemistry B* **101**(48): 9892-9900.
- Aprea, P., Caputo D., Gargiulo N., Iucolano F. and Pepe F. (2010). Modeling Carbon Dioxide Adsorption on Microporous Substrates: Comparison between Cu-BTC Metal–Organic Framework and 13X Zeolitic Molecular Sieve. *Journal of Chemical & Engineering Data* **55**(9): 3655-3661.
- Ateeq, M., Shaw A., Garrett R. and Dickson P. (2016). Feasibility study on using microwave sensing technique to analyse silver-based products. *Journal of Electromagnetic Waves and Applications*: 1-17.
- Bhadra, S., Thomson D., and Bridges G. (2015). Near-Field Coupled RFID Tag for Carbon Dioxide Concentration Sensing. *USNC-URSI Radio Science Meeting (Joint with AP-S Symposium)*. Canada: 203.
- Biesinger, M. C., Lau L. W. M., Gerson A. R., and Smart R. S. C. (2010). Resolving surface chemical states in XPS analysis of first row transition metals, oxides and hydroxides: Sc, Ti, V, Cu and Zn. *Applied Surface Science* **257**(3): 887-898.
- Casco, M. E., Fernandez-Catala J., Martinez-Escandell M., Rodriguez-Reinoso F., Ramos-Fernandez E. V., and Silvestre-Albero J. (2015). Improved mechanical stability of HKUST-1 in confined nanospace. *Chemical Communications* **51**(75): 14191-14194.
- Chen, P., Schönebaum S., Simons T., Rauch D., Dietrich M., Moos R., and U. Simon (2015). Correlating the Integral Sensing Properties of Zeolites with Molecular Processes by Combining Broadband Impedance and DRIFT Spectroscopy—A New Approach for Bridging the Scales. *Sensors* **15**(11): 28915.

- Chen, W. T., Stewart K. M. E., Carroll J., Mansour R., Abdel-Rahman E., and Penlidis A. (2013). Novel gaseous phase ethanol sensor implemented with underloaded RF resonator for sensor-embedded passive chipless rfids. *2013 Transducers & Eurosensors XXVII: The 17th International Conference on Solid-State Sensors, Actuators and Microsystems (TRANSDUCERS & EUROSENSORS XXVII)*.
- Chiang, C.-J., Tsai K.-T., Lee Y.-H., Lin H.-W., Yang Y.-L., Shih C.-C., Lin C.-Y., Jeng H.-A., Weng Y.-H., Cheng Y.-Y., Ho K.-C., and Dai C.-A. (2013). In situ fabrication of conducting polymer composite film as a chemical resistive CO₂ gas sensor. *Microelectronic Engineering* **111**: 409-415.
- Chowdhury, P., Bikkina C., Meister D., Dreisbach F. and Gumma S. (2009). Comparison of adsorption isotherms on Cu-BTC metal organic frameworks synthesized from different routes. *Microporous and Mesoporous Materials* **117**(1-2): 406-413.
- Cismaru, A., Aldrigo M., Radoi A. and Dragoman M. (2016). Carbon nanotube-based electromagnetic band gap resonator for CH₄ gas detection. *Journal of Applied Physics* **119**(12): 124504.
- Deng, H., Yi H., Tang X., Yu Q., Ning P., and Yang L. (2012). Adsorption equilibrium for sulfur dioxide, nitric oxide, carbon dioxide, nitrogen on 13X and 5A zeolites. *Chemical Engineering Journal* **188**: 77-85.
- Dietrich, M., Rauch D., Porch A., and Moos R. (2014). A Laboratory Test Setup for in Situ Measurements of the Dielectric Properties of Catalyst Powder Samples under Reaction Conditions by Microwave Cavity Perturbation: Set up and Initial Tests. *Sensors (Basel, Switzerland)* **14**(9): 16856-16868.

- Dietrich, M., Rauch D., Simon U., Porch A. and Moos R. (2015). Ammonia storage studies on H-ZSM-5 zeolites by microwave cavity perturbation: correlation of dielectric properties with ammonia storage. *J. Sens. Sens. Syst.* **4**(2): 263-269.
- Dobrovolsky, Y., Leonova L., and Nadkhina S. (1995). Working electrodes for low-temperature CO₂-sensors. *Ionics* **1**(3): 228-234.
- Ebrahimi, A., Withayachumnankul W., Al-Sarawi S. and Abbott D. (2014). High-Sensitivity Metamaterial-Inspired Sensor for Microfluidic Dielectric Characterization. *IEEE Sensors Journal* **14**(5): 1345-1351.
- Ebrahimi, A., Withayachumnankul W., Al-Sarawi S. F., and Abbott D. (2014). Metamaterial-Inspired Rotation Sensor With Wide Dynamic Range. *IEEE Sensors Journal* **14**(8): 2609-2614.
- Epp, J. (2016). 4 - X-ray diffraction (XRD) techniques for materials characterization. *Materials Characterization Using Nondestructive Evaluation (NDE) Methods*, Woodhead Publishing: 81-124.
- Galindo-Romera, G., Herraiz-Mart F. J., Gil M., Martínez-Martínez J. J., and Segovia-Vargas D. (2016). Submersible Printed Split-Ring Resonator-Based Sensor for Thin-Film Detection and Permittivity Characterization. *IEEE Sensors Journal* **16**(10): 3587-3596.
- Giannakopoulos, I. G., Kouzoudis D., Grimes C. A., and Nikolakis V. (2005). Synthesis and Characterization of a Composite Zeolite–Metglas Carbon Dioxide Sensor. *Advanced Functional Materials* **15**(7): 1165-1170.
- Dunne J.A., Sircar S., Gorte R.J., Myers A.L. (1996). Calorimetric heats of adsorption and adsorption isotherm of O₂, N₂, Ar, CO₂, CH₄, C₂H₆, and SF₆ on silicalite,. *Langmuir* **12**: 5888–5895.

- Gutierrez-Sevillano J. J., Vicent-Luna J.M, Dubbeldam D., and Calero S. (2013). Molecular Mechanisms for Adsorption in Cu-BTC Metal Organic Framework. *The Journal of Physical Chemistry C* **117**: 11357.
- Jung, S., Kim Y., Kim S.-J., Kwon T.-H., Huh S., and Park S. (2011). Bio-functionalization of metal-organic frameworks by covalent protein conjugation. *Chemical Communications* **47**(10): 2904-2906.
- Korostynska, O., Mason A., and Al-Shamma'a A. (2014). Microwave sensors for the non-invasive monitoring of industrial and medical applications. *Sensor Review* **34**(2): 182-191.
- Korostynska, O., Mason A., Ortoneda-Pedrola M., and Al-Shamma'a A. (2014). Electromagnetic wave sensing of NO₃ and COD concentrations for real-time environmental and industrial monitoring. *Sensors and Actuators B: Chemical* **198**: 49-54.
- Kot, P., Shaw A., Jones K. O., Cullen J. D., Mason A., and Al-Shamma'a A. I. (2015). The feasibility of electromagnetic waves in determining the moisture content of concrete blocks. *2015 9th International Conference on Sensing Technology (ICST)*.
- Kreno, L. E., Hupp J. T., and Van Duyne R. P. (2010). Metal–Organic Framework Thin Film for Enhanced Localized Surface Plasmon Resonance Gas Sensing. *Analytical Chemistry* **82**(19): 8042-8046.
- Kumar, P., Deep A., and Kim K.-H. (2015). Metal organic frameworks for sensing applications. *TrAC Trends in Analytical Chemistry* **73**: 39-53.
- Leiner, M. J. P. (1991). Luminescence chemical sensors for biomedical applications: scope and limitations. *Analytica Chimica Acta* **255**(2): 209-222.

- Liang, Z., Marshall M., and Chaffee A. L. (2009). Comparison of Cu-BTC and zeolite 13X for adsorbent based CO₂ separation. *Energy Procedia* **1**(1): 1265-1271.
- Liu, J., Sun F., Zhang F., Wang Z., Zhang R., Wang C., and Qiu S. (2011). In situ growth of continuous thin metal-organic framework film for capacitive humidity sensing. *Journal of Materials Chemistry* **21**(11): 3775-3778.
- Liu, J., Wang Y., Benin A. I., Jakubczak P., Willis R. R., and LeVan M. D. (2010). CO₂/H₂O Adsorption Equilibrium and Rates on Metal Organic Frameworks: HKUST-1 and Ni/DOBDC. *Langmuir* **26**(17): 14301-14307.
- Liu, Y., Bailey P., Noakes T. C. Q., Thompson G. E., Skeldon P. and Alexander M. R. (2004). Chemical environment of copper at the surface of a CuAl₂ model alloy: XPS, MEIS and TEM analyses. *Surface and Interface Analysis* **36**(4): 339-346.
- Lübbbers, D. W. and Opitz N. (1975). The pCO₂-/pO₂-optode: a new probe for measurement of pCO₂ or pO₂ in fluids and gases (authors transl). *Zeitschrift fur Naturforschung. Section C: Biosciences* **30**(4): 532-533.
- McKinlay, A. C., Morris R. E., Horcajada P., Férey G., Gref R., Couvreur P., and Serre C. (2010). BioMOFs: Metal–Organic Frameworks for Biological and Medical Applications. *Angewandte Chemie International Edition* **49**(36): 6260-6266.
- Morán-Lázaro, J. P., Blanco O., Rodríguez-Betancourt V. M., Reyes-Gómez J., and Michel C. R. (2016). Enhanced CO₂-sensing response of nanostructured cobalt aluminate synthesized using a microwave-assisted colloidal method. *Sensors and Actuators B: Chemical* **226**: 518-524.
- Rowell, J. L. C. and Yaghi O. M. (2006). Effects of Functionalization, Catenation, and Variation of the Metal Oxide and Organic Linking Units on the Low-Pressure Hydrogen

- Adsorption Properties of Metal-organic Frameworks. *Journal of the American Chemical Society* **128**(4): 1304-1315.
- Rowell, J. L. C. and Yaghi O. M. (2006). Effects of Functionalization, Catenation, and Variation of the Metal Oxide and Organic Linking Units on the Low-Pressure Hydrogen Adsorption Properties of Metal–Organic Frameworks. *Journal of the American Chemical Society* **128**(4): 1304-1315.
- Sala, O. E., Stuart Chapin F., Armesto J. J., Berlow E., Bloomfield J., Dirzo R., Huber-Sanwald E., Huenneke L. F., Jackson R. B., Kinzig A., Leemans R., Lodge D. M., Mooney H. A., Oesterheld M. N., Poff N. L., Sykes M. T., Walker B. H., Walker M., and Wall D. H. (2000). Global Biodiversity Scenarios for the Year 2100. *Science* **287**(5459): 1770-1774.
- Singh, V. K. and Anil Kumar E. (2016). Measurement and analysis of adsorption isotherms of CO₂ on activated carbon. *Applied Thermal Engineering* **97**: 77-86.
- Sohrabi, A., Shaibani P. M., Zarifi M. H., Daneshmand M., and Thundat T. (2014). A novel technique for rapid vapor detection using swelling polymer covered microstrip ring resonator. *2014 IEEE MTT-S International Microwave Symposium (IMS2014)*.
- Stegmeier, S., Fleischer M., Tawil A., Hauptmann P., Egly K., and Rose K. (2009). Mechanism of the interaction of CO₂ and humidity with primary amino group systems for room temperature CO₂ sensors. *Procedia Chemistry* **1**(1): 236-239.
- Thomas, C. D., Cameron A., Green R. E., Bakkenes M., Beaumont L. J., Collingham Y. C., Erasmus B. F. N., De Siqueira M. F., Grainger A., Hannah L., Hughes L., Huntley B., Van Jaarsveld A. S., Midgley G. F., Miles L., Ortega-Huerta M. A., Townsend Peterson A., Phillips O. L., and Williams S. E. (2004). Extinction risk from climate change. *Nature* **427**(6970): 145-148.

- Usman, M., Mendiratta S. and Lu K.-L. (2015). Metal–Organic Frameworks: New Interlayer Dielectric Materials. *ChemElectroChem* **2**(6): 786-788.
- Wagner, T., Haffer S., Weinberger C., Klaus D. and Tiemann M. (2013). Mesoporous materials as gas sensors. *Chemical Society Reviews* **42**(9): 4036-4053.
- Wales, D. J., Grand J., Ting V. P., Burke R. D., Edler K. J., Bowen C. R., Mintova S., and Burrows A. D. (2015). Gas sensing using porous materials for automotive applications. *Chemical Society Reviews* **44**(13): 4290-4321.
- Wang, B., Long J., and Teo K. (2016). Multi-Channel Capacitive Sensor Arrays. *Sensors* **16**(2): 150.
- Wark, M., Rohlffing Y., Altindag Y., and Wellmann H. (2003). Optical gas sensing by semiconductor nanoparticles or organic dye molecules hosted in the pores of mesoporous siliceous MCM-41. *Physical Chemistry Chemical Physics* **5**(23): 5188-5194.
- Wu, H., Simmons J. M., Srinivas G., Zhou W., and Yildirim T. (2010). Adsorption Sites and Binding Nature of CO₂ in Prototypical Metal-Organic Frameworks: A Combined Neutron Diffraction and First-Principles Study. *The Journal of Physical Chemistry Letters* **1**(13): 1946-1951.
- Yang, H., Xu Z., Fan M., Gupta R., Slimane R. B., Bland A. E. , and Wright I. (2008). Progress in carbon dioxide separation and capture: A review. *Journal of Environmental Sciences* **20**(1): 14-27.
- Zarifi, M. H. and Daneshmand M. (2016). Liquid sensing in aquatic environment using high quality planar microwave resonator. *Sensors and Actuators B: Chemical* **225**: 517-521.

- Zarifi, M. H., Farsinezhad S., Abdolrazzaghi M., Daneshmand M., and Shankar K. (2016). Selective microwave sensors exploiting the interaction of analytes with trap states in TiO₂ nanotube arrays. *Nanoscale* **8**(14): 7466-7473.
- Zarifi, M. H., Farsinezhad S., Shankar K., and Daneshmand M. (2015). Liquid Sensing Using Active Feedback Assisted Planar Microwave Resonator. *IEEE Microwave and Wireless Components Letters* **25**(9): 621-623.
- Zarifi, M. H., Fayaz M., Goldthorp J., Abdolrazzaghi M., Hashisho Z., and Daneshmand M. (2015). Microbead-assisted high resolution microwave planar ring resonator for organic-vapor sensing. *Applied Physics Letters* **106**(6): 062903.
- Zarifi, M. H., Rahimi M., Daneshmand M., and Thundat T. (2016). Microwave ring resonator-based non-contact interface sensor for oil sands applications. *Sensors and Actuators B: Chemical* **224**: 632-639.
- Zarifi, M. H., Shariaty P., Hashisho Z., and Daneshmand M. (2017). A non-contact microwave sensor for monitoring the interaction of zeolite 13X with CO₂ and CH₄ in gaseous streams. *Sensors and Actuators B: Chemical*.
- Zarifi, M. H., Sohrabi A., Shaibani P. M., Daneshmand M., and Thundat T. (2015). Detection of Volatile Organic Compounds Using Microwave Sensors. *IEEE Sensors Journal* **15**(1): 248-254.
- Zarifi, M. H., Thundat T., and Daneshmand M. (2015). High resolution microwave microstrip resonator for sensing applications. *Sensors and Actuators A: Physical* **233**: 224-230.
- Zhou, Y., Jiang Y., Xie T., Tai H., and Xie G. (2014). A novel sensing mechanism for resistive gas sensors based on layered reduced graphene oxide thin films at room temperature. *Sensors and Actuators B: Chemical* **203**: 135-142.

Zybaylo, O., Shekhah O., Wang H., Tafipolsky M., Schmid R., Johannsmann D. and Woll C. (2010). A novel method to measure diffusion coefficients in porous metal-organic frameworks. *Physical Chemistry Chemical Physics* **12**(28): 8093-8098.

CHAPTER 7. CONCLUSIONS AND RECOMMENDATIONS

This chapter summarizes the main conclusions of the research work presented here, and provides some recommendations for future research. This study is mainly focused on effective methods to capture CO₂ using solid sorbents. At the early stage of this study, activated carbon was synthesized from oil sands coke and the effect of different activation agents and heating methods was investigated (Chapter 3). In order to enhance the performance of as-synthesized activated carbons, amine impregnation was proposed and the function of different amines was compared in terms of amine loading, amine type, humidity and capture capacity (Chapter 4). In the next phase, a new class of porous materials (MOFs) was proposed as solid sorbents for CO₂ and their capacity was fortified at atmospheric pressure by incorporating them onto the surface of carbon nanotubes (Chapter 5). Finally, the application of MOF materials for monitoring CO₂ was studied using a microwave resonator sensor (Chapter 6).

7.1. Conclusions

1) Coke activation using KOH provides microporous activated carbons with low ash and sulfur content, while adding MgO template widens the pores of the carbon and results in a mesoporous activated carbon. The research findings showed that there is an optimum ratio in KOH and MgO to be added to the coke which could enhance the sorption capacity of carbon. FTIR analyses confirmed the decrease in surface basic groups upon activation in CO₂ which yielded activated carbons with 25% lower CO₂ adsorption capacity compared to those activated in N₂.

2) Amongst three amines (DEA, MDEA, and TEPA) utilized for activated carbon impregnation, DEA offered the highest potential for CO₂ capture with 5.63 mmol/g adsorption capacity for AC-DEA sample. It was discovered that there is an

optimum in amine loading which further increase, causes blockage of accessible volume of pores following by decrease in adsorption capacity. Increasing temperature from 50 to 75 °C yielded in a lower adsorption capacity possibly due to the exothermic nature of CO₂ reaction with amines. The presence of 20% humidity in the feed stream enhanced the capture capacity of AC-MDEA samples.

3) The metal organic framework MOF-74 was successfully embedded onto carbon nanotube bucky papers via plasma treatment. Low exposure, one side plasma treatment with O₂/Ar resulted in an improved interfacial interaction between MOF and CNT, which the synthesized sample showed almost three times higher adsorption capacity compared to the parent MOF. Long exposure (7 min) plasma treatment causes surface saturation of active sites. Also, using NH₃ as plasma gas introduced mostly carboxylic groups on the surface of CNT-BP which was not efficient enough to enhance the wettability of bucky paper surface compared to O₂/Ar.

4) During the adsorption of CO₂ on MOF-199 and zeolite 13X, the dielectric properties of adsorbents were monitored using a microwave resonator sensor by screening changes in resonant frequency. Our study showed the potential of detecting low amounts of CO₂ (~5 vol. %) using MOF-199. For all three adsorbents (2 types of MOF-199 and zeolite 13X), adsorption isotherms were obtained by volumetric adsorption and related to the shift in resonant frequency. Despite the lower adsorption capacity of MOF-199 for low CO₂ concentrations (<45 vol.%), it has demonstrated higher sensitivity than zeolite 13X, which can be related to the initial dielectric properties of the fresh bed materials.

7.2. Recommendations

Based on the course of the current research and its findings, it is recommended that further research be conducted to include: application to other MOFs, adsorption tests under real flue gas composition, and study the sensor performance in non-dry gas streams.

1) In this study MOF-74 was synthesized and embedded on CNT-BPs for CO₂ adsorption. This technique can be applied to other MOFs such as ZIF which are hydrophobic and include a comparison among these two families of MOFs.

2) In the current work, the adsorption tests were conducted for the single component adsorption (i.e. CO₂ and N₂), however it is recommended to perform adsorption tests at real flue gas composition for multi-component adsorption.

3) During the CO₂ monitoring study by microwave sensor, the humidity parameter was fixed for all the experiments. Further work is required to study the sensor function in the presence of different levels of humidity and improve the selectivity performance of selected adsorbents

BIBLIOGRAPHY

- Abdelgwad A. H. , Said T. M. , Gody A. M. (2014). Microwave Detection of Water Pollution in Underground Pipelines. *International Journal of Wireless and Microwave Technologies* **4**(3): 1-15.
- Adatoz, E., Avcı A. K., and Keskin S. (2015). Opportunities and challenges of MOF-based membranes in gas separations. *Separation and Purification Technology* **152**: 207-237.
- Afshar, S., Salimi E., Braasch K., Butler M., Thomson D. and Bridges G. (2015). Multi-frequency DEP cytometer employing a microwave interferometer for the dielectric analysis of micro-particles. *2015 IEEE MTT-S International Microwave Symposium*.
- Ago, H., Kugler T., Cacialli F., Salaneck W. R., Shaffer M. S. P., Windle A. H., and Friend R. H. (1999). Work Functions and Surface Functional Groups of Multiwall Carbon Nanotubes. *The Journal of Physical Chemistry B* **103**(38): 8116-8121.
- Ahmad, F., Daud W. M. A. W., Ahmad M. A., Radzi R., and Azmi A. A. (2013). The effects of CO₂ activation, on porosity and surface functional groups of cocoa (*Theobroma cacao*) – Shell based activated carbon. *Journal of Environmental Chemical Engineering* **1**(3): 378-388.
- Ahmadpour, A. and Do D. D. (1996). The preparation of active carbons *from* coal by chemical and physical activation. *Carbon* **34**(4): 471-479.
- Aksoylu, A. E., Madalena M., Freitas A., Pereira M. F. R., and Figueiredo J. L. (2001). The effects of different activated carbon supports and support modifications on the properties of Pt/AC catalysts. *Carbon* **39**(2): 175-185.

- Alauzun, J., Mehdi A., Reya C. and Corriu R. J. P. (2005). CO₂ as a Supramolecular Assembly Agent: A Route for Lamellar Materials with a High Content of Amine Groups. *Journal of the American Chemical Society* **127**(32): 11204-11205.
- Allen, E. W. (2008). Process water treatment in Canada's oil sands industry: I. Target pollutants and treatment objectives. *Journal of Environmental Engineering and Science* **7**(2): 123-138.
- Allendorf, M. D., Houk R. J. T., Andruszkiewicz L., Talin A. A., Pikarsky J., Choudhury A., Gall K. A. and Hesketh P. J. (2008). Stress-Induced Chemical Detection Using Flexible Metal–Organic Frameworks. *Journal of the American Chemical Society* **130**(44): 14404-14405.
- Ameloot, R., Stappers L., Fransaeer J., Alaerts L., Sels B. F., and De Vos D. E. (2009). Patterned Growth of Metal-Organic Framework Coatings by *Electrochemical Synthesis*. *Chemistry of Materials* **21**(13): 2580-2582.
- Anbia, M. and Hoseini V. (2012). Development of MWCNT@MIL-101 hybrid composite with enhanced adsorption capacity for carbon dioxide. *Chemical Engineering Journal* **191**: 326-330.
- Anderson, P. A., Armstrong A. R., Porch A., Edwards P. P. and Woodall L. J. (1997). Structure and Electronic Properties of Potassium-Loaded Zeolite L. *The Journal of Physical Chemistry B* **101**(48): 9892-9900.
- Apra, P., Caputo D., Gargiulo N., Iucolano F. and Pepe F. (2010). Modeling Carbon Dioxide Adsorption on Microporous Substrates: Comparison between Cu-BTC Metal–Organic Framework and 13X Zeolitic Molecular Sieve. *Journal of Chemical & Engineering Data* **55**(9): 3655-3661.

- Arstad, B., Fjellvag H., Kongshaug K. O., Swang O., and Blom R. (2008). Amine functionalised metal organic frameworks (MOFs) as adsorbents for carbon dioxide. *Adsorption* **14**(6): 755-762.
- ASTM (2006). Standard Test Method for Determination of Iodine Number of Activated Carbon D4607, American Society for Testing and Materials.
- Ateeq, M., Shaw A., Garrett R. and Dickson P. (2016). Feasibility study on using microwave sensing technique to analyse silver-based products. *Journal of Electromagnetic Waves and Applications*: 1-17.
- Atkinson, J. D., Zhang Z., Yan Z., and Rood M. J. (2013). Evolution and impact of acidic oxygen functional groups on activated carbon fiber cloth during NO oxidation. *Carbon* **54**: 444-453.
- Bae, Y. S., Dubbeldam D., Nelson A., Walton K. S., Hupp J. T., and Snurr R. Q. (2009). Strategies for Characterization of Large-Pore Metal-Organic Frameworks by Combined Experimental and Computational Methods. *Chemistry of Materials* **21**(20): 4768-4777.
- Bae, Y. S., Lee C. Y., Kim K. C., Farha O. K., Nickias P., Hupp J. T., Nguyen S. T., and Snurr R. Q. (2012). High Propene/Propane Selectivity in Isostructural Metal–Organic Frameworks with High Densities of Open Metal Sites. *Angewandte Chemie International Edition* **51**(8): 1857-1860.
- Bandosz, T. J. (2006). Activated carbon surfaces in environmental remediation, Oxford,UK.
- Bao, Z., Yu L., Ren Q., Lu X., and Deng S. (2011). Adsorption of CO₂ and CH₄ on a magnesium-based metal organic framework. *Journal of Colloid and Interface Science* **353**(2): 549-556.

- Barton, D., Bradley J. W., Gibson K. J., Steele D. A., and Short R. D. (2000). An In Situ Comparison between VUV Photon and Ion Energy Fluxes to Polymer Surfaces Immersed in an RF Plasma. *The Journal of Physical Chemistry B* **104**(30): 7150-7153.
- Barton, D., Bradley J. W., Steele D. A., and Short R. D. (1999). Investigating Radio Frequency Plasmas Used for the Modification of Polymer Surfaces. *The Journal of Physical Chemistry B* **103**(21): 4423-4430.
- Basu, S., Cano-Odena A., and Vankelecom I. F. J. (2011). MOF-containing mixed-matrix membranes for CO₂/CH₄ and CO₂/N₂ binary gas mixture separations. *Separation and Purification Technology* **81**(1): 31-40.
- Bernini, M. C., Garcia Blanco A. A., Villarroel-Rocha J., Fairen-Jimenez D., Sapag K., Ramirez-Pastor A. J., and Narda G. E. (2015). Tuning the target composition of amine-grafted CPO-27-Mg for capture of CO₂ under post-combustion and air filtering conditions: a combined experimental and computational study. *Dalton Transactions* **44**(43): 18970-18982.
- Bhadra, S., Thomson D., and Bridges G. (2015). Near-Field Coupled RFID Tag for Carbon Dioxide Concentration Sensing. *USNC-URSI Radio Science Meeting (Joint with AP-S Symposium)*. Canada: 203.
- Bianco, A., Kostarelos K., and Prato M. (2005). Applications of carbon nanotubes in drug delivery. *Current opinion in chemical biology* **9**(6): 674-679.
- Biemmi, E., Scherb C., and Bein T. (2007). Oriented Growth of the Metal Organic Framework Cu₃(BTC)₂(H₂O)₃·xH₂O Tunable with Functionalized Self-Assembled Monolayers. *Journal of the American Chemical Society* **129**(26): 8054-8055.

- Biesinger, M. C., Lau L. W. M., Gerson A. R., and Smart R. S. C. (2010). Resolving surface chemical states in XPS analysis of first row transition metals, oxides and hydroxides: Sc, Ti, V, Cu and Zn. *Applied Surface Science* **257**(3): 887-898.
- Birbara, P. J., Filburn T. P., Michels H. and Nalette T. A. (2002). Sorbent system and method for absorbing carbon dioxide from the atmosphere of a closed habitable environment. *U. S. Patent. US6364938 B1*.
- Bloch, E. D., Britt D., Lee C., Doonan C. J., Uribe-Romo F. J., Furukawa H., Long J. R., and Yaghi O. M. (2010). Metal Insertion in a Microporous Metal–Organic Framework Lined with 2,2'-Bipyridine. *Journal of the American Chemical Society* **132**(41): 14382-14384.
- Bonenfant, D., Mimeault M., and Hausler R. (2003). Determination of the Structural Features of Distinct Amines Important for the Absorption of CO₂ and Regeneration in Aqueous Solution. *Industrial & Engineering Chemistry Research* **42**(14): 3179-3184.
- Bradshaw, D., Garai A., and Huo J. (2012). Metal-organic framework growth at functional interfaces: thin films and composites for diverse applications. *Chemical Society Reviews* **41**(6): 2344-2381.
- Britt, D., Furukawa H., Wang B., Glover T. G., and Yaghi O. M. (2009). Highly efficient separation of carbon dioxide by a metal-organic framework replete with open metal sites. *Proceedings of the National Academy of Sciences* **106**(49): 20637-20640.
- Bullin J. A. and Polasek J. C. (1990). The use of MDEA and mixtures of amines for bulk CO₂ removal. *Sixty-Ninth GPA Annual Convention*, Lakewood, Colorado
- Buonocore, F., Trani F., Ninno D., Matteo A. D., Cantele G., and Iadonisi G. (2008). Ab initio calculations of electron affinity and ionization potential of carbon nanotubes. *Nanotechnology* **19**(2): 025711.

- Bux, H., Feldhoff A., Cravillon J., Wiebcke M., Li Y. S., and Caro J. (2011). Oriented Zeolitic Imidazolate Framework-8 Membrane with Sharp H₂/C₃H₈ Molecular Sieve Separation. *Chemistry of Materials* **23**(8): 2262-2269.
- Caballero, A., Dexpert H., Didillon B., LePeltier F., Clause O., and Lynch J. (1993). In situ x-ray absorption spectroscopic study of a highly dispersed platinum-tin/alumina catalyst. *The Journal of Physical Chemistry* **97**(43): 11283-11285.
- Carne, A., Carbonell C., Imaz I., and Maspoch D. (2011). Nanoscale metal-organic materials. *Chemical Society Reviews* **40**(1): 291-305.
- Casco, M. E., Fernandez-Catala J., Martinez-Escandell M., Rodriguez-Reinoso F., Ramos-Fernandez E. V., and Silvestre-Albero J. (2015). Improved mechanical stability of HKUST-1 in confined nanospace. *Chemical Communications* **51**(75): 14191-14194.
- Caskey, S. R., Wong-Foy A. G., and Matzger A. J. (2008). Dramatic Tuning of Carbon Dioxide Uptake via Metal Substitution in a Coordination Polymer with Cylindrical Pores. *Journal of the American Chemical Society* **130**(33): 10870-10871.
- Centrone, A., Yang Y., Speakman S., Bromberg L., Rutledge G. C., and Hatton T. A. (2010). Growth of Metal–Organic Frameworks on Polymer Surfaces. *Journal of the American Chemical Society* **132**(44): 15687-15691.
- Chakraborty, T., Bucknum M. J., and Castro E. A. (2013). Computational and Experimental Chemistry: Developments and Applications, Apple Academic Press.
- Chang, A. C. C., Chuang S. S. C., Gray M., and Soong Y. (2003). In-Situ Infrared Study of CO₂ Adsorption on SBA-15 Grafted with Y-(Aminopropyl)triethoxysilane. *Energy & Fuels* **17**(2): 468-473.

- Chang, C. F., Chang C. Y., and Tsai W. T. (2000). Effects of Burn-off and Activation Temperature on Preparation of Activated Carbon from Corn Cob Agrowaste by CO₂ and Steam. *Journal of Colloid and Interface Science* **232**(1): 45-49.
- Chatti, R., Bansiwala A. K., Thote J. A., Kumar V., Jadhav P., Lokhande S. K., Biniwale R. B., Labhsetwar N. K., and Rayalu S. S. (2009). Amine loaded zeolites for carbon dioxide capture: Amine loading and adsorption studies. *Microporous and Mesoporous Materials* **121**(1-3): 84-89.
- Chen, C., Liang B., Ogino A., Wang X, and Nagatsu M. (2009). Oxygen Functionalization of Multiwall Carbon Nanotubes by Microwave-Excited Surface-Wave Plasma Treatment. *The Journal of Physical Chemistry C* **113**(18): 7659-7665.
- Chen, C., Ogino A., Wang X., and Nagatsu M. (2010). Plasma treatment of multiwall carbon nanotubes for dispersion improvement in water. *Applied Physics Letters* **96**(13): 131504.
- Chen, H. and Hashisho Z. (2012). Effects of microwave activation conditions on the properties of activated oil sands coke. *Fuel Processing Technology* **102**(0): 102-109.
- Chen, H. and Hashisho Z. (2012). Fast preparation of activated carbon from oil sands coke using microwave-assisted activation. *Fuel* **95**: 178-182.
- Chen, P., Schönebaum S., Simons T., Rauch D., Dietrich M., Moos R., and U. Simon (2015). Correlating the Integral Sensing Properties of Zeolites with Molecular Processes by Combining Broadband Impedance and DRIFT Spectroscopy—A New Approach for Bridging the Scales. *Sensors* **15**(11): 28915.
- Chen, W. T., Stewart K. M. E., Carroll J., Mansour R., Abdel-Rahman E., and Penlidis A. (2013). Novel gaseous phase ethanol sensor implemented with underloaded RF resonator for sensor-embedded passive chipless rfids. *2013 Transducers & Eurosensors XXVII*:

*The 17th International Conference on Solid-State Sensors, Actuators and Microsystems
(Transducers & Eurosensors XXVII).*

- Cheng, H. (2014). Integrated microwave resonator/antenna structures for sensor and filter applications, *Thesis for Doctor of Philosophy*, University of Central Florida.
- Cherbański, R. and Molga, E. (2009). Intensification of desorption processes by use of microwaves-An overview of possible applications and industrial perspectives. *Chemical Engineering and Processing: Process Intensification*, **48**: 48-58.
- Cherbański, R., Komorowska-Durka M., Stefanidis G. D., and Stankiewicz A. I. (2011). Microwave Swing Regeneration vs Temperature Swing Regeneration, Comparison of Desorption Kinetics. *Industrial & Engineering Chemistry Research* **50**(14): 8632-8644.
- Chevallier, P., Castonguay M., Turgeon S., Dubrulle N., Mantovani D., McBreen P. H., Wittmann J. C., and Laroche G. (2001). Ammonia RF-Plasma on PTFE Surfaces: Chemical Characterization of the Species Created on the Surface by Vapor-Phase Chemical Derivatization. *The Journal of Physical Chemistry B* **105**(50): 12490-12497.
- Chiang, C.-J., Tsai K.-T., Lee Y.-H., Lin H.-W., Yang Y.-L., Shih C.-C., Lin C.-Y., Jeng H.-A., Weng Y.-H., Cheng Y.-Y., Ho K.-C., and Dai C.-A. (2013). In situ fabrication of conducting polymer composite film as a chemical resistive CO₂ gas sensor. *Microelectronic Engineering* **111**: 409-415.
- Cho, H.Y., Yang D.A., Kim J., Jeong S.Y., and Ahn W.S. (2012). CO₂ adsorption and catalytic application of Co-MOF-74 synthesized by microwave heating. *Catalysis Today* **185**(1): 35-40.
- Choi, S., Drese J. H., and Jones C. W. (2009). Adsorbent Materials for Carbon Dioxide Capture from Large Anthropogenic Point Sources. *ChemSusChem* **2**(9): 796-854.

- Chowdhury, P., Bikkina C., and Gumma S. (2009). Gas Adsorption Properties of the Chromium-Based Metal Organic Framework MIL-101. *The Journal of Physical Chemistry C* **113**(16): 6616-6621.
- Chowdhury, P., Bikkina C., Meister D., Dreisbach F. and Gumma S. (2009). Comparison of adsorption isotherms on Cu-BTC metal organic frameworks synthesized from different routes. *Microporous and Mesoporous Materials* **117**(1–2): 406-413.
- Chue, K. T., Kim J. N., Yoo , Cho S. H. , and Yang R. T. (1995). Comparison of Activated Carbon and Zeolite 13X for CO₂ Recovery from Flue Gas by Pressure Swing Adsorption. *Industrial & Engineering Chemistry Research* **34**(2): 591-598.
- Chung, D. D. L. (2001). Electromagnetic interference shielding effectiveness of carbon materials. *Carbon* **39**(2): 279-285.
- Cismaru, A., Aldrigo M., Radoi A. and Dragoman M. (2016). Carbon nanotube-based electromagnetic band gap resonator for CH₄ gas detection. *Journal of Applied Physics* **119**(12): 124504.
- Coates, J. (2006). Interpretation of Infrared Spectra, A Practical Approach. Encyclopedia of Analytical Chemistry, John Wiley & Sons, Ltd.
- Contarini, S., Barbini M., Del Piero G., Gambarotta E., Mazzamurro G., Riocci M., Zappelli P., Gale J., and Kaya Y. (2003). Solid Sorbents for the Reversible Capture of Carbon Dioxide. *Greenhouse Gas Control Technologies - 6th International Conference*. Oxford, Pergamon: 169-174.
- CSIRO (2008). Post-Combustion Capture (PCC). *COAL21 Post Combustion CO₂ Capture Meeting*, Canberra

- Cummings A. L., Veatch F. C., Keller A. E., Mecum S. M. and Kammiller R. M. (1990). An analytical method for determining bound and free alkanolamines in heat stable salt contaminated solutions. *AICHE 1990 Summer national meeting symposium gas processing*, Ponca City, OK.
- Dabrowski, A., Podkoscielny P., Hubicki Z., and Barczak M. (2005). Adsorption of phenolic compounds by activated carbon: a critical review. *Chemosphere* **58**(8): 1049-1070.
- D'Alessandro, D. M., and T. McDonald (2010). Toward carbon dioxide capture using nanoporous materials. *Pure and Applied Chemistry*. **83**: 57.
- D'Alessandro, D. M., Smit B., and Long J. R. (2010). Carbon Dioxide Capture: Prospects for New Materials. *Angewandte Chemie International Edition* **49**(35): 6058-6082.
- Datsyuk, V., Kalyva M., Papagelis K., Parthenios J., Tasis D., Siokou A., Kallitsis I., and Galiotis C. (2008). Chemical oxidation of multiwalled carbon nanotubes. *Carbon* **46**(6): 833-840.
- Davies, M. (2006). Corrosion: Environments and Industries *ASM Handbook*_ASM International. **13C**: 727 - 735.
- Davini, P. (2002). Flue gas treatment by activated carbon obtained from oil-fired fly ash. *Carbon* **40**(11): 1973-1979.
- De Jonge, R. J., Breure A. M., and Van Andel J. G. (1996). Reversibility of adsorption of aromatic compounds onto powdered activated carbon (PAC). *Water Research* **30**(4): 883-892.
- Debatin, F., Thomas A., Kelling A., Hedin N., Bacsik Z., Senkovska I., Kaskel S., Junginger M., Müller H., Schilde U., Jäger C., Friedrich A., and Holdt H. J. (2010). In Situ Synthesis of an Imidazolate-4-amide-5-imidate Ligand and Formation of a Microporous Zinc–Organic

- Framework with H₂-and CO₂-Storage Ability. *Angewandte Chemie International Edition* **49**(7): 1258-1262.
- Deng, H., Yi H., Tang X., Yu Q., Ning P., and Yang L. (2012). Adsorption equilibrium for sulfur dioxide, nitric oxide, carbon dioxide, nitrogen on 13X and 5A zeolites. *Chemical Engineering Journal* **188**: 77-85.
- Díaz-García, M., Mayoral Á., Díaz I., and Sánchez-Sánchez M. (2014). Nanoscaled M-MOF-74 Materials Prepared at Room Temperature. *Crystal Growth & Design* **14**(5): 2479-2487.
- Dietrich, M., Rauch D., Porch A., and Moos R. (2014). A Laboratory Test Setup for in Situ Measurements of the Dielectric Properties of Catalyst Powder Samples under Reaction Conditions by Microwave Cavity Perturbation: Set up and Initial Tests. *Sensors (Basel, Switzerland)* **14**(9): 16856-16868.
- Dietrich, M., Rauch D., Simon U., Porch A. and Moos R. (2015). Ammonia storage studies on H-ZSM-5 zeolites by microwave cavity perturbation: correlation of dielectric properties with ammonia storage. *J. Sens. Sens. Syst.* **4**(2): 263-269.
- Dietzel, P. D. C., Besikiotis V., and Blom R. (2009). Application of metal-organic frameworks with coordinatively unsaturated metal sites in storage and separation of methane and carbon dioxide. *Journal of Materials Chemistry* **19**(39): 7362-7370.
- Dietzel, P. D. C., Blom R., and Fjellvåg H. (2008). Base-Induced Formation of Two Magnesium Metal-Organic Framework Compounds with a Bifunctional Tetratopic Ligand. *European Journal of Inorganic Chemistry* **2008**(23): 3624-3632.
- Di-Panfilo, R. and Egiebor N. O. (1996). Activated carbon production from synthetic crude coke. *Fuel Processing Technology* **46**(3): 157-169.

- Dobrovolsky, Y., Leonova L., and Nadkhina S. (1995). Working electrodes for low-temperature CO₂-sensors. *Ionics* **1**(3): 228-234.
- Donaldson, T. L. and Nguyen Y. N. (1980). Carbon Dioxide Reaction Kinetics and Transport in Aqueous Amine Membranes. *Industrial & Engineering Chemistry Fundamentals* **19**(3): 260-266.
- Dong-Il Jang and Park S. J. (2011). Influence of Amine Grafting on Carbon Dioxide Adsorption Behaviors of Activated Carbons. *Bulletin of the korean chemical society* **32**(9): 3377-3381.
- D'Souza, F. and Kadish K. M. (2014). Handbook of Carbon Nano Materials: (In 2 Volumes)Volume 5: Graphene — Fundamental PropertiesVolume 6: Graphene — Energy and Sensor Applications.
- Dumée, L. F., Feng C., He L., Allieux F.M., Yi Z., Gao W., Banos C., Davies J. B. and Kong L. (2014). Tuning the grade of graphene: Gamma ray irradiation of free-standing graphene oxide films in gaseous phase. *Applied Surface Science* **322**(0): 126-135.
- Dumée, L. F., Sears K., Marmiroli B., Amenitsch H., Duan X., Lamb R., Buso D., Huynh C., Hawkins S., Kentish S., Duke M., Gray S., Innocenzi P., Hill A. J., and Falcaro P. (2013). A high volume and low damage route to hydroxyl functionalization of carbon nanotubes using hard X-ray lithography. *Carbon* **51**: 430-434.
- Dumée, L., He L., Hill M., Zhu B., Duke M., Schutz J., She F., Wang H., Gray S., Hodgson P., and Kong L. (2013) Seeded growth of ZIF-8 on the surface of carbon nanotubes towards self-supporting gas separation membranes. *Journal of Materials Chemistry A* **1**(32): 9208-9214.

- Dumée, L., Sears K., Schütz J., Finn N., Duke M., and Gray S. (2013). Influence of the Sonication Temperature on the Debundling Kinetics of Carbon Nanotubes in Propan-2-ol. *Nanomaterials* **3**(1): 70.
- Dunne J.A., Sircar S., Gorte R.J., Myers A.L. (1996). Calorimetric heats of adsorption and adsorption isotherm of O₂, N₂, Ar, CO₂, CH₄, C₂H₆, and SF₆ on silicalite,. *Langmuir* **12**: 5888–5895.
- Dunne, L. J. and Manos G. (2010). Adsorption and Phase Behaviour in Nanochannels and Nanotubes. New York.
- Durá, G., Budarin V. L., Castro-Osma J. A., Shuttleworth P. S., Quek S. C. Z., Clark J. H., and North M. (2016). Importance of Micropore–Mesopore Interfaces in Carbon Dioxide Capture by Carbon-Based Materials. *Angewandte Chemie International Edition* **55**(32): 9173-9177.
- Ebrahimi, A., Withayachumnankul W., Al-Sarawi S. and Abbott D. (2014). High-Sensitivity Metamaterial-Inspired Sensor for Microfluidic Dielectric Characterization. *IEEE Sensors Journal* **14**(5): 1345-1351.
- Ebrahimi, A., Withayachumnankul W., Al-Sarawi S. F. and Abbott D. (2014). Metamaterial-Inspired Rotation Sensor With Wide Dynamic Range. *IEEE Sensors Journal* **14**(8): 2609-2614.
- Ebrahimi, A., Withayachumnankul W., Al-Sarawi S. F., and Abbott D. (2014). Metamaterial-Inspired Rotation Sensor With Wide Dynamic Range. *IEEE Sensors Journal* **14**(8): 2609-2614.
- Eddaoudi, M., Moler D. B., Li H., Chen B., Reineke T. M., O'Keeffe M., and Yaghi O. M. (2001). Modular Chemistry: Secondary Building Units as a Basis for the Design of

- Highly Porous and Robust Metal–Organic Carboxylate Frameworks. *Accounts of Chemical Research* **34**(4): 319-330.
- Epp, J. (2016). 4 - X-ray diffraction (XRD) techniques for materials characterization. *Materials Characterization Using Nondestructive Evaluation (NDE) Methods*, Woodhead Publishing: 81-124.
- Fedorak, P. M. and Coy D. L. (2006). Oil sands cokes affect microbial activities. *Fuel* **85**(12–13): 1642-1651.
- Felten, A., Eckmann A., Pireaux J. J., Krupke R. and Casiraghi C. (2013). Controlled modification of mono- and bilayer graphene in O₂, H₂ and CF₄ plasmas. *Nanotechnology* **24**(35): 355705.
- Ferrari, A. C. and Basko D. M. (2013). Raman spectroscopy as a versatile tool for studying the properties of graphene. *Nat Nano* **8**(4): 235-246.
- Figueroa, J. D., Fout T., Plasynski S., McIlvried H., and Srivastava R. D. (2008). Advances in CO₂ capture technology—The U.S. Department of Energy's Carbon Sequestration Program. *International Journal of Greenhouse Gas Control* **2**(1): 9-20.
- Foo, K. Y. and Hameed B. H. (2012). Mesoporous activated carbon from wood sawdust by K₂CO₃ activation using microwave heating. *Bioresource Technology* **111**(0): 425-432.
- Fout T., J. T. M. and Jones A. P. (2009). DOE/NETL's Carbon Capture R&D Program for Existing Coal-Fired Power Plants. Energy, National Energy Technology Laboratory
- Franchi, R. S., Harlick P. J. E., and Sayari A. (2005). Applications of Pore-Expanded Mesoporous Silica. 2. Development of a High-Capacity, Water-Tolerant Adsorbent for CO₂. *Industrial & Engineering Chemistry Research* **44**(21): 8007-8013.

- Freguia, S. and Rochelle G. T. (2003). Modeling of CO₂ capture by aqueous monoethanolamine. *AIChE Journal* **49**(7): 1676-1686.
- Fryxell, G. E. and Cao G. (2012). Environmental Applications of Nanomaterials: Synthesis, Sorbents and Sensors. *World Scientific*
- Furimsky, E. (1998). Gasification of oil sand coke: Review. *Fuel Processing Technology* **56**(3): 263-290.
- Furukawa, H., Ko N., Go Y. B., Aratani N., Choi S. B., Choi E., Yazaydin Ö., Snurr R. Q., O’Keeffe M., Kim J., and Yaghi O. M. (2010). Ultrahigh Porosity in Metal-Organic Frameworks. *Science* **329**(5990): 424-428.
- Galindo-Romera, G., Herraiz-Mart F. J., Gil M., Martínez-Martínez J. J., and Segovia-Vargas D. (2016). Submersible Printed Split-Ring Resonator-Based Sensor for Thin-Film Detection and Permittivity Characterization. *IEEE Sensors Journal* **16**(10): 3587-3596.
- Garcia, S., Gil M. V., Martin C. F., Pis J. J., Rubiera F., and Pevida C. (2011). Breakthrough adsorption study of a commercial activated carbon for pre-combustion CO₂ capture. *Chemical Engineering Journal* **171**(2): 549-556.
- Gascon, J., Aguado S., and Kapteijn F. (2008). Manufacture of dense coatings of Cu₃(BTC)₂ (HKUST-1) on α -alumina. *Microporous and Mesoporous Materials* **113**(1-3): 132-138.
- Gauden, P. A. and Wisniewski M. (2007). CO₂ sorption on substituted carbon materials: Computational chemistry studies. *Applied Surface Science* **253**(13): 5726-5731.
- Gholidoust, A., Atkinson J. D., and Hashisho Z. (2017). Enhancing CO₂ Adsorption via Amine-Impregnated Activated Carbon from Oil Sands Coke. *Energy & Fuels* **31**(2): 1756-1763.

- Giannakopoulos, I. G., Kouzoudis D., Grimes C. A., and Nikolakis V. (2005). Synthesis and Characterization of a Composite Zeolite–Metglas Carbon Dioxide Sensor. *Advanced Functional Materials* **15**(7): 1165-1170.
- Goeders, K. M., Colton J. S., and Bottomley L. A. (2008). Microcantilevers: Sensing Chemical Interactions via Mechanical Motion. *Chemical Reviews* **108**(2): 522-542.
- Gomes, H. T., Machado B. F., Ribeiro A., Moreira I., Rosario M. R., Silva A.M.T., Figueiredo J. L., and Faria J. L. (2008). Catalytic properties of carbon materials for wet oxidation of aniline. *Journal of Hazardous Materials* **159**(2-3): 420-426.
- Granite, E. J. and Pennline H. W. (2002). Photochemical Removal of Mercury from Flue Gas. *Industrial & Engineering Chemistry Research* **41**(22): 5470-5476.
- Gray, M. L., Soong Y., Champagne K. J., Baltrus J., Stevens Jr R. W., Toochinda P., and Chuang S. S. C. (2004). CO₂ capture by amine-enriched fly ash carbon sorbents. *Separation and Purification Technology* **35**(1): 31-36.
- Gutiérrez-Sevillano, J. J., Vicent-Luna J. M., Dubbeldam D., and Calero S. (2013). Molecular Mechanisms for Adsorption in Cu-BTC Metal Organic Framework. *The Journal of Physical Chemistry C* **117**(21): 11357-11366.
- Ham, S. W., Hong H. P., Kim J. H., Min S. J., and Min N. K. (2014). Effect of Oxygen Plasma Treatment on Carbon Nanotube-Based Sensors. *Journal of Nanoscience and Nanotechnology* **14**(11): 8476-8481.
- Hamon, M. A., Chen J., Hu H., Chen Y., Itkis M. E., Rao A. M., Eklund P. C., and Haddon R. C. (1999). Dissolution of Single-Walled Carbon Nanotubes. *Advanced Materials* **11**(10): 834-840.

- Hasib-ur-Rahman, M., Sijaj M., and Larachi F. (2010). Ionic liquids for CO₂ capture: Development and progress. *Chemical Engineering and Processing: Process Intensification* **49**(4): 313-322.
- He, X., Li R., Qiu J., Xie K., Ling P., Yu M., Zhang X., and Zheng M. (2012). Synthesis of mesoporous carbons for supercapacitors from coal tar pitch by coupling microwave-assisted KOH activation with a MgO template. *Carbon* **50**(13): 4911-4921.
- Hermes, S., Schröder F., Chelmowski R., Wöll C., and Fischer R. A. (2005). Selective Nucleation and Growth of Metal–Organic Open Framework Thin Films on Patterned COOH/CF₃-Terminated Self-Assembled Monolayers on Au(111). *Journal of the American Chemical Society* **127**(40): 13744-13745.
- Heydari-Gorji, A., Belmabkhout Y., and Sayari A. (2011). Polyethylenimine-Impregnated Mesoporous Silica: Effect of Amine Loading and Surface Alkyl Chains on CO₂ Adsorption. *Langmuir* **27**(20): 12411-12416.
- Ho, M. T., Allinson G. W., and Wiley D. E. (2008). Reducing the Cost of CO₂ Capture from Flue Gases Using Pressure Swing Adsorption. *Industrial & Engineering Chemistry Research* **47**(14): 4883-4890.
- Hou, Z., Cai B., Liu H., and Xu D. (2008). Ar, O₂, CHF₃, and SF₆ plasma treatments of screen-printed carbon nanotube films for electrode applications. *Carbon* **46**(3): 405-413.
- Houshmand, A., Daud W., Lee M.G., and Shafeeyan M. (2012) Carbon Dioxide Capture with Amine-Grafted Activated Carbon. *Water, Air, & Soil Pollution* **223**(2): 827-835.
- Hu, Z. and Srinivasan M. P. (2001). Mesoporous high-surface-area activated carbon. *Microporous and Mesoporous Materials* **43**(3): 267-275.

- Huang, H. Y., Yang R. T., Chinn D. , and Munson C. L. (2002). Amine-Grafted MCM-48 and Silica Xerogel as Superior Sorbents for Acidic Gas Removal from Natural Gas. *Industrial & Engineering Chemistry Research* **42**(12): 2427-2433.
- Hussain, S., Amade R., Jover E., and Bertran E. (2012). Functionalization of carbon nanotubes by water plasma. *Nanotechnology* **23**(38): 385604.
- Hutson, N. D., Speakman S. A., and Payzant E. A. (2004). Structural Effects on the High Temperature Adsorption of CO₂ on a Synthetic Hydrotalcite. *Chemistry of Materials* **16**(21): 4135-4143.
- Hutson, N. D., Speakman S. A., and Payzant E. A. (2004). Structural Effects on the High Temperature Adsorption of CO₂ on a Synthetic Hydrotalcite. *Chemistry of Materials* **16**(21): 4135-4143.
- Huynh, C. P. and Hawkins S. C. (2010). Understanding the synthesis of directly spinnable carbon nanotube forests. *Carbon* **48**(4): 1105-1115.
- IPCC (2001). *Climate Change 2001: Impacts, Adaptation and Vulnerability*.
- Jack, T. R., Sullivan E. A., and Zajic J. E. (1979). Comparison of the structure and composition of cokes from the thermal cracking of Athabasca Oil Sands bitumen. *Fuel* **58**(8): 585-588.
- Jadhav, P. D., Chatti R. V., Biniwale R. B., Labhsetwar N. K., Devotta S., and Rayalu S. S. (2007). Monoethanol Amine Modified Zeolite 13X for CO₂ Adsorption at Different Temperatures. *Energy & Fuels* **21**(6): 3555-3559.
- Jahan, M., Bao Q., Yang J.X., and Loh K. P. (2010). Structure-Directing Role of Graphene in the Synthesis of Metal–Organic Framework Nanowire. *Journal of the American Chemical Society* **132**(41): 14487-14495.

- Jankowska, H., Świątkowski A., and Choma J. (1991). Active carbon, E. Horwood.
- Jiang, X., Gu J., Bai X., Lin L., and Zhang Y. (2009). The influence of acid treatment on multi-walled carbon nanotubes. *Pigment & Resin Technology* **38**(3): 165-173.
- Jiao, Y., Morelock C. R., Burtch N. C., Mounfield W. P., Hungerford J. T., and Walton K. S. (2015). Tuning the Kinetic Water Stability and Adsorption Interactions of Mg-MOF-74 by Partial Substitution with Co or Ni. *Industrial & Engineering Chemistry Research* **54**(49): 12408-12414.
- Jung, S., Kim Y., Kim S.-J., Kwon T.-H., Huh S., and Park S. (2011). Bio-functionalization of metal-organic frameworks by covalent protein conjugation. *Chemical Communications* **47**(10): 2904-2906.
- Junkar, I., Vesel A., Cvelbar U., Mozetič M., and Strnad S. (2009). Influence of oxygen and nitrogen plasma treatment on polyethylene terephthalate (PET) polymers. *Vacuum* **84**(1): 83-85.
- Kamarudin, K. S. N. and Mat H. (2009). Synthesis and modification of micro and mesoporous materials as CO₂ adsorbents, *Thesis for Master of Science, University of Technology of Malaysia*.
- Kang, S., Jian-chun J., and Dan-dan C. (2011). Preparation of activated carbon with highly developed mesoporous structure from *Camellia oleifera* shell through water vapor gasification and phosphoric acid modification. *Biomass and Bioenergy* **35**(8): 3643-3647.
- Karousis, N., Tagmatarchis N., and Tasis D. (2010). Current progress on the chemical modification of carbon nanotubes. *Chemical Reviews* **110**(9): 5366-5397.

- Kawano, T., Kubota M., Onyango M. S., Watanabe F., and Matsuda H. (2008). Preparation of activated carbon from petroleum coke by KOH chemical activation for adsorption heat pump. *Applied Thermal Engineering* **28**(8–9): 865-871.
- Keskin, S., Van Heest T. M., and Sholl D. S. (2010). Can Metal–Organic Framework Materials Play a Useful Role in Large-Scale Carbon Dioxide Separations? *ChemSusChem* **3**(8): 879-891.
- Khalil, S. H., Aroua M. K., and Daud W. M. A. W. (2012). Study on the improvement of the capacity of amine-impregnated commercial activated carbon beds for CO₂ adsorbing. *Chemical Engineering Journal* **183**(0): 15-20.
- Khan, M., Filiz V., Bengtson G., Shishatskiy S., Rahman M., and Abetz V. (2012). Functionalized carbon nanotubes mixed matrix membranes of polymers of intrinsic microporosity for gas separation. *Nanoscale Research Letters* **7**(1): 1-12.
- Kim, Y. K., Hyun S. M., Lee J. H., Kim T. K., Moon D., and Moon H. R. (2016). Crystal-Size Effects on Carbon Dioxide Capture of a Covalently Alkylamine-Tethered Metal-Organic Framework Constructed by a One-Step Self-Assembly. *Scientific Reports* **6**: 19337.
- Klinowski, J., Almeida Paz F. A., Silva P., and Rocha J. (2011). Microwave-Assisted Synthesis of Metal-Organic Frameworks. *Dalton Transactions* **40**(2): 321-330.
- Ko, Y. G., Shin S. S. , and Choi U. S. (2011). Primary, secondary, and tertiary amines for CO₂ capture: Designing for mesoporous CO₂ adsorbents. *Journal of Colloid and Interface Science* **361**(2): 594-602.
- Koh, C. A., Montanari T., Nooney R. I., Tahir S. F. , and Westacott R. E. (1999). Experimental and Computer Simulation Studies of the Removal of Carbon Dioxide from Mixtures with Methane Using AlPO₄-5 and MCM-41. *Langmuir* **15**(18): 6043-6049.

- Korostynska, O., Mason A., and Al-Shamma'a A. (2014). Microwave sensors for the non-invasive monitoring of industrial and medical applications. *Sensor Review* **34**(2): 182-191.
- Korostynska, O., Mason A., Ortoneda-Pedrola M., and Al-Shamma'a A. (2014). Electromagnetic wave sensing of NO₃ and COD concentrations for real-time environmental and industrial monitoring. *Sensors and Actuators B: Chemical* **198**: 49-54.
- Kot, P., Shaw A., Jones K. O., Cullen J. D., Mason A., and Al-Shamma'a A. I. (2015). The feasibility of electromagnetic waves in determining the moisture content of concrete blocks. *9th International Conference on Sensing Technology (ICST)*.
- Kreno, L. E., Hupp J. T., and Van Duyne R. P. (2010). Metal–Organic Framework Thin Film for Enhanced Localized Surface Plasmon Resonance Gas Sensing. *Analytical Chemistry* **82**(19): 8042-8046.
- Kreno, L. E., Leong K., Farha O. K., Allendorf M., Van Duyne R. P., and Hupp J. T. (2012). Metal–Organic Framework Materials as Chemical Sensors. *Chemical Reviews* **112**(2): 1105-1125.
- Krishnankutty, N. and Vannice M. A. (1995). Effect of Pretreatment on Surface Area, Porosity, and Adsorption Properties of a Carbon Black. *Chemistry of Materials* **7**(4): 754-763.
- Kumar, P., Deep A., and Kim K. H. (2015). Metal organic frameworks for sensing applications. *TrAC Trends in Analytical Chemistry* **73**: 39-53.
- Kumar, R. (1989). Adsorption column blowdown: adiabatic equilibrium model for bulk binary gas mixtures. *Industrial & Engineering Chemistry Research* **28**(11): 1677-1683.

- Küsgens, P., Siegle S., and Kaskel S. (2009). Crystal Growth of the Metal—Organic Framework $\text{Cu}_3(\text{BTC})_2$ on the Surface of Pulp Fibers. *Advanced Engineering Materials* **11**(1-2): 93-95.
- Lashaki, M. J., Fayaz M., Wang H., Hashisho Z., Philips J. H., Anderson J. E., and Nichols M. (2012). Effect of Adsorption and Regeneration Temperature on Irreversible Adsorption of Organic Vapors on Beaded Activated Carbon. *Environmental Science & Technology* **46**(7): 4083-4090.
- Leal, O., Bolivar C., Ovalles C. S., Garcia J. J., and Espidel Y. (1995). Reversible adsorption of carbon dioxide on amine surface-bonded silica gel. *Inorganica Chimica Acta* **240**(1-2): 183-189.
- Lee, C. S., Ong Y. L., Aroua M. K., and Daud W. M. A. W. (2013) Impregnation of palm shell-based activated carbon with sterically hindered amines for CO_2 adsorption. *Chemical Engineering Journal* **219**(0): 558-564.
- Lee, D., Jin Y., Jung N., Lee J., Lee J., Jeong Y. S., and Jeon S. (2011). Gravimetric Analysis of the Adsorption and Desorption of CO_2 on Amine-Functionalized Mesoporous Silica Mounted on a Microcantilever Array. *Environmental Science & Technology* **45**(13): 5704-5709.
- Lee, S. C., Chae H. J., Lee S. J., Choi B. Y., Yi C. K., Lee J. B., Ryu C. K., and Kim J. C. (2008). Development of Regenerable MgO -Based Sorbent Promoted with K_2CO_3 for CO_2 Capture at Low Temperatures. *Environmental Science & Technology* **42**(8): 2736-2741.
- Lee, S. C., Chae H. J., Lee S. J., Choi B. Y., Yi C. K., Lee J. B., Ryu C. K., and Kim J. C. (2008). Development of Regenerable MgO -Based Sorbent Promoted with K_2CO_3 for CO_2 Capture at Low Temperatures. *Environmental Science & Technology* **42**(8): 2736-2741.

- Lee, S. H. and Choi C. S. (2000). Chemical activation of high sulfur petroleum cokes by alkali metal compounds. *Fuel Processing Technology* **64**(1–3): 141-153.
- Leiner, M. J. P. (1991). Luminescence chemical sensors for biomedical applications: scope and limitations. *Analytica Chimica Acta* **255**(2): 209-222.
- Leiner, M. J. P. (1991). Luminescence chemical sensors for biomedical applications: scope and limitations. *Analytica Chimica Acta* **255**(2): 209-222.
- Li, J.R., Kuppler R. J., and Zhou H.C. (2009). Selective gas adsorption and separation in metal-organic frameworks. *Chemical Society Reviews* **38**(5): 1477-1504.
- Li, L., Tang L., Liang X., Liu Z., and Yang Y. (2016). Adsorption Performance of Acetone on Activated Carbon Modified by Microwave Heating and Alkali Treatment. *Journal of Chemical Engineering of Japan* **49**(11): 958-966.
- Li, P., Ge B., Zhang S., Chen S., Zhang Q., and Zhao Y. (2008). CO₂ Capture by Polyethylenimine-Modified Fibrous Adsorbent. *Langmuir* **24**(13): 6567-6574.
- Li, S., Liao G., Liu Z., Pan Y., Wu Q., Weng Y., Zhang X., Yang Z., and Tsui O. K. C. (2014). Enhanced water flux in vertically aligned carbon nanotube arrays and polyethersulfone composite membranes. *Journal of Materials Chemistry A* **2**(31): 12171-12176.
- Li. S., Wang Z.J., Chang T-T (2014) Temperature Oscillation Modulated Self-Assembly of Periodic Concentric Layered Magnesium Carbonate Microparticles. *PLoS ONE* **9**(2): e88648.
- Li, W., Zhang Y., Li Q., and Zhang G. (2015). Metal–organic framework composite membranes: Synthesis and separation applications. *Chemical Engineering Science* **135**: 232-257.
- Liang, Z., Marshall M., and Chaffee A. L. (2009). CO₂ Adsorption-Based Separation by Metal Organic Framework (Cu-BTC) versus Zeolite (13X). *Energy & Fuels* **23**(5): 2785-2789.

- Liang, Z., Marshall M., and Chaffee A. L. (2009). Comparison of Cu-BTC and zeolite 13X for adsorbent based CO₂ separation. *Energy Procedia* **1**(1): 1265-1271.
- Liangcheng, Y., Xinlei W., Ted L. F., Richard S. G., and Yuanhui Z. (2013). Impedance-Based Moisture Sensor Design and Test for Gas-Phase *Biofilter* Applications. *American Society of Agricultural and Biological Engineers* **56**(4). 1613-1621.
- Lin, R., Ge L., Diao H., Rudolph V., and Zhu Z. (2016). Propylene/propane selective mixed matrix membranes with grape-branched MOF/CNT filler. *Journal of Materials Chemistry A* **4**(16): 6084-6090.
- Lin, R., Ge L., Liu S., Rudolph V., and Zhu Z. (2015). Mixed-Matrix Membranes with Metal–Organic Framework-Decorated CNT Fillers for Efficient CO₂ Separation. *ACS Applied Materials & Interfaces* **7**(27): 14750-14757.
- Lin, T., Bajpai V., Ji T., and Dai L. (2003). Chemistry of carbon nanotubes. *Australian journal of chemistry* **56**(7): 635-651.
- Lin, Y.C., Lin C.Y., and Chiu P.W. (2010). Controllable graphene N-doping with ammonia plasma. *Applied Physics Letters* **96**(13): 133110.
- Liou, T. H. (2010). Development of mesoporous structure and high adsorption capacity of biomass-based activated carbon by phosphoric acid and zinc chloride activation. *Chemical Engineering Journal* **158**(2): 129-142.
- Littel, R. J., Versteeg G. F., and Van Swaaij W. P. M. (1992). Kinetics of CO₂ with primary and secondary amines in aqueous solutions II. Influence of temperature on zwitterion formation and deprotonation rates. *Chemical Engineering Science* **47**(8): 2037-2045.

- Liu, J., Sun F., Zhang F., Wang Z., Zhang R., Wang C., and Qiu S. (2011). In situ growth of continuous thin metal-organic framework film for capacitive humidity sensing. *Journal of Materials Chemistry* **21**(11): 3775-3778.
- Liu, J., Wang Y., Benin A. I., Jakubczak P., Willis R. R., and LeVan M. D. (2010). CO₂/H₂O Adsorption Equilibrium and Rates on Metal Organic Frameworks: HKUST-1 and Ni/DOBDC. *Langmuir* **26**(17): 14301-14307.
- Liu, Y., Bailey P., Noakes T. C. Q., Thompson G. E., Skeldon P. and Alexander M. R. (2004). Chemical environment of copper at the surface of a CuAl₂ model alloy: XPS, MEIS and TEM analyses. *Surface and Interface Analysis* **36**(4): 339-346.
- Liu, Y., Chen T., Lu T., Sun Z., Chua D. H. C., and Pan L. (2015). Nitrogen-doped porous carbon spheres for highly efficient capacitive deionization. *Electrochimica Acta* **158**: 403-409.
- Liu, Y., Zeng G., Pan Y., and Lai Z. (2011). Synthesis of highly c-oriented ZIF-69 membranes by secondary growth and their gas permeation properties. *Journal of Membrane Science* **379**(1-2): 46-51.
- Lu, H. (2012). Interfacial Synthesis of Metal-organic Frameworks. *Thesis for Master of Science, McMaster University*.
- Lübbers, D. W. and Opitz N. (1975). The pCO₂-/pO₂-optode: a new probe for measurement of pCO₂ or pO₂ in fluids and gases (authors transl). *Zeitschrift für Naturforschung. Section C: Biosciences* **30**(4): 532-533.
- Ma, P. C., Siddiqui N. A., Marom G., and Kim J.K. (2010). Dispersion and functionalization of carbon nanotubes for polymer-based nanocomposites: A review. *Composites Part A: Applied Science and Manufacturing* **41**(10): 1345-1367.

- Macia-Agullo, J. A., Moore B. C., Cazorla-Amoros D., and Linares-Solano A. (2004). Activation of coal tar pitch carbon fibres: Physical activation vs. chemical activation. *Carbon* **42**(7): 1367-1370.
- Mahajan, A., Kingon A., Kukovecz Á., Konya Z., and Vilarinho P. M. (2013). Studies on the thermal decomposition of multiwall carbon nanotubes under different atmospheres. *Materials Letters* **90**: 165-168.
- Mahurin, S. M., Lee J. S., Wang X., and Dai S. (2011). Ammonia-activated mesoporous carbon membranes for gas separations. *Journal of Membrane Science* **368**(1–2): 41-47.
- Majumder, M., Chopra N., Andrews R., and Hinds B. J. (2005). Nanoscale hydrodynamics: Enhanced flow in carbon nanotubes. *Nature* **438**(7064): 44-44.
- Maroto-Valer, M. M., Tang Z., and Zhang Y. (2005). CO₂ capture by activated and impregnated anthracites. *Fuel Processing Technology* **86**(14-15): 1487-1502.
- Marsh, H. and Rodriguez-Reinoso F. (2006). *Activated Carbon*, Elsevier Ltd: Oxford: 243-365.
- Matsuura, T. (2009). Membrane Separation Technologies. *Wastewater Recycling, Reuse, and Reclamation*. S. Vigneswaran, EOLSS Publications. **I**: 98-135.
- Mattson, J. A., Mark H. B., Malbin M. D., Weber W. J. and Crittenden J. C. (1969). Surface chemistry of active carbon: Specific adsorption of phenols. *Journal of Colloid and Interface Science* **31**(1): 116-130.
- McEvoy, N., Nolan H., Ashok Kumar N., Hallam T., and Duesberg G. S. (2013). Functionalisation of graphene surfaces with downstream plasma treatments. *Carbon* **54**: 283-290.
- McGrath, M. P. and Pham A. (2006). Carbon Nanotube Based Microwave Resonator Gas Sensors. *International Journal of High Speed Electronics and Systems* **16**(04): 913-935.

- McKinlay, A. C., Morris R. E., Horcajada P., Férey G., Gref R., Couvreur P., and Serre C. (2010). BioMOFs: Metal–Organic Frameworks for Biological and Medical Applications. *Angewandte Chemie International Edition* **49**(36): 6260-6266.
- Menendez, J. A., Phillips J., Xia B., and Radovic L. R. (1996). On the Modification and Characterization of Chemical Surface Properties of Activated Carbon: In the Search of Carbons with Stable Basic Properties. *Langmuir* **12**(18): 4404-4410.
- Merenda, A. (2015). Development of gate keepers gas separation membranes by selective growth of metal organic frameworks on the tips of carbon nanotubes. *Thesis for Master of Science, Politecnico di Torino*
- Miller, S. R., Pearce G. M., Wright P. A., Bonino F., Chavan S., Bordiga S., Margiolaki I., Guillou N., Férey G., Bourrelly S., and Llewellyn P. L. (2008). Structural Transformations and Adsorption of Fuel-Related Gases of a Structurally Responsive Nickel Phosphonate Metal–Organic Framework, Ni-STA-12. *Journal of the American Chemical Society* **130**(47): 15967-15981.
- Millward, A. R. and Yaghi O. M. (2005). Metal-Organic Frameworks with Exceptionally High Capacity for Storage of Carbon Dioxide at Room Temperature. *Journal of the American Chemical Society* **127**(51): 17998-17999.
- Morán-Lázaro, J. P., Blanco O., Rodríguez-Betancourt V. M., Reyes-Gómez J., and Michel C. R. (2016). Enhanced CO₂-sensing response of nanostructured cobalt aluminate synthesized using a microwave-assisted colloidal method. *Sensors and Actuators B: Chemical* **226**: 518-524.
- Morbideilli M., Gavriilidis A., and Varma A. (2001). *Catalyst design*, Cambridge University Press, UK: 149-150.

- Morishita, T., Tsumura T., Toyoda M., Przepiorski J., Morawski A. W., Konno H., and Inagaki M. (2010). A review of the control of pore structure in MgO-templated nanoporous carbons. *Carbon* **48**(10): 2690-2707.
- Morita, S., Hattori S., D'Agostino R. (1990). Applications of Plasma Polymers - Plasma Deposition, Treatment, and Etching of Polymers. San Diego, Academic Press: 423-461.
- Mueller, U., Schubert M., Teich F., Puetter H., Schierle-Arndt K., and Pastre J. (2006). Metal-organic frameworks-prospective industrial applications. *Journal of Materials Chemistry* **16**(7): 626-636.
- Mulgundmath, V. and Tezel F. H. (2010). Optimisation of carbon dioxide recovery from flue gas in a TPSA system. *Adsorption* **16**(6): 587-598.
- Nalette, T. A., Papale W., and Filburn T. P. (2004). Carbon dioxide scrubber for fuel and gas emissions. U. S. Patent. **6755892**.
- National Center for Biotechnology Information. PubChem Compound Database (2017); (a) CID=74819, <https://pubchem.ncbi.nlm.nih.gov/compound/74819>; (b) CID=8113, <https://pubchem.ncbi.nlm.nih.gov/compound/8113>; (c) CID=7767, <https://pubchem.ncbi.nlm.nih.gov/compound/7767>; (d) CID=8197, <https://pubchem.ncbi.nlm.nih.gov/compound/8197>
- Nayak, A. K., Ghosh R., Santra S., Guha P. K., and Pradhan D. (2015). Hierarchical nanostructured WO₃-SnO₂ for selective sensing of volatile organic compounds. *Nanoscale* **7**(29): 12460-12473.
- Olajire, A. A. (2010). CO₂ capture and separation technologies for end-of-pipe applications – A review. *Energy* **35**(6): 2610-2628.

- Ostermann, R., Cravillon J., Weidmann C., Wiebcke M., and Smarsly B. M. (2011). Metal-organic framework nanofibers viaelectrospinning. *Chemical Communications* **47**(1): 442-444.
- Patrick, J. W. (1995). Porosity in Carbons: Characterization and Applications, Wiley.
- Petit, C. and Bandosz T. J. (2011). Synthesis, Characterization, and Ammonia Adsorption Properties of Mesoporous Metal–Organic Framework (MIL(Fe))–Graphite Oxide Composites: Exploring the Limits of Materials Fabrication. *Advanced Functional Materials* **21**(11): 2108-2117.
- Petit, C., Mendoza B., and Bandosz T. J. (2010). Hydrogen Sulfide Adsorption on MOFs and MOF/Graphite Oxide Composites. *Journal of chemical physics and physical chemistry* **11**(17): 3678-3684.
- Pevida, C., Plaza M. G., Arias B., Feroso J., Rubiera F., and Pis J. J. (2008). Surface modification of activated carbons for CO₂ capture. *Applied Surface Science* **254**(22): 7165-7172.
- Pichon, A., Lazuen-Garay A., and James S. L. (2006). Solvent-free synthesis of a microporous metal-organic framework. *CrystEngComm* **8**(3): 211-214.
- Pipatsantipong, S., Rangsunvigit P., and Kulprathipanja S. (2012). Towards CO₂ adsorption enhancement via polyethyleneimine impregnation. *International Journal of Chemical and Biological Engineering* **6**: 291-295.
- Pirngruber, G. D., Cassiano-Gaspar S., Louret S., Chaumonnot A., and Delfort B. (2009). Amines immobilized on a solid support for postcombustion CO₂ capture: A preliminary analysis of the performance in a VSA or TSA process based on the adsorption isotherms and kinetic data. *Energy Procedia* **1**(1): 1335-1342.

- Plaza, M. G., Pevida C., Arenillas A., Rubiera F., and Pis J. J. (2007). CO₂ capture by adsorption with nitrogen enriched carbons. *Fuel* **86**(14): 2204-2212.
- Plaza, M. G., Pevida C., Arias B., Feroso J., Rubiera F., and Pis J. J. (2009). A comparison of two methods for producing CO₂ capture adsorbents. *Energy Procedia* **1**(1): 1107-1113.
- R. Veneman, Kamphuis H., and Brilman D. W. F. (2013). Post combustion CO₂ capture using supported amine sorbents: A process integration study. *Energy Procedia*: 1-9.
- Rackley, S. A. (2010). *Carbon Capture and Storage*, Butterworth-Heinemann/Elsevier.
- Rao, A. B., and Rubin E.S. (2002). A Technical, Economic and Environmental Assessment of Amine-based CO₂ Capture Technology for Power Plant Greenhouse Gas Control, *Environmental Science & Technology*, **36** (20): 4467–4475.
- Rathore, R. S., Srivastava D. K., Agarwal A. K., and Verma N. (2010). Development of surface functionalized activated carbon fiber for control of NO and particulate matter. *Journal of Hazardous Materials* **173**(1): 211-222.
- Rauscher, H., Perucca M., and Buyle G. (2010). Plasma Technology for Hyperfunctional Surfaces: Food, Biomedical and Textile Applications, *Wiley*.
- Rivera-Tinoco, R. and Bouallou C. (2010). Comparison of absorption rates and absorption capacity of ammonia solvents with MEA and MDEA aqueous blends for CO₂ capture. *Journal of Cleaner Production* **18**(9): 875-880.
- Robeson, L. M. (1991). Correlation of *separation* factor versus permeability for polymeric membranes. *Journal of Membrane Science* **62**(2): 165-185.
- Robeson, L. M. (2008). The upper bound revisited. *Journal of Membrane Science* **320**(1–2): 390-400.

- Rowse, J. L. C. and Yaghi O. M. (2006). Effects of Functionalization, Catenation, and Variation of the Metal Oxide and Organic Linking Units on the Low-Pressure Hydrogen Adsorption Properties of Metal-organic Frameworks. *Journal of the American Chemical Society* **128**(4): 1304-1315.
- Saha, D. and Deng S. (2010). Adsorption equilibrium and kinetics of CO₂, CH₄, N₂O, and NH₃ on ordered mesoporous carbon. *Journal of Colloid and Interface Science* **345**(2): 402-409.
- Saha, D. and Deng S. (2010). Adsorption equilibrium and kinetics of CO₂, CH₄, N₂O, and NH₃ on ordered mesoporous carbon. *Journal of Colloid and Interface Science* **345**(2): 402-409.
- Sala, O. E., Stuart Chapin F., Armesto J. J., Berlow E., Bloomfield J., Dirzo R., Huber-Sanwald E., Huenneke L. F., Jackson R. B., Kinzig A., Leemans R., Lodge D. M., Mooney H. A., Oesterheld M. N., Poff N. L., Sykes M. T., Walker B. H., Walker M., and Wall D. H. (2000). Global Biodiversity Scenarios for the Year 2100. *Science* **287**(5459): 1770-1774.
- Sanchez-Lainez, J., Zornoza B., Mayoral A., Berenguer-Murcia A., Cazorla-Amoros D., Tellez C., and Coronas J. (2015). Beyond the H₂/CO₂ upper bound: one-step crystallization and separation of nano-sized ZIF-11 by centrifugation and its application in mixed matrix membranes. *Journal of Materials Chemistry A* **3**(12): 6549-6556.
- Sartori, G. and Savage D. W. (1983). Sterically hindered amines for carbon dioxide removal from gases. *Industrial & Engineering Chemistry Fundamentals* **22**(2): 239-249.
- Satyapal, S., Filburn T., Trela J., and Strange J. (2001). Performance and Properties of a Solid Amine Sorbent for Carbon Dioxide Removal in Space Life Support Applications. *Energy & Fuels* **15**(2): 250-255.

- Shackley, S. and Gough C. (2006). Carbon Capture and Its Storage: An Integrated Assessment, *Ashgate*.
- Shawwa, A. R., Smith D. W., and Segó D. C. (2001). Color and chlorinated organics removal from pulp mills wastewater using activated petroleum coke. *Water Research* **35**(3): 745-749.
- Shieh, Y.-T., Liu G.-L., Wu H.-H., and Lee C.-C. (2007). Effects of polarity and pH on the solubility of acid-treated carbon nanotubes in different media. *Carbon* **45**(9): 1880-1890.
- Simmons, J. M., Wu H., Zhou W., and Yildirim T. (2011). Carbon capture in metal-organic frameworks-a comparative study. *Energy & Environmental Science* **4**(6): 2177-2185.
- Singh, G., Botcha V. D., Narayanam P. K., Sutar D. S., Talwar S. S., Srinivasa R. S., and Major S. S. (2013). Effect of ammonia plasma treatment on graphene oxide LB monolayers. *AIP Conference Proceedings* **1512**(1): 702-703.
- Singh, V. K. and Anil Kumar E. (2016). Measurement and analysis of adsorption isotherms of CO₂ on activated carbon. *Applied Thermal Engineering* **97**: 77-86.
- Siriwardane, R. V., Shen M. S., Fisher E. P., and Poston J. A. (2001). Adsorption of CO₂ on Molecular Sieves and Activated Carbon. *Energy & Fuels* **15**(2): 279-284.
- Small, C., Hashisho Z., and Ulrich A. C. (2012). Preparation and characterization of activated carbon from oil sands coke. *Fuel* **92**(1): 69-76.
- Small, C., Ulrich A., and Hashisho Z. (2012). Adsorption of Acid Extractable Oil Sands Tailings Organics onto Raw and Activated Oil Sands Coke. *Journal of Environmental Engineering* **138**(8): 833-840.

- Smith, B., Wepasnick K., Schrote K. E., Cho H. H., Ball W. P., and Fairbrother D. H. (2009). Influence of surface oxides on the colloidal stability of multi-walled carbon nanotubes: A structure– property relationship. *Langmuir* **25**(17): 9767-9776.
- Sohrabi, A., Shaibani P. M., Zarifi M. H., Daneshmand M., and Thundat T. (2014). A novel technique for rapid vapor detection using swelling polymer covered microstrip ring resonator. *2014 IEEE MTT-S International Microwave Symposium (IMS2014)*.
- Srikanth, C. S. and Chuang S. S. C. (2012). Spectroscopic Investigation into Oxidative Degradation of Silica-Supported Amine Sorbents for CO₂ Capture. *ChemSusChem* **5**(8): 1435-1442.
- Stavropoulos, G. G. and Zabaniotou A. A. (2009). Minimizing activated carbons production cost. *Fuel Processing Technology* **90**(7–8): 952-957.
- Steen, M. L., Butoi C. I., and Fisher E. R. (2001). Identification of Gas-Phase Reactive Species and Chemical Mechanisms Occurring at Plasma–Polymer Surface Interfaces. *Langmuir* **17**(26): 8156-8166.
- Stegmeier, S., Fleischer M., Tawil A., Hauptmann P., Egly K., and Rose K. (2009). Mechanism of the interaction of CO₂ and humidity with primary amino group systems for room temperature CO₂ sensors. *Procedia Chemistry* **1**(1): 236-239.
- Sullivan, P., Moate J., Stone B., Atkinson J. D., Hashisho Z., and Rood M. J. (2012). Physical and chemical properties of PAN-derived electrospun activated carbon nanofibers and their potential for use as an adsorbent for toxic industrial chemicals. *Adsorption* **18**(3): 265-274.

- Sumida, K., Rogow D. L., Mason J. A., McDonald T. M., Bloch E. D., Herm Z. R., Bae T. H., and Long J. R. (2012). Carbon Dioxide Capture in Metal–Organic Frameworks. *Chemical Reviews* **112**(2): 724-781.
- Sun, Y., Wang Y., Zhang Y., Zhou Y., and Zhou L. (2007). CO₂ sorption in activated carbon in the presence of water. *Chemical Physics Letters* **437**(1-3): 14-16.
- Supasinee Pipatsantipong, P. R., Santi Kulprathipanja (2012). Towards CO₂ adsorption enhancement via polyethyleneimine impregnation. *International Journal of Chemical and Biological Engineering* **6**: 291-295.
- Suslick, K. S., Hammerton D. A., and Cline R. E. (1986). Sonochemical hot spot. *Journal of the American Chemical Society* **108**(18): 5641-5642.
- Sveningsson, M., Morjan R. E., Nerushev O. A., Sato Y., Bäckström J., Campbell E. E. B., and Rohmund F. (2001). Raman spectroscopy and field-emission properties of CVD-grown carbon-nanotube films. *Applied Physics A* **73**(4): 409-418.
- Taborski, J., Wüstenhagen V., Väterlein P., and Umbach E. (1995). Precoverage-dependent molecular orientation of big organic adsorbates: NDCA on Ni(111) and O/Ni(111). *Chemical Physics Letters* **239**(4–6): 380-386.
- Tang, S., Lu N., Wang J. K., Ryu S. K., and Choi H. S. (2007). Novel Effects of Surface Modification on Activated Carbon Fibers Using a Low Pressure Plasma Treatment. *The Journal of Physical Chemistry C* **111**(4): 1820-1829.
- Tarka, T. J., Ciferno J. P., McMahan L. G. , and Fauth D. (2006). CO₂ Capture Systems Using Amine Enhanced Solid Sorbents. *5th Annual Conference on Carbon Capture & Sequestration, Alexandria, VA, USA.*

- Thomas, C. D., Cameron A., Green R. E., Bakkenes M., Beaumont L. J., Collingham Y. C., Erasmus B. F. N., De Siqueira M. F., Grainger A., Hannah L., Hughes L., Huntley B., Van Jaarsveld A. S., Midgley G. F., Miles L., Ortega-Huerta M. A., Townsend Peterson A., Phillips O. L., and Williams S. E. (2004). Extinction risk from climate change. *Nature* **427**(6970): 145-148.
- Thompson, M. (2008). CHNS Elemental Analyzers. *The Royal Society of Chemistry* **29**.
- Tontiwachwuthikul, P., Wee A. G. H., Idem R., Maneeintr K. , Fan G.J. , Amornvadee V., Amr H., Aroonwilas A. , Chakma A. (2011). Method of capturing carbon dioxide from gas streams. *US Patent, US 7910078 B2*
- Tranchemontagne, D. J., Mendoza-Cortes J. L., O'Keeffe M., and Yaghi O. M. (2009). Secondary building units, nets and bonding in the chemistry of metal-organic frameworks. *Chemical Society Reviews* **38**(5): 1257-1283.
- Ugarte N.P. and Swider-Lyons K. E. (2005). Low-Platinum tin-oxide electrocatalysts for PEM fuel cell cathodes. *Proton Conducting Membrane Fuel Cells III*. M. Murthy and T. F. Fuller: 67-73.
- Usman, M., Mendiratta S. and Lu K.-L. (2015). Metal–Organic Frameworks: New Interlayer Dielectric Materials. *ChemElectroChem* **2**(6): 786-788.
- Vaidhyanathan, R., Iremonger S. S., Dawson K. W. , and Shimizu G. K. H. (2009). An amine-functionalized metal organic framework for preferential CO₂ adsorption at low pressures. *Chemical Communications* (35): 5230-5232.
- Vandsburger, L., Swanson E., Tavares J., Meunier J. L., and Coulombe S. (2009). Stabilized aqueous dispersion of multi-walled carbon nanotubes obtained by RF glow-discharge treatment. *Journal of Nanoparticle Research* **11**(7): 1817-1822.

- Veawab, A., Aroonwilas A., Chakma A., and Tontiwachwuthikul P. (2008). Solvent Formulation for CO₂ Separation from Flue Gas Streams, Faculty of Engineering, University of Regina.
- Veawab, A., Tontiwachwuthikul P. , and Chakma A. (1999). Corrosion Behavior of Carbon Steel in the CO₂ Absorption Process Using Aqueous Amine Solutions. *Industrial & Engineering Chemistry Research* **38**(10): 3917-3924.
- Vesel, A. and Mozetic M. (2008). Modification of PET surface by nitrogen plasma treatment. *Journal of Physics: Conference Series* **100**(1): 012027.
- Vesel, A., Junkar I., Cvelbar U., Kovac J., and Mozetic M. (2008). Surface modification of polyester by oxygen- and nitrogen-plasma treatment. *Surface and Interface Analysis* **40**(11): 1444-1453.
- Wagner, T., Haffer S., Weinberger C., Klaus D. and Tiemann M. (2013). Mesoporous materials as gas sensors. *Chemical Society Reviews* **42**(9): 4036-4053.
- Wales, D. J., Grand J., Ting V. P., Burke R. D., Edler K. J., Bowen C. R., Mintova S., and Burrows A. D. (2015). Gas sensing using porous materials for automotive applications. *Chemical Society Reviews* **44**(13): 4290-4321.
- Walton, K. S., Millward A. R., Dubbeldam D., Frost H., Low J. J., Yaghi O. M., and Snurr R. Q. (2007). Understanding Inflections and Steps in Carbon Dioxide Adsorption Isotherms in Metal-Organic Frameworks. *Journal of the American Chemical Society* **130**(2): 406-407.
- Wang, B., Long J., and Teo K. (2016). Multi-Channel Capacitive Sensor Arrays. *Sensors* **16**(2): 150.

- Wang, P., Liu Z. G., Chen X., Meng F. L., Liu J. H., and Huang X. J. (2013). UV irradiation synthesis of an Au-graphene nanocomposite with enhanced electrochemical sensing properties. *Journal of Materials Chemistry A* **1**(32): 9189-9195.
- Wang, S. C., Chang K. S., and Yuan C. J. (2009). Enhancement of electrochemical properties of screen-printed carbon electrodes by oxygen plasma treatment. *Electrochimica Acta* **54**(21): 4937-4943.
- Wang, X., Li X., Zhang L., Yoon Y., Weber P. K., Wang H., Guo J., and Dai H. (2009). N-doping of graphene through electrothermal reactions with ammonia. *Science* **324**(5928): 768-771.
- Wang, Y., Chyu M. K., and Wang Q. M. (2014). Passive wireless surface acoustic wave CO₂ sensor with carbon nanotube nanocomposite as an interface layer. *Sensors and Actuators A: Physical* **220**: 34-44.
- Wark, M., Rohlfing Y., Altindag Y., and Wellmann H. (2003). Optical gas sensing by semiconductor nanoparticles or organic dye molecules hosted in the pores of mesoporous siliceous MCM-41. *Physical Chemistry Chemical Physics* **5**(23): 5188-5194.
- Wei, J., Liao L., Xiao Y., Zhang P., and Shi Y. (2010) Capture of carbon dioxide by amine-impregnated as-synthesized MCM-41. *Journal of Environmental Sciences* **22**(10): 1558-1563.
- Wiltshire, J., Khlobystov A., Li L., Lyapin S., Briggs G., and Nicholas R. (2004). Comparative studies on acid and thermal based selective purification of HiPCO produced single-walled carbon nanotubes. *Chemical Physics Letters* **386**(4): 239-243.
- Wong S. and Bioletti R. (2002). Carbon Dioxide Separation Technologies. Edmonton, Alberta, *Alberta Research Council Inc (ARC)*

- Wong, S. (2009). Module 2: CO₂ capture: Post combustion flue gas separation.
- Woo, S.W., Dokko K., Nakano H., and Kanamura K. (2009). Incorporation of polyaniline into macropores of three-dimensionally ordered macroporous carbon electrode for electrochemical capacitors. *Journal of Power Sources* **190**(2): 596-600.
- Wu, H., Simmons J. M., Liu Y., Brown C. M., Wang X. S., Ma S., Peterson V. K., Southon P. D., Kepert C. J., Zhou H. C., Yildirim T., and Zhou W. (2010). Metal–Organic Frameworks with Exceptionally High Methane Uptake: Where and How is Methane Stored? *Chemistry – A European Journal* **16**(17): 5205-5214.
- Wu, H., Simmons J. M., Srinivas G., Zhou W., and Yildirim T. (2010). Adsorption Sites and Binding Nature of CO₂ in Prototypical Metal-Organic Frameworks: A Combined Neutron Diffraction and First-Principles Study. *The Journal of Physical Chemistry Letters* **1**(13): 1946-1951.
- Wu, M., Zha Q., Qiu J., Han X., Guo Y., Li Z., Yuan A., and Sun X. (2005). Preparation of porous carbons from petroleum coke by different activation methods. *Fuel* **84**(14–15): 1992-1997.
- Xia, Y., Mokaya R., Grant D. M., and Walker G. S. (2011). A simplified synthesis of N-doped zeolite-templated carbons, the control of the level of zeolite-like ordering and its effect on hydrogen storage properties. *Carbon* **49**(3): 844-853.
- Xia, Y., Yang Z., and Mokaya R. (2010). Templated nanoscale porous carbons. *Nanoscale* **2**(5): 639-659.

- Xie, J., Yan N., Qu Z., and Yang S. (2012). Synthesis, characterization and experimental investigation of Cu-BTC as CO₂ adsorbent from flue gas. *Journal of Environmental Sciences* **24**(4): 640-644.
- Xiong, R., Ida J. , and Lin Y. S. (2003). Kinetics of carbon dioxide sorption on potassium-doped lithium zirconate. *Chemical Engineering Science* **58**(19): 4377-4385.
- Xu, B., Peng L., Wang G., Cao G., and Wu F. (2010). Easy synthesis of mesoporous carbon using nano-CaCO₃ as template. *Carbon* **48**(8): 2377-2380.
- Xu, D. P., Yoon S. H., Mochida I., Qiao W. M., Wang Y. G., and Ling L. C. (2008). Synthesis of mesoporous carbon and its adsorption property to biomolecules. *Microporous and Mesoporous Materials* **115**(3): 461-468.
- Xu, P., Li X., Yu H., and Xu T. (2014). Advanced Nanoporous Materials for Micro-Gravimetric Sensing to Trace-Level Bio/Chemical Molecules. *Sensors* **14**(10): 19023.
- Xu, X., Song C., Andresen J. M., Miller B. G., and Scaroni A. W. (2002). Novel Polyethylenimine-Modified Mesoporous Molecular Sieve of MCM-41 Type as High-Capacity Adsorbent for CO₂ Capture. *Energy & Fuels* **16**(6): 1463-1469.
- Xu, X., Song C., Miller B. G., and Scaroni A. W. (2005). Adsorption separation of carbon dioxide from flue gas of natural gas-fired boiler by a novel nanoporous Molecular basket adsorbent. *Fuel Processing Technology* **86**(14-15): 1457-1472.
- Xu, X., Song C., Miller B. G., and Scaroni A. W. (2005). Influence of Moisture on CO₂ Separation from Gas Mixture by a Nanoporous Adsorbent Based on Polyethylenimine-Modified Molecular Sieve MCM-41. *Industrial & Engineering Chemistry Research* **44**(21): 8113-8119.

- Xu, X., Song C., Wincek R., Andresen J. M., Scaroni A. W., Miller B. G. (2003). Separation of CO₂ from Power Plant Flue Gas Using a Novel CO₂ “Molecular Basket” Adsorbent *Fuel Chemistry Division Preprints* **48**(1): 162.
- Yamagiwa, H., Sato S., Fukawa T., Ikehara T., Maeda R., Mihara T., and Kimura M. (2014). Detection of Volatile Organic Compounds by Weight-Detectable Sensors coated with Metal-Organic Frameworks. *Scientific Reports* **4**: 6247.
- Yang, D., Velamakanni A., Bozoklu G., Park S., Stoller M., Piner R. D., Stankovich S., Jung I., Field D. A., Ventrice C. A., and Ruoff R. S. (2009). Chemical analysis of graphene oxide films after heat and chemical treatments by X-ray photoelectron and Micro-Raman spectroscopy. *Carbon* **47**(1): 145-152.
- Yang, H., Xu Z., Fan M., Gupta R., Slimane R. B., Bland A. E. , and Wright I. (2008). Progress in carbon dioxide separation and capture: A review. *Journal of Environmental Sciences* **20**(1): 14-27.
- Yang, J. and Qiu K. (2010). Preparation of activated carbons from walnut shells via vacuum chemical activation and their application for methylene blue removal. *Chemical Engineering Journal* **165**(1): 209-217.
- Yang, S. J., Cho J. H., Nahm K. S., and Park C. R. (2010). Enhanced hydrogen storage capacity of Pt-loaded CNT@MOF-5 hybrid composites. *International Journal of Hydrogen Energy* **35**(23): 13062-13067.
- Yang, Y., Li H., Chen S., Zhao Y., and Li Q. (2010). Preparation and Characterization of a Solid Amine Adsorbent for Capturing CO₂ by Grafting Allylamine onto PAN Fiber. *Langmuir* **26**(17): 13897-13902.

- Yazaydin, A. Ö., Snurr R. Q., Park T. H., Koh K., Liu J., LeVan M. D., Benin A. I., Jakubczak P., Lanuza M., Galloway D. B., Low J. J., and Willis R. R. (2009). Screening of Metal–Organic Frameworks for Carbon Dioxide Capture from Flue Gas Using a Combined Experimental and Modeling Approach. *Journal of the American Chemical Society* **131**(51): 18198-18199.
- Yin, C. Y., Aroua M. K., and Daud W. M. A. W. (2008). Polyethyleneimine impregnation on activated carbon: Effects of impregnation amount and molecular number on textural characteristics and metal adsorption capacities. *Materials Chemistry and Physics* **112**(2): 417-422.
- Yoo, Y., Lai Z., and Jeong H. K. (2009). Fabrication of MOF-5 membranes using microwave-induced rapid seeding and solvothermal secondary growth. *Microporous and Mesoporous Materials* **123**(1–3): 100-106.
- Yoon, S., Oh S. M., Lee C. W., and Ryu J. H. (2011). Pore structure tuning of mesoporous carbon prepared by direct templating method for application to high rate supercapacitor electrodes. *Journal of Electroanalytical Chemistry* **650**(2): 187-195.
- Yu, K., Zhu Z., Zhang Y., Li Q., Wang W., Luo L., Yu X., Ma H., Li Z., and Feng T. (2004). Change of surface morphology and field emission property of carbon nanotube films treated using a hydrogen plasma. *Applied Surface Science* **225**(1–4): 380-388.
- Yue, M. B., Chun Y., Cao Y., Dong X., and Zhu J. H. (2006). CO₂ Capture by As-Prepared SBA-15 with an Occluded Organic Template. *Advanced Functional Materials* **16**(13): 1717-1722.
- Zacher, D., Shekhah O., Woll C., and Fischer R. A. (2009). Thin films of metal-organic frameworks. *Chemical Society Reviews* **38**(5): 1418-1429.

- Zanganeh, K. E., Shafeen A., and Salvador C. (2009). CO₂ Capture and Development of an Advanced Pilot-Scale Cryogenic Separation and Compression Unit. *Energy Procedia* **1**(1): 247-252.
- Zarifi, M. H. and Daneshmand M. (2016). Liquid sensing in aquatic environment using high quality planar microwave resonator. *Sensors and Actuators B: Chemical* **225**: 517-521.
- Zarifi, M. H., Farsinezhad S., Abdolrazzaghi M., Daneshmand M., and Shankar K. (2016). Selective microwave sensors exploiting the interaction of analytes with trap states in TiO₂ nanotube arrays. *Nanoscale* **8**(14): 7466-7473.
- Zarifi, M. H., Farsinezhad S., Shankar K., and Daneshmand M. (2015). Liquid Sensing Using Active Feedback Assisted Planar Microwave Resonator. *IEEE Microwave and Wireless Components Letters* **25**(9): 621-623.
- Zarifi, M. H., Fayaz M., Goldthorp J., Abdolrazzaghi M., Hashisho Z., and Daneshmand M. (2015). Microbead-assisted high resolution microwave planar ring resonator for organic-vapor sensing. *Applied Physics Letters* **106**(6): 062903.
- Zarifi, M. H., Rahimi M., Daneshmand M., and Thundat T. (2016). Microwave ring resonator-based non-contact interface sensor for oil sands applications. *Sensors and Actuators B: Chemical* **224**: 632-639.
- Zarifi, M. H., Shariaty P., Hashisho Z., and Daneshmand M. (2017). A non-contact microwave sensor for monitoring the interaction of zeolite 13X with CO₂ and CH₄ in gaseous streams. *Sensors and Actuators B: Chemical*.
- Zarifi, M. H., Sohrabi A., Shaibani P. M., Daneshmand M., and Thundat T. (2015). Detection of Volatile Organic Compounds Using Microwave Sensors. *IEEE Sensors Journal* **15**(1): 248-254.

- Zarifi, M. H., Thundat T., and Daneshmand M. (2015). High resolution microwave microstrip resonator for sensing applications. *Sensors and Actuators A: Physical* **233**: 224-230.
- Zelenak, V., Halamova D., Gaberova L., Bloch E., and Llewellyn P. (2008). Amine-modified SBA-12 mesoporous silica for carbon dioxide capture: Effect of amine basicity on sorption properties. *Microporous and Mesoporous Materials* **116**(1-3): 358-364.
- Zhang, Z., Guan J., and Ye Z. (1998). R and D Note: Separation of a Nitrogen-Carbon Dioxide Mixture by Rapid Pressure Swing Adsorption. *Adsorption* **4**(2): 173-177.
- Zhang, Z., Wang K., Atkinson J. D., Yan X., Li X., Rood M. J., and Yan Z. (2012). Sustainable and hierarchical porous Enteromorpha prolifera based carbon for CO₂ capture. *Journal of Hazardous Materials* **229–230**: 183-191.
- Zhang, Z., Xu M., Wang H., and Li Z. (2010). Enhancement of CO₂ adsorption on high surface area activated carbon modified by N₂, H₂ and ammonia. *Chemical Engineering Journal* **160**(2): 571-577.
- Zhao, B., Zhang L., Wang X., and Yang J. (2012). Surface functionalization of vertically-aligned carbon nanotube forests by radio-frequency Ar/O₂ plasma. *Carbon* **50**(8): 2710-2716.
- Zhao, J., Losego M. D., Lemaire P. C., Williams P. S., Gong B., Atanasov S. E., Blevins T. M., Oldham C. J., Walls H. J., Shepherd S. D., Browe M. A., Peterson G. W., and Parsons G. N. (2014). Highly Adsorptive, MOF-Functionalized Nonwoven Fiber Mats for Hazardous Gas Capture Enabled by Atomic Layer Deposition. *Advanced Materials Interfaces* **1**(4): 1400040-n/a
- Zhao, Z., Li Z., and Lin Y. S. (2009). Adsorption and Diffusion of Carbon Dioxide on Metal–Organic Framework (MOF-5). *Industrial & Engineering Chemistry Research* **48**(22): 10015-10020.

- Zhou, Y., Jiang Y., Xie T., Tai H., and Xie G. (2014). A novel sensing mechanism for resistive gas sensors based on layered reduced graphene oxide thin films at room temperature. *Sensors and Actuators B: Chemical* **203**: 135-142.
- Zhuang, J. L., Ar D., Yu X. J., Liu J. X. and Terfort A. (2013). Patterned Deposition of Metal-Organic Frameworks onto Plastic, Paper, and Textile Substrates by Inkjet Printing of a Precursor Solution. *Advanced Materials* **25**(33): 4631-4635.
- Zu, D. D., Lu L., Liu X. Q., Zhang D. Y., and Sun L. B. (2014). Improving Hydrothermal Stability and Catalytic Activity of Metal–Organic Frameworks by Graphite Oxide Incorporation. *The Journal of Physical Chemistry C* **118**(34): 19910-19917.
- Zybaylo, O., Shekhah O., Wang H., Tafipolsky M., Schmid R., Johannsmann D. and Woll C. (2010). A novel method to measure diffusion coefficients in porous metal-organic frameworks. *Physical Chemistry Chemical Physics* **12**(28): 8093-8098.

APPENDIX A: SUPPLEMENTARY DATA FOR CHAPTER 3

X-ray Photo electron Spectroscopy Measurement

In a XPS spectrum, peak intensities of different elements correspond to their atomic percentage present in a sample. The atomic percentage of each element then can be easily converted to weight percentage by multiplying by its molecular weight.

Table A1. The atomic percentage of different N1s components determined from relative area of corresponding XPS spectra

Sample	Pyridinic-N (%)	Pyrrolic-N (%)	Graphitic-N (%)	Oxidized-N (%)
Delayed coke	12.32	46.72	38.65	2.31
AC	39.51	29.73	28.85	1.92

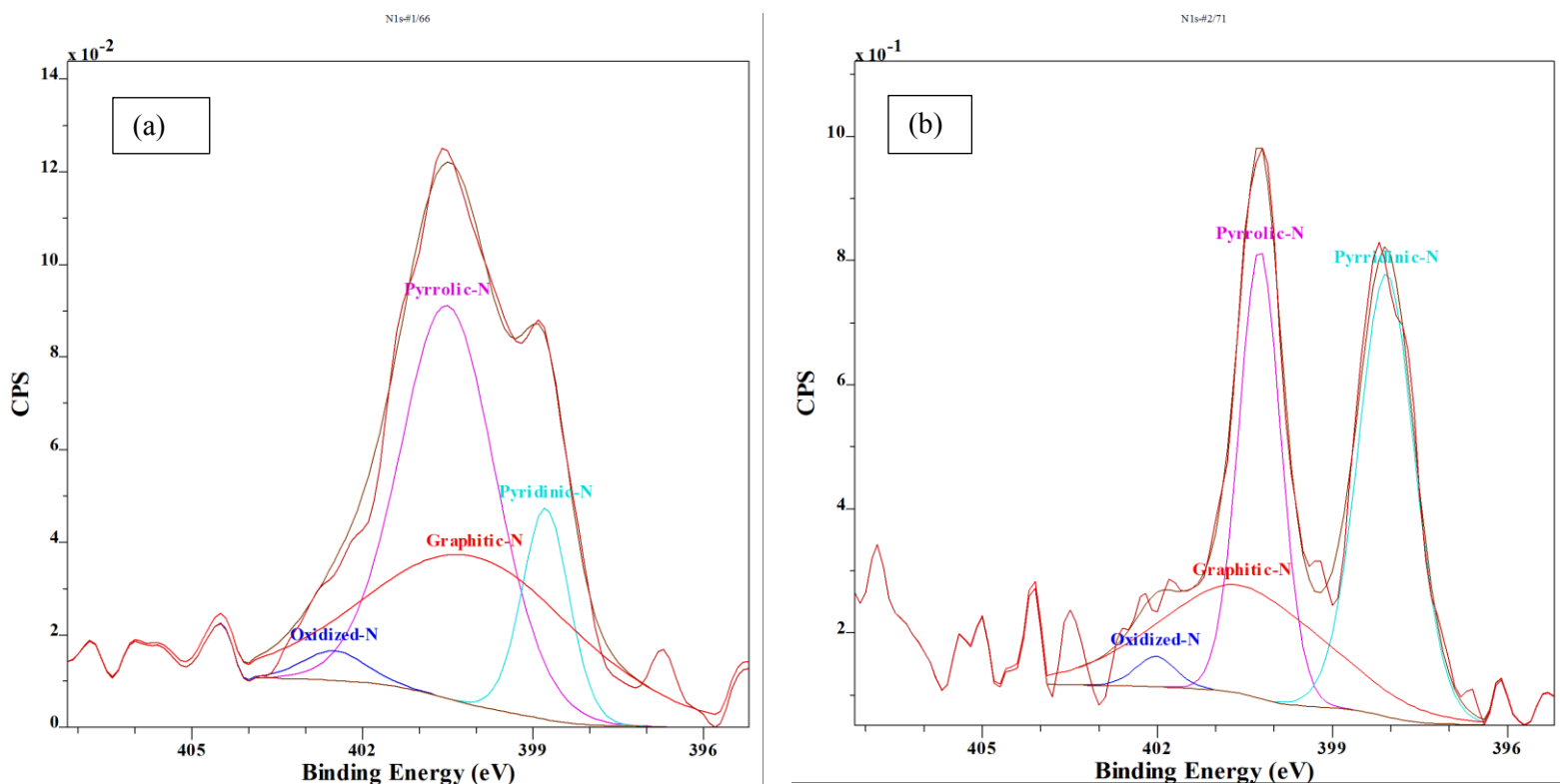
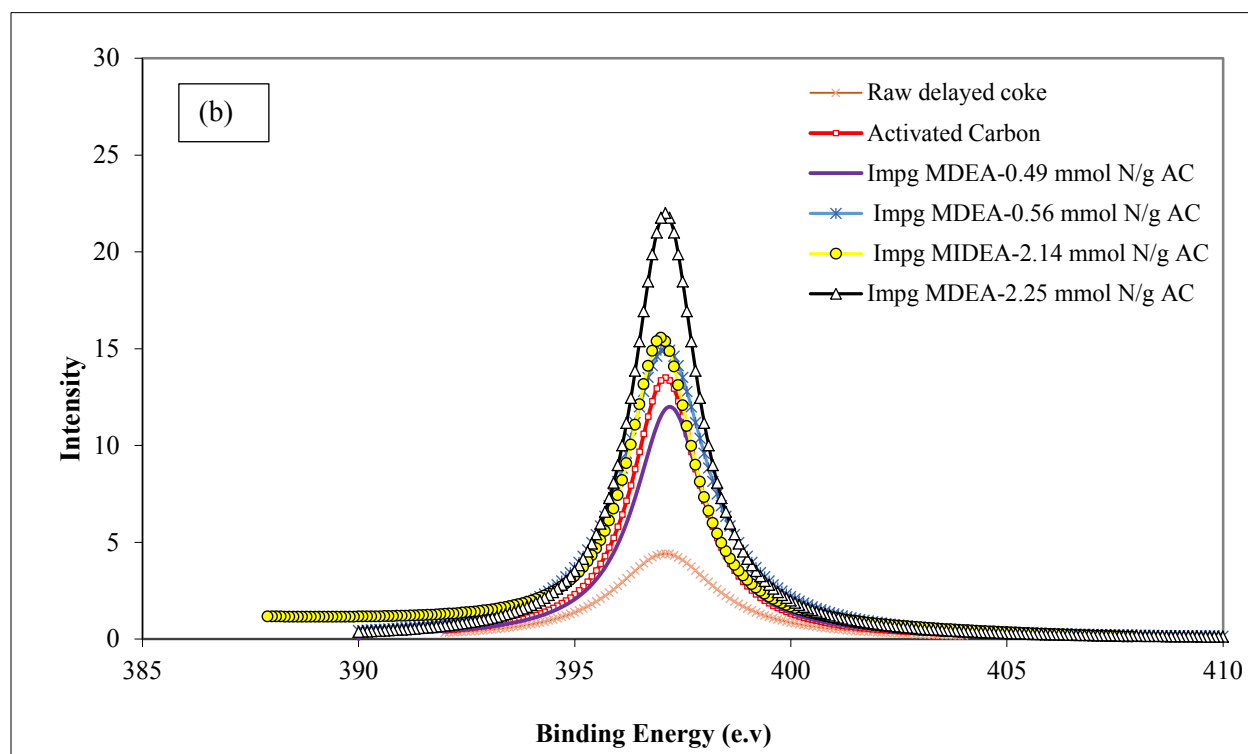
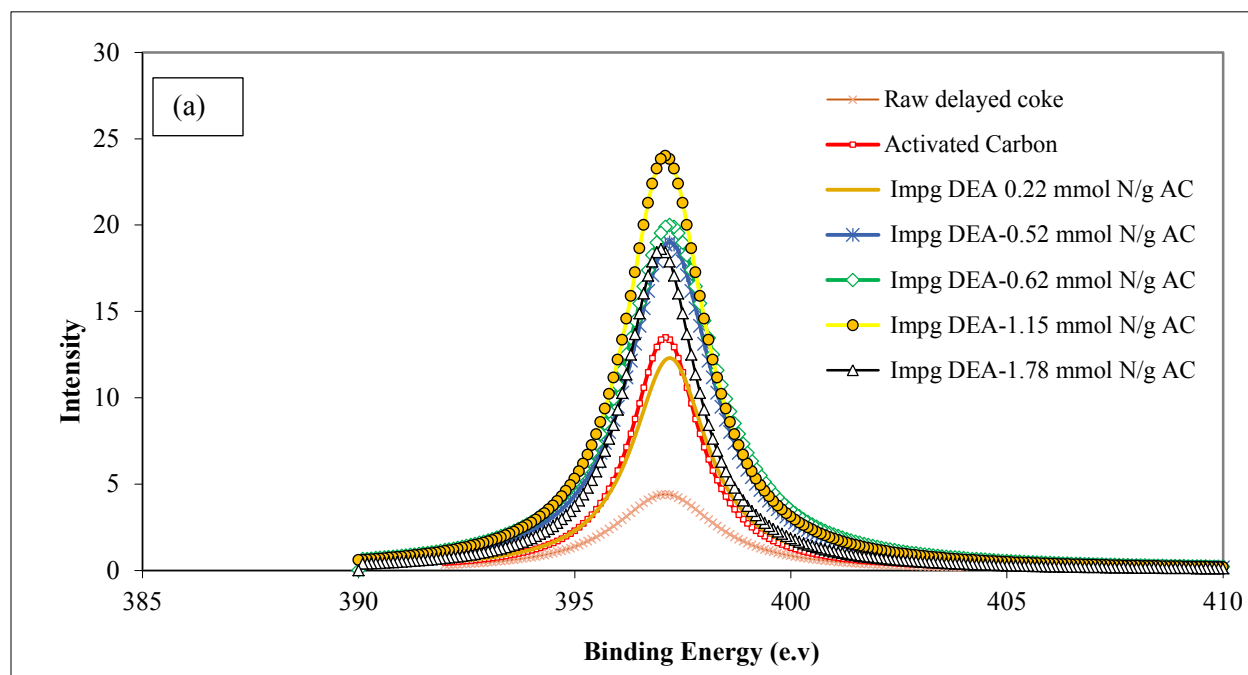


Figure A1. De-convoluted N1s spectra of (a) raw and (b) activated coke



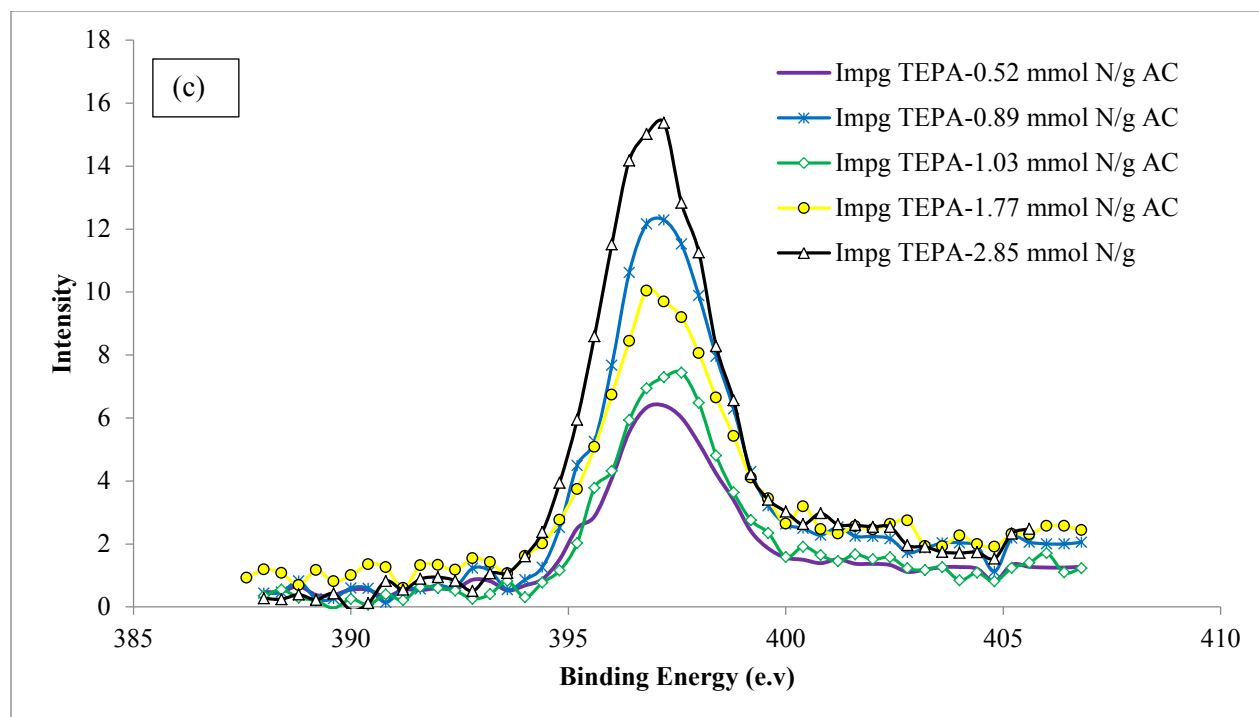


Figure A2. N1s spectra of raw and activated coke, and (a) AC-DEA samples, (b) AC-MDEA samples, and (c) AC-TEPA samples

APPENDIX B: SUPPLEMENTARY DATA FOR CHAPTER 5

Table B1. Curve fitting results of XPS C1s spectra for O₂/Ar plasma treatment

Sample	Sp ² %	Sp ³ %	C-O %	C=O %	O-C=O %
	284.1 ±0.2ev	285.1 ±0.2ev	286.2 ±0.2ev	287.2 ±0.2ev	288.9 ±0.2ev
Virgin CNT-BP	58.5	28.0	1.9	9.4	2.2
Plasma treated CNT-BP, O ₂ /Ar, 3min	28.1	43.6	13.1	12.9	2.3
Plasma treated CNT-BP, O ₂ /Ar, 5min	20.8	44.3	5.4	29.4	0.1
Plasma treated CNT-BP, O ₂ /Ar, 7min	19.2	43.0	3.4	24.4	9.9

Table B2. Curve fitting results of XPS C1s spectra for NH₃ plasma treatment

Sample	C-C %	C-O, C-N %	O=C-N, C=O %	O-C=O %
	284.8ev	286.4ev	287.4ev	288.8ev
Virgin CNT-BP	85.9	6.2	5.3	2.6
Plasma treated CNT-BP, NH ₃ , 3min	62.7	23.1	–	14.2
Plasma treated CNT-BP, NH ₃ , 5min	54.0	31.7	–	14.3
Plasma treated CNT-BP, NH ₃ , 7min	33.8	30.8	24.2	11.2

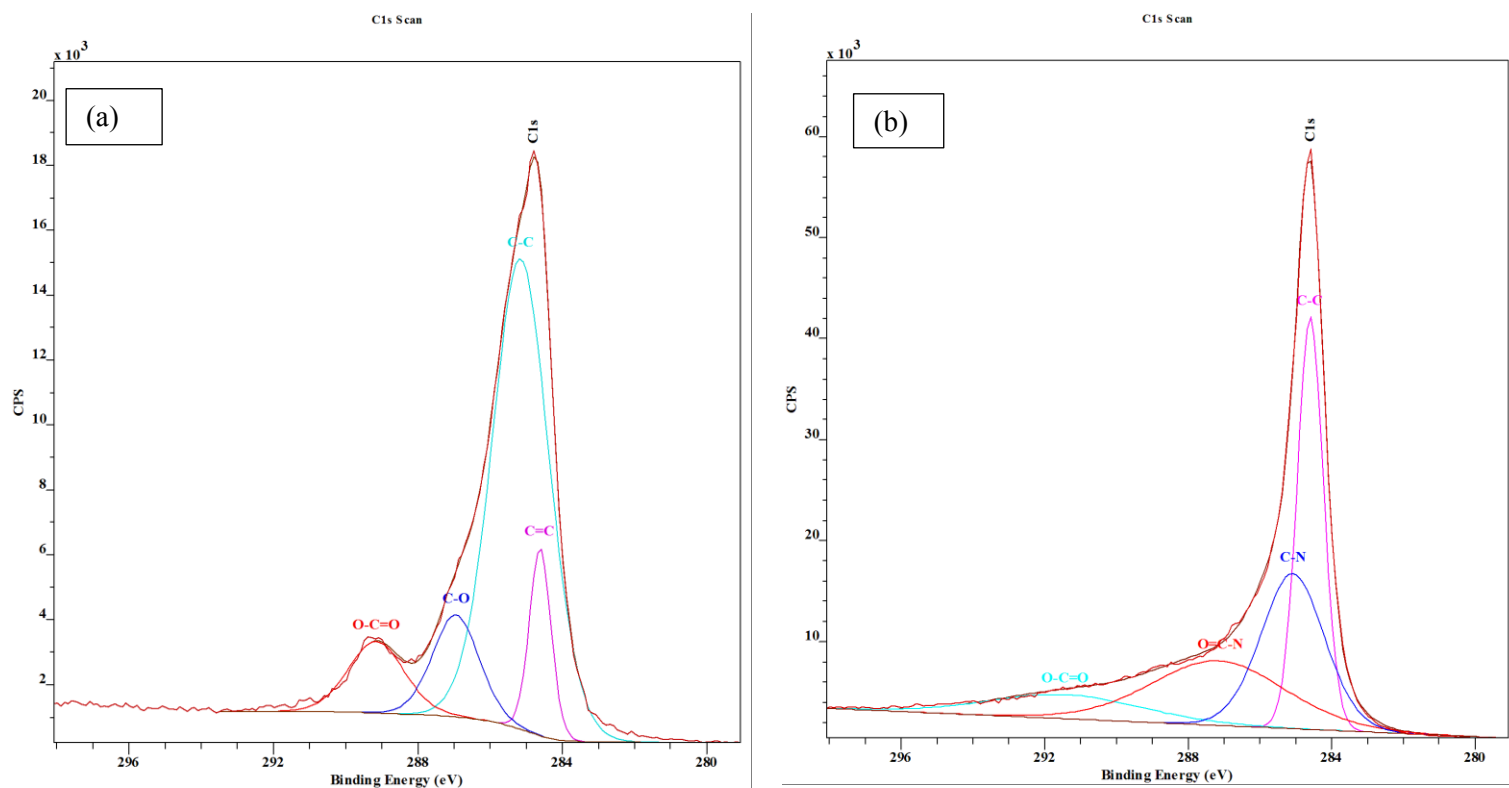


Figure B1. Carbon 1s electron spectra for (a) double side plasma treated CNT-BP with O_2/Ar for 7 min, and (b) double side plasma treated CNT-BP with NH_3 for 7 min

Table B3. Raman feature of CNT-BP before and after plasma treatment with O_2/Ar and NH_3

Sample	Peak (cm^{-1})	Intensity (a.u.)	I_D/I_G
Virgin CNT-BP	(D) 1342.67	24014.6	0.51
	(G) 1570.65	47067.2	
Single side plasma treated CNT-BP, NH_3 , 3min	(D) 1342.67	20630.1	0.60
	(G) 1571.86	34135.9	

Single side plasma treated CNT-BP, O ₂ /Ar, 3min	(D) 1342.67	13836.5	0.69
	(G) 1573.07	19954.9	

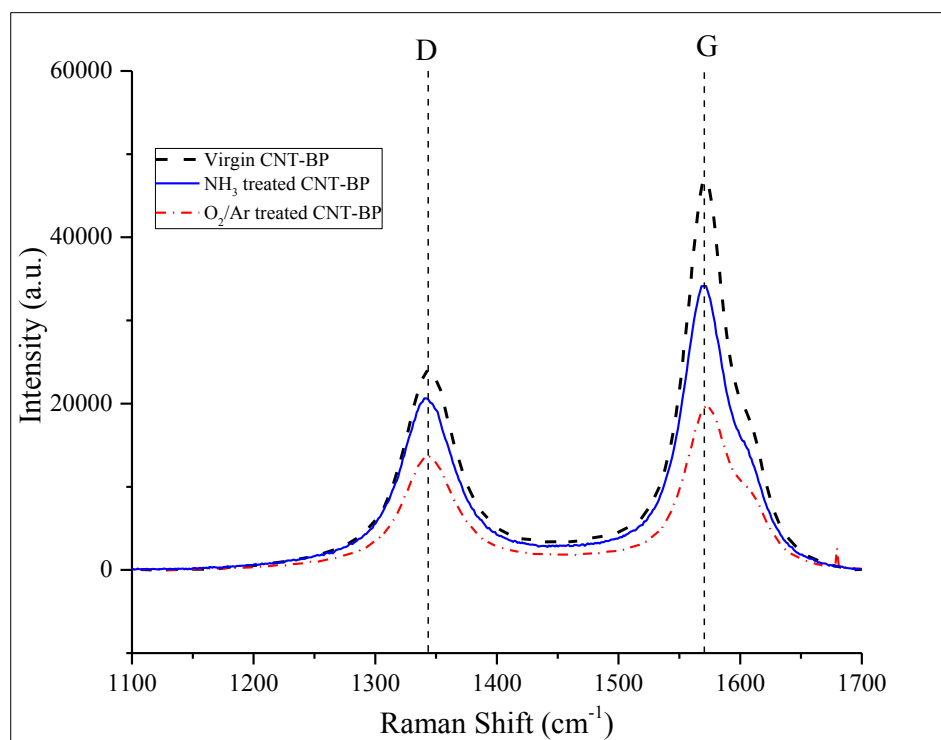


Figure B2. Raman spectrum of virgin CNT-BP, and single side plasma treated CNT-BP with O₂/Ar and NH₃ for 3 min

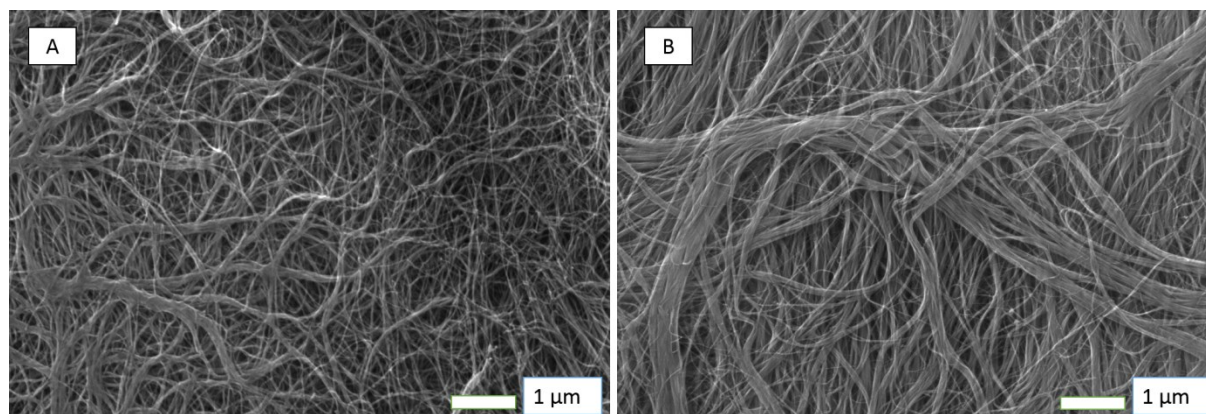


Figure B3. SEM images of (a) virgin and (b) single side plasma treated CNT-BP with O_2/Ar for 15min

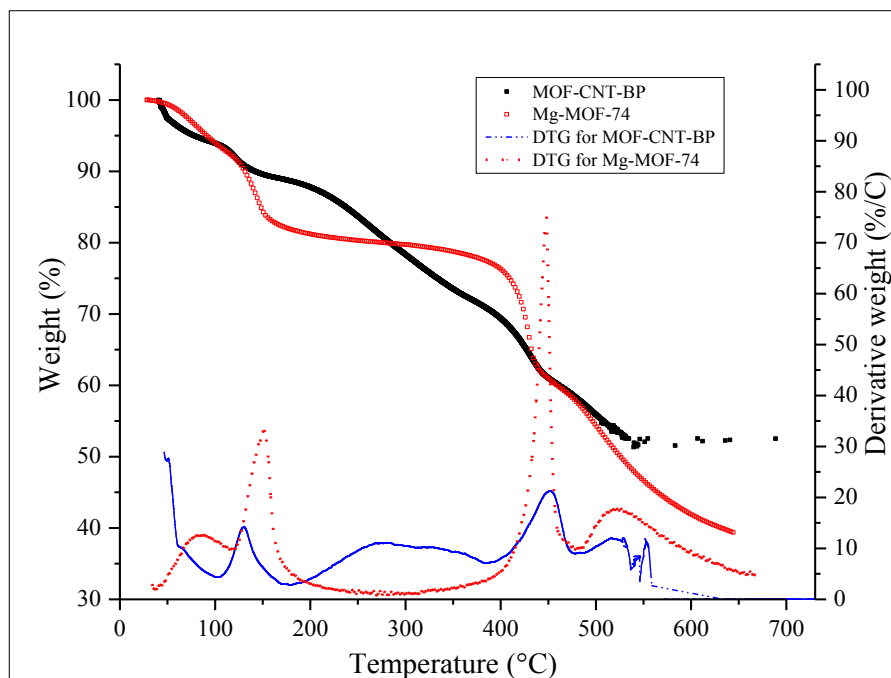


Figure B4. Gravimetric analysis of the Mg-MOF-74 decomposition for Mg-MOF-74 and MOF-CNT-BP (single side treated CNT-BP with O_2/Ar for 3 min, 20 h crystallization)